DISSERTATION

POSTMORTEM RETRIEVAL ANALYSIS OF CANINE TOTAL HIP ARTHROPLASTY

Submitted by

Carolyn Patlovany Skurla

Department of Mechanical Engineering

In partial fulfillment of the requirements

For the Degree of Doctor of Philosophy

Colorado State University

Fort Collins, Colorado

Summer 2002

ProQuest Information and Learning Company
300 North Zeeb Road
P.O. Box 1346
Ann Arbor, MI 48106-1346

COLORADO STATE UNIVERSITY

June 27, 2002

WE HEREBY RECOMMEND THAT THE DISSERTATION PREPARED UNDER OUR SUPERVISION BY CAROLYN PATLOVANY SKURLA ENTITLED POSTMORTEM RETRIEVAL ANALYSIS OF CANINE TOTAL HIP ARTHROPLASTY BE ACCEPTED AS FULFILLING IN PART REQUIREMENTS FOR THE DEGREE OF DOCTOR OF PHILOSOPHY.

Committee on Graduate Work

Advisor

Department Head

ABSTRACT OF DISSERTATION

POSTMORTEM RETRIEVAL ANALYSIS OF CANINE TOTAL HIP ARTHROPLASTY

With the aging of the human population in the United States comes a demand for increasingly advanced medical care options for the elderly. The average number of total hip arthroplasties (THAs) performed each year in the United States has increased from 204.000 in 1988 to 249.000 in 1995 with an estimated increase to 359.000 by 2030. The economic impact of THAs in the United States was estimated at $3.7 billion in 1995, and that figure will continue to increase.

The dog is commonly used as an animal model in human orthopaedic prosthetic development. In addition, THAs are performed clinically in dogs to treat diseased joints, alleviate pain, and increase function. This procedure has been performed at the Colorado State University Veterinary Teaching Hospital for over 20 years, but the long-term clinical performance of cemented THA in dogs was unknown.

This dissertation research involved performing engineering analysis on canine THA implants that had been implanted in client-owned dogs and were retrieved postmortem with the dual goal of improving our understanding of the dog as a model for human THA and of improving the clinical success of canine THA. Much has been learned about the performance and failure mechanisms of THAs in humans through postmortem retrieval studies, and that knowledge could not be gained in any other way.

The femoral and acetabular components were mechanically tested to assess the stability of the implant within the bone and the bone cement. The quality of the femoral cement mantle was assessed using radiographs of the intact and sliced femora. The acetabular components, made of ultra high molecular weight polyethylene (UHMWPE), were measured for volumetric wear and graded for types and location of damage to the UHMWPE. Wear debris was isolated from soft tissues surrounding the joint. The results of this study were also compared with similar findings in human postmortem retrieval studies in order to assess whether THA implants wear and fail by similar mechanisms in humans and dogs.

The incidence of aseptic loosening was alarmingly high for both the femoral and acetabular components in the dog with more than half of all components being loose. Surprisingly, the prostheses that had been implanted in dogs with bilateral THA tended to perform better than those implanted in dogs with unilateral THA. Just as human postmortem studies led to changes in human THA surgical technique, the results of this dissertation research are already leading to changes in the surgical paradigm for veterinary orthopedic surgeons across the country.

Carolyn Patlovany Skurla
Mechanical Engineering Department
Colorado State University
Fort Collins, CO 80523
Summer 2002

ACKNOWLEDGEMENTS

First, I thank my beloved husband, Richard, who commuted to Denver or Boulder for seven years to enable me to pursue this degree. He was my biggest supporter throughout this long period, and he paid a high price. He and the dogs kept me grounded, sane, and loved. Next, I thank my parents, Raymond and Cecilia Patlovany, who gave my brothers and me the gifts of love, faith, and education. I think I got a bit carried away with the education part.

My teachers and fellow students at Catholic Biblical School and my friends at John XXIII Catholic Community gave me a life outside of my pursuit of a Ph.D and words of wisdom to live by. My friend and fellow Ph.D. candidate, Fr. Marcel Zibognon, gave me the goal of someday helping him attain his dream of building a university to help lift his country, Ivory Coast, out of poverty.

My committee encouraged and challenged me to make my research better. My adviser, Susan James has been mentor and friend over the course of my very long journey. Don Radford, my only other original committee member, was always helpful, fair, and challenging. Donna Wheeler and Elizabeth Pluhar were added late in my dissertation journey, but they provided me with a sense of renewed excitement in my work when I needed it most. Erick Egger, as my "honorary committee member," stuck with me through the entire journey and was a valuable source of information, assistance, and encouragement.

PREFACE

This dissertation is organized as a series of journal articles or technical communications. As a result, there are some redundancies in the literature review, discussion, and conclusion among the chapters, and I apologize in advance for any confusion or difficulty that this may cause. Some of these redundancies were reduced for the purposes of this dissertation by referring to tables and figures outside of each chapter. The basic organization of this dissertation is as follows:

- Chapter 1 contains a brief introductory literature review and an explanation of the motivation for this research project.
- Chapter 2 contains the results of an owner assessment survey that was mailed to owners of THA dogs. This journal article was published in its entirety in *Journal of the American Veterinary Medical Association* in October 2000.
- Chapter 3 is the first of three journal articles being prepared for submission. This chapter describes the testing of the femoral components and the results of the analysis of this data.
- Chapter 4 is the second of three journal articles being prepared for submission. This chapter describes the testing of the acetabular components and the results of the analysis of this data.
- Chapter 5 is the third of three journal articles being prepared for submission. This chapter describes the method used to digest soft tissue specimens to isolate wear

debris. The data analysis was performed to look for wear debris and acetabular component data that correlated with the dependent variables for the femoral component and to look for wear debris and femoral component data that correlated with the dependent variables for the acetabular component.

- Chapter 6 is the first of two technical communications being prepared for submission. This chapter summarizes the results, discussion, and conclusions from chapters 3, 4, and 5 that were particularly relevant to the veterinary orthopaedic surgeon.
- Chapter 7 is the second of two technical communications being prepared for submission. This chapter summarizes the results, discussion, and conclusions from chapters 3, 4, and 5 that were relevant to the biomedical researcher or human orthopaedic surgeon.
- Chapter 8 describes future work resulting from this dissertation research.

TABLE OF CONTENTS

Chapter 1

Introduction and Motivation

1.1. Introduction

1.1.1. Human Total Hip Arthroplasty

Total hip arthroplasty (THA) procedures are performed in humans in order to replace a diseased hip joint with a new, artificial, articulating surface designed to alleviate pain and increase function. A variety of prosthetic devices are used, but the most common devices consist of an ultra high molecular weight polyethylene (UHMWPE) acetabular component and a metallic femoral component, usually made of cobalt-chromium (Co-Cr) or titanium (Ti-6Al-4V) alloys. Cemented components are held in place using polymethyl methacrylate (PMMA) bone cement. Cementless prostheses are also commonly used [1].

The number of total joint arthroplasties (TJAs) and THAs performed in the United States increases each year (*See Table 1.1*) [2]. The economic impact of all THAs in the United States was conservatively estimated at $10 billion per year in 1995 with THAs comprising $3.7 billion of that estimate [3]. This impact will continue to increase with the aging of the baby-boomer population.

Despite many improvements in prosthetic design and surgical technique since the

advent of THA surgery, the failure rate due to aseptic loosening remains high [4-6]. A review of the literature with regard to incidence rates for aseptic loosening of femoral and acetabular components appears in the introductory sections of Chapters 3 and 4.

Human implants that are retrieved at the time of revision surgery provide valuable information to the biomedical researcher. Unfortunately, secondary failure mechanisms and damage induced at the time of revision may obscure the initiating causes of failure; therefore, the analysis of THA implants retrieved at revision surgery has limited usefulness in identifying the initiating events of aseptic loosening.

Autopsy retrieval studies are problematic because of the lack of control over the experimental design; however, autopsy retrieval studies of human THA implants that were considered to be clinically successful at the time of the patients' death provided insight into the earliest failure initiators [7-11]. This information could not have been gained in any other fashion. The initiating failure event for cemented femoral components was found to be mechanical in nature [7-9], beginning with debonding of the PMMA/metal interface at the proximal and distal ends of the femoral stem. By contrast, the primary failure mechanism for acetabular components appears to be biological in nature [9-11]. Submicron-sized UHMWPE wear particles become dispersed into the joint capsule and initiate a complex biological reaction, resulting in osteolysis and the interposition of soft tissue at the bone/PMMA interface. More detailed descriptions of these initiating failure events appear in the introductory sections of Chapters 3 and 4. Insights into initiating failure mechanisms in human THA have led to improvements in surgical technique and implant design.

1.1.2. Dogs as an Animal Model for Human THA

Dogs are commonly used as an animal model in orthopaedic prosthetic development and testing. According to An and Friedman [12], dogs have the "closest *in vivo* condition to the human except for non-human primates." Factors that make the dog preferable over other higher level vertebrates (i.e., goats, sheep, pigs) are availability of basic data about the species, ease of handling, and modest housing requirements.

There have been many experimental studies performed on healthy dogs with no evidence of degenerative joint disease (DJD), but there are too many to review here. A review of a subset of these studies [13-21] shows that the most recent studies have been performed using experimental, cementless implants that are unavailable for clinical use in dogs with DJD. These experimental studies were performed using from 8 to 54 dogs, with study durations ranging from 3 weeks to 3 years, although most had durations of 24 months or less. The short duration of these studies contrasts sharply with the implant durations of human autopsy retrievals, cited in the studies above [7-11], with implant durations ranging from 2 weeks to 21 years. Harris warns in a review article, "...short-term results do not necessarily predict the future" [22]. The examples he cited were studies on femoral head allografts and acetabular cement fixation that showed excellent results with a 0% failure rate at 4.5 years for the femoral allografts and a 2% loosening rate for acetabular components at 6 years. However, the failure rate for femoral allografts was 33% by 6 years, and the socket loosening rate had increased to 42% by 11 years after surgery.

Most of these canine studies did not limit the dog's activity after surgery as much as surgeons limit the activity of client-owned, clinical dogs after THA. Because the

implants used were unavailable to veterinary surgeons for clinical use. these studies are of little use to the veterinary clinical surgeon dealing with clinical THA cases in dogs.

1.1.3. Canine Total Hip Arthroplasty

While not as common as the human procedure. clinical THAs are performed in dogs for much the same reasons as in humans. Acceptable success rates were not attained until the Richards Canine II total hip prosthesis (*See Figure 1.1*) was introduced in 1974 [23].

While it is unknown how many THAs are performed in dogs in the United States. approximately one to two THAs per week are performed at the Colorado State University Veterinary Teaching Hospital (CSU VTH). This procedure has been performed at the CSU VTH for over 20 years. The surgical paradigm in existence at the CSU VTH at the beginning of this study held that dogs with bilateral DJD could be treated adequately with unilateral THA. Feedback from veterinary orthopaedic surgeons and owners indicated that dogs with bilateral DJD and unilateral THA would adjust their gait after surgery and carry more weight on their implanted hip than on their intact. diseased hip.

Seven retrospective studies [24-30] that provided survivorship data on clinical canine THAs are more thoroughly presented in the introductory sections of Chapters 3 and 4 (*See Tables 3.1 & 4.3*). Briefly. these studies presented data regarding the incidence of aseptic loosening requiring revision surgery for both femoral and acetabular components. This data was based on a combination of follow-up office visits and subjective owner surveys. Indications from these studies were that the incidence of aseptic loosening requiring revision was low in canine THA.

1.1.3.1. Canine THA Implant Designs

The cemented THA implant used clinically in dogs is very similar to human

implants. There have been three implant designs used at the CSU VTH. All designs had a non-metal backed acetabular component that was machined from UHMWPE bar stock (*See Figure 1.2*). There is a major difference between the shapes of the human and canine acetabular components. The canine acetabular component has a 45° fire hydrant cut-out that is placed dorsally when implanted in the dog. All three femoral components were collared. The collar, according to Harris [31], serves to increase PMMA pressurization during implantation, reduce subsidence, reduce micromotion during gait, and increase load transfer to the proximal medial bone in order to decrease stress shielding and disuse osteoporosis of the proximal femur.

The first implant design used was the Richards (Smith & Nephew Richards, Memphis, TN) and consisted of a monolithic Co-Cr femoral component (*See Figures 1.1 & 1.3*). The shape of the proximal cross-section is rectangular (*See Figure 1.4*), and the distal tip is tapered. This implant came in large, medium, and small sizes. Sharp corners, such as those seen in this implant design, have been shown to be associated with stress concentrations in the PMMA [32]. One human postmortem retrieval study [8] found that radially oriented fractures were usually located at or near sharp corners of the prosthesis.

The second design, the BioMedtrix #1 (BioMedtrix, Inc., Allendale, NJ), had a modular femoral component with a Ti-6Al-4V stem and Co-Cr head (*See Figures 1.4 & 1.5*). This implant design has been reported to be related to a high rate of aseptic loosening [30]. This femoral component had sharp corners on the lateral aspect of the proximal stem (*See Figure 1.5*). As with the Richards femoral component, sharp corners are known to cause stress concentrations in the PMMA [32]. The distal one-third of the femoral stem was round with grooves running the length of the component on the cranial

and caudal sides of the stem. The implants were sized according to the diameter of the distal stem, and most common sizes ranged from 6 to 9 mm in diameter in 1 mm increments. The same modular femoral head, 17 mm in diameter, was used for all femoral components in the most common size range. A 5 mm femoral component was also available, and this implant had a femoral head that was smaller in diameter.

The third design, the BioMedtrix #2, is the current commercially available design with a modular femoral component made entirely of Co-Cr (*See Figures 1.4 & 1.5*). The sharp corners were removed from this design, and the proximal portion of the femoral stem is thinner than the BioMedtrix #1 in the cranial-to-caudal direction. The proximal cross-section (*See Figure 1.4*) is approximately oval in shape with the lateral end being thicker than the medial end. The shape of the distal third of the femoral stem and the sizes are same as for the BioMedtrix #1.

For the remainder of this dissertation, the three implant designs will be referred to as Richards, BioMedtrix #1, and BioMedtrix #2.

1.2. Motivation

Prior to the present study, there had been no postmortem retrieval studies of clinical THA that provided information with regard to mechanical stability and wear in canine THA. The long-term performance of clinical canine THA implants was unknown except through the retrospective studies. The manner and degree of UHMWPE wear and damage were unknown.

This dissertation research involved performing engineering analysis on canine THA implants that had been implanted in client-owned dogs and were retrieved postmortem

with the dual goal of improving our understanding of the dog as a model for human THA and of improving the clinical success of canine THA. Much has been learned about the performance and failure mechanisms of THA in humans through postmortem retrieval studies [7-11], and that knowledge could not be gained in any other way. Despite the fact that the dog is the orthopaedic model of choice for THA, little was known about the long-term performance of these implants in the dog. It was unknown whether THAs in dogs would display the same initiating failure mechanisms as those seen in humans. Experimental studies rarely extended for longer than two years, and the implants in this dissertation range in duration *in situ* from 8 months to 11 years and 8 months. Just as human postmortem studies led to changes in human THA surgical technique, the intent of this research was that the results would lead to improvements in surgical technique and implant design for canine THA. In addition, a better understanding of long-term clinical performance of canine THA in comparison to that seen in humans would lead to a better understanding of the suitability of the dog as an orthopaedic model for human THA.

In order to compare the clinical canine THA findings of this study to similar studies in humans, human retrieval studies from the literature needed to be carefully chosen. The studies must be on human implants made from similar materials, implanted using similar attachment methods, and measured using similar methods. The humans studies selected were those performed on cemented THA with non-metal backed acetabular components made from UHMWPE that were articulated against metallic femoral components.

1.3. References

1) Kaplan SS. Biomaterial-Host Interactions: Consequences, Determined by Implant Retrieval Analysis. *Medical Progress Through Technology*, 1994; 20: 209-230.

2) Praemer A. Furner S. Rice DP. *Musculoskeletal Conditions in the United States*. American Academy of Orthopaedic Surgeons. Rosemont. IL; 1999.

3) Mushinski M. Average Charges for a Total Hip Arthroplasty: Geographic Variations. 1995. *Statistical Bulletin (Metropolitan Life Insurance Company)*. 1996; 77: 21-28.

4) Mulroy WF. Estok DM. Harris WH. Total Hip Arthroplasty with Use of So-Called Second-Generation Cementing Techniques: A Fifteen-Year-Average Follow-Up Study. *The Journal of Bone and Joint Surgery*. 1995; 77-A: 1845-1852.

5) Klapach AS. Callaghan JJ. Goetz D. Olejniczak JP. Johnston RC. Charnley Total Hip Arthroplasty With Use of Improved Cementing Techniques: A Minimum Twenty-Year Follow-Up Study. *The Journal of Bone and Joint Surgery*. 2001; 83-A: 1840-1848.

6) Iorio R. Eftekhar NS. Kobayashi S. Grelsamer RP. Cemented Revision of Failed Total Hip Arthroplasty: Survivorship Analysis. *Clinical Orthopaedics and Related Research*. 1995; 316: 121-130.

7) Maloney WJ. Jasty M. Burke DW. O'Connor DO. Zalenski EB. Bragdon C. Harris WH. Biomechanical and Histologic Investigation of Cemented Total Hip Arthroplasties: A Study of Autopsy-Retrieved Femurs After *In Vivo* Cycling. *Clinical Orthopaedics and Related Research*. 1989; 249: 129-140.

8) Jasty M. Maloney WJ. Bragdon CR. O'Connor DO. Haire T. Harris WH. The Initiation of Failure in Cemented Femoral Components of Hip Arthroplasties. *The Journal of Bone and Joint Surgery*. 1991; 73-B: 551-558.

9) Schmalzried TP. Maloney WJ. Jasty M. Kwong LM. Harris WH. Autopsy Studies of the Bone-Cement Interface in Well-Fixed Cemented Total Hip Arthroplasties. *The Journal of Arthroplasty*. 1993; 8: 179-188.

10) Schmalzried TP. Kwong LM. Jasty M. Sedlacek RC. Haire TC. O'Connor DO. Bragdon CR. Kabo JM. Malcolm AJ. Harris WH. The Mechanism of Loosening of Cemented Acetabular Components in Total Hip Arthroplasty: Analysis of Specimens Retrieved at Autopsy. *Clinical Orthopaedics and Related Research*. 1992; 274: 60-78.

11) Jasty M. Goetz DD. Bragdon CR. Lee KR. Hanson AE. Elder JR. Harris WH. Wear of Polyethylene Acetabular Components in Total Hip Arthroplasty: An Analysis of One Hundred and Twenty-Eight Components Retrieved at Autopsy or Revision Operations. *The Journal of Bone and Joint Surgery*. 1997; 79-A: 349-358.

12) An YH. Friedman RJ. Animal Selections in Orthopaedic Research. *Animal Models in Orthopaedic Research*. edited by An YH. Friedman RJ. CRC Press. Boca Raton.

Chapter 3: 1998: 39-57.

13) Anderson GI. Podworny N. Jain R. Kwok AWL. Waddell JP. Hydroxyapatite Application Effect on Micromotion Around Acetabular and Femoral Components in the Dog. *Transactions of Fifth World Biomaterials Congress*. 1996: 176.

14) Bobyn JD. Jacobs JJ. Tanzer M. Urban RM. Aribindi R. Sumner DR. Turner TM. Brooks CE. The Susceptibility of Smooth Implant Surfaces to Periimplant Fibrosis and Migration of Polyethylene Wear Debris. *Clinical Orthopaedics and Related Research*. 1995: 311: 21-39.

15) Bobyn JD. Pilliar RM. Binnington AG. Szivek JA. The Effect of Proximally and Fully Porous-Coated Canine Hip Stem Design on Bone Modeling. *Journal of Orthopaedic Research*. 1987: 5: 393-408.

16) Dowd JE. Schwendeman LJ. Macaulay W. Doyle JS. Shanbhag AS. Wilson S. Herndon JH. Rubash HE. Aseptic Loosening in Uncemented Total Hip Arthroplasty in a Canine Model. *Clinical Orthopaedics and Related Research*. 1995: 319: 106-121.

17) Finkelstein JA. Anderson GI. Waddell JP. Richards RR. Hearn TC. Schemitsh E. A Study of Micromotion and Appositional Bone Growth to a Canine Madreporic-Surfaced Femoral Component. *The Journal of Arthroplasty*. 1994: 9: 317-324.

18) Harvey EJ. Bobyn JD. Stackpool GJ. Tanzer M. Comparative Peri-Implant Femoral Bone Remodeling with Isoelastic and Hypoelastic Noncemented Canine Hip Prostheses. *Transactions of the 43rd Meeting of the Orthopaedic Research Society*. 1997: 307.

19) Maistrelli GL. Mahomed N. Fornasier V. Antonelli L. Li Y. Binnington A. Functional Osseointegration of Hydroxyapatite-Coated Implants in a Weight-Bearing Canine Model. *The Journal of Arthroplasty*. 1993: 8: 549-554.

20) Vanderby Jr R. Manley PA. Kohles SS. McBeath AA. Fixation Stability of Femoral Components in a Canine Hip Replacement Model. *Journal of Orthopaedic Research*. 1992: 10: 300-309.

21) Walenciak MT. Zimmerman MC. Harten RD. Ricci JL. Stamer DT. Biomechanical and Histological Analysis of an HA Coated. Arc Deposited CPTi Canine Hip Prosthesis. *Journal of Biomedical Materials Research*. 1996: 31: 465-474

22) Harris WH. The First 32 Years of Total Hip Arthroplasty: One Surgeon's Perspective. *Clinical Orthopaedics and Related Research*. 1992: 274: 6-11.

23) Montgomery RD. Milton JL. Pernell R. Aberman HM. Total Hip Arthroplasty for Treatment of Canine Hip Dysplasia. *The Veterinary Clinics of North America: Small*

Animal Practice. 1992: 22: 703-719.

24) Lewis RH. Jones Jr JP. A Clinical Study of Canine Total Hip Arthroplasty. *Veterinary Surgery*. 1980: 9: 20-23.

25) Gofton N. Sumner-Smith G. Total Hip Prosthesis for Revision of Unsuccessful Excision Arthroplasty. *Veterinary Surgery*. 1982: 11: 134-139.

26) Olmstead ML. Hohn RB. Turner TM. A five-year study of 221 total hip replacements in the dog. *Journal of the American Veterinary Medical Association*. 1983: 183: 191-194.

27) Parker RB. Bloomberg MS. Bitetto W. Rodkey WG. Canine Total Hip Arthroplasty: A Clinical Review of 20 Cases. *Journal of the American Veterinary Medical Association*. 1984: 20: 97-104.

28) Olmstead ML. Total Hip Replacement in the Dog. *Seminars in Veterinary Medicine and Surgery (Small Animal)*. 1987: 2: 131-140.

29) Paul HA. Bargar WL. A Modified Technique for Canine Total Hip Replacement. *Journal of the American Animal Hospital Association*. 1987: 23: 13-18.

30) Edwards MR. Egger EL. Schwarz PD. Aseptic Loosening of the Femoral Implant after Cemented Total Hip Arthroplasty in Dogs: 11 Cases in 10 Dogs (1991-1995). *Journal of the American Veterinary Medical Association*. 1997: 211: 580-586.

31) Harris WH. Is It Advantageous to Strengthen the Cement-Metal Interface and Use a Collar for Cemented Femoral Components of Total Hip Replacements? *Clinical Orthopaedics and Related Research*. 1992: 285: 67-72.

32) Huiskes R. Verdonschot N. BioMechanics of Artificial Joints: The Hip. *Basic Orthopaedic Biomechanics, 2nd ed.*. edited by Mow VC. Hayes. WC. Lippincott-Raven Publishers. Philadelphia. Chapter 11: 1997: 395-460.

1.4. Tables

Table 1.1		
Survey Years	**TJA / Year in US**	**THA / Year in US**
1985-1988	531.000	204.000
1993-1995	648.000	249.000
2030 (Projected)		359.000

Table 1.1 – Survey data for average number of total joint arthroplasties and total hip arthroplasties performed per year in the United States [2].

1.5. Figures

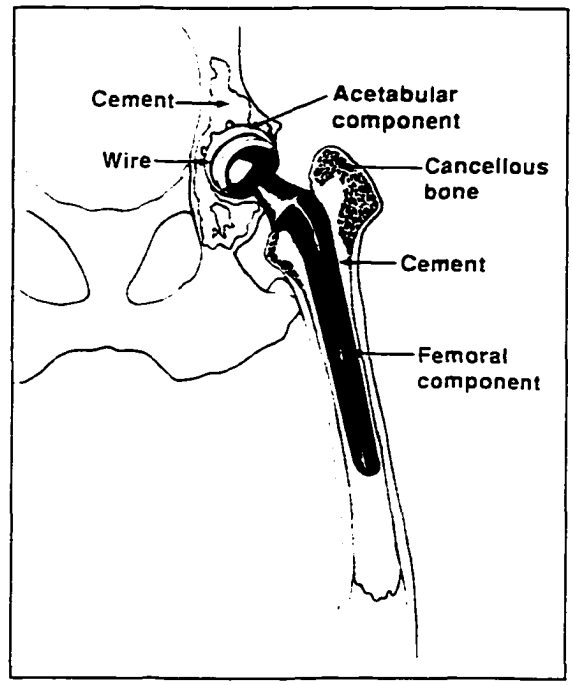

Figure 1.1 – Schematic drawing of radiograph of a canine total hip prosthesis [23]. Copyright W.B. Saunders Company 1992. Used with permission. All rights reserved.

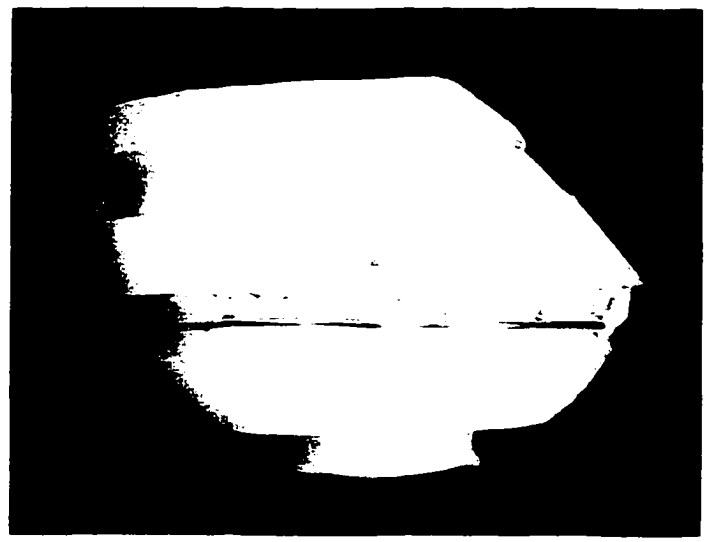

Figure 1.2 – Side view of a BioMedtrix acetabular implant. Note the 45° "fire-hydrant" cut-out in the upper rim.

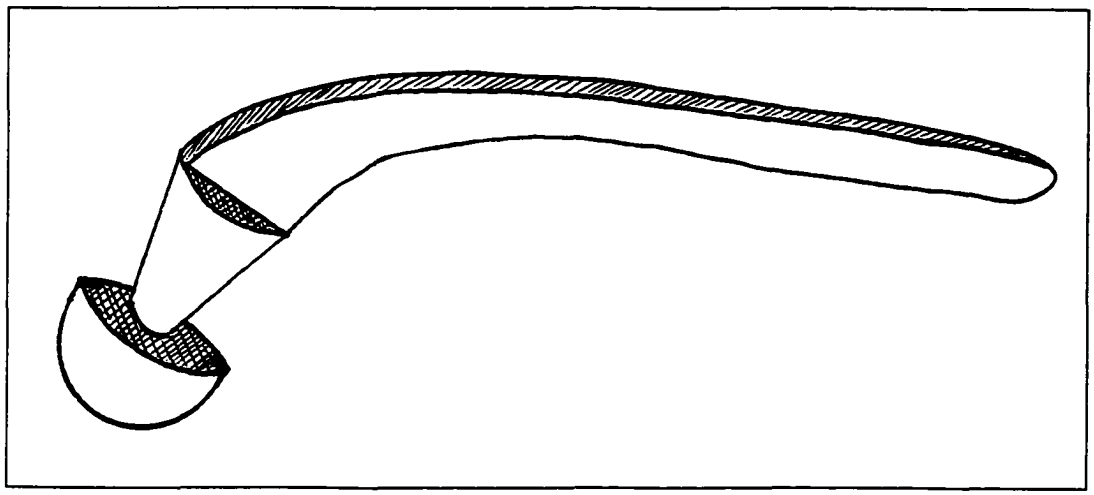

Figure 1.3 – Schematic drawing of a Richards femoral component.

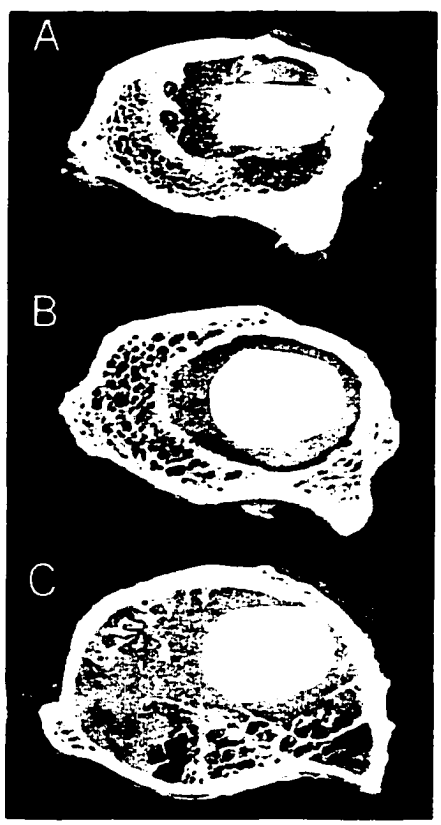

Figure 1.4 – Cross-sectional geometry of proximal end of femoral stem. (A) Richards has rectangular stem with sharp corners. (B) BioMedtrix #1 has a more rounded shape with sharp corners on the lateral aspect. (C) BioMedtrix #2 has a more oval shape.

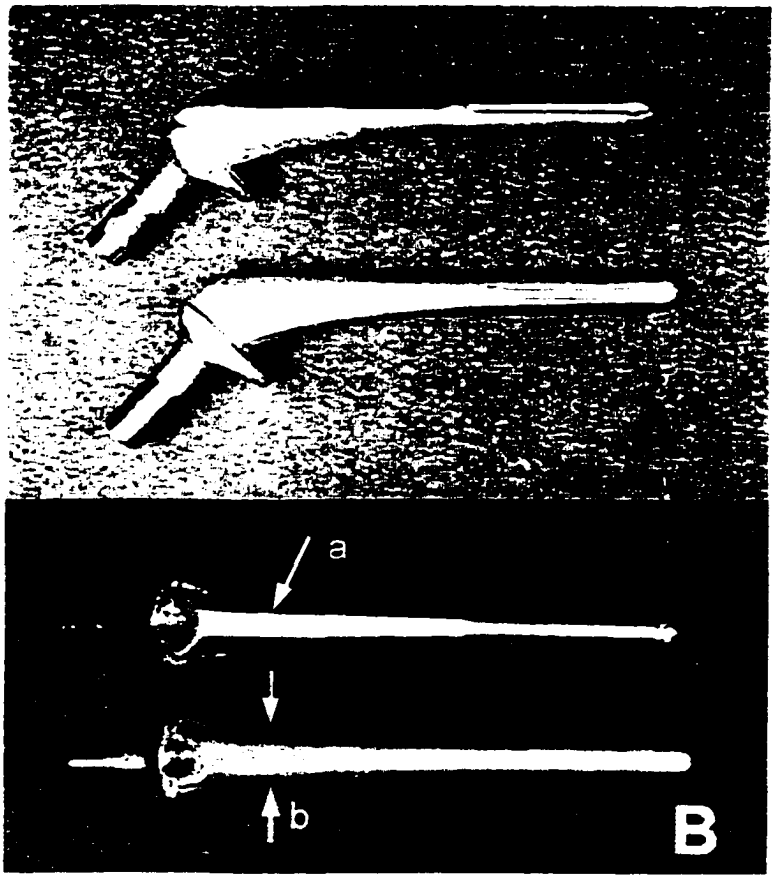

Figure 1.5 – (A) Cranial or caudal view of BioMedtrix #1 (top) and BioMedtrix #2 (bottom) femoral components. Note the sharp corners on the BioMedtrix #1 (See arrow). (B) Lateral view of BioMedtrix #1 (top) and BioMedtrix #2 (bottom) femoral components. Note the sharp corners (a – see arrow) on the BioMedtrix #1. Note the narrower dimensions (b – see arrows) in the cranial-caudal direction of the BioMedtrix #2.

Chapter 2

Owner Assessment of the Outcome of Total Hip Arthroplasty in Dogs

This Chapter, with the exception of the Addendum, was previously published as: [Skurla CT, Egger EL, Schwarz PD, James SP. Owner Assessment of the Outcome of Total Hip Arthroplasty in Dogs. Journal of the American Veterinary Medical Association. 2000; 217: 1010-1012.] Copyright JAVMA 2000. Used with permission. All rights reserved.

2.1. Abstract

Surveys were mailed to owners of 353 dogs that underwent total hip arthroplasty (THA) between 1982 and 1996 to evaluate the owners' perceptions of the outcomes of their dogs' surgery. The response rate was 41%. For owners who responded to the survey, time from surgery to completion of the questionnaire ranged from 6 months to 11 years. Overall, 122 respondents (84.1%) rated results of THA in their dog as excellent or good.

2.2. Introduction

In 1983, Olmstead *et al.* [1] reported on outcome of 216 dogs that underwent total hip arthroplasty (THA) between 1976 and 1981, using a commercially available one-piece,

cemented, cobalt-chromium prosthesis [a]. Follow-up time ranged from 4 weeks to 5 years, and hip joint function, assessed on the basis of "locomotive ability," was graded as excellent in 172 (79.6%) dogs and good in 25 (11.6%). In a later study involving dogs in which THA was performed between 1981 and 1984, using the same prosthesis, [2] Olmstead reported that 139 of 146 dogs (95.2%) had satisfactory function. In 1995, [3] Olmstead reported on outcome of 41 dogs in which THA had been performed, using a modular titanium alloy femoral prosthesis with a cobalt-chromium head [b]. Follow-up time ranged from 2 to 15 months, and owners of 40 of the 41 (98%) dogs reported an improvement in their dogs' quality of life after surgery.

Other authors have also reported outcomes of dogs undergoing THA with cemented prostheses. Gofton and Sumner-Smith [4] reported excellent results for 3 dogs that underwent THA: follow-up time ranged from 8 to 18 months. Lewis and Jones [5] reported that 16 of 20 THA implants were still in place 19 to 34 months after surgery, and that outcome was excellent for 12 (75%) of the 16 and good for 2 (13%). Parker *et al.* [6] reported on outcome of 23 THA performed between 1979 and 1982 in 20 dogs. Follow-up time ranged from 6 months to 4.5 years, and outcome was assessed through clinical evaluation and owner interviews. Results were excellent for 8 THA (35%) and good for 10 (44%). Paul and Bargar [7] evaluated results of 65 THA with a minimum of 6 months of follow-up, and reported that 7 (11%) had complications.

Surgeons at the Colorado State University Veterinary Teaching Hospital have been performing THA in dogs for more than 15 years. Although anecdotal evidence seemed to indicate a high level of owner satisfaction with the outcome of their dogs' surgery, no formal survey had ever been performed at this institution to assess the impact of this

procedure on dogs and their owners. The purpose of the study reported here, therefore, was to evaluate owners' perceptions of the outcomes of dogs that have undergone THA. None of the previous studies discussed above include the current commercially available prosthesis, using a modular femoral component made entirely of cobalt-chromium [b]. The longest follow-up previously reported was 5 years, and this study included longer follow-ups of up to 11 years. This study provided more detailed owner ratings, as described in the results section, than previous studies. However, since this study did not include repeated measures on individual dogs, it is not possible to determine if the surgical outcome deteriorates with time.

2.3. Materials and Methods

A questionnaire (*See Appendix A*) was developed, using validated questionnaires developed for assessing outcome of THA in human patients, [8,9] and mailed to 353 owners of dogs that had undergone unilateral or bilateral THA at the veterinary teaching hospital between 1982 and 1996. Owners were asked to complete and return the survey in a postage-paid envelope. Additional written comments were encouraged. Owners of dogs that had undergone bilateral THA were asked to report separately on each side. Owners were asked if their dogs were currently alive or dead and, if their dogs were dead, when and how their dogs had died.

Responses were tabulated. To demonstrate the level of non-response bias, age and weight of the dogs at the time of surgery were compared between respondents and non-respondents, using a t-test for samples with unequal variances.

Three prostheses have been used for THA at the Veterinary Teaching Hospital. The

first consisted of an ultrahigh molecular weight polyethylene acetabular cup matched with a one-piece cobalt-chromium alloy femoral prosthesis [a]. The second consisted of an ultrahigh molecular weight polyethylene acetabular cup and a modular femoral prosthesis that consisted of a titanium alloy femoral stem with a rounded distal tip and a cobalt-chromium femoral head [b]. The third was similar to the second but had a slightly different geometry and was made entirely of cobalt-chromium [b].

2.4. Results

One hundred forty-five responses were returned for a 41% response rate. Ninety-nine (68.2%) respondents reported that their dogs were still alive at the time of the survey. Age and weight of the dogs at the time of THA were not significantly different ($P > 0.02$) between respondents and non-respondents.

Owners reported that 70 of the 145 dogs were receiving pain medication daily (n = 40; 27.6%) or several times a week (30; 20.7%) prior to surgery. An additional 17 dogs (11.7%) were receiving pain medication infrequently and 55 (37.9%) were not receiving any pain medication prior to surgery (owners of 3 dogs did not respond). By comparison, only 26 dogs were receiving pain medication daily (19; 13.1%) or several times a week (7; 4.8%) after surgery. Twenty-three (15.9%) were receiving pain medication infrequently, and 84 (57.9%) were not receiving any pain medication (owners of 12 dogs did not respond). Owners of 98 dogs (67.6%) indicated that surgery completely relieved their dogs' pain, and 33 (22.8%) indicated that surgery appeared to decrease the amount of pain. Only 3 (2.1%) indicated that surgery did not decrease the amount of pain; whereas, 9 (6.2%) indicated that their dogs were not in pain prior to surgery, and 2 did

not respond. One hundred three owners (71%) reported that THA substantially increased their dogs' function, and 31 (21.4%) indicated that THA increased their dogs' function somewhat. Only 5 (3.4%) indicated that their dogs' function was unchanged after surgery, and 3 (2.1%) indicated that their dogs' function was worse (3 owners did not respond). Overall, 106 owners (73.1%) rated results of the procedure as excellent, 16 (11%) rated it as good, 8 (5.5%) rated it as fair, and 9 (6.2%) rated it as poor (6 owners did not respond).

When asked if the expense of the surgery was justifiable, given the outcome, 92.5% of owners gave a positive answer (definitely yes, 120 [82.8%]; probably yes, 14 [9.7%]), and only 10 indicated that the expense was probably not (4; 2.8%) or definitely not (6; 4.1%) justifiable (1 did not respond). Asked if they would make the same decision to have the surgery for their dogs again, 93.1% of the owners answered in the affirmative (definitely yes, 126 [86.9%]; probably yes, 9 [6.2%]) and only 7 indicated that they probably (4; 2.8%) or definitely (3; 2.1%) would not (3 did not respond).

Fifty owners (34.5%) indicated that their dogs' quality of life was more improved after surgery than they had thought possible, 69 (47.6%) reported a great improvement, 13 (9%) reported a moderate improvement, and 4 (2.8%) reported a slight improvement. Only 2 (1.4%) reported no improvement in their dogs' quality of life, and 1 (0.7%) reported a worsening (6 did not respond). Eighty owners (55.2%) reported that, compared with the period prior to THA, their dogs' health was better, 36 (24.8%) reported that their dogs' health was the same, and 9 (6.2%) reported that their dogs' health was worse (20 did not respond).

Seventy-four owners (51%) reported that their dogs could now run at will without

restrictions, and 14 (9.7%) reported that their dogs could run for half a day without causing discomfort. However, 9 (6.2%) reported that an hour of running caused apparent discomfort, 12 (8.3%) reported that less than 30 minutes of running caused apparent discomfort, and 14 (9.7%) reported that their dogs could not run without causing apparent discomfort (22 owners did not respond). Ninety-five owners (65.5%) reported that their dogs could now walk at will without restrictions, and 10 (6.9%) reported that their dogs could walk for half a day without causing discomfort. However, 11 (7.6%) reported that an hour of walking caused apparent discomfort, 11 (7.6%) reported that less than 30 minutes of walking caused apparent discomfort, and 5 (3.4%) reported that their dogs could not walk without causing apparent discomfort (13 owners did not respond).

The 88 postsurgical "no responses" (i.e., excluding the question regarding pain before THA) were investigated, and owners of 23 (50%) of the 46 dogs that were no longer alive accounted for 50 (56.8%) of the "no responses." A small percentage (18; 18.8%) of owners of THA dogs that were still alive accounted for 38 (43.2%) of the "no response" answers. Some written comments indicated that owners thought that none of the answers applied to them. The remaining owners of 104 THA dogs answered each postsurgical question.

Time from initial surgery to death, revision surgery, or survey response ranged from 6 months to 11 years. Some owners of dogs with the longest term follow-up wrote comments that led us to believe that dogs had done well during the first few years after surgery, but that their condition had seemed to deteriorate in recent years. Several owners of dogs that underwent unilateral THA indicated that they thought their dogs would have done better in old age if they had undergone bilateral surgery. Many

commented on other health problems, unrelated to THA, that made answering the questions more difficult. Two owners indicated that they wished they had had more information about the recovery period after THA.

2.5. Discussion

Results of the present study suggest that owners are generally satisfied with the results of THA in their dogs, that they believe the expense of surgery is justifiable, given the outcome, and that they believe THA had a positive effect on their dogs' health and well-being. The 41% response rate is high for a mailed survey [10] and ages and weights of dogs at the time of surgery were not significantly different between respondents and non-respondents; however, results must still be interpreted with some caution, as there may have been some degree of non-response bias. In addition, the survey included dogs that underwent THA during a 14-year period. A variety of prostheses were used, surgeries were performed by a number of surgeons, and surgical techniques likely improved with time. We did not attempt to correlate results of the survey with date of surgery or prosthesis type, and we recommend that future studies be designed to examine these factors and others that may be associated with outcome.

Owner surveys necessarily provide subjective results, but results of the present study seem to compare favorably with results of previous studies in which follow-up evaluation included clinical examination. The present study, however, involved more detailed owner ratings and a longer follow-up time, ranging from 6 months to 11 years. In addition, results of a single individual [1-3] dominated the previous studies, and the present study provides results for a separate large population (141 dogs) that underwent

surgery at a different institution with different surgeons and different implants. Since the results of this study agree with previous studies, these results can be generalized to the overall population of surgeons using the same prostheses and prescribed surgical techniques.

We suggest that in the future, a tracking system similar to that used for human patients undergoing THA be established for dogs undergoing THA. This would involve administration of a similar survey prior to and at various set times after (e.g., 6 months and 1, 2, and 5 years) surgery, so that a dog's condition before THA could be compared with its condition after. This would also allow investigators to determine whether outcome deteriorates over time.

Dog owners faced with making a decision about whether to have this surgery for their dogs may benefit from information provided by owners who previously faced this decision. This is an expensive surgery that requires close supervision during the recovery period, and some owners may be discouraged by the expense and time commitment during the postoperative period. Results of surveys of owners who have gone through this procedure with their dogs may be a useful educational tool for owners faced with making a decision about whether to agree to THA for their dogs.

[a] Richards Canine II Hip Prosthesis, Smith & Nephew Richards Inc., Memphis, TN

[b] Modular Canine Total Hip Replacement System, BioMedtrix, Allendale, NJ

2.6. References

1) Olmstead ML, Hohn RB, Turner TM. A Five-Year Study of 221 Total Hip Replacements in the Dog. *Journal of the American Veterinary Medical Association,*

1983: 183: 191–194.

2) Olmstead ML. Total Hip Replacement in the Dog. *Seminars in Veterinary Medicine and Surgery (Small Animal)*. 1987: 2: 131–140.

3) Olmstead ML. The Canine Cemented Modular Total Hip Prosthesis. *Journal of the American Animal Hospital Association*. 1995: 31: 109-124.

4) Gofton N. Sumner-Smith G. Total Hip Prosthesis for Revision of Unsuccessful Excision Arthroplasty. *Veterinary Surgery*. 1982: 11: 134–139.

5) Lewis RH. Jones Jr JP. A Clinical Study of Canine Total Hip Arthroplasty. *Veterinary Surgery*. 1980: 9: 20–23.

6) Parker RB. Bloomberg MS. Bitetto W. *et al.*. Canine Total Hip Arthroplasty: A Clinical Review of 20 Cases. *Journal of the American Veterinary Medical Association*. 1984: 20: 97–104.

7) Paul HA. Bargar WL. A Modified Technique for Canine Total Hip Replacement. *Journal of the American Animal Hospital Association*. 1987: 23: 13–18.

8) Johanson NA. Charlson ME. Szatrowski TP. *et al.*. A Self-Administered Hip-Rating Questionnaire for the Assessment of Outcome After Total Hip Replacement. *The Journal of Bone and Joint Surgery*. 1992: 74-A: 587–597.

9) Katz JN. Phillips CB. Poss R. *et al.*. The Validity and Reliability of a Total Hip Arthroplasty Outcome Evaluation Questionnaire. *The Journal of Bone and Joint Surgery*. 1995: 77-A: 1528–1534.

10) Buttle F. Thomas G. Questionnaire Color and Mail Survey Response Rate. *Journal of the Market Research Society*. 1997: 39(4): 625–627.

2.7. Addendum

This survey served a dual purpose with regard to this dissertation. The first purpose was for outcome assessment, as described above. The second purpose (*See Appendix A – questions 15 & 17*) was as a recruitment tool for donations to the Colorado State University Orthopaedic Implant Retrieval Program (CSU OIRP). At the end of the survey, owners were asked if their dogs were still alive. If the dogs were still alive,

owners were asked whether they might consider donation of their dogs' hemepelves and femora at the time of their dogs' death. Of those 99 (68.3%) respondents whose dogs were still alive at the time of the survey, 79 (79.7%) expressed interest in the donation program and were subsequently sent instructions for donation.

Free euthanasia and cremation services were offered for those owners who could bring their dogs to the CSU Veterinary Teaching Hospital (VTH). For those owners unable to bring their dogs to the CSU VTH, provisions were made with their local veterinarians to assist in the collection of the remains. If the owner lived in Colorado, the local veterinarian was asked to store the dog's remains until they could be picked up and transported to the CSU VTH. If the owner lived outside of Colorado, the local veterinarian's assistance was sought for coordinating the shipment of the dog's remains to the CSU VTH. In those cases, free shipment was offered to the owner. In all cases, free cremation services were offered to the owners.

This was the only major donor recruitment tool used for the present study. In addition, owners who brought their dogs into the CSU VTH for THA or follow-up visits were informed of the OIRP and provided with a donor information packet if they expressed interest in the program.

Chapter 3

Postmortem Retrieval Analysis of the Femoral Component in Clinical Total Hip Arthroplasty in Dogs

3.1. Introduction

3.1.1. Human Total Hip Arthroplasty

Despite many improvements in prosthetic design and surgical technique since the advent of total hip arthroplasty (THA) surgery in humans, the failure rate due to aseptic loosening remains high. Mulroy *et al.* [1], in survivorship analysis of cemented THA, defined two levels of failure for femoral components: aseptic loosening requiring revision surgery, and asymptomatic femoral components showing radiographic evidence of loosening. Aseptic loosening of the femoral component resulted in revision surgery in 2% of cases at 15 years follow-up. Of those patients surviving at 15 years follow-up with the original femoral component in place, an additional 7% showed radiographic evidence of loosening (i.e., debonding of the polymethyl methacrylate (PMMA)/metal interface; less than 1 mm cement mantle at one or more points). Thus 9% of femoral components showed evidence of aseptic loosening at 15 years after primary THA surgery. Klapach *et al.* [2], reporting on survivorship analysis at another center, found aseptic loosening of the femoral component resulting in revision surgery in 3% of cases at 15 years follow-up

and in 8% of cases at 20 years follow-up. An additional 3% of cases showed radiographic evidence of loosening for a total of 6% of femoral components showing evidence of aseptic loosening at 15 years follow-up. At 20 years follow-up. an additional 8% of cases showed radiographic evidence of loosening for a total 16% of femoral components showing evidence of aseptic loosening.

Iorio *et al.* [3] performed follow-up studies of cemented THA after revision surgery and found radiographic evidence of loosening of the revised femoral component in 1% of cases at 5 years and 33% of cases at 10 years. Since the 33% aseptic loosening rate 10 years after revision surgery [3] is greater than the 9% aseptic loosening rate 15 years after primary surgery [1]. it is vital for the biomedical research community to work towards improving the longevity of the primary THA and avoiding revision surgery.

Autopsy retrieval studies of human THA implants that were considered to be functioning well at the time of the patients' death provided the knowledge that the initiating failure event for cemented femoral components was mechanical in nature [4-6]. Debonding of the PMMA/metal interface and fractures in the cement mantle were commonly found in firmly implanted femoral implants. The debonding process began proximally and distally and progressed toward the middle of the femoral stem. Radial fractures in the bone cement. not visible on clinical radiographs. were commonly seen with the initiating point at sharp corners on the femoral component. These fractures were most commonly seen in areas where the cement mantle was thin or in association with voids in the cement. Fractures were rarely seen in cement mantles thicker than 2 mm. Fractures were rarely seen to initiate from the bone/PMMA interface. Schmalzried *et al.*, [6] reported that femoral components with no evidence of radiographic loosening moved

less than 100 μm under physiologic loading conditions. The actual raw data, published in these studies, will be compared to the results from this study and discussed in greater detail in the discussion section of this chapter.

Ebramzadeh, *et al.*, [7] correlated radiographic analysis with survival analysis on 836 clinical cases of cemented THA in humans. Femoral components with proximal medial cement mantle thickness ranging from 2-5 mm had a more successful outcome than those with either thinner or thicker cement mantles. Those femoral components at greatest risk for aseptic loosening were:

1. Those with proximal medial cement thicknesses greater than 10 mm;
2. Those with more than 5 mm of proximal medial cancellous bone;
3. Those that filled less than half of the medullary canal;
4. Those that were implanted in more than 5 degrees varus.

In a finite element analysis (FEA) study by Ramaniraka, *et al.* [8], similar findings with regard to cement mantle thickness were found. Shear stress at the proximal end and distal tip of the femoral component and micromotion increased when the cement mantle was 2 mm thick. The optimal cement mantle thickness was found to be 3-5 mm.

In a review of THA biomechanics, Huiskes and Verdonschot [9] describe stress transfer in a composite structure and state that stress patterns depend on the bonding characteristics at the interfaces and the relative magnitudes of the elastic moduli. The part with the greatest stiffness will carry more of the load. The elastic moduli [9] of the most common THA materials and of bone are:

1. Cobalt-chromium (Co-Cr) alloy = 200-220 GPa;
2. Titanium (Ti-6Al-4V) alloy = 100-130 GPa;

3. PMMA = 2-3 GPa;

4. Cortical bone = 15-20 GPa;

5. Cancellous bone = 500-1500 MPa.

Thus, since the metallic femoral components have the highest elastic moduli, they will carry more of the load. The load that is normally carried by the bone is carried by the femoral implant and the bone, causing stress shielding of the bone which in turn leads to disuse osteoporosis after THA [9].

Stresses in a composite structure cannot be assumed to be uniform and cannot be determined by dividing the load to be transferred by the area available for load transfer [9]. Peak values of stress occur, depending on the material characteristics and the geometry of the structure. Stresses increase in structures that have features such as notches, sharp corners, and holes. Such features are described as stress concentrators.

In addition, stresses in a composite may be generated indirectly due to variations in the amount of deformation that each component undergoes as a result of the different moduli [9]. If, at the interface, one material expands or deforms more laterally than the other, shear forces developed at the interface resist the expansion. The ultimate strengths of the interfaces, tested in shear, are 5-8 MPa at the metal/PMMA interface and 2-4 MPa at the bone/PMMA interface [9]. There are also significant increases in PMMA stresses when the PMMA/metal bond changes from bonded to debonded and frictionless. This leads to progressive damage to the PMMA after debonding at the interface.

Huiskes and Verdonschot [9] also describe the load transfer between the femoral stem and the PMMA as being realized by shear stresses at the interface. The same can be said of the bone/PMMA interface. There are three regions of load transfer in a femoral

component: proximal, middle, and distal. There are stress concentrations at the proximal and distal ends. The distal and proximal regions are load transfer regions, and the middle region is an area of load sharing. The stress is concentrated at the proximal and distal ends. If the percentage of the load carried by the middle portion is increased, the proximal load transfer decreases while the distal load transfer increases. If the percentage of the load carried by the middle portion is decreased, the proximal load transfer increases while the distal load transfer decreases. Thus a stiffer femoral stem increases distal interface stresses. Also, peak interface stresses at the proximal and distal ends do not necessarily decrease when the stem is lengthened. However, if the stem is shortened to the point that the middle portion disappears, interface stresses will increase in the distal and proximal regions. The concentration of shear stresses at the proximal and distal load transfer regions help explain why the human autopsy retrieval studies [4-6] found the first evidence of debonding of the PMMA/metal interface at the proximal and distal ends of the femoral stem.

3.1.2. Differences Between Canine and Human

3.1.2.1. Femoral Morphology

There are a number of interspecies differences in the morphology of the femur that need to be taken into account in the context of comparing THA performance in the dog to that in the human. The angle between the femoral shaft and the femoral neck is approximately 5° greater in the dog than in the human (136.7° vs. 131.5°) as is the anteversion angle of the femoral head and neck (14.9° vs. 10.0°) [10]. The length of the femoral neck relative to the length of the femur is much shorter in the dog than in the human [10-12]. Human femora exhibit age-related changes, particularly in the female

[10-11]. The anteversion angle of the femoral head and neck and the angle between the long axis of the femur and the femoral neck are reported to decrease with age in the human, but age-related changes have not been observed in canine femora. The lack of age-related changes in canine bone has serious implications in the analysis of data and the drawing of conclusions from studies using the dog to model the response of bone in elderly humans to THA designs and materials.

There is a difference in the curvature between human and canine femora [10-11]. The maximum anterior bow in the human femur is located near the middle of the femoral shaft. With the length of the femoral shaft measured from the condyles to the greater trochanter, the maximum anterior bow is located at 45% of the femoral shaft length distal to the greater trochanter. The maximum cranial (anterior) bow in the canine femur, by contrast, is located at 65% of the femoral shaft length distal to the greater trochanter. As a result, the proximal portion of the bone into which a femoral component would be implanted is straighter in the canine femur than in the human femur. In addition, the canine femur is bowed to a greater degree than the human femur [11].

There are differences in cross-sectional geometry with the canine femur having thinner cortical bone and a larger medullary canal relative to the length of the femoral shaft [12]. In addition, the canine femur flares more proximally than the human femur. Since the cortical area remains constant, the cortex becomes markedly thinner in the canine proximal femur than in the human femur.

Another difference noted between studies performed by Bloebaum *et al.* [11] on greyhound femora and that performed by Sumner *et al.* [12] on adult mongrel femora was that there are morphological differences in femora among breeds of dogs.

3.1.2.2. Hip Joint Loading

There are obvious interspecies differences in the loading and weight bearing of the hips since humans are bipeds and dogs are quadrupeds. One important difference is that dogs carry most of their weight, between 53% and 65%, on their front legs [13].

Page *et al.* [13] determined the magnitude and direction of the peak joint reaction force (JRF) for the dog during a walking gait cycle using instrumented femoral components implanted in dogs. The peak JRF was measured in three-legged stance (i.e., when the opposite hind leg was off the ground). To orient the JRF, Davy *et al.* [14] defined a coordinate system whereby the z-axis lies on the shaft of the femoral neck (*See Figure 3.1*). The x-axis is perpendicular to the neck and is directed laterally and dorsally. The y-axis is directed cranially on the right femoral component (*As shown in Figure 3.1*) and caudally on the left femoral component. All figures following refer to the right femoral component. The cone angle, θ, is the angle between the JRF and the z-axis. The polar angle, ϕ, is the angle between the projection of the JRF onto the x-y plane and the x-axis. The peak JRF in the dog was measured as 1.50-1.65 times body weight (BW) at $\theta = 28°$ and $\phi = 20°$ [14, 15]. This means that the peak JRF is directed caudally (posteriorly), ventrally (inferiorly), and laterally on the head of the femur. This contrasts with the peak JRF in the human, which is estimated at 2.40-5.00 times BW with $\theta = 30°$ and $\phi = 15°$ [14]. The human peak JRF is also directed posteriorly, inferiorly, and laterally; however, the major difference between species are that the magnitude of the human JRF is considerably greater and ϕ is 5° less in the human.

As a result of the peak JRF in dogs, a torsional moment about the shaft was calculated at 1.6 N-m [13]. Canine knees are flexed more in three-legged stance than

human knees are in single-legged stance. both during walking gait. The canine femur is 20° off vertical.

Dogs can make subtle adjustments in their gait and do not consistently load their hip joints between gait cycles. Dogs display wide variation in their walking gait cycles. and they also walk with sideways torso movement (i.e.. crab walking) [16]. There are also considerable differences in joint angles among different breeds of dogs.

Despite the differences in gait loading between humans and dogs. measurements to determine the magnitude and direction of the principle strain in canine and human femora have found the direction is similar in both species (i.e.. within 15-20 degrees off the long axis of the femur). but the magnitude of the strain in the canine femur is much less than that in the human femur [17-18].

3.1.3. Canine Total Hip Arthroplasty

While not as common as the human procedure. clinical cemented THAs are performed in dogs for much the same reasons as in humans. Acceptable success rates were not attained until the Richards Canine II total hip prosthesis was introduced in 1974 [19]. In a review of seven retrospective studies [20-26]. (*See Table 3.1*). aseptic loosening of the femoral component requiring revision surgery was reported in 19 (3.0%) of 625 THA cases. To the best of the author's knowledge. there have been no studies that provide follow-up data on canine femoral components that display radiographic evidence of loosening in clinical cases.

While it is unknown how many THAs are performed in dogs in the United States. approximately one to two THAs per week are performed at the Colorado State University Veterinary Teaching Hospital (CSU VTH). This procedure has been performed at the

CSU VTH for over 20 years. The surgical paradigm in existence at the CSU VTH at the beginning of this study held that dogs with bilateral degenerative joint disease (DJD) could be treated adequately with unilateral THA. Feedback from veterinary orthopaedic surgeons and owners indicated that dogs with bilateral DJD and unilateral THA would adjust their gait after surgery and carry more weight on their implanted hip than on their intact, diseased hip.

3.1.3.1. Canine THA Implant Designs

The cemented THA implant used in dogs is very similar to human implants. There have been three implant designs used at the CSU VTH, and they are described in Section 1.1.3.1 of Chapter 1.

3.1.3.2. Analysis of Clinical Radiographs

Edwards *et al.* [26] studied radiographs obtained after the primary THA in 152 cases over a 4-year period using the BioMedtrix #1 design. In only 37 (24.3%) cases was the distal tip of the femoral component well centered within the medullary canal. The remaining 115 (75.6%) distal tips were in contact with the endosteal surface. Eleven cases (7.2%) were diagnosed with aseptic loosening of the femoral implant requiring revision surgery. In all eleven of the revision cases, the distal tip of the femoral component was in contact with the endosteal surface and an asymmetric periosteal reaction was apparent in the region adjacent to the endosteal contact. All eleven of the revised implants were loose at the PMMA/metal interface at revision surgery and displayed polishing of the femoral stem caused by rotation of the femoral stem within the cement mantle. When 194 cases of THA using the Richards implant were reviewed, no cases of aseptic loosening were identified radiographically despite the fact that endosteal

contact by the distal tip was apparent in many cases. Improper positioning of the implant and prosthesis design were offered as possible contributing factors to aseptic loosening.

3.1.3.3. Postmortem Retrieval Analysis of Canine THA

Prior to this dissertation research, there had been no postmortem retrieval studies performed on clinical canine THAs. Since only experimental studies of relatively short duration in healthy dogs using cementless implants [27-35] had been performed before this, the long-term performance of clinical THA in dogs was unknown except through retrospective studies of clinical cases performed using office visits and subjective owner responses to phone surveys [20-26]. The survey study performed at CSU [36] (*See Chapter 2*) indicated a very high positive response from owners, but engineering analysis on clinical canine THA had not been published. Since human postmortem retrieval studies [4-6] had provided invaluable information with regard to the initiating failure events of human THA, it was hoped that similarly valuable information could be found about canine THA in order to determine how well these implants were performing and whether improvements to implant design and surgical technique should be made.

3.1.3.4. Mechanical Testing for Femoral Implant Stability

In order to compare the clinical canine THA findings of this study to similar studies in humans, human retrieval studies from the literature must be chosen carefully. These studies must be on human implants made from similar materials, implanted using similar attachment methods, and measured using similar methods used for this study. Unfortunately, studies of this nature are difficult to find. Three studies [4-6] describe testing performed on 16 (or a subset thereof) human femoral component that were retrieved at autopsy. Femoral components were acutely implanted in contralateral intact

femora to serve as firm controls. The firm controls were tested to verify that no damage was done to the clinical specimens during mechanical testing. Loose controls were not created and tested. The testing was not performed to assess stability of the bone/PMMA and PMMA/metal interfaces. Testing similar to that performed as subsidence and medial-lateral (ML) translational testing between the bone and metal in this dissertation study (described below) was performed in addition to purely rotational loading on the femoral head, the method used to assess femoral component stability during human revision surgery. The greatest micromotion was measured using the purely rotational loading on the femoral head. The investigators did not provide criteria to determine loose from firmly implanted femoral components. However, four specimens were osteoporotic in appearance and exhibited peak rotational micromotion of 88 μm or more.

3.2. Hypotheses

There were three hypotheses in this portion of the study. The first was that the initiating failure event for canine femoral components would be similar to that observed in human THA. Mechanical debonding of the PMMA from the metal implant was expected to be found as the initiating event. The second hypothesis was that the incidence of aseptic loosening of the femoral component (i.e., the percentage of postmortem retrievals that were considered to be loose based on mechanical testing) would not be as high in dogs as in humans due to lower peak joint forces in dogs. The third hypothesis was that unilateral components would perform similarly to bilateral implants. Thus, dogs only need to be subjected to one surgery rather than two in order to treat bilateral hip dysplasia in their dogs.

3.3. Methods

3.3.1. Preliminary Processing

Thirty-eight implants with hemipelves and femora were donated by owners at the time of their dogs' death, whether by natural causes or euthanasia. There were 29 dogs, 9 with bilateral THA, for a total of 18 bilateral and 20 unilateral implants (*See Table 3.2*). Approval from the institutional animal use and care committee was not required for this study since the animals were donated to the CSU VTH after their deaths. Owners signed a standard donation form.

Demographic data (e.g., weight, surgeon, surgery date) were collected from the clinical charts. Clinical radiographs, if available, were collected.

Specimens were stored in a freezer at -20°C until testing began. After removal of soft tissue, the femora were photographed for journalistic purposes. High contrast, contact radiographs in cranial-caudal (CC) and medial-lateral (ML) views were made using Kodak Xomat LS 8x10 Industrial Film (Eastman Kodak Company, Rochester, NY) in a Faxitron Cabinet X-Ray System (Model 43855A, Faxitron X-Ray Corporation, Wheeling, IL) (*See Figure 3.2*).

3.3.2. Mechanical Testing to Assess Implant Stability

In order to facilitate comparison of canine data with previously published human data, an existing methodology for measuring stability of the femoral component was adapted from human postmortem retrieval studies [4, 37-38]. If the femoral implant, upon manual manipulation, moved either ±3 mm in subsidence (i.e., movement of the implant down the axial length of the femur) or ±10° in ML translation, the implant was classified as "grossly loose" and was not tested. The intent of this test method was to be

non-destructive in order to allow for further analysis after the mechanical testing. The intent of this test was not to measure strain at the interfaces but rather to classify the femoral component as loose or firmly implanted at the two interfaces.

Relative motion was measured between the bone and PMMA as well as between the bone and the prosthesis. This resulted in a measurement of the stability of the bone/PMMA and of the PMMA/metal interfaces. A special jig (*See Figure 3.3*) was developed to hold the femur in the correct position on the MTS biaxial mechanical testing system (MTS Corporation. Eden Prairie. MN) so that the load would be applied to the head of the femur in the direction of the peak JRF (*See Section 3.1.2.2. above*) as determined by Page *et al.* [13]. Since the load cell on the MTS was on the bottom. the femur was mounted upside down so that the femoral head was toward the load cell.

3.3.2.1. Calibration of the Relative Motion Device

A relative motion device (RMD) as described by O'Connor *et al.* [38] was used (*See Figure 3.4*). The detailed methodology for the procedure is listed in Appendix B. Briefly. a jig was developed for calibration. Part 1 of the RMD (RMD "t") was mounted (*See Figures 3.4 & 3.5*) to the aluminum component. which acted as the bone. A piece of Teflon™ acted as the implant against which the pin of the RMD rested. Part 2 of the device threaded onto Part 1 so that the head of the pin and the rim of Part 2 were level. An extensometer (10 mm gage length. MTS. Eden Prairie. MN) was mounted with one blade on the head of the pin and the other blade on Part 2. A 2-inch micrometer was used as an actuator to move the Teflon™ under the aluminum in 13 μm (0.0005 inch) increments. Extensometer readings were taken after each time the actuator was advanced. Approximately 20 readings were taken for each curve.

Ninety-five percent confidence intervals were calculated on calibration curves for each of three RMD "t"s (*See Appendix B for sample calibration curves*). A correction factor for each RMD "t" was calculated so that the extensometer measurement could be converted to the distance traveled by the tip of the RMD pin. To calculate motion at the tip of the pin, the extensometer reading was divided by the correction factor. The 95% prediction confidence limits for the calibration curves had a range of 24 μm (±12 μm).

3.3.2.2. Mechanical Testing Method

From the contact radiographs, thickness of the bone and bone cement (in ML view) as well as placement of the implant within the femur (in CC view) were measured in order to determine placement of a 6.4 mm (0.25 inch) diameter hole to be drilled through the bone. The hole was placed on the cranial side of the femur at least 1 cm distal to the lower edge of the implant collar in the widest part of the femur and implant. The RMD "t" was cemented to the bone after the hole was drilled through the bone to the PMMA. The test was performed in the widest, flattest part of the femur in order to ensure a good bond between the bone and the epoxy used to glue the RMD "t" into position. The RMD worked very well in studies of human THA, but human femora are considerably larger than canine femora. Due to the small radius of curvature of the femur at the distal end of the femoral component, it was very difficult to attain a good bond between the bone and the RMD "t" at that level. The distal end of the femoral component was the desired location for relative motion measurements, but the proximal end of the femur provided the best location for gluing the RMD "t" firmly into position long enough to complete the test. The canine femora were extremely fatty, and great care had to be taken to ensure a good bond between the bone and the RMD "t." After drilling the hole in the femur, the

surface of the bone had to be roughened with sandpaper and then swabbed with alcohol and then with ether in order to defat the bone.

Part 2 of the device threaded onto Part 1. The RMD pin was placed through the hole in the bone with the pointed end of the pin in contact with the PMMA. An extensometer measured movement between the head of the pin and Part 2 of the RMD when a force was applied to the head of the femoral component. When the extensometer blades were placed perpendicular to the long axis of the femur (*See Figure 3.4*), the measurements reflected subsidence of the implant within the femur. When the extensometer blades were placed parallel to the long axis of the femur, the measurements reflected ML translation of the implant within the femur. Two tests, one for subsidence and one for ML translation, were performed to measure relative motion at the bone/PMMA interface. Next the hole was extended through the PMMA to the metal implant. The procedure was repeated to measure the motion of the prosthesis relative to the bone in subsidence and ML translation. The order of the tests (subsidence first or ML translation first) at each interface were randomized.

In human retrieval studies by Schmalzried *et al.* [6], human femora were tested for implant stability using a peak load of 2.5 times BW on a 45.4 kg (100 lbs) person regardless of the body weight of the donor. One modification required for the canine retrieval study was that the peak load needed to be normalized to the actual weight of the dog. The retrievals were taken from dogs ranging in size from 18.1 kg (40 lbs) to 66.2 kg (146 lbs), and it would have been inappropriate to select one peak load due to the wide range in sizes of the femora. Peak loading in three-legged stance in the canine hip is calculated at 1.5 to 1.65 times BW [13, 15]. Since the intent of this test was to be non-

destructive. the peak load was normalized to the dog's BW. A peak load of 75% of 1.5 times BW was selected. This peak load was divided by five to provide a loading sequence that started with a 9 N (2 lbf) pre-load and ramped in increments to the peak load before returning to zero (*See Appendix C for detailed methodology*). Each incremental load was ramped up for 5 seconds. and each load increment was held for 10 seconds. The stepped loading was meant to allow for viscoelastic deformation of the composite construct of bone. PMMA. and implant and to prevent brittle failure of the construct. Data was acquired every 0.25 second. Data collected included. extensometer displacement. crosshead displacement. force. and time. The test was repeated four times for each test condition: the order of testing at each interface (i.e., subsidence first or ML translation first) was randomized. The bone/PMMA micromotion measurement was subtracted from the bone/metal micromotion measurement in order to calculate the relative motion between the PMMA and metal. The maximum micromotion achieved at the peak load during the each of the four test conditions was used to categorize the implant as loose or firmly implanted.

Schmalzried *et al.* [6] considered the human implant to be well-fixed if the motion relative to the bone was less than 100 μm. Since human femora are so much larger than canine femora. this criterion needed to be adjusted downward. Control femora were created to determine the criteria for classification of "loose" vs. "firm." Canine femora were harvested from cadavers. The "firm" control had a femoral component implanted in it by a veterinary orthopaedic surgeon using standard surgical procedure. The "loose" control was prepared in a similar manner. but the metal implant was moved constantly in subsidence while the PMMA cured in order to create a loose PMMA/metal interface.

The control femora were tested using the same method as that used for the retrievals.

Micromotion measurements taken of the firm control were 2 μm in both subsidence and ML translation at the bone/PMMA interface and 10 μm in subsidence and 6 μm in ML translation between the bone and metal. Micromotion measurements taken of the loose control were 10 μm in subsidence and 4 μm in ML translation at the bone/PMMA interface and 57 μm in subsidence and 40 μm in ML translation between the bone and metal. Since the PMMA/metal interface was the only interface that was disrupted in the loose control and since the disruption was in subsidence only, the subsidence measurement at this interface were used as the criteria to classify the femoral component as loose or firmly implanted in both directions at both interfaces. The RMD error (*See Section 3.3.2.1*) was ±12 μm; therefore, 45 μm (i.e., 57 μm minus 12 μm) was determined as the critical value for classifying an implant as loose or firmly implanted. The femoral implants were classified as "loose" if relative motion of greater than or equal to 45 μm was measured in subsidence or ML translation at either interface.

The calculated PMMA/metal relative motion measurements were classified as "loose" if the bone/metal measurement was greater than the bone/PMMA measurement and the bone/metal measurement was greater than 45 μm.

3.3.3. Analysis of Contact Radiographs

The CC and ML contact radiographs of the femora were marked for modified Gruen zones (GZs) [39-40] (*See Figure 3.6*). First, a line was drawn down the long axis of the femur. Next, a line perpendicular to the long-axis line was drawn at the intersection of the collar and the stem of the femoral component. A second line perpendicular to the long axis of the femur was drawn just proximal to the distal tip of the implant so that the

rounded tip of the implant did not fall between the two lines. Two additional perpendicular lines were placed so that the distance between the original two perpendicular lines was divided into thirds. Seven zones were marked on each radiographic view. Zones 1-7 were marked on the CC view, as shown, with the proximal lateral zone labeled zone 1 and the proximal medial zone labeled zone 7. Zones 8-14 were marked on the ML view, as shown, with the proximal cranial zone labeled zone 8 and the proximal caudal side labeled zone 14.

A "Femoral Radiograph Evaluation Form" (*See Appendix D - Grading of Femoral Radiographs*), based on similar forms used in human studies [40], was developed with the assistance of three veterinary orthopaedic surgeons. Radiographic features determined to be most clinically relevant to canine THA by the surgeons were minimum and maximum thickness of the cement mantle in each zone; presence and size of voids, cracks, and radiolucencies; alignment of the implant within the femur (e.g., anteversion, retroversion, or normoversion); and contact of the distal tip of the implant with bone. An orthopaedic veterinary surgeon measured and assessed the radiographs.

3.3.4. Transverse Sectioning of Femoral Components

The CC contact radiographs, marked with modified Gruen zones 1-7 (*See Figure 3.6*) and used previously in the radiographic evaluation, were used to plan the location of the slices (*See Appendix E -Slicing of Femora*). Slices, perpendicular to the long axis of the femur, were planned to facilitate histological and radiographic studies as well as the needs of this study. For each of the three Gruen zones (i.e., 1/7, 2/6, 3/5), two-2 mm thick slices were planned for future radiographic and microscopic analysis (*See Figure 3.7*). A 2 mm slice was taken 3 mm distal to the proximal end of the Gruen zone, and

another was taken 3 mm proximal to the distal end of the Gruen zone. A seventh-2 mm slice was taken 3 mm distal to the distal tip of the femoral implant. The slices from the center of each Gruen zone and from the Gruen zone boundaries were preserved and saved for future histological analysis. Each slice was preserved in 70% ethanol.

Photographs and contact radiographs (*See Figure 3.8*) were made of each set of seven-2 mm thick slices. Since previous human and canine studies [4-6, 26] found a relationship between aseptic loosening and placement of the distal tip of the femoral component, the sixth 2 mm slice (slice taken 3 mm proximal to the distal end of zone 3/5) was considered to be the most clinically relevant slice for digital image analysis, and this was the only slice analyzed in the present study (*See Figures 3.7 & 3.8*).

3.3.5. Digital Image Analysis

Scion Image (Scion Corporation, Frederick, MD, Release Beta 3b), digital image analysis shareware based on NIH Image for Macintosh, was downloaded from the web site for the National Institutes for Health (www.nih.gov). The contact radiographs were digitized and the sixth 2 mm slice (3 mm proximal to the distal end of zone 3/5) (*See Figures 3.7 & 3.8*) was analyzed. The area of and centroid location of the metal implant, PMMA, and cortical bone were calculated (*See Figure 3.9*). The minimum and maximum thicknesses of the PMMA cement mantle were calculated. From the centroid locations, three distances were calculated: from metal centroid to PMMA centroid (*From point 1 to point 2 in Figure 3.9*), from metal centroid to bone centroid (*From point 1 to point 3 in Figure 3.9*), and from PMMA centroid to bone centroid (*From point 2 to point 3 in Figure 3.9*). These distances were measures of how well the metal implant was centralized within the cement mantle. A template (*See Figure 3.10*) was used to identify

in which quadrant of the femur (i.e., cranial, medial, caudal, lateral) the femoral component was in contact with the endosteum. The same designation was determined if the minimum PMMA thickness was less than 2 mm.

3.3.6. Statistical Analysis

Statistical analysis was performed using SAS software (SAS Institute, Cary, NC). Statistical analysis was performed with the assistance of the Center for Applied Statistical Expertise (CASE) in the Statistics Department at CSU. The low number of specimens and the large number of variables in this study presented challenges for statistician and researcher.

The SAS factor procedure [41] was used to perform principal component analysis in order to identify highly correlated variables. These results were analyzed in combination with expert opinion of engineers and veterinary surgeons in order to select variables that could be combined into index variables and thus reduce dimensionality (i.e., number of variables). Square root transformations were used for those indices that did not have a normal distribution in order to allow the use of parametric statistics.

Simple and multiple linear regression analyses were performed with bone/PMMA index, bone/metal index, PMMA/metal subsidence, and PMMA/metal ML translation (from mechanical testing) as the dependent variables. For multiple linear regression, two model selection methods were used in attempting to determine the best model for predicting the selected dependent variables [41-42]. The best selection method calculates the coefficient of determination (R^2) for all possible models for each number of variables being considered (e.g., one to four variables models). The models with the greatest R^2 are selected for each number of variables (*See Appendix F for sample output*). The

backward selection method starts by fitting the multiple regression model containing all the possible independent variables. At each step, the variable that makes the smallest contribution to the model (i.e., smallest F statistic) is deleted. This process continues until an F statistic for a particular model meets the significance criteria that is preset by the investigator.

In addition, simple linear regression for all variables vs. implant duration were also performed to look for time-dependent trends.

3.4. Results

Twenty-nine dogs, 9 with bilateral implants, were donated (*See Table 3.2*) for a total of 38 implants. Nine femoral components that had been implanted in dogs with bilateral THA (hereafter referred to as bilateral implants) and three femoral components that had been implanted in dogs with unilateral THA (hereafter referred to as unilateral implants) were Richards. Eight bilateral implants and 14 unilaterals were BioMedtrix #1. One bilateral and three unilaterals were BioMedtrix #2. Implant durations ranged from 8 months to 11 years and 8 months. The sizes of the dogs ranged from an 18.2 kg (40 lbs) Brittany Spaniel to a 66.4 kg (146 lbs) Newfoundland. Using one-way analysis of variance (ANOVA) there were no significant differences in age or weight between the implant designs.

3.4.1. Preliminary Processing

The owner of one dog reported that his dog was paralyzed in her hindquarters before the decision for euthanasia was made. The owner had been told by his veterinarian that the dog had a degenerative neurological condition that caused the paralysis. When the

joint capsule surrounding the THA was opened. the femoral component was so loose that it could easily bc slipped from the femur. Another owner reported that her dog displayed progressive difficulty with the hind limbs in walking. especially up stairs in the home. This implant was also so loose that it could easily be slipped from the femur. Both of these femoral components were BioMedtrix #1 with the Ti-6Al-4V femoral stem. Both of the femoral components displayed severe discoloration of the bone (i.e.. yellow and black) and surrounding soft tissues. The femora were also misshapen. The blackening has been reported in the human literature [43] as a sign of Ti-6Al-4V wear debris in the tissues. In both cases there was considerable damage to the lateral side of the implant with scratches in the metal indicating that the implant had rotated within the femur. One of these femoral components was polished to a mirror finish on the lateral side.

Another owner reported that her dog was paralyzed in his hindquarters before the decision for euthanasia was made. This dog had a torn ligament in the contralateral knee. The veterinarian diagnosed a degenerative neurological condition. In this case. the femoral component was firmly implanted.

In three cases. the dog had undergone revision surgery of the femoral component only. One of these cases was a particularly difficult surgical case because the contralateral hind limb had been amputated. In this case. the femur broke at the distal tip of the femoral component shortly after the primary THA. Revision surgery followed. and a bone plate and cerclage wires were used to repair the femur.

In three cases. when the joint capsule was cut open there were large fragments of PMMA loose within the joint. Some of the fragments were up to 1 cm in length. One of these cases was the contralateral amputee. and the joint capsule between the femoral neck

and the greater trochanter was packed with PMMA debris.

One unique case had a diagnosis of trauma rather than DJD. The dog suffered multiple severe injuries in a fall from the back of a pickup truck traveling at highway speed. One hip joint was repaired with THA. The contralateral femur no longer had a femoral head. The dog lived for seven years after THA, serving as an ambassador for the local chapter of the Society for the Prevention of Cruelty to Animals. The femoral component was grossly loose upon manual manipulation.

Eight of the retrievals (including the first two mentioned above) had notable blackening of the bone and soft tissues around the joint capsule. The femora were misshapen and/or discolored in half of these cases. In all but one of these cases, the implant was the BioMedtrix #1, as expected since this discoloration is commonly associated with Ti-6Al-4V wear debris [43]. In the eighth case, the femoral component had been revised and the current implant was a BioMedtrix #2; however, the year of the initial surgery fell during the time that the BioMedtrix #1 component was being implanted, indicating that the first implant was most likely Ti-6Al-4V.

Nine (23.7%) femoral components were classified as "grossly loose" upon manual manipulation of the femoral component. Mechanical testing was not performed on these femoral components.

3.4.2. Mechanical Testing to Assess Implant Stability

Twenty-nine femoral components were mechanically tested (*See Table 3.3*). The femoral implants were classified as "loose" if relative motion of greater than or equal to 45 μm was measured in subsidence or ML translation at either interface. The criteria derived from testing the controls was reinforced by the mechanical testing results. In all

four test conditions (i.e., subsidence or ML translation at each interface), there was a break in the data around 45 μm (*See Figure in Appendix C*) between the firmly implanted and loose femoral components. At the bone/PMMA interface in subsidence, the maximum measurement for a firmly implanted component was 37 μm, and the minimum measurement for a loose implant was 81 μm, a break of 44 μm. For ML translation at the bone/PMMA interface, the maximum measurement for a firmly implanted component was 40 μm, and the minimum measurement for a loose implant was 60 μm, a break of 20 μm. For subsidence relative motion between the bone and metal, the maximum measurement for a firmly implanted component was 17 μm, and the minimum measurement for a loose implant was 72 μm, a break of 55 μm. For ML translation between the bone and metal, the maximum measurement for a firmly implanted component was 39 μm, and the minimum measurement for a loose implant was 64 μm, a break of 25 μm. The difference between the bone/PMMA and bone/metal relative motion measurements was calculated as micromotion at the PMMA/metal interface. The femoral component was classified as loose at the PMMA/metal interface if the bone/metal measurement was greater than the bone/PMMA measurement and if the bone/metal measurement was greater than 45 μm.

Of the postmortem retrievals that were mechanically tested (*See Table 3.3*), 14 tested as firmly implanted (48.3% of tested femora, 36.8% of total). Six of the firmly implanted femoral components were Richards (5 bilateral, 1 unilateral), 7 were BioMedtrix #1 (5 bilateral, 2 unilateral), and 1 was BioMedtrix #2 (unilateral).

If an implant tested as loose in any direction at any interface (i.e., loose designation in one of four tests or two calculations) the implant was classified as loose. Fifteen

femoral components (51.7% of tested femora, 39.5% of total) tested as loose. Two implants (*See Table 3.3*), both Richards (one unilateral, one bilateral) tested loose only at the PMMA/metal interface in subsidence. Five femoral components tested loose at the PMMA/metal interface in both subsidence and ML translation. Two were Richards (both bilateral), 2 were BioMedtrix #1 (one bilateral, one unilateral), and one was BioMedtrix #2 (unilateral). One implant (bilateral BioMedtrix #1) tested loose in both directions at the PMMA/metal interface and in ML translation at the bone/PMMA interface. Another implant (unilateral BioMedtrix #1) tested loose in both directions at the PMMA/metal interface and in subsidence at the bone/PMMA interface. One unilateral BioMedtrix #1 component tested loose at the bone/PMMA interface and firm at the PMMA/metal interface. The femoral slice used for digital image analysis showed that the femoral component was in contact with the lateral endosteal bone, and there appeared to be soft tissue between the bone and the PMMA. One bilateral BioMedtrix #1 implant tested loose in all measurements except in ML translation at the PMMA/metal interface. The femoral component has a substantial cement mantle around the entire distal tip, although the tip is located caudal-medial within the femoral canal. There are two voids in the PMMA at the cranial bone/PMMA interface, and there appears to be a lucency between the bone and PMMA. The remaining four loose femoral components, all unilaterals (3 BioMedtrix #1, 1 BioMedtrix #2), tested loose in both directions at both interfaces.

3.4.3. Statistical Analysis

Frequency distributions of categorical results of femoral implant stability were calculated (*See Figure 3.11*). Although not statistically significant by Chi-Square analysis, there appears to be a trend that Richards femoral components are more stable

than BioMedtrix #1 or BioMedtrix #2. Using the non-parametric Kruskal-Wallis test, micromotion measured for unilaterals was significantly greater than for bilaterals in subsidence at both interfaces and in ML translation at the PMMA/metal interface ($p<0.05$) (*See Figure 3.12*). When micromotion measurements were compared between implant designs using the Kruskal-Wallis test, there were no significant differences, but there was a trend that BioMedtrix #1 implants were less stable than Richards and that BioMedtrix #2 implants were less stable than BioMedtrix #1. When micromotion measurements were compared between manufacturers (i.e., all BioMedtrix implants combined into one category) using the two-sample t-test for unequal variances (*See Figure 3.13*), there was significantly more micromotion measured for the BioMedtrix than Richards implants in ML translation at both interfaces and in subsidence at the bone/PMMA interface ($p<0.05$). Using repeated measures analysis with the subject being each case and the repeated measure being the four micromotion measurements, the subsidence measurement at the PMMA/metal interface was significantly greater ($p<0.05$) than the other three measurements, and the ML translation measurement at the PMMA/metal interface was significantly greater than ML translation at the bone/PMMA interface.

Using factor analysis combined with the expert opinion of engineers and veterinary surgeons, a number of indices were formed by taking the mean of highly correlated variables. Only variables with similar units (e.g., mm) were combined. Factor analysis was performed in order to reduce the dimensionality (i.e., number of variables). If the distribution of an index appeared to be non-normal, the index was transformed (i.e., square root) to allow for the use of parametric statistical analysis. The index variables

that were defined in this manner are defined and named (*See Table 3.4*). Additional (*See Glossary C for names and descriptions of variables*) variables were defined by combining original and index variables, and those are also defined and named (*See Table 3.4*). During multiple regression analysis, it was found that the bone/PMMA index (*See Table 3.4 for index definitions*) correlated positively with the GZ 4 index and negatively correlated with the GZ 11 index. The measurements taken in Gruen zones 4 and 11 reflect the width of the medullary canal in CC and ML views (*See Figure 3.6*); thus, there was a shape effect that correlated with the bone/PMMA index (*See Figure 3.14*). When the medullary canal was wider in the ML direction than in the CC direction, there was a tendency toward greater motion at the bone/PMMA interface. Conversely, those femora that were wider in the CC direction than in the ML direction tended to be more firmly implanted. Therefore, two shape indices were defined (*See Table 3.4*).

The dependent variables chosen were the bone/PMMA index, the bone/metal index, and the PMMA/metal index. Simple linear correlations were calculated with all independent variables against the dependent variables. Simple linear correlations were also calculated against implant duration in order to look for time-dependent trends. Results from simple linear correlations are presented (*See Table 3.5*). Some of the stronger relationships include a negative correlation between implant duration and age (*See Figure 3.15*) and a positive correlation between the bone/metal index and distance 3 (*See Figure 3.16*).

Multiple linear regression was performed using backward selection and best selection methods in an attempt to find a model that could be used to predict failure of the femoral component (*See Table 3.6 for examples of possible models; see Appendix F for*

sample SAS output). It was hoped that this analysis would identify variables that were unnecessary to collect in future studies of this type with the goal of further reducing the dimensionality of the data. Unfortunately, no clear-cut model of choice presented itself, due in part to the low number of specimens in this study. Variables that appeared most often in these models are presented (*See Table 3.7*).

3.5. Discussion

3.5.1. Comparison to Human Postmortem Retrieval Studies

Despite the fact that postmortem retrieval studies are difficult to control for statistical power, human studies have already proven the value of the information that can only be obtained from THAs that are considered to be performing well and retrieved postmortem as opposed to revision retrievals [4-6]. Statistical analysis of postmortem retrieval data was not included in the human studies; however, valuable qualitative information was still obtained from these human studies.

More than half of the femoral components (63.2%) in this study were loose, and this contrasts sharply with the 84% positive response to the subjective owner survey discussed in Chapter 2 [36]. Nine of 38 (23.7%) of the canine femoral components were loose upon manual manipulation. This is much higher than the 1 of 16 (6.2%) human femoral components, retrieved at autopsy, that was loose upon manual manipulation [4-6]. This grossly loose human femoral component was completely debonded at the PMMA/metal interface and had soft tissue between the metal and PMMA. The three studies [4-6] of human postmortem retrievals examined 16 asymptomatic femoral components or a subset thereof. Fifteen of 16 femoral components displayed no

radiographic evidence of loosening.

In order to compare the clinical canine THA findings of this study to similar studies in humans, human postmortem retrieval studies from the literature must be carefully chosen. These studies must be on human femoral components made from similar materials, implanted using similar attachment methods, and measured using similar methods to those used in this study. Unfortunately, studies of this nature are difficult to find. Three different mechanical testing methods were used to test for implant stability in the human studies [4-6], one of which was adapted for use in this study. One testing method used for the human femoral components involved the application of torsion to the femoral head in a manner similar to that used during revision surgery to assess the stability of the femoral component *in situ*. The second method used was the one adapted for testing the canine postmortem retrievals. A first-generation RMD was mounted to the femur and micromotion of the metallic implant relative to the bone was measured in subsidence and ML translation while the femur was loaded in single-leg stance loading, a physiologic loading condition. Unfortunately, only motion of the femoral component relative to the bone was measured in these studies. No attempt was made to test the integrity of the bone/PMMA interface. The third test method was just like the second test method except that the femur was loaded to mimic loads experienced during stair climbing, another physiologic loading condition.

Firmly implanted controls were created in the human postmortem retrieval studies [4-6] in order to verify that no damage was done to the clinical specimens during testing. Unfortunately, loose controls were not created, and only Schmalzried *et al.* [6] provided any criteria (i.e., less than 100 μm motion) for categorizing a femoral component as

"well-fixed." However, no explanation was provided for how the criteria were derived. In addition, no statistical analysis were provided on the data from any of these three studies. To complicate the matter even further, the principal investigator at this laboratory referred to these studies in a review article and provided a figure of 50 μm of micromotion as the criteria to categorize loose from firmly implanted femoral components [44].

All three of these studies were performed in the same laboratory on the same specimens, but there were some contradictions in the results of the three studies. Jasty *et al.* [5] described four of the femora, those with the greatest micromotion using the torsion apparatus, as osteoporotic. A fifth osteoporotic femur was not tested using this method because it had broken during single-leg stance loading [4]. Jasty *et al.* [5] implied that these 5 (31.2%) femoral components were loose, since these five femora were described separately and in greater detail than the remaining 10. In that case, 6 (37.5%) of the retrievals would have been classified as loose. By contrast, Schmalzried *et al.* [6] examined a subset of ten of these 16 femoral components that were described as "well-fixed." The criteria for inclusion of the ten femora in this study were that they moved less than 100 μm under physiologic loading conditions (i.e., the single-leg stance and stair climbing test conditions). However, there was a disconnect between the results of the torsional loading and the physiologic loading. Two of the femoral components that moved less than 100 μm under physiologic loading conditions had the two highest micromotion measurements under torsional loading. These two femora had been described by Jasty *et al.* [5] as osteoporotic and loose. Thirteen of the 16 femoral components were tested under physiologic loading conditions, and two moved more than

100 μm, the criteria for "well-fixed" provided by Schmalzried *et al.* [6]. Based on these criteria, 2 (15.4%) of the 13 tested femoral components would be classified as loose. If the one femoral component that was grossly loose upon manual manipulation were included, 3 (21.4%) of 14 femoral components would be classified as loose. Since the mechanical testing performed under physiologic loading is similar to that used in this study (i.e., at the PMMA/metal interface), these are the numbers that will be used for comparison to the canine postmortem retrieval data. To complicate the matter even further, the principal investigator at this laboratory referred to these studies in a review article and provided a figure of 50μm of micromotion for stable femoral components [44].

To recap, 1 (7.1%) of 14 human femoral components, retrieved postmortem, were loose upon manual manipulation. This is much lower than the 9 (23.7%) of 38 canine femoral components, retrieved postmortem, that were loose upon manual manipulation in the present study. As a result of mechanical testing, an additional 2 (14.3%) human femoral components and 15 (39.5%) canine femoral components were classified as loose. This gave a total of 3 (21.4%) of 14 human femoral components and 24 (63.2%) of 38 canine femoral components class that were classified as loose by similar criteria. The incidence of aseptic loosening of the femoral component in canine THA is much greater than that seen in the human autopsy retrieval studies.

3.5.2. Other Findings

More thorough follow-up with objective methods of evaluation needs to be incorporated to ensure the best quality of life for canine THA patients. For example, gait analysis with a force plate could be used to pinpoint a change in weight bearing on the

implanted leg that may indicate problems with the implant.

When a femoral component becomes loose in a human THA patient, that person usually complains of thigh pain [45] to their surgeon, and the component is revised soon afterward. Dogs mask pain well [46], and from owner feedback it is apparent that most owners were unaware of the possibility that their dogs' THA femoral components had loosened. For two of three dogs that were paralyzed in or partially paralyzed in their hind quarters, the owners were told by their veterinarians that the dogs had degenerative neurological conditions. This may not have been the case at all. Perhaps the completely loose femoral component was causing bone pain to a degree that prevented the dog from walking. Another possibility may be that the loose femoral component caused nerve damage while it rotated about within the femur, thus leading to paralysis in the hindquarters.

Most humans undergoing THA are elderly and relatively sedentary. Most orthopaedic surgeons will avoid performing this surgery in any patient under the age of 50. THA is not as successful in young patients [9, 44, 47-48]. Young, active patients will wear their implants much more quickly, thus requiring more frequent revision surgeries. Since the primary surgery has the greatest chance for a successful outcome and since each subsequent revision surgery has decreasing chances for a successful outcome, surgeons prefer to limit the number of potential revisions surgeries by avoiding performing THA in young patients.

From speaking with owners and veterinary orthopaedic surgeons, the expectation with canine THA is that the dog will lead an active life. This contrasts sharply with the expectations of the average human THA patient. It may be more appropriate to compare

canine THA to THA performed in the young human patient.

Bilateral THA in dogs performed better than unilateral THA (*See Figure 3.12*). Richards implants appear to have performed better than either BioMedtrix design (*See Figure 3.13*). Both of these perceptions may be skewed by the fact that the majority of Richards implants (9 of 12) were retrieved from bilateral THAs. However, the importance of the bilateral vs. unilateral factor is illustrated (*See Table 3.3*) by examining the firmly implanted specimens. BioMedtrix #1 implants, known to have an early aseptic loosening problem [26], comprised half of the firmly implanted components (7 of 14); however, 5 of these were bilaterals. This is also reinforced by examining the grossly loose components (*See Table 3.3*). Six of the 9 grossly loose specimens were BioMedtrix #1 unilaterals.

From the plot of implant duration vs. age of the dog at surgery (*See Figure 3.15*), it appears that the earliest THAs were performed on young dogs, and over time the ages of dogs undergoing this surgery were progressively older. However, another explanation for this relationship may be that dogs of all ages underwent THA surgery, but the older ones reached the end of their lives sooner while the younger dogs undergoing THA at the same time are still thriving. This may also explain why the implants with the longest durations were implanted in younger dogs. Older dogs receiving THA surgery in those years would have already died before this study commenced.

Improper positioning of the distal tip of the implant, resulting in thin cement mantles or contact of the distal tip with endosteal bone, has been implicated as a predictor of aseptic loosening of the femoral component in both human and canine THA [4-6, 26]. A minimum of 2 mm thick PMMA is needed in order to reduce stress concentrations in the

cement mantle. The findings of the present study support the previous findings. Measures of cement mantle thickness on contact radiographs of intact femora in Gruen zones 2 and 3 (i.e., middle and distal thirds of lateral side in CC view) were negatively correlated with loosening at both interfaces in several of the possible models identified in the multiple linear regression analysis. The sites with the greatest incidence of endosteal contact or very thin PMMA were caudal (11), caudal-lateral (7) or lateral (5).

Another surprising finding in this study that resulted from the sophisticated statistical analysis methods was related to the shape of the medullary canal of the femur. In the analysis of contact radiographs made of the intact femora, measurements of the width of the femoral canal were made distal to the distal tip of the femoral component in Gruen zones 4 (GZ 4 - in CC view) and 11 (GZ 11 - in ML view) (*See Figure 3.6*). The measurement made in the CC view reflected the width of the femoral canal in the ML direction. The measurement made in the ML view reflected the width of the femoral canal in the CC direction. A shape effect (*See Figure 3.14*) was detected during multiple linear regression analysis. The measures of loosening of the femoral component were positively correlated with the ML width of the femoral canal (in CC view) and were negatively correlated with the CC width of the femoral canal (in ML view). This meant that femora that were wider in the ML direction and narrower in the CC direction tended to have loose femoral components; whereas, femora that were wider in the CC direction and narrower in the ML direction tended to have firmly implanted femoral components.

This shape finding is reinforced by observations made with regard to the cross-sectional geometry of the distal stem of the Richards versus the BioMedtrix femoral components. The Richards femoral component was more rectangular in shape, and the

thinner aspect was in the CC direction. The BioMedtrix designs are both round at the distal end of the femoral stem with two small grooves (one on the cranial side and the other on the caudal side) that run the distal length of the femoral stem. Perhaps the Richards components were thin enough in the CC direction that, even in femora that were thin in the CC direction, an adequate PMMA cement mantle could be achieved to maintain femoral implant stability for long periods of time. Thin cement mantles have been found, in both human and canine THA, to be predictors of future aseptic loosening of the femora components [4-6], and an FEA study [8] found increased shear stress and micromotion at the PMMA/metal interface when the PMMA thickness was 2 mm or less. Thus, future designs for canine femoral components need to utilize a more rectangular or oval shape on the distal end of the femoral stem with the thinner aspect being in the CC direction in order to ensure that the cement mantle will be sufficiently thick in all directions around the distal tip of the femoral component. An implant that is thinner in the CC direction would be less likely to experience contact of the distal tip with caudal endosteum at the cranial bow of the femur.

Another possible explanation for the better performance of the Richard implants may be the stronger distal taper of the Richards implant in comparison to the BioMedtrix components. Huiskes and Verdonschot [9] stated that in cases where the femoral stem had a very prominent taper at the distal tip, distal stresses were reduced. Perhaps distal stresses were reduced with the Richards femoral component in comparison to the BioMedtrix components thus protecting the bond at the PMMA/metal interface.

Two postmortem retrievals from the present study had femoral components that were so loose they could easily be removed from the femora. Both of the femoral components

had damage on the lateral side of the femoral stem. One implant was scratched in a manner that indicated that the implant had been rotating within the stem. The other femoral component was polished to a mirror finish on the lateral side of the femoral stem. These observations in combination with statements from orthopaedic veterinary surgeons performing revision THA, led to an early belief that rotational stability was the key issue for the redesign of a canine femoral component. However, the mechanical testing data for the femoral components did not support these early observations. Of the 29 femoral components (*See Table 3.3*) that were mechanically tested (9 were so loose that they were not tested), 14 tested as firmly implanted (i.e., firm in both subsidence and ML translation at both the bone/PMMA and PMMA/metal interfaces). Six femoral components tested as loose in all four tests, and five tested loose in both directions at the PMMA/metal interface but firm in both directions at the bone/PMMA interface. One implants tested loose at the bone/PMMA interface and firm at the PMMA/metal interface in both rotation and ML translation, and a second implant tested firm at the PMMA/metal interface in ML translation and loose in all other directions at both interfaces. The remaining four femoral components were unique. Two implants tested loose only at the PMMA/metal interface in subsidence. One implant tested loose in both directions at the PMMA/metal interface and in ML translation at the bone/PMMA interface. One implant tested loose in both directions at the PMMA/metal interface and in subsidence at the bone/PMMA interface.

Considering that there were only five implants that had a mismatch between subsidence and ML translation testing at the same interface, it is difficult to draw definitive conclusions. However, three of these five implants tested as loose in

subsidence and firm in ML translation at the same interface, in direct contradiction to the belief that rotational stability is the key. These results provide preliminary data to support published reports from human postmortem retrieval studies that indicate that femoral components fail mechanically at the PMMA/metal interface first with debonding of the PMMA/metal interface as the initiating event [4-6]. This failure in canine THA, as in human THA, appears to be in subsidence first. Despite the fact that the shear strength of the PMMA/metal interface (i.e., 5-8 MPa [9]) is greater than the shear strength of the bone/PMMA interface (i.e., 2-4 MPa [Huiskes]), the PMMA/metal interface appears to be the first point of failure in both human and canine THA. There is a smaller surface area for the PMMA/metal interface than for the bone/PMMA interface thus providing less interface for load transfer at the PMMA/metal interface. The smaller surface area for the same load will cause increased stress at this interface. In addition, the metallic femoral component is stiffer than the bone and PMMA, and the stiffer component in a composite carries more of the load [9]. Thus, given the larger load carried by the femoral implant and the smaller surface area for load transfer, the PMMA/metal interface is the most likely point for the initiating failure event to occur.

These results indicate that the rotational damage seen on the femoral components is not related to initiating failure events. However, further research and an increase in the number of tested specimens is required to verify these findings. The data seem to suggest that perhaps the initial failure occurs in subsidence. Eventually, as the debonding of the PMMA/metal interface progresses, the PMMA cracks and the femoral component begins to rotate within the cement mantle, thus causing the rotational markings on the femoral stems. This rotational scoring and burnishing would result from secondary or tertiary

failure mechanisms.

Human THA results have improved with modifications in implant design and cementing technique. Considering that 63.2% of the canine femoral implants in this study were loose, redesign of the femoral component for better stability is needed. The shape of the Richards femoral stem was more rectangular than either of the BioMedtrix #2 femoral stems that were round on the distal end with two small grooves that ran parallel to the femoral stem. Despite the fact that the Richards femoral components had been implanted using earlier surgical techniques, these implants tended to remain firmly implanted.

The surgical paradigm for canine THA at the CSU VTH has changed as a result of this study. Unilateral THA for dogs with bilateral DJD is no longer considered to be adequate. Surgeons are suggesting bilateral surgery more frequently in dogs with bilateral DJD, although the additional cost of bilateral surgery remains an issue with many owners. Surgeons are taking greater care with preparation of the femur and acetabulum before placement of the implants. Surgeons at the CSU VTH are using state-of-the-art cementing techniques, including vacuum mixing to reduce voids, pressurization, use of cement plugs in the medullary canal, and centralization of the distal tip within the medullary canal. These measures led to improved success in human THA, and similar results are hoped for in canine THA in future follow-up studies.

3.6. Conclusions

This is the first report that provides benchmark data on femoral implant stability and cement mantle quality in postmortem retrievals of clinical canine THAs.

Hypothesis #1 in the present study was that the canine femoral component would fail in a manner similar to that seen in human THA. Human postmortem retrieval studies [4-6] found mechanical failure of the femoral component that initiated with debonding of the PMMA from the metal implant. In the present study, seven of the loose femoral components tested loose at the PMMA/metal interface and firm at the bone/PMMA interface, supporting hypothesis #1. This hypothesis is further supported since, by repeated measures analysis, subsidence micromotion at the PMMA/metal interface was significantly greater than the other three micromotion measures.

The second hypothesis was that incidence of aseptic loosening of the femoral component would not be as pronounced in dogs as in humans due to lower peak JRFs in dogs. This hypothesis was not found to be true since 63.2% of the femoral components were either loose or grossly loose. This percentage is much greater than the 6 to 9% of human femoral components showing evidence of aseptic loosening at 15 years after primary THA [1-2]. THA in young, more active human patients has been shown to fail more quickly than in older sedentary patients [9, 44, 47-48], and THA in dogs may also experience a high incidence of aseptic loosening due to the activity level of the dog.

The third hypothesis was that unilateral components would perform adequately in comparison to bilateral implants. This hypothesis was not found to be true, and this was the most surprising finding of this study. Owners and veterinary surgeons reported that after unilateral surgery the dogs placed more weight on the implanted side than the diseased, intact limb. This may have resulted in possible overloading and early failure of the unilateral THAs. Bilateral femoral components were significantly more stable than unilateral components, but these findings may be skewed since nine of the 12 Richards

implants were bilaterals.

Despite the fact that the Richards implants were the earliest implant design used and implanted using earlier generations of surgical techniques with poorer quality cement mantles. these implant performed better than either of the BioMedtrix designs. This may be directly related to the bilateral vs. unilateral question since 9 of 12 Richards retrievals were from bilateral cases and since 5 of the firmly implanted components were BioMedtrix #1 bilaterals as well. Edwards *et al.* [26] found no cases of surgical revision for aseptic loosening of the Richards femoral component despite the fact that many of them had the distal tip of the implant in contact with bone. The BioMedtrix #1 implant design was associated with early aseptic loosening problems [26]. and the present study confirmed this finding: however. unilateral BioMedtrix #1 implants predominated in those implants that were grossly loose.

Despite the problems with aseptic loosening found in this study. THA remains a valuable option in the treatment of DJD in dogs. Improved surgical techniques and implant design coupled with more thorough follow-up using objective (i.e.. force plate gait analysis) and subjective (i.e.. owner surveys) test methods will lead to a decrease in aseptic loosening in the future.

3.7. Acknowledgements

Daniel O'Connor and Charles Bragdon – for technical assistance on the mechanical testing method for the femoral components: Dan Frankel. DVM – for radiographic analysis: Elizabeth Pluhar. DVM – for radiographic analysis; Erick Egger. DVM – for assistance in making of control femora and radiographic analysis and for radiographic

analysis: BioMedtrix, Inc. – for donation of 2 new femoral components: Howmedica – for donation of PMMA bone cement: Liza Eschbach & Diane Beranek for technical assistance in sectioning femora using the Exakt™ bone saw: Jim zum Brunnen – for statistical data analysis assistance.

3.8. References

1) Mulroy WF, Estok DM, Harris WH. Total Hip Arthroplasty with Use of So-Called Second-Generation Cementing Techniques: A Fifteen-Year-Average Follow-Up Study. *The Journal of Bone and Joint Surgery*, 1995; 77-A: 1845-1852.

2) Klapach AS, Callaghan JJ, Goetz DD, Olejniczak JP, Johnston RC. Charnley Total Hip Arthroplasty With Use of Improved Cementing Techniques: A Minimum Twenty-Year Follow-Up Study. *The Journal of Bone and Joint Surgery*, 2001; 83-A: 1840-1848.

3) Iorio R, Eftekhar NS, Kobayashi S, Grelsamer RP. Cemented Revision of Failed Total Hip Arthroplasty: Survivorship Analysis. *Clinical Orthopaedics and Related Research*, 1995; 316: 121-130.

4) Maloney WJ, Jasty M, Burke DW, O'Connor DO, Zalenski EB, Bragdon C, Harris WH. Biomechanical and Histologic Investigation of Cemented Total Hip Arthroplasties: A Study of Autopsy-Retrieved Femurs After *In Vivo* Cycling. *Clinical Orthopaedics and Related Research*, 1989; 249: 129-140.

5) Jasty M, Maloney WJ, Bragdon CR, O'Connor DO, Haire T, Harris WH. The Initiation of Failure in Cemented Femoral Components of Hip Arthroplasties. *The Journal of Bone and Joint Surgery*, 1991; 73-B: 551-558.

6) Schmalzried TP, Maloney WJ, Jasty M, Kwong LM, Harris WH. Autopsy Studies of the Bone-Cement Interface in Well-Fixed Cemented Total Hip Arthroplasties. *The Journal of Arthroplasty*, 1993; 8: 179-188.

7) Ebramzadeh E, Sarmiento A, McKellop HA, Llinas A, Gogan W. The Cement Mantle in Total Hip Arthroplasty: Analysis of Long-Term Radiograpic Results. *The Journal of Bone and Joint Surgery*, 1994; 76-A: 77-87.

8) Ramaniraka NA, Rakotomanana LR, Leyvraz PF. The Fixation of the Cemented Femoral Component: Effects of Stem Stiffness, Cement Thickness and Roughness of the Cement-Bone Surface. *The Journal of Bone and Joint Surgery*; 2000; 82-B: 297-303.

9) Huiskes R. Verdonschot N. BioMechanics of Artificial Joints: The Hip. *Basic Orthopaedic Biomechanics, 2nd ed.*, edited by Van C. Mow and Wilson C. Hayes. Lippincott-Raven Publishers. Philadelphia. Chapter 11: 1997: 395-460.

10) Kuo TY. Skedros JG. Bloebaum RD. Comparison of Human. Primate. and Canine Femora: Implications for Biomaterials Testing in Total Hip Replacement. *Journal of Biomedical Materials Research.* 1998: 40: 475-489.

11) Bloebaum RD. Ota DT. Skedros JG. Mantas JP. Comparison of Human and Canine External Femoral Morphologies in the Context of Total Hip Replacement. *Journal of Biomedical Materials Research.* 1993: 27: 1149-1159.

12) Sumner DRJ. Devlin TC. Winkelman D. Turner TM. The Geometry of the Adult Canine Proximal Femur. *Journal of Orthopaedic Research.* 1990: 8: 671-677.

13) Page AE. Allan C. Jasty M. Harrigan TP. Bragdon CR. Harris WH. Determination of Loading Parameters in the Canine Hip *in Vivo*. *Journal of Biomechanics.* 1993: 26: 571-579.

14) Davy DT. Kotzar GM. Brown RH. Heiple KG. Goldberg VM. Heiple Jr KG. Berilla J. Burstein AH. Telemetric Force Measurements across the Hip after Total Hip Arthroplasty. *The Journal of Bone and Joint Surgery.* 1988: 70-A: 45-50.

15) Arnoczky SP. Torzilli PA. Biomechanical Analysis of Forces Acting About the Canine Hip. *American Journal of Veterinary Research.* 1981: 42: 1581-1585.

16) Adrian MJ. Roy WE. Karpovich PV. Normal Gait of the Dog: An Electrogoniometric Study. *American Journal of Veterinary Research.* 1966: 27: 90-95.

17) Finlay JB. Chess DG. Harkie WR. Rorabeck CH. Bourne RB. An Evaluation of Three Loading Configurations for the In Vitro Testing of Femoral Strains in Total Hip Arthroplasty. *Journal of Orthopaedic Research.* 1991: 9: 749-759.

18) Jasty M. Page A. Henshaw R. Bragdon C. Cargill E. Harris WH. Long Duration Measurement of In Vivo Strain Distribution in the Canine Femur. *Transactions of the 34th Annual Meeting of the Orthopaedic Research Society.* 1988: 236.

19) Montgomery RD. Milton JL. Pernell R. Aberman HM. Total Hip Arthroplasty for Treatment of Canine Hip Dysplasia. *The Veterinary Clinics of North America: Small Animal Practice.* 1992: 22: 703-719.

20) Lewis RH. Jones Jr JP: A Clinical Study of Canine Total Hip Arthroplasty. *Veterinary Surgery.* 1980: 9: 20-23.

21) Gofton N. Sumner-Smith G: Total Hip Prosthesis for Revision of Unsuccessful

Excision Arthroplasty. *Veterinary Surgery*. 1982; 11: 134-139.

22) Olmstead ML. Hohn RB. Turner TM: A Five-Year Study of 221 Total Hip Replacements in the Dog. *Journal of the American Veterinary Medical Association*. 1983; 183: 191-194.

23) Parker RB. Bloomberg MS. Bitetto W. Rodkey WG: Canine Total Hip Arthroplasty: A Clinical Review of 20 Cases. *Journal of the American Veterinary Medical Association*. 1984; 20: 97-104.

24) Olmstead ML: Total Hip Replacement in the Dog. *Seminars in Veterinary Medicine and Surgery (Small Animal)*. 1987; 2: 131-140.

25) Paul HA. Bargar WL. A Modified Technique for Canine Total Hip Replacement. *Journal of the American Animal Hospital Association*. 1987; 23: 13-18.

26) Edwards MR. Egger EL. Schwarz PD: Aseptic Loosening of the Femoral Implant after Cemented Total Hip Arthroplasty in Dogs: 11 Cases in 10 Dogs (1991-1995). *Journal of the American Veterinary Medical Association*. 1997; 211: 580-586.

27) Anderson GI. Podworny N. Jain R. Kwok AWL. Waddell JP. Hydroxyapatite Application Effect on Micromotion Around Acetabular and Femoral Components in the Dog. *Transactions of Fifth World Biomaterials Congress*. 1996: 176.

28) Bobyn JD. Jacobs JJ. Tanzer M. Urban RM. Aribindi R. Sumner DR. Turner TM. Brooks CE. The Susceptibility of Smooth Implant Surfaces to Periimplant Fibrosis and Migration of Polyethylene Wear Debris. *Clinical Orthopaedics and Related Research*. 1995; 311: 21-39.

29) Bobyn JD. Pilliar RM. Binnington AG. Szivek JA. The Effect of Proximally and Fully Porous-Coated Canine Hip Stem Design on Bone Modeling. *Journal of Orthopaedic Research*. 1987; 5: 393-408.

30) Dowd JE. Schwendeman LJ. Macaulay W. Doyle JS. Shanbhag AS. Wilson S. Herndon JH. Rubash HE. Aseptic Loosening in Uncemented Total Hip Arthroplasty in a Canine Model. *Clinical Orthopaedics and Related Research*. 1995; 319: 106-121.

31) Finkelstein JA. Anderson GI. Waddell JP. Richards RR. Hearn TC. Schemitsh E. A Study of Micromotion and Appositional Bone Growth to a Canine Madreporic-Surfaced Femoral Component. *The Journal of Arthroplasty*. 1994; 9: 317-324.

32) Harvey EJ. Bobyn JD. Stackpool GJ. Tanzer M. Comparative Peri-Implant Femoral Bone Remodeling with Isoelastic and Hypoelastic Noncemented Canine Hip Prostheses. *Transactions of the 43rd Meeting of the Orthopaedic Research Society*, 1997: 307.

33) Maistrelli GL. Mahomed N. Fornasier V. Antonelli L. Li Y. Binnington A. Functional Osseointegration of Hydroxyapatite-Coated Implants in a Weight-Bearing Canine Model. *The Journal of Arthroplasty*. 1993; 8: 549-554.

34) Vanderby Jr R. Manley PA. Kohles SS. McBeath AA. Fixation Stability of Femoral Components in a Canine Hip Replacement Model. *Journal of Orthopaedic Research*. 1992; 10: 300-309.

35) Walenciak MT. Zimmerman MC. Harten RD. Ricci JL. Stamer DT. Biomechanical and Histological Analysis of an HA Coated. Arc Deposited CPTi Canine Hip Prosthesis. *Journal of Biomedical Materials Research*. 1996; 31: 465-474

36) Skurla CT. Egger EL. Schwarz PD. James SP. Owner Assessment of the Outcome of Total Hip Arthroplasty in Dogs. *Journal of the American Veterinary Medical Association*. 2000; 217: 1010-1012.

37) Burke DW. O'Connor DO. Zalenski EB. Jasty M. Harris WH. Micromotion of Cemented and Uncemented Femoral Components. *The Journal of Bone and Joint Surgery*. 1991; 73-B: 33-37.

38) O'Connor DO. Burke DW. Sedlacek RC. Lozynsky AJ. Harris WH. A New Method for Measuring Relative Motion Between a Total Joint Component and Adjacent Cortical Bone. *Proceedings from the 19th Annual Meeting of the Society for Biomaterials*. 1993; 16: 122.

39) Gruen TA. McNeice GM. Amstutz HC. "Modes of Failure" of Cemented Stem-Type Femoral Components: A Radiographic Analysis of Loosening. *Clinical Orthopaedics and Related Research*. 1979; 141: 17-27.

40) Johnston RC. Fitzgerald Jr RH. Harris WH. Poss R. Müller ME. Sledge CB. Clinical and Radiographic Evaluation of Total Hip Replacement: A Standard System of Terminology for Reporting Results. *The Journal of Bone and Joint Surgery*. 1990; 72-A: 161-168.

41) SAS Institute. Inc. *SAS/STAT User's Guide. Version 6. 4th ed.*. SAS Institute. Inc., Cary. NC. 1990.

42) Ott RL. More on Multiple Regression. *An Introduction to Statistical Methods and Data Analysis. 4th ed.* Duxbury Press. Belmont. California. Chapter 12; 1993: 647-766.

43) Witt JD. Swann M. Metal Wear and Tissue Response in Failed Titanium Alloy Total Hip Replacements. *The Journal of Bone and Joint Surgery*. 1991; 73-B: 559-563.

44) Harris WH. Sledge CB. Total Hip and Total Knee Replacement (First of Two Parts). *New England Journal of Medicine*. 1990; 323: 725-731.

45) Georgiou AP. Cunningham JL. Accurate Diagnosis of Hip Prosthesis Loosening Using a Vibrational Technique. *Clinical Biomechanics*. 2001: 16: 315-323.

46) Johnston SA. Overview of Pain in the Lame Patient. *Veterinary Clinics of North America: Small Animal Practice*. 2001: 31: 39-53.

47) Callaghan JJ. Forest EE. Sporer SM. Goetz DD. Johnston RC. Total Hip Arthroplasty in the Young Adult. *Clinical Orthopaedics and Related Research*. 1997: 344: 257- 262.

48) Callaghan JJ. Results of Primary Total Hip Arthroplasty in Young Patients. *The Journal of Bone and Joint Disease*. 1993: 75-A: 1728-1734.

3.9. Tables

Table 3.1				
Study	**Nbr of Cases**	**Nbr (Pct) of Cases with Aseptic Loosening of the Femoral Component**	**Implant Design**	**Follow-Up Period (months)**
Lewis & Jones (1980) [20]	20	7 (35.0%)	Richards	19-34
Gofton & Sumner-Smith (1982) [21]	3	0 (0.0%)	Richards (1): Other (2)	8-18
Olmstead (1983) [22]	216	0 (0.0%)	Richards	1-72
Parker (1984) [23]	23	0 (0.0%)	Richards	6-42
Olmstead (1987) [24]	146	1 (0.7%)	Richards	1-36
Paul & Barger (1987) [25]	65	0 (0.0%)	Richards	6-42
Edwards (1997) [26]	152	11 (7.2%)	BioMedtrix #1	26-74
Combined	**625**	**19 (3.0%)**		

Table 3.1 - Literature review of previous outcomes assessment studies of canine total hip arthroplasties for aseptic loosening (requiring revision surgery) of the femoral component [20-26].

Table 3.2			
Implant Design	**Unilateral**	**Bilateral**	**Total**
Richards	3	9	**12**
BioMedtrix #1	14	8	**22**
BioMedtrix #2	3	1	**4**
Total	**20**	**18**	**38**

Table 3.2 – Postmortem retrievals of canine THA received at the CSU VTH, by implant design.

Table 3.3							
Mfr	Bilateral/ Unilateral	Bone/PMMA		Bone/Metal		PMMA/Metal	
		Sub	Trans	Sub	Trans	Sub	Trans
BioMedtrix #1	Bilateral	F	F	F	F	F	F
BioMedtrix #1	Bilateral	F	F	F	F	F	F
BioMedtrix #1	Bilateral	F	F	F	F	F	F
BioMedtrix #1	Bilateral	F	F	F	F	F	F
BioMedtrix #1	Bilateral	F	F	F	F	F	F
Richards	Bilateral	F	F	F	F	F	F
Richards	Bilateral	F	F	F	F	F	F
Richards	Bilateral	F	F	F	F	F	F
Richards	Bilateral	F	F	F	F	F	F
Richards	Bilateral	F	F	F	F	F	F
BioMedtrix #1	Unilateral	F	F	F	F	F	F
BioMedtrix #1	Unilateral	F	F	F	F	F	F
BioMedtrix #2	Unilateral	F	F	F	F	F	F
Richards	Unilateral	F	F	F	F	F	F
Richards	Bilateral	F	F	L	F	L	F
Richards	Unilateral	F	F	L	F	L	F
BioMedtrix #1	Bilateral	F	F	L	L	L	L
Richards	Bilateral	F	F	L	L	L	L
Richards	Bilateral	F	F	L	L	L	L
BioMedtrix #1	Unilateral	F	F	L	L	L	L
BioMedtrix #2	Unilateral	F	F	L	L	L	L
BioMedtrix #1	Bilateral	F	L	L	L	L	L
BioMedtrix #1	Unilateral	L	F	L	L	L	L
BioMedtrix #1	Unilateral	L	L	L	L	F	F
BioMedtrix #1	Bilateral	L	L	L	L	L	F
BioMedtrix #1	Unilateral	L	L	L	L	L	L
BioMedtrix #1	Unilateral	L	L	L	L	L	L
BioMedtrix #1	Unilateral	L	L	L	L	L	L
BioMedtrix #2	Unilateral	L	L	L	L	L	L
BioMedtrix #2	Bilateral	L *	L *	L *	L *	L *	L *
Richards	Bilateral	L *	L *	L *	L *	L *	L *
BioMedtrix #1	Unilateral	L *	L *	L *	L *	L *	L *
BioMedtrix #1	Unilateral	L *	L *	L *	L *	L *	L *
BioMedtrix #1	Unilateral	L *	L *	L *	L *	L *	L *
BioMedtrix #1	Unilateral	L *	L *	L *	L *	L *	L *
BioMedtrix #1	Unilateral	L *	L *	L *	L *	L *	L *
BioMedtrix #1	Unilateral	L *	L *	L *	L *	L *	L *
Richards	Unilateral	L *	L *	L *	L *	L *	L *

Table 3.3 – Results of mechanical testing of femoral components. F = firmly implanted: L = loose: L * = grossly loose (not mechanically tested).

Table 3.4			
Index Variable Name	**Data Source**	**Original Variables**	**Transform Used**
Bone/PMMA index	Mechanical testing	Subsidence (bone/PMMA)	Square root of mean
		ML translation (bone/PMMA)	
Bone/Metal index	Mechanical testing	Subsidence (bone/metal)	Square root of mean
		ML translation (bone/metal)	
GZ 2-3 index	Radiographs of intact femora	Min PMMA thickness (Gruen zone 2)	Square root of mean
		Max PMMA thickness (GZ 2)	
		Min PMMA thickness (GZ 3)	
		Max PMMA thickness (GZ 3)	
GZ 4 index	Radiographs of intact femora	Min PMMA thickness (GZ 4)	Square root of mean
		Max PMMA thickness (GZ 4)	
GZ 5-6 index	Radiographs of intact femora	Min PMMA thickness (GZ 5)	Square root of mean
		Max PMMA thickness (GZ 5)	
		Min PMMA thickness (GZ 6)	
		Max PMMA thickness (GZ 6)	
GZ 9-10 index	Radiographs of intact femora	Min PMMA thickness (GZ 9)	Square root of mean
		Max PMMA thickness (GZ 9)	
		Min PMMA thickness (GZ 10)	
		Max PMMA thickness (GZ 10)	
GZ 11 index	Radiographs of intact femora	Min PMMA thickness (GZ 11)	Square root of mean
		Max PMMA thickness (GZ 11)	
GZ 12-13 index	Radiographs of intact femora	Min PMMA thickness (GZ 12)	Square root of mean
		Max PMMA thickness (GZ 12)	
		Min PMMA thickness (GZ 13)	
		Max PMMA thickness (GZ 13)	
Void index	Radiographs of intact femora	Number of voids in CC view	Square root of mean
		Number of voids in ML view	
Radiolucency index 1	Radiographs of intact femora	Length of radiolucencies in CC view (bone/PMMA interface)	0 = no radioluc.; 1 = radioluc. detected
		Width of radioluc.(CC view, bone/PMMA interface)	
		Length of radioluc. (ML view, bone/PMMA interface)	
		Width of radioluc. (ML view, bone/PMMA interface)	
Radiolucency index 2	Radiographs of intact femora	Length of radioluc. (CC view, PMMA/metal interface)	0 = no radioluc.; 1 = radioluc. detected
		Width of radioluc.(CC view, PMMA/metal interface)	

		Length of radioluc. (ML view. PMMA/metal interface)	
		Width of radioluc. (ML view. PMMA/metal interface)	
Crack index	Radiographs of intact femora	Length of cracks in PMMA (CC view)	0 = no cracks; 1 = cracks detected
		Length of cracks in PMMA (ML view)	
Area index	Slice analysis	Area of metal implant	Mean
		Area of PMMA	
Distance index	Slice analysis	Distance between PMMA and metal centroids	Square root of mean
		Distance between Bone and metal centroids	
Shape Index 1	Radiographs of intact femora	GZ 4 index	Mean of 2 indices.
		GZ 11 index	
Shape Index 2	Radiographs of intact femora	Difference between GZ 4 index and GZ 11 index	Difference between 2 indices.
Additional Problem	Radiographs of intact femora & Chart	Separates unilaterals with other disease conditions into one group and bilaterals and unilaterals with unilateral DJD into a second group.	1 = unilat. With other disease; 0 = others
BM1	Chart	Implant design	1 = BioMed #1; 0 = others
BM2	Chart	Implant design	1 = BioMed #2; 0 = others

Table 3.4 – Name and definition of index variables created from factor analysis and used in multiple linear regression analysis.

Table 3.5					
Dependent Variable	**Independent Variable**	**Pearson's rho**	**R^2**	**p**	**Power**
Bone/PMMA Index	Radiolucency Index 1	0.452	0.204	0.009	0.766
	Implant Duration	-0.438	0.192	0.016	0.701
Bone/Metal Index	Distance 3	0.590	0.348	0.001	0.956
	Shape Index 2	0.441	0.194	0.019	0.673
	Number of Implants	-0.438	0.192	0.017	0.686
	Radiolucency Index 1	0.384	0.148	0.043	0.534
PMMA/Metal Subsidence	Bone area	0.378	0.143	0.047	0.518
PMMA/Metal ML Translation	Void index	-0.394	0.156	0.042	0.541
	BM2 index	0.429	0.184	0.023	0.645
Implant Duration	Age at Surgery	-0.540	0.291	<0.001	0.947
	Radiolucency Index 1	-0.458	0.210	0.008	0.779
	Min. PMMA	-0.352	0.124	0.045	0.526

Table 3.5 – Results of simple linear regression analysis by dependent variable in order of descending R^2. The sign of the Pearson's rho indicates whether the correlation between the dependent and independent variables is negative or positive.

Table 3.6					
Selection Method	**Dependent Variable**	**Model R^2 / p**	**Independent Variable**	**Parameter Estimate**	**Par. p**
Backward	Bone/PMMA index	0.735 <0.001	Area index	-0.076	0.004
			GZ 5-6 index	5.539	0.001
			Distance index	-6.502	<0.001
			Shape index 1	2.453	<0.001
			Shape index 2	6.853	<0.001
			BM1 index	4.744	<0.001
Best – 2 variable	Bone/PMMA index	0.518 <0.001	Implant duration	-0.797	<0.001
			Shape index 2	7.377	<0.001
Best – 2 variable	Bone/PMMA index	0.449 0.001	GZ 12-13 index	-5.686	0.006
			Radioluc. Index 1	6.928	<0.001
Best – 3 variable	Bone/PMMA index	0.628 <0.001	Implant duration	-0.858	<0.001
			GZ 2-3 index	-3.530	0.007
			Shape index 2	8.034	<0.001
Best – 4 variable	Bone/PMMA index	0.671 <0.001	Implant duration	-0.853	<0.001
			Area index	-0.045	0.083
			GZ 5-6 index	1.265	0.386
			Shape index 2	7.421	<0.001
Backward	Bone/metal index	0.765 <0.001	Area index	-0.190	<0.001
			Shape index 1	3.124	0.001
			Shape index 2	3.077	0.002
			BM1 index	6.993	<0.001
			BM2 index	11.270	<0.001
Best – 2 variable	Bone/metal index	0.496 <0.001	Area index	-0.128	0.001
			Number of implants	-7.246	<0.001
Best – 2 variable	Bone/metal index	0.457 <0.001	GZ 2-3 index	-7.901	0.001
			Radioluc. index 1	8.854	<0.001
Best – 3 variable	Bone/metal index	0.600 <0.001	GZ 2-3 index	-7.480	<0.001
			Crack index	6.570	0.006
			Number of implants	-7.126	<0.001
Best – 4 variables	Bone/metal index	0.688 <0.001	Implant duration	-0.599	0.021
			GZ 2-3 index	-7.226	<0.001
			Crack index	8.204	<0.001
			Number of implants	-5.772	0.001

Table 3.6 – Representative example of results of multiple linear regression analysis using backward and best model selection methods. The parameter estimate indicates whether the correlation is negative or positive.

Table 3.7			
Dependent Variable	**Correlation Direction**	**Independent Variable**	**Data Source**
Bone/PMMA Index	Positive	BM1 index	Chart
		GZ 5-6 index	Radiographic evaluation
		Shape index 1	
		Shape index 2	
		Radiolucency index 1	
	Negative	Implant duration	Chart
		GZ 12-13 index	Radiographic evaluation
		GZ 2-3 index	
		Area index	Slice evaluation
Bone/metal index	Positive	BM1 index	Chart
		BM2 index	
		GZ 5-6 index	Radiographic evaluation
		Shape index 1	
		Shape index 2	
		Radiolucency index 1	
		Crack index	
	Negative	Implant duration	Chart
		Nbr of implants	
		GZ 2-3 index	Radiographic evaluation
		Area index	Slice evaluation

Table 3.7 – Trends found during multiple linear regression analysis.

3.10. Figures

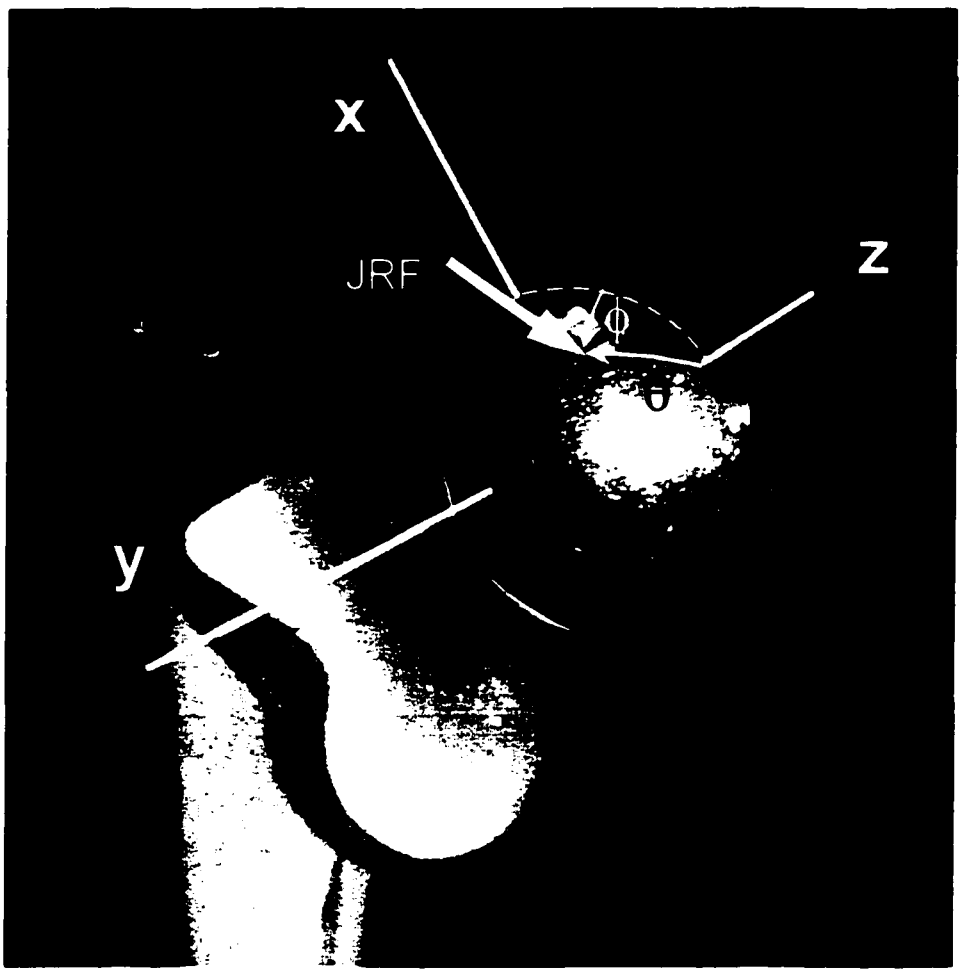

Figure 3.1 – Photograph of BioMedtrix #2 femoral component marked with coordinate system. Origin is the center of the femoral head. The z-axis runs parallel to the femoral neck. The x-axis is perpendicular to the femoral neck and is directed laterally and dorsally. The y-axis in the right femoral component (as shown) is directed cranially. θ = cone angle. ϕ = polar angle. JRF = joint reaction force.

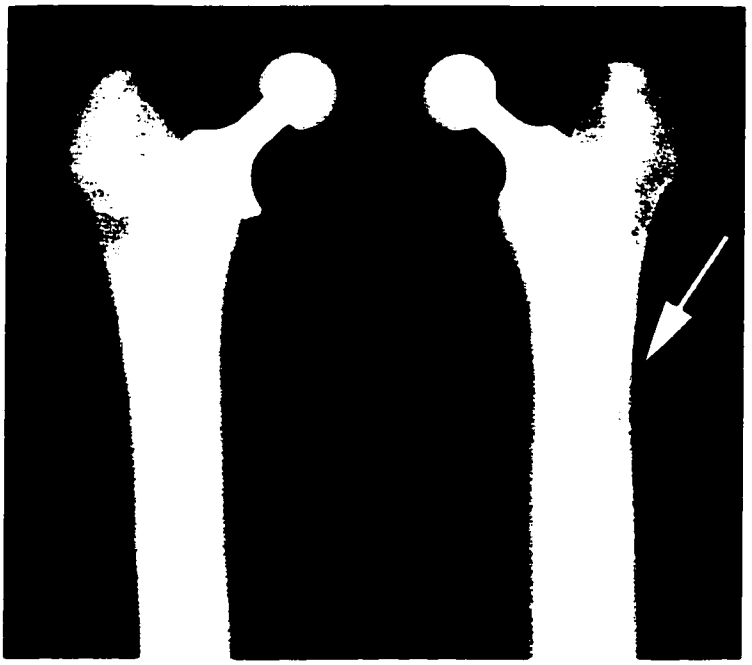

Figure 3.2 – Contact radiograph of bilateral canine THA. Femoral component shown on the right was grossly loose. Note arrow pointing to radiolucency at bone/PMMA interface and crack extending from bone/PMMA interface to PMMA/metal interface. Femoral component shown on left was firmly implanted.

Figure 3.3 - Femur (wrapped in saline-soaked towels and mounted in custom test jig) being tested for implant stability. The femur is mounted upside down so that the femoral head is toward the load cell. An extensometer is mounted to the relative motion device.

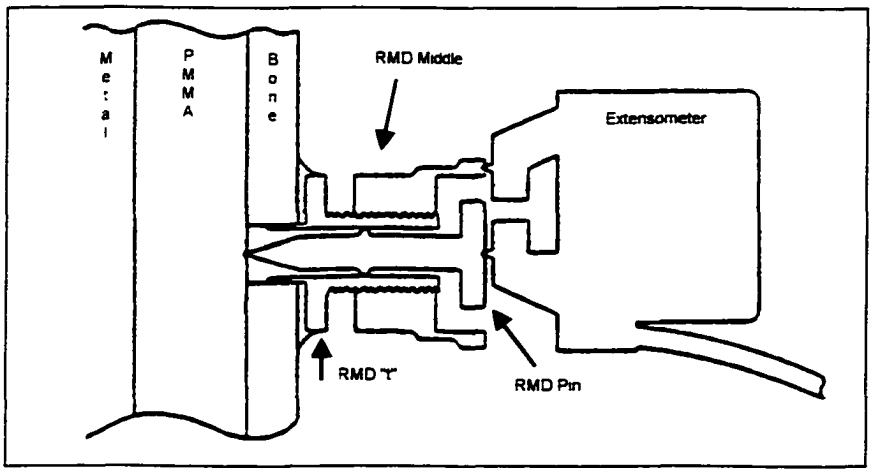

Figure 3.4 – Schematic drawing of relative motion device (RMD) being used to measure relative motion at the bone/PMMA interface of a femoral component. The extensometer is mounted for testing in subsidence. Adapted from O'Connor, *et al.* [38].

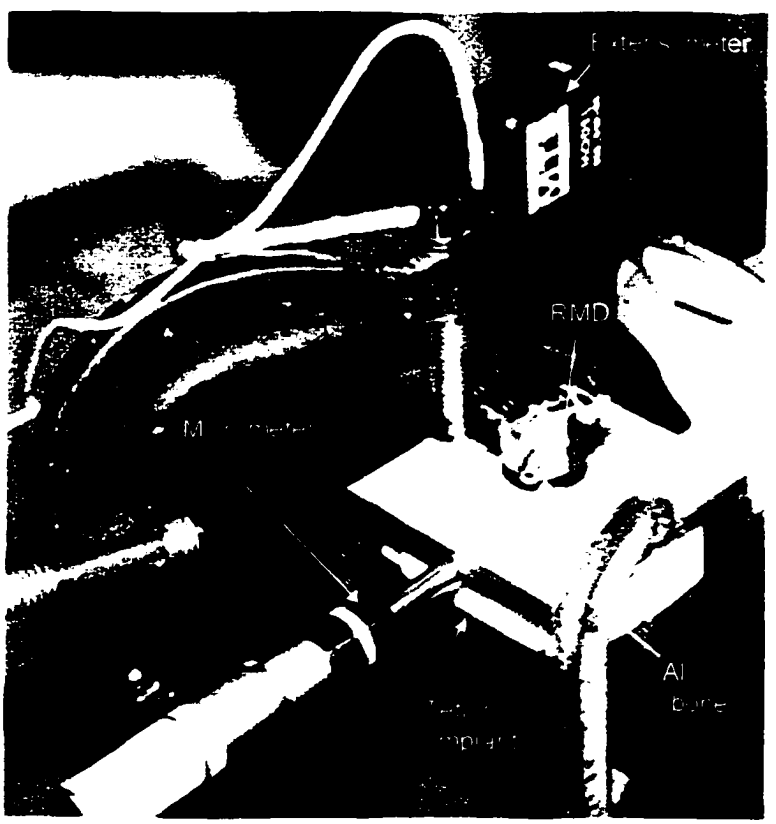

Figure 3.5 – Photograph taken during calibration of relative motion device (RMD).

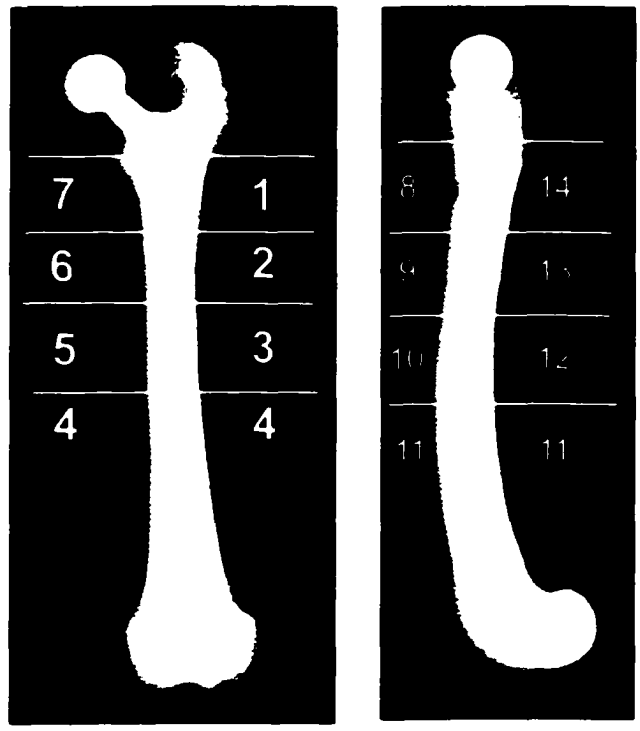

Figure 3.6 – Cranial-caudal (left) and medial-lateral (right) contact radiographs with modified Gruen zones marked.

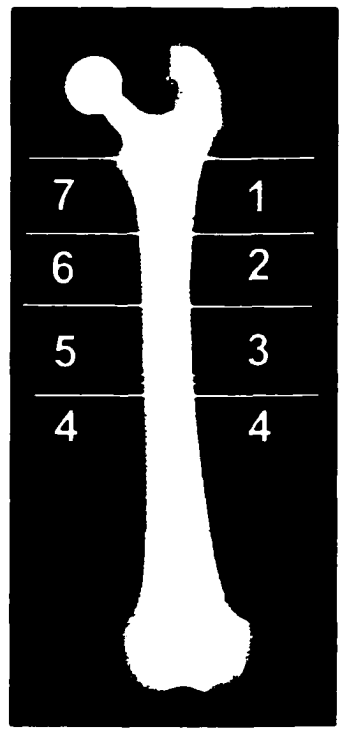

Figure 3.7 – Location of sixth-2 mm transverse slices taken from femora.

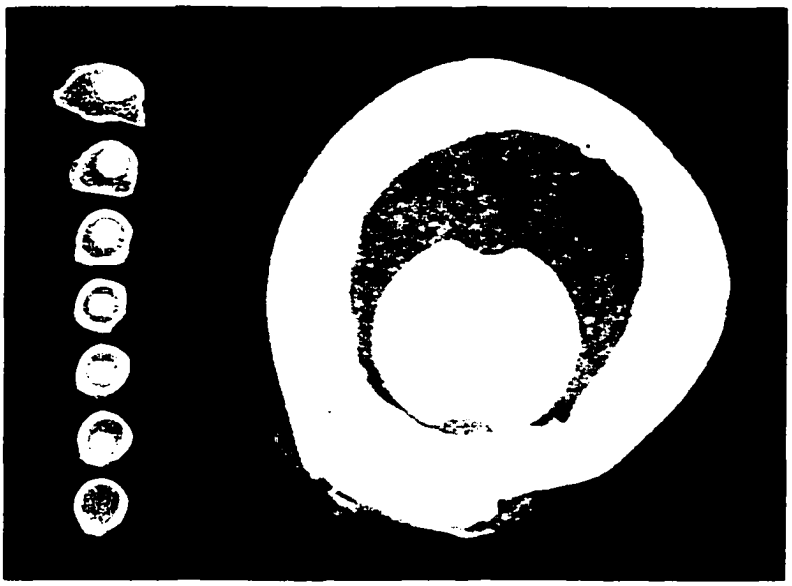

Figure 3.8 – (Left) Contact radiograph of seven-2 mm thick slices of canine femur implanted with THA. (Right) Enlarged view of sixth slice.

Figure 3.9 – Two femoral slices with measurements taken during digital image analysis marked on them. Lines are marked to indicate the locations where the maximum and minimum thicknesses PMMA were measured. (1) = centroid of the metal implant; (2) = centroid of PMMA; (3) = centroid of bone; distance 1 = distance from (1) to (2); distance 2 = distance from (1) to (3); distance 3 = distance from (2) to (3).

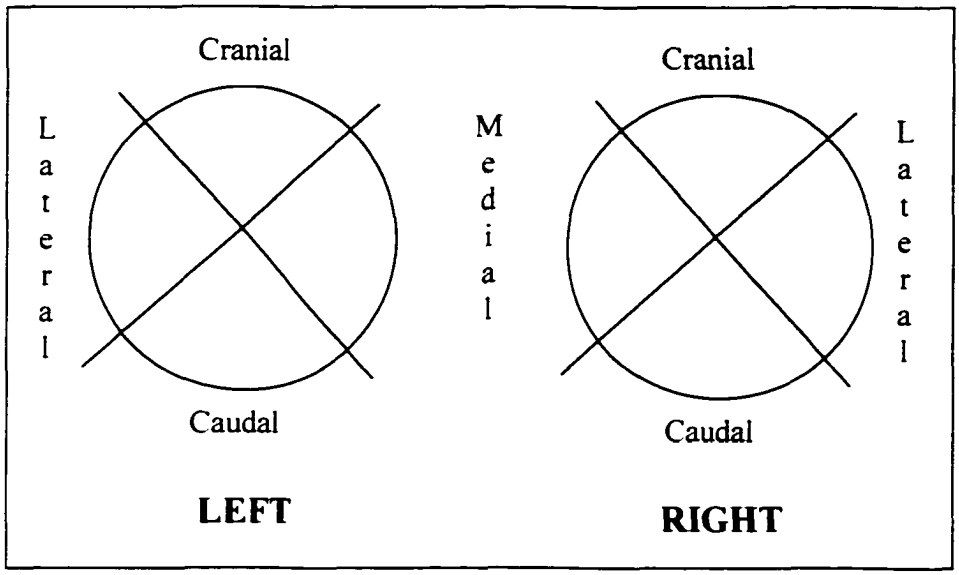

Figure 3.10 – Template used to identify quadrant in which distal tip of femoral component was in contact with endosteal bone.

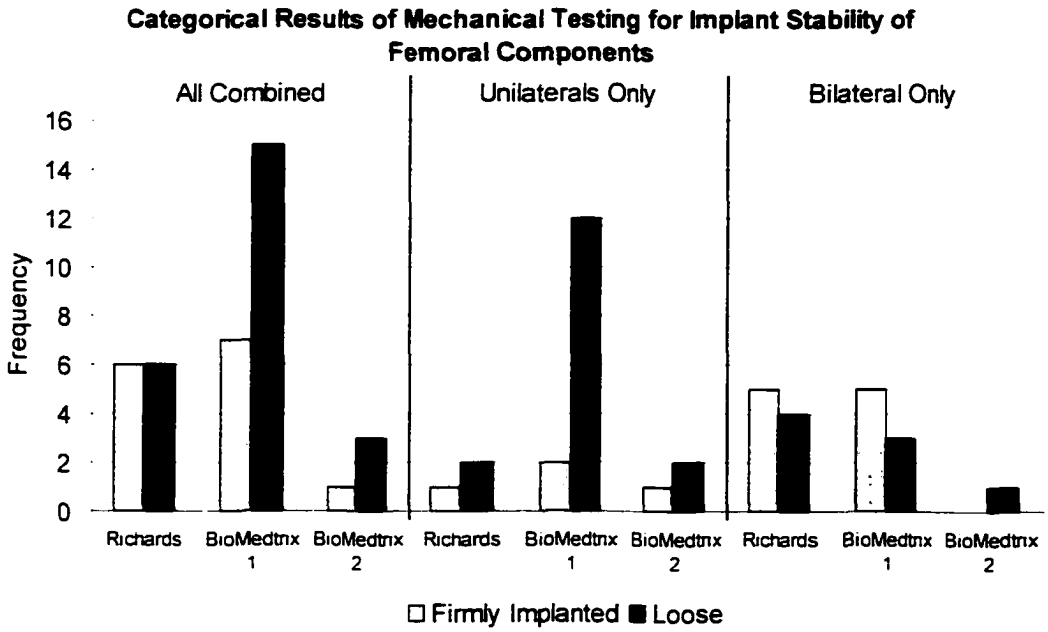

Figure 3.11 – Categorical results of non-destructive mechanical testing of femora for implant stability.

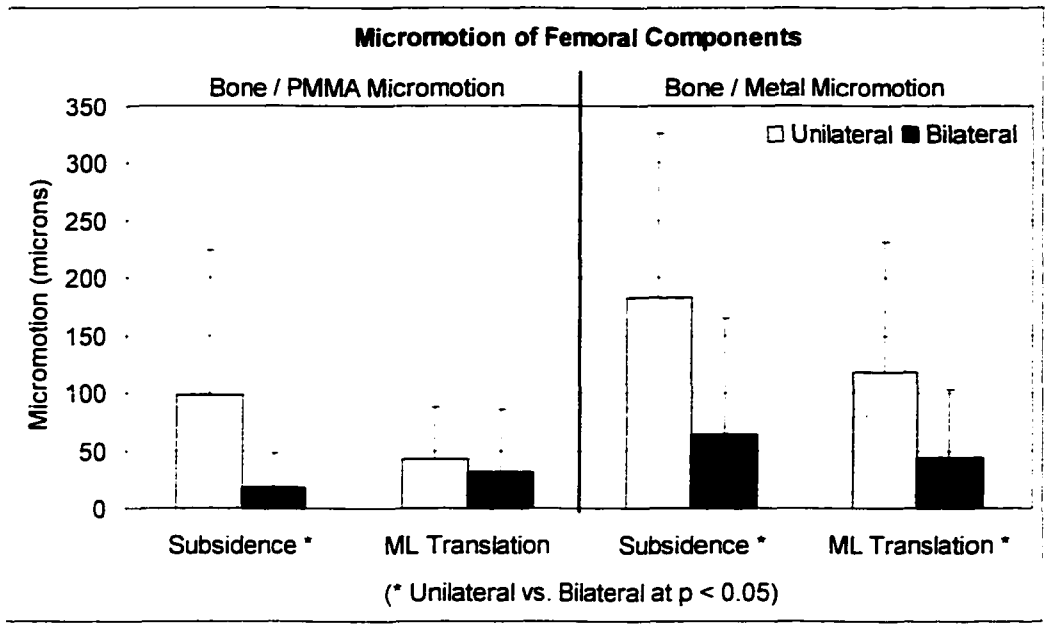

Figure 3.12 – Micromotion of unilateral vs. bilateral implants at each interface and in each test direction.

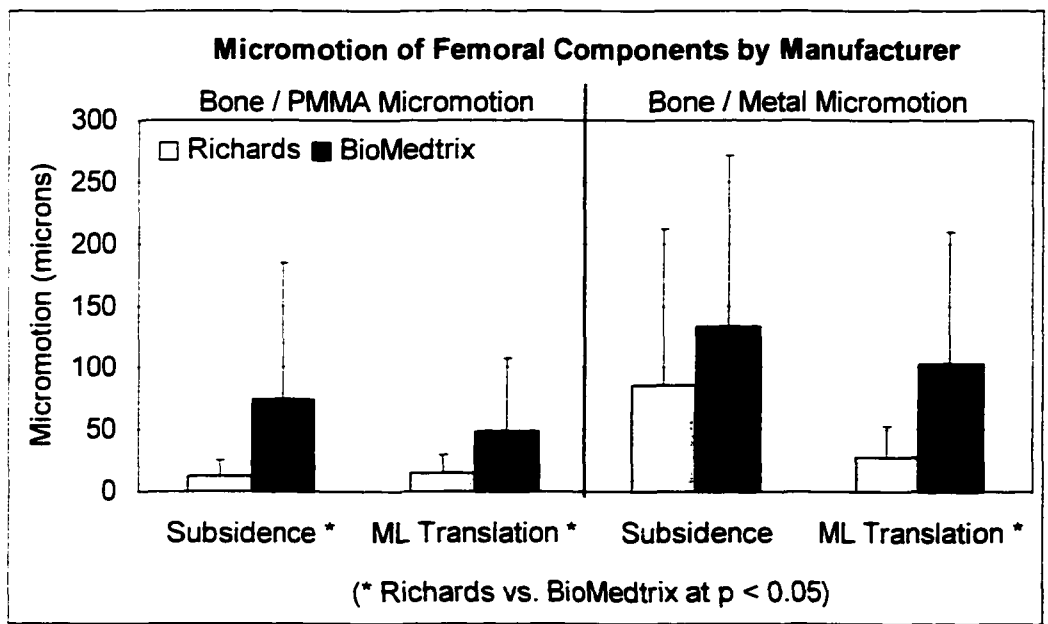

Figure 3.13 – Micromotion measurements by manufacturer at each interface and in each test direction.

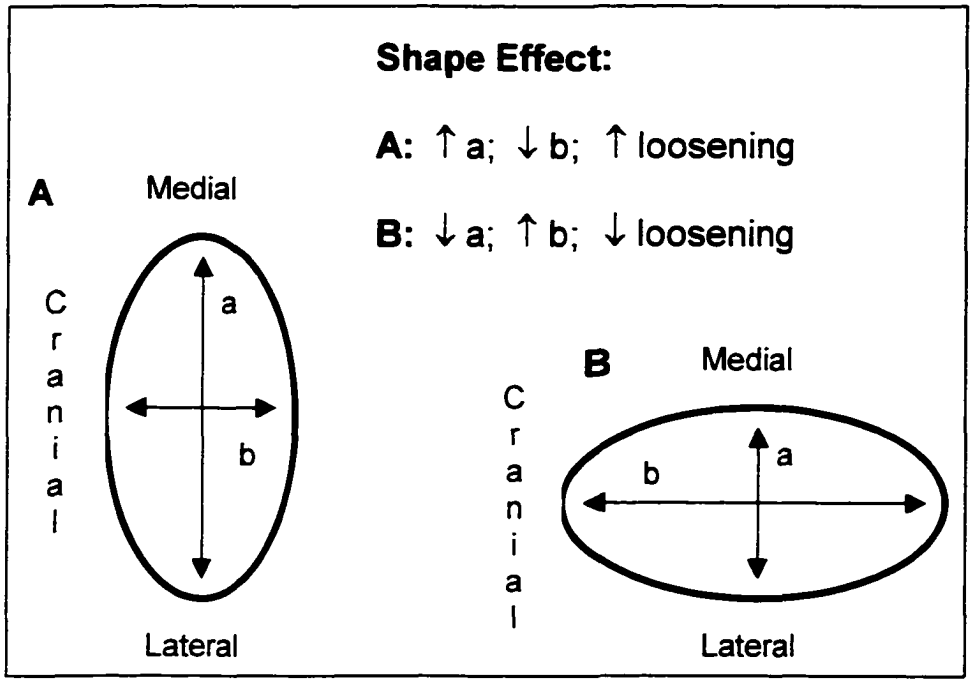

Figure 3.14 – Shape effect of femoral medullary canal on loosening of femoral component.

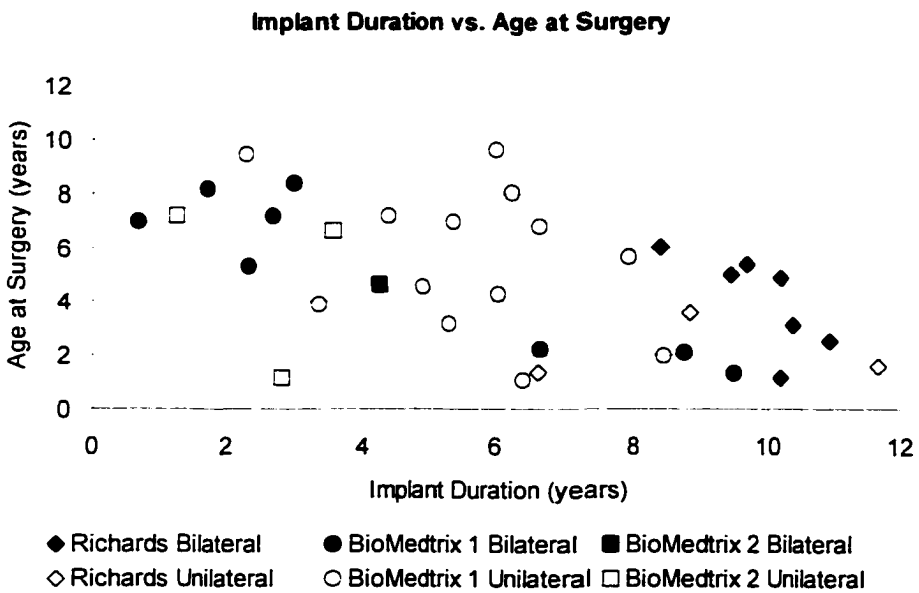

Figure 3.15 – Significant negative correlation between implant duration and age at surgery ($R^2 = 0.274$, $p = 0.002$).

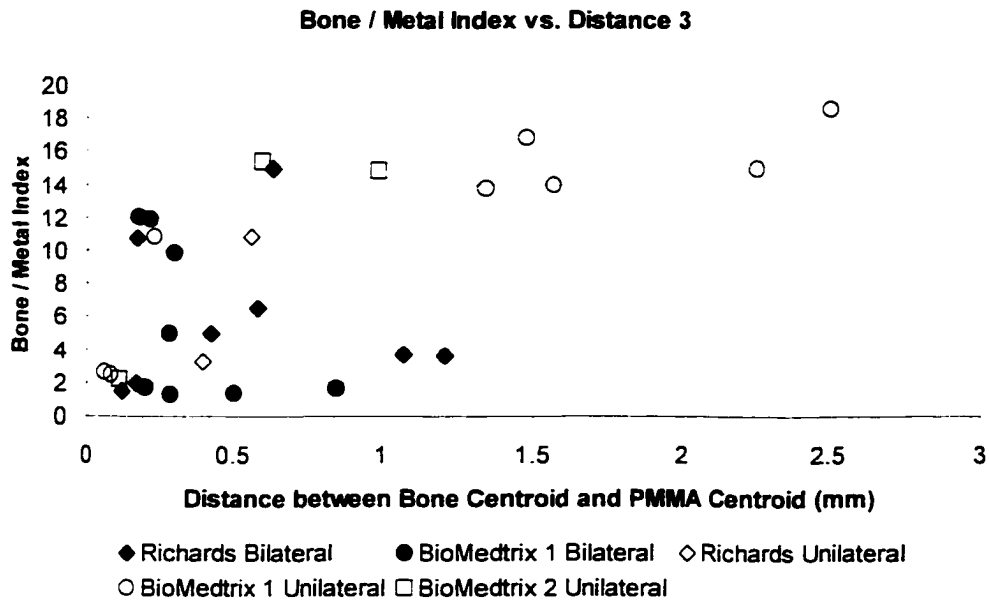

Figure 3.16 – Significant positive correlation between bone/metal index and distance between PMMA centroid and bone centroid ($R^2 = 0.348$. $p = 0.001$).

Chapter 4

Postmortem Retrieval Analysis of the Cemented Acetabular Component in Clinical Total Hip Arthroplasty in Dogs

4.1. Introduction

4.1.1. Human Total Hip Arthroplasty

One of the most common complications following total hip arthroplasty (THA) in humans is aseptic loosening. In human THA, Mulroy *et al.* [1] defined two levels of failure for cemented acetabular components that were non-metal backed and made of ultra high molecular weight polyethylene (UHMWPE): aseptic loosening requiring revision surgery, and asymptomatic acetabular components showing radiographic evidence of loosening. Aseptic loosening of the acetabular component resulted in revision surgery in 10% of cases after 15 years follow-up. The rate of aseptic loosening based on radiographic evidence of loosening (i.e., radiolucency) without revision surgery was 42%. Thus 52% of acetabular components showed evidence of aseptic loosening at 15 years after primary THA surgery. Klapach *et al.* [2], in performing survivorship analysis for cemented non-metal backed UHMWPE components at another center, reported aseptic loosening of the acetabular component resulting in revision surgery in 12% of cases at 15 years follow-up and 16% of cases at 20 years follow-up. An

additional 10% of cases showed radiographic evidence of loosening for a total of 22% of acetabular components showing evidence of aseptic loosening at 15 years follow-up. At 20 years follow-up, an additional 14% of cases showed radiographic evidence of loosening for a total 29% of acetabular components showing evidence of aseptic loosening.

Iorio *et al.* [3] performed follow-up studies of cemented acetabular components, made of non-metal backed UHMWPE, after revision surgery and found radiographic evidence of loosening of the acetabular component in 5% of cases at 5 years and 26% of cases at 10 years. The rate of loosening of cemented acetabular components increases with time, especially after the first ten years [1, 4-6]. This leads to a large number of relatively late failures of acetabular components, and the increase in the rate of loosening can be exponential in nature. However, loosened acetabular components can remain clinically asymptomatic [4-5].

A review of human retrieval studies (*See Table 4.1*) [7-9] revealed that the volumetric wear rates (VWRs) of UHMWPE acetabular components that were articulated against metal femoral heads were higher for components retrieved at revision, considered to have failed, than for postmortem retrieved components, considered clinically successful.

Research on human THA over the last decade has implicated wear of the UHMWPE acetabular component as one of the main causes of aseptic loosening [8]. The primary failure mechanism for human acetabular components appears to be biological in nature, in contrast to mechanical failure of the bone cement seen on the femoral side [4, 10]. Aseptic loosening of the acetabular component begins with the generation of UHMWPE

wear debris that is dispersed into the synovial fluid that is in contact with the intraarticular edge of the bone/polymethyl methacrylate (PMMA) bone cement interface. Small UHMWPE particles enter pores in the exposed surface of the interface and cause macrophages to trigger localized bone resorption [4-5]. Soft tissue forms in the spaces previously occupied by bone. This process proceeds from the intraarticular surface toward the dome of the acetabular cup. The actual raw data, published in these autopsy retrieval studies, will be compared to the results from this study and discussed in greater detail in the discussion section of this chapter.

In a review of THA biomechanics, Huiskes and Verdonschot [11] explain that the development of an adequate finite element analysis (FEA) model for THA is not a trivial exercise. The structure of the acetabulum is more complex than the femur and is more difficult to reduce to simpler geometries for modeling purposes. Consequently, fewer stress analyses have been performed on the acetabulum, and there is little information available about the local stresses in and around the acetabular implant and the surrounding cement mantle.

The elastic moduli of the materials used for the acetabular component are considerably different than those for the femoral component (*See Section 3.1.1*). The elastic moduli of the most common acetabular component materials and bone are [11]:

1. UHMWPE = 1 GPa;
2. PMMA = 2-3 GPa;
3. Cortical bone = 15-20 GPa;
4. Cancellous bone = 500-1500 MPa.

There is a higher percentage of cancellous bone in contact with the PMMA on the

acetabular side compared with the femoral side. As described in the review of stress transfer in a composite in Section 3.1.1, the material that is the most stiff will carry more of the load [11]. UHMWPE's elastic modulus is less than PMMA and 2 orders of magnitude less than that of the metallic femoral components. In the case of the acetabular component, the PMMA would be the stiffer material, and more of the load would be carried by the PMMA. Cortical bone has the highest elastic modulus, but cancellous bone predominates on the acetabular side. Huiskes and Verdonschot [11] also state that as the UHMWPE thickness increases, the stress becomes more evenly distributed, thus decreasing stress concentrations in the PMMA.

4.1.1.1. Volumetric Wear Measurements

In order to compare the clinical canine THA findings of this study to similar studies in humans, human retrieval studies from the literature must be carefully chosen. These studies must be on human implants made from similar materials, implanted using similar attachment methods, and measured for volumetric wear using a fluid displacement method similar to the one used in this study. Thus the data from Jasty *et al.* [8] was used as the main source of comparative data for volumetric wear measurements. Data from Sychterz, *et al.* [7] provided volumetric wear data for comparison purposes using a different measurement technique (*See Table 4.1*). Jasty *et al.* [8] used a fluid displacement method for measuring total volumetric wear (TVW) similar that used in this study. Twenty-two human autopsy retrieved, UHMWPE, cemented acetabular components that had been articulated against Co-Cr femoral heads had a volumetric wear rate (VWR) of 35.0 mm^3 per year, which was higher than the 21.6 mm^3 per year [7] measured using a gravimetric and shadowgraph method. In the gravimetric method used

by Sychterz *et al.* [7], a large volume of ethanol was used to fill the entire acetabular cup. The cup was weighed empty and full of liquid; however, ethanol evaporates quickly and introduces error into the measurement. In the shadowgraph method, a mold is made of the articulating surface, and a shadow of the mold is projected against a wall in order to measure wear. This indirect measurement method introduces possible error with the making of the mold since the casting material shrinks during curing [12] and introduces error. The shadowgraph method is only a two-dimensional measurement; however, the fluid displacement method measures wear in three dimensions.

The fluid displacement method reduces error by using the same unworn femoral head, and a small volume of fluid is used to measure wear. The fluid used is vegetable oil that is less volatile than ethanol. Since a smaller volume than in the gravimetric method is used in the fluid displacement method, the difference in volumes between the worn and unworn acetabular components makes up a greater percentage of the total liquid volume thus making the measurement technique less sensitive to error.

Revision retrievals displayed a higher VWR of 62.0 mm^3 per year [8]. This is expected since revision retrievals are considered to have failed during service while the autopsy retrievals are considered to be clinically successful. In addition, Sychterz *et al.* [7] reported a VWR of 47.9 mm^3 per year for cementless, metal-backed UHMWPE autopsy retrievals. This was lower than the VWR of 94.0 mm^3 per year that Jasty *et al.* [8] reported for cemented metal-backed UHMWPE revision retrievals. Sychterz *et al.* [7] suggested that the higher wear in the metal-backed acetabular components was in part due to the fact that the UHMWPE liner was very thin. Huiskes and Verdonschot [?] stated that as the UHMWPE thickness increases, the stress becomes more evenly

distributed. thus decreasing stress concentrations which may cause the higher wear rates.

4.1.1.2. Wear Grading

Retrieved human UHMWPE acetabular cups usually exhibit a characteristic wear pattern [13]. A smooth. highly polished. high wear region is usually distinct from a low wear region. A wear ridge commonly separates the two regions. Machine lines are often still visible in the low wear region. While there is plentiful information in the literature regarding grading of UHMWPE wear. there is considerable disagreement between investigators as to the types of damage that are identified and graded. The types of UHMWPE damage commonly reported on retrievals of human UHMWPE implants are described as:

1. Creep (or permanent plastic deformation) [7. 14-16];
2. Pitting (cratering. pin-hole sized circular or diamond shaped holes) [7-8. 14. 16];
3. Embedded PMMA debris [7-8. 14-16];
4. Embedded metal debris [7-8. 13. 15];
5. Scratching [7-8. 13-16];
6. Burnishing (polishing. abrasive wear) [7-8. 14-16];
7. Abrasion (shredding. tufting) [7-8. 14-16];
8. Delamination (flaking. peeling. large sheet removal) [8. 14-16];
9. Cracking [8];
10. Presence of wear ridge [8. 13];
11. Presence of white specks [13];
12. Yellowing (discoloration. sign of oxidative degradation) [8. 13, 17].

Commonly used scoring criteria involved a semi-quantitative, non-parametric score, based on the percentage of the surface affected by each type of damage within a specific zone on the implant [14-16]:

1. 0 = A particular damage mode is not present;
2. 1 = < 10% of the articular surface was damaged (Mild damage);
3. 2 = 10-50% of the articular surface was damaged (Moderate damage);
4. 3 = > 50% of the articular surface was damaged (Severe damage).

Sychterz *et al.* [7] divided the articulating surface of the human acetabular component by using a superior-inferior line and an anterior-posterior line to divide the articulating surface into four quadrants. Where damage modes overlapped within a zone, each damage type was graded independently [15]. This meant that a cumulative damage score for a particular zone could exceed 100% of the area.

4.1.1.3. Mechanical Testing for Acetabular Implant Stability in Human THA

Literature on stability testing of the acetabular component is not as readily available as that for stability testing of the femoral component. Ohlin *et al.* [18] performed destructive mechanical tests on human acetabular components retrieved at autopsy. No further testing could be performed on these retrievals because of the destructive nature of the test. The test method involved drilling 8 holes into the rim of the cup so that a loading jig with 8 pins could be used to apply a torque parallel to the mouth of the acetabular component.

Schmalzried *et al.* [5] performed mechanical testing of autopsy retrievals and chose to mount and test the acetabular components in an anatomical position while measuring

motion between the bone and the implant using a relative motion device developed and used for mechanical testing of the femoral component (*See Chapter 3*). Holes were drilled into the bone at the apex and posterior aspects of the acetabular component and micromotion measurements were made from the backside of the acetabular component.

Schmalzried *et al.*, [5] also tested for implant stability by applying a torque parallel to the mouth of the unloaded acetabular component. A maximum torque of 11.3 N-m (100 in-lbf) was used; however, the apparatus used to apply the torque was not fully described. Firmly implanted acetabular components moved less than 100 μm under anatomical loading conditions. Under the non-anatomical test in which a torque was applied parallel to the mouth, the maximum motion was 114 μm. The reason for using such a large load was not explained. Neither were the criteria for calling an implant firmly implanted explained. No controls were used in this study. The authors also claimed that the motion measured was at the bone/PMMA interface, but the only measurement made was between the bone and the UHMWPE acetabular component.

The majority of recent studies, in which mechanical testing for stability of acetabular components was performed, involved acute implantation of cementless acetabular components in hemipelves harvested from cadavers [19-25]. Stiehl *et al.* [20] performed destructive tests that provided little insight with regard to the present study. Some of the tests performed were non-destructive in nature with loading applied in the direction of peak joint force during the stance phase of gait [19, 21-24]. Many of them measured micromotion by drilling holes into the bone on the back-side of the implant and attaching measurement devices using a variety of sensors [21, 23-24]. The remainder of the studies measured motion between the rim of the acetabular component and the bone using a

variety of devices, such as LVDTs [19-20, 22, 25].

4.1.2. Dog as an Animal Model for Human THA

For a review of the dog as an animal model for human THA and the differences in hip joint loading between humans and dogs, see Section 3.1.2.2. in Chapter 3. Of the nine experimental studies performed on healthy dogs reviewed in Chapter 3, only one abstract [26] referred to mechanical testing for stability of the acetabular component, but few details were given with regard to the actual test technique.

4.1.2.1. Differences in Hip Joint Loading Between Dogs and Humans

Section 3.1.2.2. in Chapter 3 gives a review of the differences between canine and human femora and hip joint loading. The peak joint reaction force (JRF) in the dog in three-legged stance is directed caudally, ventrally, and laterally on the head of the femoral component [27]. Conversely, the peak JRF on the acetabular component would be directed cranially, dorsally, and medially.

4.1.3. Canine Total Hip Arthroplasty

The cemented THA implant used in dogs is very similar to human implants. There have been three implant designs used at the Colorado State University Veterinary Teaching Hospital (CSU VTH), and they are described in Section 1.1.3.1 of Chapter 1.

Briefly, all acetabular components for the three implant designs that have been used at the CSU VTH were machined from UHMWPE bar stock and were non-metal backed (*See Figure 1.2*). The Richards, BioMedtrix #1, and BioMedtrix #2 acetabular components are very similar in design. The dimensions of the different implant designs are provided (*See Table 4.2*). One major difference between human and canine acetabular components is that the canine implant has a 45° fire hydrant cut-out that is

placed dorsally in the dog to minimize impingement when the hind leg is abducted.

Aseptic loosening is a common complication in cemented canine THA. A review of six canine THA outcomes assessment studies related to cemented canine THA revealed an aseptic loosening rate of 5.5% (26 of 473 cases) for follow-up periods ranging from 1 month to 6 years (*See Table 4.3*) [28-33]. These studies defined aseptic loosening of the acetabular component as cases that required revision surgery. All of these studies involved retrospective clinical follow-up studies that involved either subjective responses from owners or office visits to an orthopaedic veterinary surgeon. No data were provided with regard to acetabular components that displayed radiographic evidence of loosening.

The 5.5% canine aseptic loosening rate requiring revision surgery had follow-up times ranging from 1 month to 6 years. To the best of the author's knowledge, no follow-up data at specific times post-THA exist for aseptic loosening of acetabular components in dogs; so, comparison to human data cannot be made. However, Mulroy *et al.* [1] reported that 10% of human acetabular components at 15 years post-THA had aseptic loosening requiring revision surgery. In order to improve surgical techniques for canine THA and to prevent this type of implant failure, the initiating events leading to aseptic loosening need to be studied and understood in both species.

The surgical paradigm in existence at the CSU VTH at the beginning of this study held that dogs with bilateral degenerative joint disease (DJD) could be treated adequately with unilateral THA. Feedback from veterinary orthopaedic surgeons and owners indicated that dogs with bilateral DJD and unilateral THA would commonly adjust their gait after surgery and carry more weight on their implanted hip than on their intact, diseased hip.

4.1.3.1. Volumetric Wear Measurements

Some interspecies differences in volumetric wear are expected since dogs load their hips differently than humans. However, to the best of the author's knowledge, there have not been prior published studies on volumetric wear of canine acetabular components that were retrieved postmortem.

4.1.3.2. Wear Grading

To the best of the author's knowledge, there have not been any reports of wear grading in canine THA that are comparable to the human studies reviewed above.

4.1.4. Mechanical Testing for Acetabular Implant Stability in Canine THA

To the best of the author's knowledge, the only report of mechanical testing for implant stability of the canine acetabular component was presented in an abstract by Anderson *et al.* [26]. The test method was not fully described. There have not been any reports of mechanical testing for implant stability of canine cemented acetabular components that had been retrieved postmortem after being implanted in clinical cases.

4.2. Hypotheses

There were five hypotheses with regard to this study. The first was that, due to lower peak joint forces and differences in hip loading between dogs and humans, volumetric wear rates would be lower and wear patterns would be less extensive in canine postmortem retrievals than those seen in human studies. The second hypothesis was that primary failure mechanisms for the acetabular component in the dog would be biological in nature, as seen in human THA. The third hypothesis was that aseptic loosening would not be as pronounced in dogs as in humans due to lower peak joint

forces. Since the expectation was for lower aseptic loosening rates in dogs, the fourth hypothesis was that acetabular implants with higher volumetric wear would be less mechanically stable, similar to results in human studies [5]. The fifth hypothesis was that unilateral components would be equivalent to bilateral implants in performance. Thus, owners need only pay for one surgery, rather than two, in order to treat DJD in their dogs.

4.3. Materials and Methods

4.3.1. Preliminary Processing

Owners donated twenty-nine dogs to the CSU Orthopaedic Implant Retrieval Program (OIRP) at the time of their dogs' deaths, due to natural causes or owner-chosen euthanasia. The Institutional Animal Care and Use Committee determined that approval was not required for this study since no experiments were performed on live animals. Nine of the dogs had bilateral THA for a total of 38 implants. Twelve of the implants were Richards, 22 were BioMedtrix #1, and 4 were BioMedtrix #2 (*See Table 3.2*). There was no difference between the BioMedtrix #1 and BioMedtrix #2 acetabular components. Demographic data (e.g., surgeon, surgery date, age at surgery) were collected from the clinical charts.

Specimens were stored in a freezer at -20°C until testing began. After removal of soft tissue, the hemipelves and acetabular components were photographed for journalistic purposes. High contrast, contact radiographs in ventral-dorsal view were made using Kodak Xomat LS 8x10 Industrial Film (Eastman Kodak Company, Rochester, NY) in a Faxitron Cabinet X-Ray System (Model 43855A, Faxitron X-Ray Corporation, Wheeling, IL).

The UHMWPE articulating surface was visually inspected for general wear patterns and photographed for documentation. Close-up photos were taken, using a macro lens, of the UHMWPE articulating surface with special attention given to visible wear patterns and any other features of interest.

4.3.2. Volumetric Wear Measurement

A simple fluid displacement method for measuring the volumetric wear of UHMWPE acetabular components was developed based on similar studies performed on retrieved human acetabular cups [12-13]. This method assumes that the difference in the gap size between a new femoral head/new acetabular cup pair and a new femoral head/worn acetabular cup pair equals the volume of UHMWPE wear (*See Figure 4.1*). The volume of the gap was accurately measured using drops of vegetable oil, which wets UHMWPE. The oil was dispensed with a known drop volume (e.g., 10 μl) using an adjustable micropipette. The accuracy and repeatability of the micropipette was tested before volumetric wear measurements commenced each day. The micropipette was set to deliver 10 μl, and the number of drops of vegetable oil necessary to fill a 1 ml volumetric flask were counted. This measure was repeated three to five times each day. The volume actually delivered by the micropipette was calculated as 8.7 μl with a 95% confidence interval of 8.77 to 8.66 μl.

A slight modification to the wear measurement method for human implants was required due to the 45° fire hydrant cut-out (*See Figure 1.2*) on the canine acetabular cup. The cup had to be tilted so that the lower rim of the cut-out was level with the ventral rim in order to maximize the amount of articulating surface that could be measured. The femoral head was then placed in the acetabular cup and secured. First, a baseline

measurement was made using the new acetabular cup/new femoral head pair. Then the wear measurement was taken using the retrieved acetabular cup/new femoral head pair. The steps involved in each test are:

1. Clean the acetabular cup and femoral head with hexane and dry:
2. Clamp the acetabular cup at an angle:
3. Place the femoral head in the cup:
4. Dispense oil from pipette while counting drops until the cup is full:
5. Repeat 4-5 times per cup.

The TVW was calculated by subtracting the average baseline measurement from the average volume measured using the retrieved acetabular cup/femoral head pair. The average standard deviation among specimens was 4.2 μl. The implant duration, in years, was calculated by subtracting the surgery date from the date of the dog's death. The VWR was calculated by dividing TVW by implant duration.

4.3.3. Wear Grading

A cursory examination of the articulating surfaces of the canine retrievals for the most commonly seen damage modes was made using a stereoscopic microscope at 8x magnification. The following damage categories were used in this study:

1. Creep:
2. Pitting:
3. Embedded PMMA debris:
4. Embedded metal debris:
5. Scratching:
6. Absence of machine marks (burnishing, polishing);

7. Abrasion (tufting);
8. Non-scratch macroscopic removal of UHMWPE;
9. Yellowing of UHMWPE.

The characteristic wear ridge, commonly seen in human retrievals [13], was not noted in the preliminary examination of the canine acetabular components. The entire surface of the canine acetabular component showed high levels of wear, and rarely were there large areas with machine marks still visible. What machine marks remained were usually worn and distorted. The presence of machine marks would indicate minimal or no wear.

Human wear grading studies break the components into specific regions [7, 14]. The canine acetabular cup has a considerably different geometry from the human acetabular component because of the 45° fire hydrant cut-out. Due to the unique geometry of the canine cup, the areas chosen for individual grading scores were (*See Figure 4.2*):

1. Quadrant I (cranial-dorsal articulating surface);
2. Quadrant II (caudal-dorsal articulating surface);
3. Quadrant III (ventral-caudal articulating surface);
4. Quadrant IV (ventral-cranial articulating surface);
5. Cranial corner (corner of 45° cut-out);
6. Caudal corner (corner of 45° cut-out);
7. Cut-out rim (rim of acetabular component along cut-out);
8. Cranial rim (cranial half of rim);
9. Caudal rim (caudal half of rim).

The scoring criteria for each zone and damage type (*See Appendix G - Wear Grading*

Form for Acetabular Component) were based on several human studies [14-16] as described above in Section 4.1.1.2.

Each acetabular component was graded twice by the same observer on different days, and scores were then averaged. The wear grading form (*See Appendix G*) was designed so that scores totaled horizontally across the page reflected the total score for each damage type across all zones. The scores that were totaled vertically down the page reflected the total damage score for each zone across all damage types. The grand total score for UHMWPE damage was in the lower right hand corner of the form. Thus, there were 18 sub-total scores and one grand total score for each specimen.

4.3.4. Mechanical Testing for Implant Stability

Mechanical testing for implant stability in autopsy retrieval studies of human THA are rarely performed, and the test methods are often destructive in nature. Due to the potential for multiple studies from the test specimens (*See Chapter 8 – Future Work*), a non-destructive testing method was desired. The intent of this test was not to measure strain at the interfaces but rather to classify the acetabular components as loose or firmly implanted.

An added complication to developing a test method for canine acetabular components was the small size of the implant compared to human acetabular components. In addition, several of the specimens included only fragments of the hemipelvis, rather than the entire hemipelvis. This posed challenges with regard to mounting each of the specimens firmly for testing purposes. With those acetabular components mounted in pelvic fragments, it would have been impossible to mount the specimens while measuring micromotion from the backside of the acetabular component

as Schmalzried *et al.* did in human studies [5]. There was also concern that drilling a 6.4 mm (one-quarter inch) diameter hole into the bone behind an acetabular component that was 29 mm or less (less than one and one-quarter inches) in diameter would destabilize the construct.

Due to the difficulties in adapting test methods used in human THA retrieval studies, a novel test method was developed (*See Figure 4.3*) based on a simple laser measurement technique [34]. Testing was not performed at each of the interfaces as in the femoral component (*See Chapter 3*) because of fears that drilling holes through the bone to the PMMA and to the implant would destabilize firmly implanted components.

4.3.4.1. Calibration of the Laser Test Method

Potential sources of error for this test method included the size of the laser reflection on the wall, the measurements made of the laboratory's dimensions, the angle of the laser mirror relative to the wall, the differing outer diameters of the different sizes of acetabular components, movement of the specimen within the grips during testing, and placement of the bone laser mirror.

An inexpensive laser pointer (Clearline Concepts Model CL2001 Laser Pointer, maximum output <5 mW, wavelength 650 nm, Class IIIA laser product, Clearline Concepts, Boonton, NJ) was selected for a two of reasons. First, the size of the laser spot on the laboratory wall was small and oval in shape. The spot from the laser pointer had an intense inner spot (approximately 3 mm x 2 mm) within a larger, more diffuse spot (approximately 7 mm x 4 mm) that was easily marked and measured (*See Appendix H*). Second, two lasers were required for this test method, and the small laser pointer could easily be mounted to a shelf attached to the upright bearing of the MTS mechanical

testing system (MTS Corporation. Eden Prairie. MN) (*See Figures 4.3 & 4.4*). Simple brackets constructed of wood and plastic cable clamps held the lasers in place. The plastic clamp was also used to depress the on/off button of the laser during testing to allow hands-free operation of the laser.

One laser was reflected off a laser mirror that was mounted to the acetabular component. and the second laser was reflected off a laser mirror that was mounted to the surrounding bone. The square laser mirrors used were 15 mm x 15 mm and had the reflective coating on the front of the laser. The placement of the UHMWPE laser mirror was consistent among the specimens. The acetabular components were mounted on the MTS so that the fire hydrant cut-out was toward the laboratory wall onto which the lasers were reflected. and the acetabular component was centered at the center of rotation of the actuator. A bone pin was placed in the cutout rim at the cranial corner on left specimens and the caudal corner on right specimens (*See Figure 4.5*). The laser mirror was attached to the bone pin with gel Super Glue™ (cyanoacrylate). The diameter of the acetabular component was the only variable that changed the placement of the UHMWPE laser mirror.

A second laser was reflected off a laser mirror that was mounted to the bone near the acetabular component. The bone laser mirror was placed caudal to left acetabular components and cranial to right acetabular components. The placement of the bone laser mirror was more variable due to the great variability in the geometry of the specimens and the placement of the bone pin (*See Figure 4.5*). This made calibration of the bone laser more difficult. As a result. the bone laser was used to verify that the hemipelvis was firmly mounted and did not move during the mechanical testing. If the bone laser spot on

the wall showed movement of the specimen, the specimen was re-mounted in the grip and the test was repeated.

The remainder of the sources of error were accounted for by the UHMWPE laser calibration method (*See Appendix H*). Movement on the wall by the UHMWPE laser spot was calibrated within a certain zone on the wall that was 3.5 mm from the center of rotation of the MTS actuator. Movement of the laser was linear for up to 5 degrees of rotation. The MTS actuator rotated through 2 degrees during the test, and the laser mirror was aimed so that the spot fell within the zone that was calibrated for 5 degrees of rotation. See Appendix H for a detailed description of the calibration of the UHMWPE laser spot movement on the laboratory wall. The calibration curves were repeated at the different radii of the acetabular components, and all curves fell within the same 95% confidence intervals for all calibration curves. Different calibration curves were not required for the different sized acetabular components. The 95% prediction confidence limits for the y-direction (i.e., horizontal movement) movement of the UHMWPE laser spot was 8.7 mm (±4.4 mm). When the calibration curve parameters were used to calculate the degrees of rotation of the acetabular component, the 95% prediction confidence limit was 0.08 degrees (±0.04 degrees).

4.3.4.2. Laser Test Method to Assess Acetabular Implant Stability

The hemipelvis was potted so that the rim of the acetabular component was level and the fire hydrant cutout faced the wall upon which the lasers were reflected. One bone pin was place in the acetabular component in the cutout rim at the corner (i.e., cranial corner for left side; caudal corner for right side). A second bone pin was placed into the bone near the acetabular component (i.e., caudal to left side; cranial to right side) (*See Figures*

4.3, 4.4, & 4.5). Front reflecting laser mirrors were mounted to the bone pins using gel Super Glue™. The UHMWPE laser mirror was aimed so that the laser spot on the wall fell within the calibrated zone (*See Section 4.3.4.1. for calibration method*). Lasers were focused on the laser mirrors and reflected onto the laboratory wall approximately 3.5 m from the center of rotation of the MTS actuator. A custom designed loading jig (*See Figure 4.5*) was used to apply a torque parallel to the rim of the acetabular component until the actuator had rotated 2 degrees.

Loose and firm controls were used to determine criteria for categorizing the acetabular components as firmly implanted, borderline, and loose. Both the loose and firm controls were implanted with a size 27 mm BioMedtrix #2 acetabular component. The firm control was implanted into a hemipelvis that was harvested from a cadaver by a veterinary orthopaedic surgeon using standard surgical technique. The loose control was implanted in a similar manner, but the acetabular component was rotated and rocked while the PMMA was curing in order to create a loose UHMWPE/PMMA interface. The criteria for categorizing an implant as firmly implanted, borderline, or loose were based on the 95% confidence interval of the calibration curve and the results of the mechanical testing of the loose and firm controls.

During testing of the controls and retrievals, a z-component (i.e., vertical movement of laser spot on the wall) as well as a y-component (i.e., horizontal movement of laser spot on the wall) were noted (*See Figures 4.4 & 4.6 for coordinate system*). The z-component of the movement was more problematic to characterize. For example, there was a larger z-motion in a firmly implanted component than in some loose components. Since the UHMWPE implant was not moving, the UHMWPE was being deformed by the

pins of the loading jig, thus causing the UHMWPE laser mirror to rock backward as the UHMWPE was deformed. In loose components, the z-motion was negligible in some and considerable in others. However, it appeared that the z-component often increased toward the end of the test when perhaps the loose implant came in contact with PMMA or bone that impeded its movement in the y-direction. The loose UHMWPE component, if loose at the UHMWPE/PMMA interface would perhaps rock within the PMMA as it rotated, thus adding a vertical component to its motion. In either case, the z-motion was difficult to use to characterize the stability of the implants. The y-motion (i.e., horizontal motion along the wall) appeared to give a very clear picture of a continuum of firmly implanted to loose acetabular components.

A laminated dry-erase poster was mounted to the laboratory wall that was 3.5 m from the center of rotation of the MTS in order to provide a smooth surface for recording the movement of the laser spots. Tractor-feed continuous form computer printer paper was taped to the laminated poster so that the laser spots at the zero position were placed with enough room to record movement in the direction in which the laser spot would be travelling. The test date, specimen identification number, side, and MTS data set name were recorded on the paper. The paper was marked with its location relative to a fixed point in the room, and a carpenter's level was used to draw level lines under both the UHMWPE and bone laser spots before testing began. The torque was applied clockwise on right specimens and counter-clockwise for a left specimen. This loading technique was chosen based on the direction of the peak joint reaction force (*See Section 3.1.2.2.*) and the most likely direction of rotation if the implant was loose. The loading sequence began with a 30 second hold at the zero degree position to allow the operator to record

the locations of the UHMWPE and bone laser spots on the paper. Then the actuator was rotated by 0.2 degrees over 10 seconds followed by a 30 second hold for each increment of rotation to allow the operator to record the locations of the laser spots on the paper. During the ramp, the MTS program collected data every 0.25 seconds. During the hold periods, data was collected every 5 seconds. The data collected were time, crosshead displacement, axial force, actuator angle, and torque. This continued through 2 degrees of actuator rotation. After the test, the paper was removed from the wall. Later, measurements were made of the y- and z-motion relative to the location of the 0 degree point and the level line drawn using the carpenter's level.

The laser spot on the wall had an intense interior oval (approximately 3 mm x 2 mm) surrounded by a larger more diffuse oval (approximately 7 mm x 4 mm). To measure displacement of the laser spot, an x was drawn through the spot to find the center. One line was drawn through the longer axis of the oval., and the other line was draw perpendicular to the first through the center of the small, intense inner spot. A line was drawn from the center of the spot to the level line drawn using the carpenter's level. Y- and z-motion measurements were made relative to the level line and the 0 degree spot.

One observation made during testing was that the movement recorded at 1 degree of actuator rotation provided a more clear picture of loose vs. firmly implanted specimens. At 2 degrees of rotation, it appeared that some of the loose implants had impinged on bone or PMMA that impeded the acetabular components' rotation. Thus, it was decided to use the data at 1 degree of actuator rotation to classify the specimens as loose or firmly implanted.

A 1 degree of actuator rotation, the firm control moved 0.05 degrees, and the loose

control moved 0.20 degrees in the y-direction. The designation of "firmly implanted" was given to any implant with recorded motion of 0.09 degrees or less (i.e., firm control's 0.05 degrees plus the 0.04 degree error calculated from the 95% prediction confidence limits of the calibration curve (*See Section 4.3.4.1.*). The designation of "loose" was given to any implant with recorded motion of 0.16 degrees or more (i.e., loose control's 0.20 degrees minus the 0.04 degree error from the 95% prediction confidence limits of the calibration curve). There were several implants with recorded movement between 0.09 and 0.16 degrees. There was no clear break in the data between loose and firmly implanted acetabular components as there had been for the femoral components (*See Chapter 3*): therefore, and "borderline" designation was given to those specimens.

Two calculations were made from the y-motion data. First, the y-motion was converted to degrees of rotation based on the parameters of the calibration curve. Second, a non-dimensionalized calculation was made by calculating the chord length of the micromotion of the acetabular component and dividing that number by the circumference of the acetabular components. This was done to normalize the measurements for the different sizes of implant. However, this calculation effectively took the degree measurement and divided it by 360 (*See formulas in Appendix I*). The data used in the data analysis was left as degrees of rotation.

4.3.5. Statistical Analysis

Statistical analysis was performed using SAS software (SAS Institute, Cary, NC). Statistical analysis was performed with the assistance of the Center for Applied Statistical Expertise (CASE) in the Statistics Department at CSU. The low number of specimens and the large number of variables in this study presented challenges for statistician and

researcher.

The SAS factor procedure [35] was used to perform principal component analysis in order to identify highly correlated variables. These results were analyzed in combination with expert opinion of engineers and veterinary surgeons in order to select variables that could be combined into index variables and thus reduce dimensionality (i.e., number of variables). Square root transformations were used for those indices that did not have a normal distribution in order to allow the use of parametric statistics.

Simple and multiple linear regression analyses were performed with the PE micromotion index (from mechanical testing), TVW, and VWR as the dependent variables. For multiple linear regression, two model selection methods were used in attempting to determine the best model for predicting the selected dependent variables [35-36]. The best selection method calculates the coefficient of determination (R^2) for all possible models for each number of variables being considered (e.g., one to four variables models). The models with the greatest R^2 are selected for each number of variables (*See Appendix F for sample output*). The backward selection method starts by fitting the multiple regression model containing all the possible independent variables. At each step, the variable that makes the smallest contribution to the model (i.e., smallest F statistic) is deleted. This process continues until an F statistic for a particular model meets the significance criteria that is preset by the investigator.

In addition, simple linear regression for all variables vs. implant duration were also performed to look for time-dependent trends.

4.4. Results

Twenty-nine dogs, 9 with bilateral implants, were donated (*See Table 3.2*) for a total of 38 implants. Implant duration ranged from 8 months to 11 years and 8 months. The weights of the dogs ranged from 18.2 kg (40 lbs) to 66.4 kg (146 lbs). Using one-way analysis of variance (ANOVA), there were no significant differences in age or weight between implant designs.

4.4.1. Preliminary Processing

Upon visual inspection of the acetabular components, the wear patterns were markedly different from human postmortem retrievals. Large areas of implant-on-implant damage included impingement on the corners and on the cut-out rim. Aggressive third body wear damage was widespread, and there was commonly a distinctive area of aggressive third body wear on the articulating surface near the ventral rim of the cup. Third body wear damage was often seen on the entire articulating surface, and some of the acetabular components were no longer supported by PMMA around the rim. Upon cutting the joint capsule open, PMMA fragments as large as 1 cm long were found loose in the joint in three retrievals. In one of these cases, small PMMA wear debris fragments were also packed within the joint capsule between the neck of the femoral component and the greater trochanter. Only one implant, retrieved from the largest dog (66.4 kg), displayed a burnished surface similar in appearance to human autopsy and revision retrievals. However, the entire articulating surface was highly polished, and there was no low wear area or wear ridge as seen in human retrievals [13].

4.4.2. Volumetric Wear

During the measurement of TVW, it was noted that, despite the 45° fire hydrant cut-

out. the entire articulating surface of the canine acetabular component was measured due to capillary action of the vegetable oil and the tilting of the acetabular component. Average VWR for all implants was 6.7 ± 4.2 mm^3 per year.

Using Tukey-Kramer multiple comparisons. TVW was significantly greater for Richards than for BioMedtrix #1 for all implants combined and for bilaterals only ($p < 0.05$) (*See Figure 4.7*). This was expected due to the fact that Richards was the first implant design used at the CSU VTH. There was no significant difference in VWR among implant designs or between unilaterals and bilaterals.

There was a significant positive correlation between TVW and implant duration (*See Table 4.5 & Figure 4.8*). This correlation was quite strong despite the presence of two outliers with extraordinarily high volumetric wear.

There was a trend toward negative correlation between implant duration and VWR (Pearson's rho = -0.30. $R^2 = 0.09$. $p = 0.08$) (*See Figure 4.9*).

4.4.3. Wear Grading

There was a significant positive correlation between the total UHMWPE wear damage score and implant duration (*See Table 4.5 & Figure 4.10*). This correlation was strong despite the presence of one outlier with the highest UHMWPE damage score of the study.

Using ANOVA and Tukey-Kramer multiple comparisons. there were no significant differences in the total wear score among implant designs or between unilaterals and bilaterals.

4.4.4. Mechanical Testing to Assess Acetabular Implant Stability

Thirty-eight acetabular components were mechanically tested (*See Table 4.6*).

Twenty (52.6%) components tested as loose. Six (15.8%) tested as borderline, and 12 (31.6%) were classified as firmly implanted. Frequency distribution of categorical results of acetabular implant stability were calculated (*See Figure 4.11*). Although not statistically significant by Chi-Square analysis, there appears to be a trend that Richards acetabular components are more than BioMedtrix #1 and BioMedtrix #2. Using ANOVA, there were no significant differences in micromotion among implant designs or between unilaterals and bilaterals.

The torque that was necessary to achieve 1 degree of actuator rotation during testing was very low. For example, the firmly implanted control had 0.8 N-m applied, and it only took 0.1 N-m to test the loose control to 1 degree. To verify this, the firm control was tested through 5 degrees of actuator rotation. The firmly implanted acetabular component did not move, and the torque did not increase: however, the pins of the loading jig tore the UHMWPE in the rim of the component.

4.4.5. Statistical Analysis

The dependent variables chosen were TVW, VWR, and PE micromotion (*See Glossary C for names and descriptions of variables*). Simple linear correlations were calculated with all variables against the dependent variables, and the results are presented (*See Table 4.5*). In addition, simple linear correlations were calculated with all variables against implant duration to detect time-related trends (*See Table 4.5*). Some of the stronger relationships include a positive correlation between implant duration and TVW (*See Figure 4.8*) and a positive correlation between implant duration and the total UHMWPE damage score (*See Figure 4.10*).

Using factor analysis combined with the expert opinion of engineers and veterinary

surgeons, a number of indices were formed by taking the mean of highly correlated variables. Only variables with similar units (e.g., mm) were combined. Factor analysis was performed in order to reduce the dimensionality (i.e., number of variables). If the distribution of an index appeared to be non-normal, the index was transformed (i.e., square root) to allow for the use of parametric statistical analysis. The index variables that were defined in this manner are defined and named (*See Table 4.4*). Other variables, described in Chapter 3, that were also used in this analysis were BM1, BM2, and additional problem (*See Glossary C for names and descriptions of variables*).

Multiple linear regression was performed using backward selection and best selection methods in an attempt to find a model that could be used to predict failure of the acetabular component (*See Table 4.7 for examples of possible models; See Appendix F for sample SAS output*). It was hoped that this analysis would identify variables that were unnecessary to collect in future studies of this type with the goal of further reducing the dimensionality of the data. Unfortunately, no clear-cut model of choice presented itself for either VWR or PE micromotion, due in part to the low number of specimens in this study. However, there did appear to be a possible model for TVW that was identified with both the backward and best selection methods (*See Table 4.7*). Variables that appeared most often in these models are presented (*See Table 4.8*).

4.5. Discussion

4.5.1. Comparison to Human Postmortem Retrieval Studies

This is the first report that provides benchmark data on acetabular component stability, UHMWPE volumetric wear measurements, and UHMWPE wear grading in

postmortem retrievals of clinical canine THAs. Despite the fact that postmortem retrieval studies are difficult to control for statistical power, the value of these studies has already been demonstrated in human THA because the information that can be obtained from studies of this type cannot be found any other way [4-5, 7-8]. Valuable qualitative information was discovered from human postmortem retrieval studies despite the lack of statistical analysis in these studies. An example of the knowledge gained from human postmortem retrieval studies was the knowledge of the biological reaction to increased generation of UHMWPE wear debris that triggered osteolysis and the subsequent interposition of soft tissue between the bone and PMMA.

More than half of the acetabular components (20 of 38: 52.6%) in this study were loose, and this contrasts sharply with the 84% positive response to the subjective owner survey discussed in Chapter 2 [9]. This is the same contrast seen with respect to the femoral components (*See Chapter 3*). This aseptic loosening rate is an order of magnitude higher than previous reports in the literature (*See Table 4.3*) for aseptic loosening of acetabular components requiring revision surgery. It is unknown whether loosened canine acetabular components remain clinically asymptomatic as occurs in human THA [4-5]. In order to assess whether aseptic loosening of the acetabular component matters clinically, more thorough clinical follow-up with objective methods of evaluation needs to be incorporated. Force plate gait analysis performed at set times post-surgery would serve to identify a change in weight bearing on the implanted leg, which may indicate problems with the implant. If the acetabular component has loosened yet remains asymptomatic, no action need be taken other than to continue thorough follow-up.

In order to compare the clinical canine THA findings of this study to similar studies in humans, human postmortem retrieval studies from the literature must be carefully chosen. These studies must be on human acetabular components made from similar materials, implanted using similar attachment methods, and measured using similar methods to those used in this study. Unfortunately, studies of this nature are difficult to find. One study [8] was found that presented analysis of human postmortem retrievals for the total volumetric wear of non-metal backed acetabular components made of UHMWPE that had been articulated against Co-Cr femoral heads (*See Table 4.1*). One study [5] was found that performed mechanical testing of human postmortem retrievals that were tested in a similar mode (i.e., torsional loading to the rim of the acetabular cup) to that used in this study. Fortunately, this study provided the raw data for each specimen.

As expected, canine VWRs were considerably lower than those measured in similar human studies. Jasty *et al.* [8] reported an average postmortem retrieval VWR of 35.0 mm^3 per year, which is an order of magnitude higher than canine VWRs in the present study of 6.7 mm^3 per year. Surprisingly, there were no significant differences in VWRs between the two different manufacturers' implants. Perhaps this is an indication of equality of UHMWPE resins and consolidation procedures between the two manufacturers.

Schmalzried *et al.* [5] performed mechanical testing on 14 human acetabular components that were retrieved at autopsy. One had been a revision implant; the remainder of the specimens were from the primary THA. By a combination of clinical symptoms, radiographic evaluation, and manual testing of the acetabular component, four

(including the revision implant) of the specimens could be classified as loose prior to mechanical testing. One implant that could not be radiographically evaluated due to radiolucent PMMA had measurable micromotion greater than one of the radiographically loose specimens; thus, this component was also classified as loose for the purposes of this comparison. Based on these criteria, 2 (14.3%) of 14 human specimens were grossly loose on manual manipulation. An additional 3 (21.4%) were classified as loose by either mechanical testing or radiographic evaluation. A total of 5 (35.7%) of 14 autopsy retrievals of human acetabular components were considered to be loose. The remainder had measured average rotational displacements of 0.29 degrees (range = 0.05 to 0.61 degrees). No loose or firmly implanted controls were used in this study to determine the mechanical testing criteria for loose or firmly implanted classification. A load of 11.3 N-m (100 in-lbf) was used in the mechanical testing by Schmalzried *et al.* [5].

The canine acetabular components classified as firm had average rotational displacements of 0.03 degrees (range = 0 to 0.08), borderline averaged 0.11 degrees (range = 0.09 to 0.15), and loose averaged 0.36 degrees (range = 0.16 to 0.76). From these results, it is clear that there was a great deal more rotational displacement measured in the firmly implanted human acetabular components than in the dog; thus it is difficult to draw conclusions from the rotational displacement between the two species. In addition, the applied torsion in the testing of the canine acetabular components was an order of magnitude lower than that used in testing the human components. The human autopsy retrieval study used a load of 11.3 N-m, whereas the firmly implanted canine control was loaded to 0.8 N-m, and the loose canine control was loaded to 0.1 N-m. The differences in the loading also makes it impossible to draw conclusions from the

mechanical testing results between species.

To recap, 2 (14.3%) of 14 human acetabular components, retrieved postmortem, were loose upon manual manipulation. There were no canine acetabular components that were grossly loose upon manual manipulation. As a result of mechanical testing, an additional 3 (21.4%) for a total of 5 (35.7%) of 14 human acetabular components were found to be loose. As a result of mechanical testing of the canine acetabular components, 20 (52.6%) of 38 specimens were found to be loose. The percentage of canine postmortem retrievals that were found to be loose was much greater than in the human postmortem retrieval study.

4.5.2. Other Findings

There was a strong positive correlation between TVW and implant duration (*See Table 4.5 & Figure 4.8*) despite the presence of two outliers with extraordinarily high volumetric wear. One was a 36 kg Newfoundland that was paralyzed in the hindquarters at the time of euthanasia. The unilateral BioMedtrix #1 femoral component was so loose that it could easily slip from the femur when the joint was cut open. The second was a dog that had undergone revision surgery after aseptic loosening of the unilateral femoral component. The femoral component implanted at revision surgery was a BioMedtrix #2 design, but the date of the primary THA fell during the time when the BioMedtrix #1 design was in use: so, the femoral component that became aseptically loose may have been a BioMedtrix #1. The original acetabular component was left in place at the time of the revision surgery: thus, the acetabular component retrieved postmortem had at one time been articulated against a femoral component that had failed. The implant duration reflected in Figure 4.8 is the duration of the acetabular component.

There was a strong positive correlation between the total UHMWPE wear damage score and implant duration (*See Table 4.5 & Figure 4.10*) despite the presence of one outlier with the highest UHMWPE damage score of the study. This dog with unilateral THA had been experiencing progressive loss of control over the hind legs until she could no longer climb the steps into the owner's home. When the joint was opened, the BioMedtrix #1 femoral component was completely loose and could be easily pulled from the femur. The femur was misshapen and discolored, usually a sign of titanium wear debris [37].

Canine acetabular cup wear patterns are considerably different than those seen in human THA [13]. There is considerably more third body wear, and there are no readily apparent distinct high wear/low wear regions. Perhaps this is an indication of the greater range of motion in a canine hip joint. Evidence of cement mantle breakdown was seen on several postmortem retrievals, and in some cases the breakdown resulted in poor support of the acetabular cup rim. The extensive third body wear seen on the canine acetabular components may be caused by loose PMMA fragments.

Impingement on the corners and along the edge of the cut-out was extensive and most likely caused by the neck of the femoral implant. This level of damage indicates that the 45° fire hydrant cut-out is not adequate impingement protection given the large range of motion in the canine joint. Perhaps the impingement of the femoral neck on the acetabular component caused high forces on the PMMA (a relatively brittle, amorphous polymer that is below its glass transition temperature at body temperature), causing it to break, thus leading to high levels of third body wear damage caused by PMMA debris between the femoral head and the UHMWPE articulating surface.

One item of note in the results of the mechanical testing of the canine acetabular components (*See Table 4.6*) was the absence of BioMedtrix size 23 and 25 components under the firmly implanted and borderline categories. This seems to support the statement in the Huiskes and Verdonschot review [11] that a thicker UHMWPE acetabular component distributes stress more uniformly and thus reduces the peak stress in the cement mantle. Perhaps the size 23 and 25 BioMedtrix acetabular components were too thin to withstand the forces applied when the femoral component impinged upon the corners and the cutout rim, passed the concentrated stresses into the PMMA, and thus caused cracking and breaking of the PMMA around the upper rim of the acetabular component with resultant aseptic loosening at the UHMWPE/PMMA interface.

Loosening of the acetabular component was positively correlated with the total UHMWPE damage score. There were no gross observations of large scale osteolysis, as reported in human THA, but future histological studies of these specimens will definitively answer whether osteolysis occurred in canine THA.

The average VWR of 6.7 mm^3 per year in the canine acetabular components was an order of magnitude lower than the 35.0 mm^3 per year reported in human autopsy retrievals [8] (*See Table 4.1*). This may mean that the dog experiences a lower UHMWPE wear debris load, which may explain why dogs do not display the level of osteolysis seen in human THA.

These two factors lead to the conclusion that the initiating event for failure of the canine acetabular component is mechanical in nature. The femoral component impingement on the acetabular component, causing implant-on-implant damage,

increased localized stress on the cement mantle, causing cracking and breakdown of the PMMA around the rim of the acetabular component. The increased damage and the lower volumetric wear in the canine acetabular points to a fundamental difference between the species. Human autopsy retrieval studies pointed to biological initiators of aseptic loosening of the acetabular component at the bone/PMMA interface. The canine acetabular components had wear rates that were an order of magnitude less than that seen in the human, thus resulting in a lower wear debris load and perhaps decreased magnitude biological reaction to wear debris in the dog. The increased third body and implant-on-implant damage and the increased aseptic loosening in the dog lead to the conclusion that the canine acetabular component may be loosening at the UHMWPE/PMMA interface because of the mechanical stress caused by implant-on-implant impingement and passed through the UHMWPE to the PMMA at the UHMWPE/PMMA interface.

The incidence of loosening in the canine acetabular components seen in this study is alarmingly high. As was seen in Chapter 3 with the femoral components, the Richards acetabular components tended to remain more firmly implanted than the BioMedtrix #1 or BioMedtrix #2 acetabular components, despite the older generation cementing techniques and longer implant durations for the Richards components. Similar to the findings of Chapter 3, the bilateral acetabular components tended to remain more firmly implanted than the unilateral acetabular components.

Human THA results have improved with advances in implant design and cementing technique. Considering that 52.6% of the canine acetabular components in the present study were loose, redesign of the acetabular component to reduce implant-on-implant damage is needed.

Great care needs to be taken during canine total hip replacement surgery to ensure that the cement mantle fully supports the acetabular component while reducing the amount of excess PMMA left in the surgical field. Reducing damage to the PMMA mantle and subsequent third body wear damage should be one of the veterinary surgeon's goals.

The surgical paradigm for canine THA has changed as a result of this study. Unilateral THA for dogs with bilateral DJD is no longer considered to be adequate. Surgeons are suggesting bilateral surgery more frequently for dogs with bilateral DJD, but the cost of the additional surgery remains an issue with owners. Surgeons are taking greater care with preparation of the femur and acetabulum before cementing of the implants. They are also taking great care to ensure that excess PMMA is removed from the surgical field in order to reduce future third body wear damage to the articulating surface.

4.6. Conclusions

This is the first report that provides benchmark data on acetabular component stability, UHMWPE volumetric wear measurements, and UHMWPE wear grading in postmortem retrievals of clinical canine THAs.

The first hypothesis in this study was that, due to lower peak joint forces and differences in hip loading, volumetric wear would be lower and wear patterns would be less extensive in canine postmortem retrievals than in human postmortem retrieval studies. This hypothesis was supported for volumetric wear only. Volumetric wear rates were an order of magnitude lower in canine acetabular components compared to human

implants. However, hypothesis one was not supported for wear patterns. Wear patterns were considerably different from and more severe than those reported in the literature for human acetabular components. There was much more implant-on-implant damage, most often seen as impingement on the corners and the cut-out rim. The degree of third-body wear damage was very high, and PMMA wear debris is the probable culprit considering that large pieces of PMMA were sometimes found loose in the joint and several implants were no longer supported PMMA around the rim. Perhaps the forces applied to the acetabular component by impingement of the femoral neck caused damage to the PMMA, leading to cracking and third-body wear.

The second hypothesis was that primary failure mechanisms for the canine acetabular component would be biological in nature, as seen in human THA. This hypothesis was not found to be true. Perhaps since UHMWPE wear is so much lower, there is less submicron wear debris available to trigger the complex biological reaction seen in human acetabular components that causes them to loosen at the bone/PMMA interface. Micromotion of the acetabular component was not correlated with implant duration; however, micromotion was positively correlated with the total UHMWPE damage score. The extensive implant-on-implant damage and the relationship between UHMWPE damage and loosening leads to the conclusion that the primary failure mechanism in canine acetabular mechanisms is mechanical in nature. The canine acetabular component probably loosens at the UHMWPE/PMMA interface due to implant-on-implant damage and higher stresses being applied by the femoral component on the corners and cutout rim of the implant.

The third hypothesis was that aseptic loosening would not be as pronounced in dogs

as in humans because of lower peak joint forces in dogs. This hypothesis was not found to be true. More than half of the acetabular components were loose.

The fourth hypothesis was that implants with higher volumetric wear would be less stable, similar to results of human studies [5]. This hypothesis was not found to be true. There was no correlation between PE micromotion and either TVW or VWR.

The fifth hypothesis was that unilateral components would perform adequately in comparison to bilateral implants. Just as in Chapter 3, this hypothesis was surprisingly found not to be true. There was a trend that bilateral acetabular components were more stable than unilateral components.

THA remains a valuable option for the treatment of DJD in dogs despite the problems found in this study. Improvements in surgical technique and implant design in conjunction with more thorough follow-up using objective (i.e., force plate gait analysis) and subjective (i.e., owner survey) techniques will lead to a decrease in aseptic loosening in the future.

4.7. Acknowledgements

Companion Animal Orthopedic Research Group (CAORG) Donations Fund at Colorado State University – for funding this project: Elisha Rentfrow - for technical assistance on the volumetric wear measurement: BioMedtrix Corporation - for donation of a new, unworn acetabular cup/femoral head pair for experimental use: Erick Egger, DVM - for assistance in making of control specimens

4.8. References

1) Mulroy WF, Estok DM, Harris WH. Total Hip Arthroplasty with Use of So-Called Second-Generation Cementing Techniques: A Fifteen-Year-Average Follow-Up Study. *The Journal of Bone and Joint Surgery*, 1995; 77-A: 1845-1852.

2) Klapach AS, Callaghan JJ, Goetz DD, Olejniczak JP, Johnston RC. Charnley Total Hip Arthroplasty With Use of Improved Cementing Techniques: A Minimum Twenty-Year Follow-Up Study. *The Journal of Bone and Joint Surgery*, 2001; 83-A: 1840-1848.

3) Iorio R, Eftekhar NS, Kobayashi S, Grelsamer RP. Cemented Revision of Failed Total Hip Arthroplasty: Survivorship Analysis. *Clinical Orthopaedics and Related Research*, 1995; 316: 121-130.

4) Schmalzried TP, Maloney WJ, Jasty M, Kwong LM, Harris WH. Autopsy Studies of the Bone-Cement Interface in Well-Fixed Cemented Total Hip Arthroplasties. *The Journal of Arthroplasty*, 1993; 8: 179-188.

5) Schmalzried TP, Kwong LM, Jasty M, Sedlacek RC, Haire TC, O'Connor DO, Bragdon CR, Kabo JM, Malcolm AJ, Harris WH. The Mechanism of Loosening of Cemented Acetabular Components in Total Hip Arthroplasty: Analysis of Specimens Retrieved at Autopsy. *Clinical Orthopaedics and Related Research*, 1992; 274: 60-78.

6) Harris WH, Sledge CB. Total Hip and Total Knee Replacement (First of Two Parts). *New England Journal of Medicine*, 1990; 323: 725-731.

7) Sychterz CJ, Moon KH, Hashimoto Y, Terefenko KM, Engh Jr CA, Bauer TW. Wear of Polyethylene Cups in Total Hip Arthroplasty: A Study of Specimens Retrieved Post Mortem. *The Journal of Bone and Joint Surgery*, 1996; 78-A: 1193-1200.

8) Jasty M, Goetz DD, Bragdon CR, Lee KR, Hanson AE, Elder JR, Harris WH. Wear of Polyethylene Acetabular Components in Total Hip Arthroplasty: An Analysis of One Hundred and Twenty-Eight Components Retrieved at Autopsy or Revision Operations. *The Journal of Bone and Joint Surgery*, 1997; 79-A: 349-358.

9) Skurla CT, Egger EL, Schwarz PD, James SP. Owner Assessment of the Outcome of Total Hip Arthroplasty in Dogs. *Journal of the American Veterinary Medical Association*, 2000; 217: 1010-1012.

10) Jasty M, Maloney WJ, Bragdon CR, O'Connor DO, Haire T, Harris WH. The Initiation of Failure in Cemented Femoral Components of Hip Arthroplasties. *The Journal of Bone and Joint Surgery*, 1991; 73-B: 551-558.

11) Huiskes R. Verdonschot N. BioMechanics of Artificial Joints: The Hip. *Basic Orthopaedic Biomechanics, 2nd ed.*, edited by Van C. Mow and Wilson C. Hayes. Lippincott-Raven Publishers. Philadelphia. Chapter 11: 1997: 395-460.

12) Biggs S. Bragdon CR. Sedlacek R. Lee K. Jasty M. Estok D. Harris WH. A New Method of Volumetric Quantification of Retrieved Polyethylene Components. *Trans Orth Res Soc*: 470. 1996.

13) James SP. Lee KR. Beauregard GP. Rentfrow ED. McLaughlin JR. Clinical Wear of 63 Ultrahigh Molecular Weight Polyethylene Acetabular Components: Effect of Starting Resin and Forming Method. *Journal of Biomedical Materials Research (Applied Biomaterials)*. 1999: 48: 374-384.

14) Hood RW. Wright TM. Burstein AH. Retrieval Analysis of Total Knee Prostheses: A Method and Its Application to 48 Total Condylar Prostheses. *Journal of Biomedical Materials Research*. 1983: 17: 829-842.

15) Engh GA. Dwyer KA. Hanes CK. Polyethylene Wear of Metal-Backed Tibial Components in Total and Unicompartmental Knee Prostheses. *The Journal of Bone and Joint Surgery*. 1992: 74-B: 9-17.

16) Wright TM. Rimnac CM. Stulberg SD. Mintz L. Tsao AK. Klein RW. McCrae C. Wear of Polyethylene in Total Joint Replacements: Observations From Retrieved PCA Knee Implants. *Clinical Orthopaedics and Related Research*. 1992: 276: 126-134.

17) Huang CH. Young TH. Lee YT. Jan JS. Cheng CK. Polyethylene Failure in New Jersey Low-Contact Stress Total Knee Arthroplasty. *Journal of Biomedical Materials Research*. 1998: 39: 153-160.

18) Ohlin A. Balkfors B. Stability of Cemented Sockets After 3-14 Years. *The Journal of Arthroplasty*. 1992: 7: 87-92.

19) Won. CH. Hearn TC. Tile M. Micromotion of Cementless Hemispherical Acetabular Components: Does Press-Fit Need Adjunctive Screw Fixation? *The Journal of Bone and Joint Surgery*. 1995: 77-B: 484-489.

20) Stiehl JB. MacMillan E. Skrade DA. Mechanical Stability of Porous-Coated Acetabular Components in Total Hip Arthroplasty. *The Journal of Arthroplasty*. 1991: 6: 295-300.

21) Kwong LM. O'Connor DO. Sedlacek RC. Krushell RJ. Maloney WJ. Harris WH. A Quantitative *In Vitro* Assessment of Fit and Screw Fixation on the Stability of a Cementless Hemispherical Acetabular Component. *The Journal of Arthroplasty*, 1994: 9: 163-170.

22) Perona PG. lawrence J. Paprosky WG. Patwardhan AG. Sartori M. Acetabular Micromotion as a Measure of Initial Implant Stability in Primary Hip Arthroplasty: An *In Vitro* Comparison of Different Methods of Initial Acetabular Component Fixation. *The Journal of Arthroplasty*. 1992; 7: 537-547.

23) Noble PC. Kamaric E. Alexander JW. Paravic V. Collier MB. Interface Micromotion of Cementless Acetabular Cups: Effect of Ingrowth Coating. *Transactions of the 43rd Annual Meeting of the Orthopaedic Research Society*. 1997: 854.

24) Cournoyer JR. Ochoa JA. Kurtz SM. Relative Motion at the Backside of a Metal-Backed Acetabular Component Under Quasistatic and Dynamic Loading. *Transactions of the 43rd Annual Meeting of the Orthopaedic Research Society*. 1997: 839.

25) Doehring TC. Saigal S. Shanbhag AS. Rubash HE. Micromotion of Acetabular Liners: Measurements Comparing the Effectiveness of Locking Mechanisms. *Transactions of the 42nd Annual Meeting of the Orthopaedic Research Society*. 1996: 427.

26) Anderson GI. Podwornv N. Jain R. Kwok AWL. Waddell JP. Hydroxyapatite Application Effect on Micromotion Around Acetabular and Femoral Components in the Dog. *Transactions of Fifth World Biomaterials Congress*. 1996: 176.

27) Page AE. Allan C. Jasty M. Harrigan TP. Bragdon CR. Harris WH. Determination of Loading Parameters in the Canine Hip *in Vivo*. *J Biomech*. 26: 571-579. 1993.

28) Lewis RH. Jones Jr JP. A Clinical Study of Canine Total Hip Arthroplasty. *Veterinary Surgery*. 1980; 9: 20-23.

29) Gofton N. Sumner-Smith G. Total Hip Prosthesis for Revision of Unsuccessful Excision Arthroplasty. *Vet Surg*. 11: 134-139. 1982.

30) Olmstead ML. Hohn RB. Turner TM. A five-year study of 221 total hip replacements in the dog. *J Am Vet Med Assoc*. 183: 191-194. 1983.

31) Parker RB. Bloomberg MS. Bitetto W. Rodkey WG. Canine Total Hip Arthroplasty: A Clinical Review of 20 Cases. *J Am Vet Med Assoc*. 20: 97-104. 1984.

32) Olmstead ML. Total Hip Replacement in the Dog. *Semin Vet Med Surg (Small Animal)*. 2: 131-140. 1987.

33) Paul HA. Bargar WL. A Modified Technique for Canine Total Hip Replacement. *J Am Anim Hosp Assoc*. 23: 13-18. 1987.

34) Radford DW. *Shape Instabilities in Composites*. Doctoral dissertation, Rensselaer Polytechnic Institute. Troy. NY. 1987.

35) SAS Institute. Inc. *SAS/STAT User's Guide, Version 6, 4th ed.*. SAS Institute. Inc.. Cary. NC. 1990.

36) Ott RL. More on Multiple Regression. *An Introduction to Statistical Methods and Data Analysis, 4th ed.* Duxbury Press. Belmont. California. Chapter 12: 1993: 647-766.

37) Witt JD. Swann M. Metal Wear and Tissue Response in Failed Titanium Alloy Total Hip Replacements. *The Journal of Bone and Joint Surgery*. 1991: 73-B: 559-563.

4.9. Tables

Table 4.1						
Study	**Nbr of Cases**	**Retr. Type**	**Fem. Head Mat'l**	**Acet. Comp. Mat'l**	**Vol. Wear Rate (mm^3/yr)**	**Wear Meas. Method Used**
Sychterz *et al.* (1996) [7]	8	Autopsy	All Co-Cr	Cemented UHMWPE	21.6	Gravimetric & shadowgraph
Sychterz *et al.* (1996) [7]	18	Autopsy	5 ceramic, 13 Co-Cr	Cement-less, metal-backed UHMWPE	47.9	Gravimetric & shadowgraph
Jasty *et al.* (1997) [8]	22	Autopsy	Co-Cr	Cemented UHMWPE	35.0	Fluid displacement
Jasty *et al.* (1997) [8]	84	Revision	4 stainless steel, 1 Ti-6Al-4V, 79 Co-Cr	Cemented UHMWPE	62.0	Fluid displacement
Jasty *et al.* (1997) [8]	22	Revision	Co-Cr	Cemented, metal-backed UHMWPE	94.0	Fluid displacement

Table 4.1 - Previous human THA outcomes reports on UHMWPE volumetric wear.

Table 4.2				
Implant Manufacturer	**Implant Size**	**Outer Diameter (mm)**	**Inner Diameter (mm)**	**UHMWPE Thickness (mm)**
Richards	Large	23.74	19.07	4.67
	Medium	20.65	15.77	4.88
BioMedtrix #1 & #2	23 mm	23	17	6.00
	25 mm	25	17	8.00
	27 mm	27	17	10.00
	29 mm	29	17	12.00

Table 4.2 – Dimensions of Richards and BioMedtrix acetabular components.

Table 4.3				
Study	**Nbr of Cases**	**Nbr (Pct) of Cases with Aseptic Loosening of the Acetabular Component**	**Implant Design**	**Follow-Up Period (months)**
Lewis & Jones (1980) [28]	20	9 (45.0%)	Richards	19-34
Gofton & Sumner-Smith (1982) [29]	3	0 (0.0%)	Richards (1): Other (2)	8-18
Olmstead (1983) [30]	216	7 (3.2%)	Richards	1-72
Parker (1984) [31]	23	3 (13.0%)	Richards	6-42
Olmstead (1987) [32]	146	5 (3.4%)	Richards	1-36
Paul (1987) [33]	65	2 (3.1%)	Richards	6-42
Combined	**473**	**26 (5.5%)**		

Table 4.3 - Literature review of previous outcomes reports on canine total hip arthroplasty for aseptic loosening of the acetabular component that required revision surgery [28-33].

Table 4.4			
Index Variable Name	**Data Source**	**Original Variables**	**Transform Used**
Quadrant index	UHMWPE wear grading	Quadrant 1 score	Mean
		Quadrant 2 score	
		Quadrant 3 score	
		Quadrant 4 score	
Rim index	UHMWPE wear grading	Cranial rim score	Mean
		Caudal rim score	
Cut-out index	UHMWPE wear grading	Cranial corner score	Mean
		Caudal corner score	
		Cut-out rim score	
Creep index	UHMWPE wear grading	Creep score	Mean
		Pitting score	
3BW index	UHMWPE wear grading	Embedded PMMA score	Mean
		Scratching score	
		Removal of machine marks score	
		Abrasion score	

		Macroscopic removal of UHMWPE score Yellowing score	
Embedded metal index	UHMWPE wear grading	Embedded metal score	1 = embedded metal detected; 0 = no detected metal debris

Table 4.4 – Name and definition of index variables created from factor analysis and used in multiple linear regression analysis.

Table 4.5					
Dependent Variable	**Independent Variable**	**Pearson's rho**	**R^2**	**p**	**Power**
TVW	Implant duration	0.534	0.285	0.001	0.941
	PE thickness	-0.486	0.236	0.002	0.901
	PE OD	-0.366	0.134	0.024	0.632
	PE ID	0.365	0.133	0.024	0.628
	PE Thickness	-0.491	0.242	0.002	0.901
	Age at surgery	-0.343	0.117	0.035	0.567
VWR	Creep index	-0.345	0.119	0.043	0.535
PE Micromotion	Torque	-0.505	0.255	0.001	0.928
	Total PE score	0.331	0.110	0.042	0.536
Implant Duration	Creep index	0.607	0.368	<0.001	0.989
	Age at surgery	-0.574	0.329	<0.001	0.974
	Cut-out index	0.538	0.289	<0.001	0.945
	Total PE score	0.504	0.254	0.002	0.902
	PE thickness	-0.401	0.161	0.017	0.684
	Quadrant index	-0.400	0.160	0.017	0.683
	PE OD	-0.392	0.154	0.020	0.661
	Rim index	0.371	0.138	0.028	0.606

Table 4.5 – Results of simple linear regression analysis by dependent variable in order of descending R^2. The sign of the Pearson's rho indicates whether the correlation between the dependent and independent variables is negative or positive.

Table 4.6				
Mfr	**Bilateral/ Unilateral**	**Duration (years)**	**Size (mm)**	**Testing Results**
BioMedtrix #1	Bilateral	8.7	27.0	Firm
BioMedtrix #1	Bilateral	2.3	27.0	Firm
BioMedtrix #1	Bilateral	6.7	27.0	Firm
Richards	Bilateral	10.2	23.7	Firm
Richards	Bilateral	10.9	20.6	Firm
Richards	Bilateral	Unk	20.6	Firm
Richards	Bilateral	9.4	23.7	Firm
Richards	Bilateral	Unk	20.6	Firm
BioMedtrix #1	Unilateral	5.3	29.0	Firm
BioMedtrix #1	Unilateral	6.0	27.0	Firm
BioMedtrix #2	Unilateral	1.2	27.0	Firm
BioMedtrix #2	Unilateral	8.0	29.0	Firm
BioMedtrix #1	Bilateral	0.7	27.0	Border
Richards	Bilateral	9.7	23.7	Border
Richards	Bilateral	10.2	20.6	Border
BioMedtrix #1	Unilateral	4.4	29.0	Border
BioMedtrix #1	Unilateral	5.3	27.0	Border
Richards	Unilateral	6.6	23.7	Border
BioMedtrix #1	Bilateral	9.5	27.0	Loose
BioMedtrix #1	Bilateral	3.0	23.0	Loose
BioMedtrix #1	Bilateral	2.7	23.0	Loose
BioMedtrix #1	Bilateral	1.7	25.0	Loose
BioMedtrix #2	Bilateral	4.2	27.0	Loose
Richards	Bilateral	10.4	20.6	Loose
Richards	Bilateral	8.4	23.7	Loose
BioMedtrix #1	Unilateral	8.4	27.0	Loose
BioMedtrix #1	Unilateral	7.9	29.0	Loose
BioMedtrix #1	Unilateral	6.6	27.0	Loose
BioMedtrix #1	Unilateral	2.3	23.0	Loose
BioMedtrix #1	Unilateral	6.7	29.0	Loose
BioMedtrix #1	Unilateral	3.4	29.0	Loose
BioMedtrix #1	Unilateral	6.4	25.0	Loose
BioMedtrix #1	Unilateral	Unk	29.0	Loose
BioMedtrix #1	Unilateral	6.0	27.0	Loose
BioMedtrix #1	Unilateral	4.9	25.0	Loose
BioMedtrix #2	Unilateral	6.8	27.0	Loose
Richards	Unilateral	8.8	23.7	Loose
Richards	Unilateral	11.7	20.6	Loose

Table 4.6 – Results of mechanical testing of acetabular components. F = firmly implanted: B = borderline: L = loose.

Table 4.7					
Selection Method	**Dependent Variable**	**Model R^2 / p**	**Independent Variable**	**Parameter Estimate**	**Par. p**
Backward	TVW *	0.590	Implant duration	0.004	<0.001
		<0.001	PE ID	0.013	<0.001
Best – 2 variable	TVW *	0.590	Implant duration	0.004	<0.001
		<0.001	PE ID	0.013	<0.001
Best – 2 variable	TVW	0.529	BMI	-0.019	0.007
		0.001	PE ID	0.011	0.005
Best – 3 variable	TVW	0.641	Implant duration	0.005	<0.001
		<0.001	PE ID	0.012	0.001
			Creep index	-0.002	0.357
Best – 4 variable	TVW	0.710	Implant duration	0.004	0.005
		<0.001	BMI	-0.011	0.149
			PE ID	0.011	0.005
			Creep index	-0.003	0.240
Backward	VWR	None			
Best – 2 variable	VWR	0.347	PE thickness	-0.0006	0.022
		0.009	Creep index	-0.001	0.006
Best – 2 variable	VWR	0.315	PE OD	-0.0006	0.048
		0.018	Creep index	-0.001	0.007
Best – 3 variable	VWR	0.458	PE thickness	-0.0008	0.001
		<0.001	Creep index	-0.001	<0.001
			Embedded metal index	0.005	0.003
Best – 4 variables	VWR	0.491	PE thickness	-0.0008	0.002
		<0.001	Quadrant index	-0.0002	0.514
			Creep index	-0.002	<0.001
			Embedded metal index	0.005	0.002
Backward	PE micromotion	None			
Best – 2 variables	PE micromotion	0.197	Torque	-0.725	0.010
		0.027	Creep index	-0.019	0.300
Best – 2 variables	PE micromotion	0.177	Weight	0.003	0.361
		0.031	Torque	-0.731	0.010
Best – 3 variables	PE micromotion	0.274	Implant duration	0.019	0.122
		0.023	Torque	-0.767	0.006
			Creep index	-0.042	0.078
Best – 4 variables	PE micromotion	0.317	Implant duration	0.016	0.198
		0.025	Torque	-0.693	0.013
			Cut-out index	0.033	0.192
			Creep index	-0.064	0.030

Table 4.7 - Representative example of results of multiple linear regression analysis using backward and best model selection methods. The parameter estimate indicates whether the correlation is negative or positive. * = Clear-cut superior model for dependent variable. TVW.

Table 4.8			
Dependent Variable	**Correlation Direction**	**Independent Variable**	**Data Source**
TVW	Positive	Implant duration	Chart
		UHMWPE inner diameter	
	Negative	BMI index	
		Creep index	Wear grading
VWR	Positive	Embedded metal index	
	Negative	UHMWPE thickness	Chart
		UHMWPE outer diameter	
		Creep index	Wear grading
		Quadrant index	
PE micromotion	Negative	Creep index	Wear grading
		Torque	Mechanical testing

Table 4.8 – Trends found during multiple linear regression analysis.

4.10. Figures

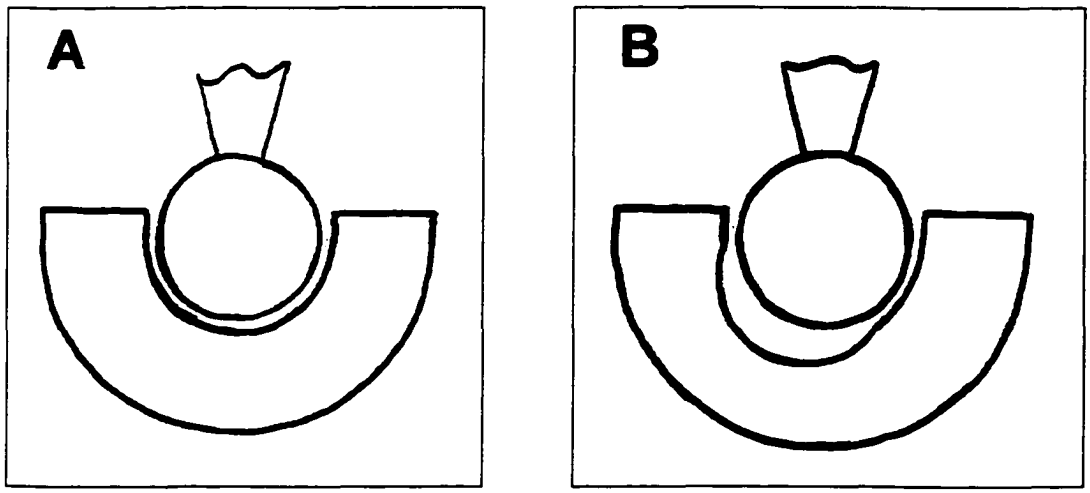

Figure 4.1 – Schematic drawing of the volumetric wear measurement method. In (A) an unworn, new femoral head is placed into an unworn, new acetabular component. In (B) the same unworn, new femoral head is placed into the retrieved acetabular component. The volumes of the gaps are measured. The difference between (B) and (A) is the volume of UHMWPE that has worn away.

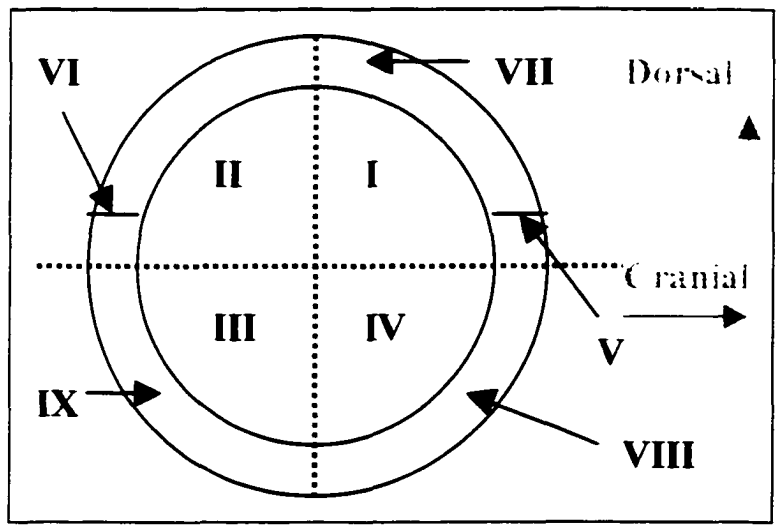

Figure 4.2 – Schematic drawing of canine acetabular component with quadrants and areas marked for individual wear grading scores. I = Cranial dorsal articulating surface, II = Caudal dorsal articulating surface, III = Caudal ventral articulating surface, IV = Cranial ventral articulating surface, V = Cranial corner, VI = Caudal corner, VII = Cut-out rim, VIII = Cranial rim, IX = Caudal rim.

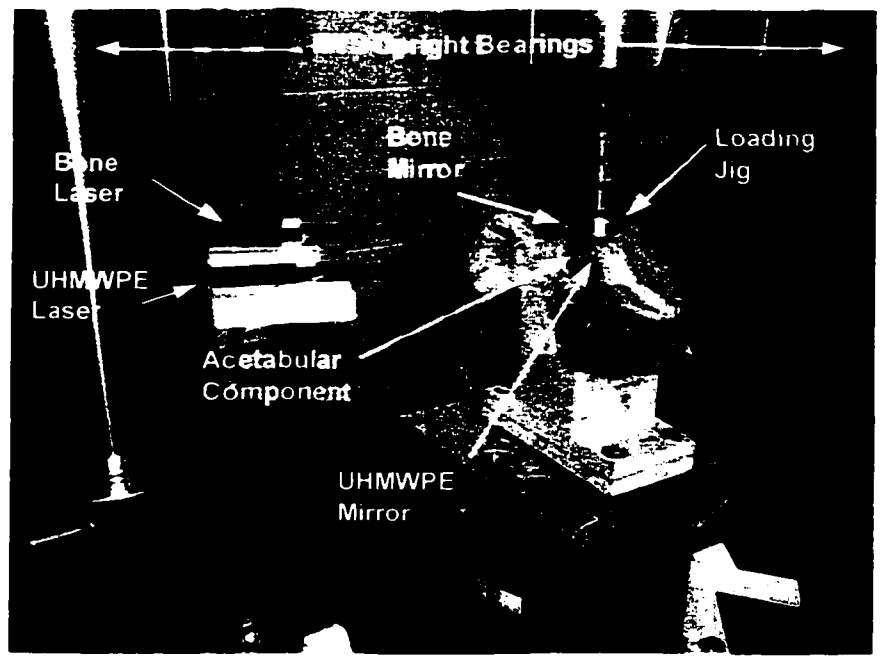

Figure 4.3 – Photograph of test set-up on the MTS mechanical testing system for the mechanical testing for implant stability of the acetabular component.

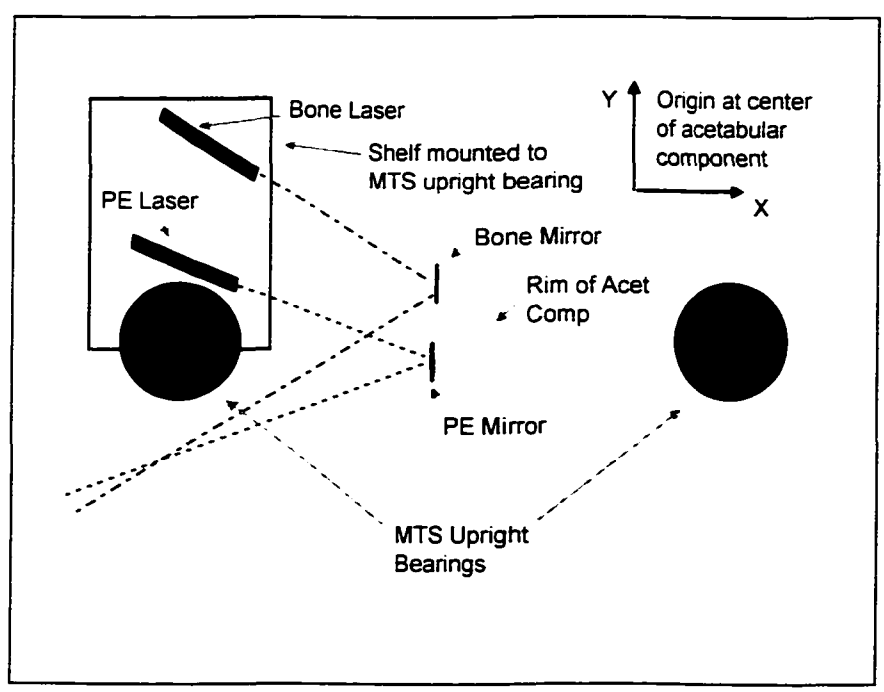

Figure 4.4 – Close-up schematic drawing of mechanical testing set-up on the MTS as shown in Figure 4.3.

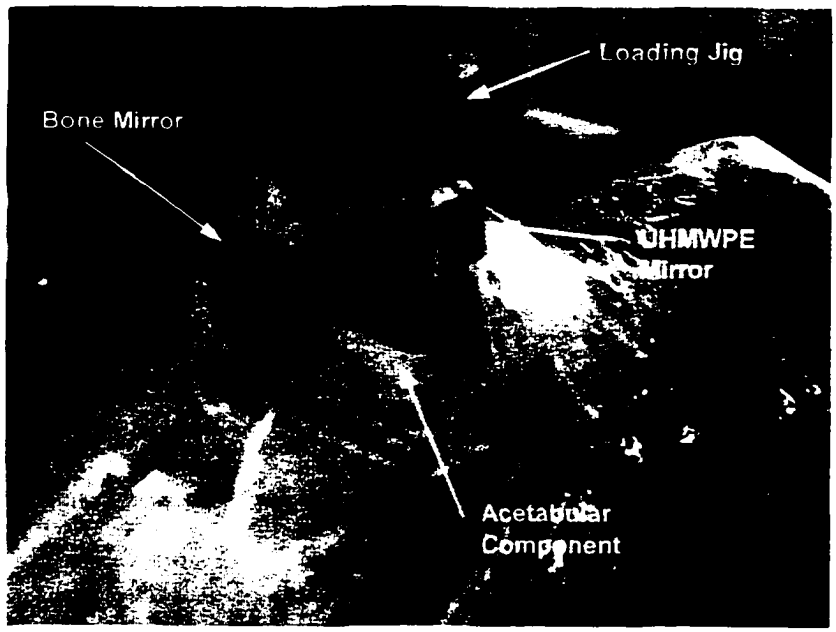

Figure 4.5 – Close-up photo of the loading jig and laser mirrors mounted to a test specimen.

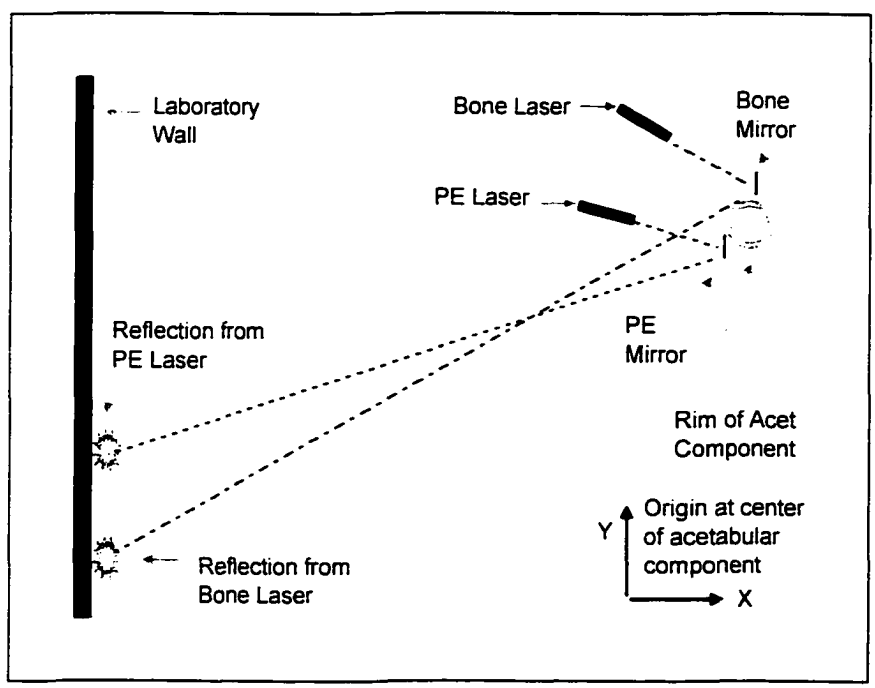

Figure 4.6 – Schematic drawing of broader view of mechanical testing set-up in the laboratory.

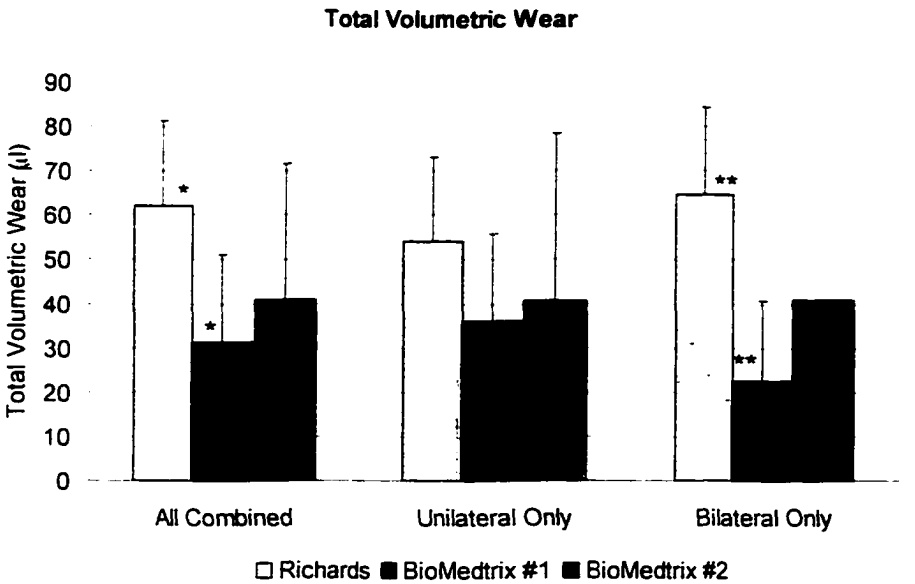

Figure 4.7 – Average TVW by implant design for all combined, unilateral implants only, and bilateral implants only. For all combined and bilateral only, total volumetric wear is significantly greater for Richards than BioMedtrix #1 ($p < 0.05$).

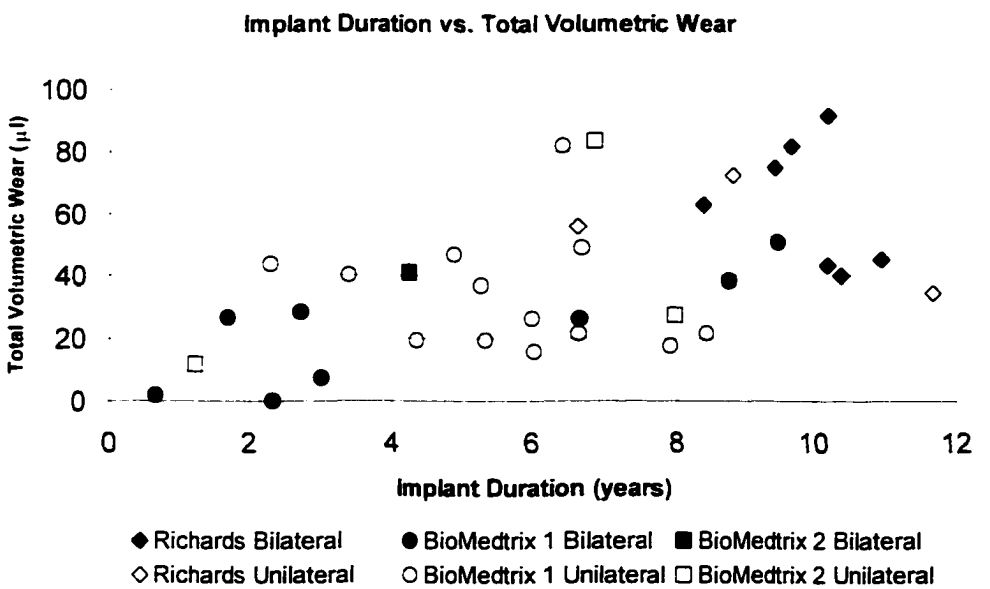

Figure 4.8 – Significant positive correlation between TVW and ID ($p=0.001$, $R^2=0.29$).

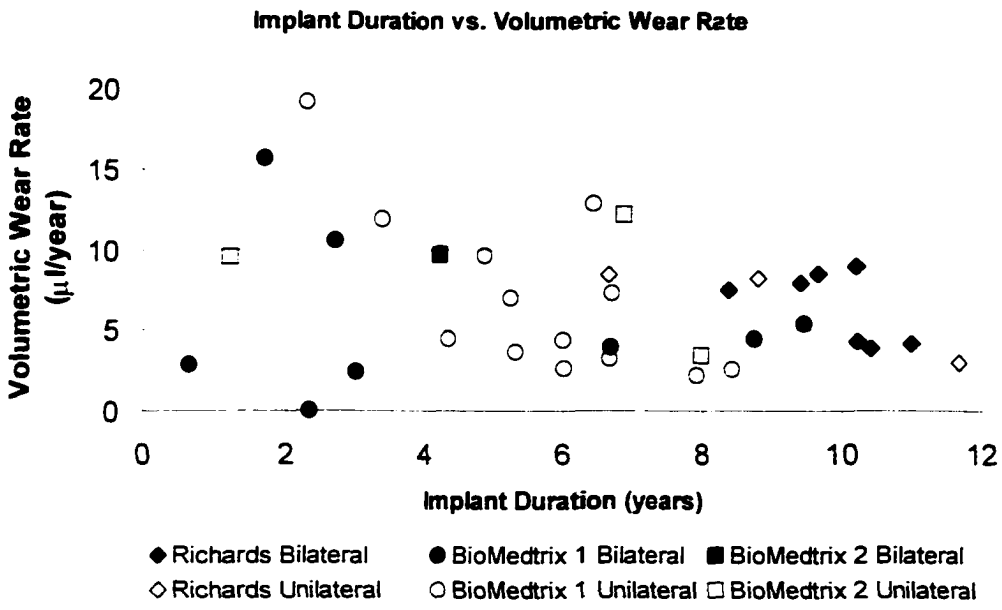

Figure 4.9 – Non-significant correlation between VWR and implant duration (Pearson's rho = -0.30, R^2 = 0.09, p = 0.08). Negative trend indicates that VWR may not be constant with time.

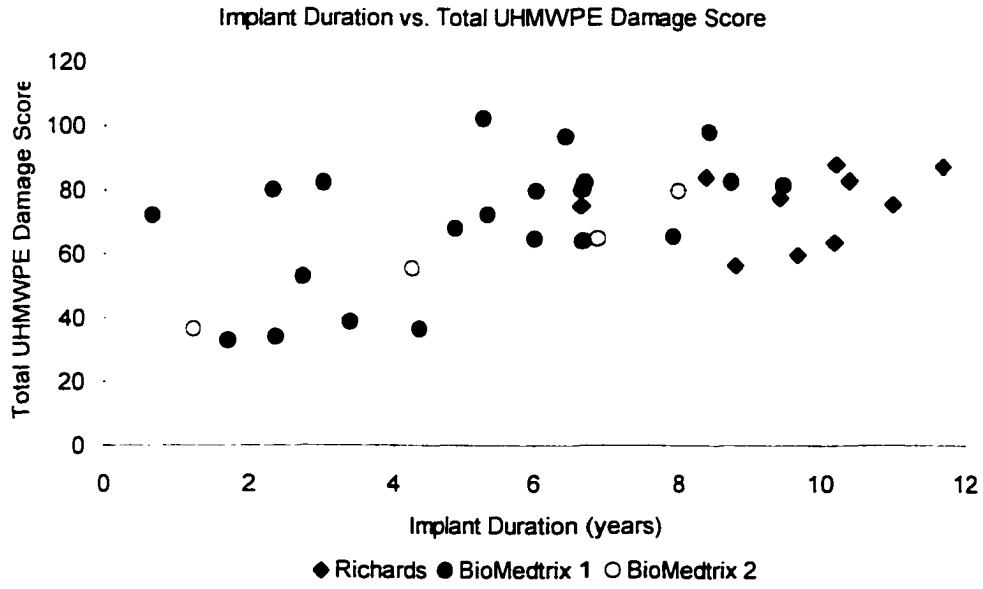

Figure 4.10 – Significant correlation between total UHMWPE damage score and implant duration.

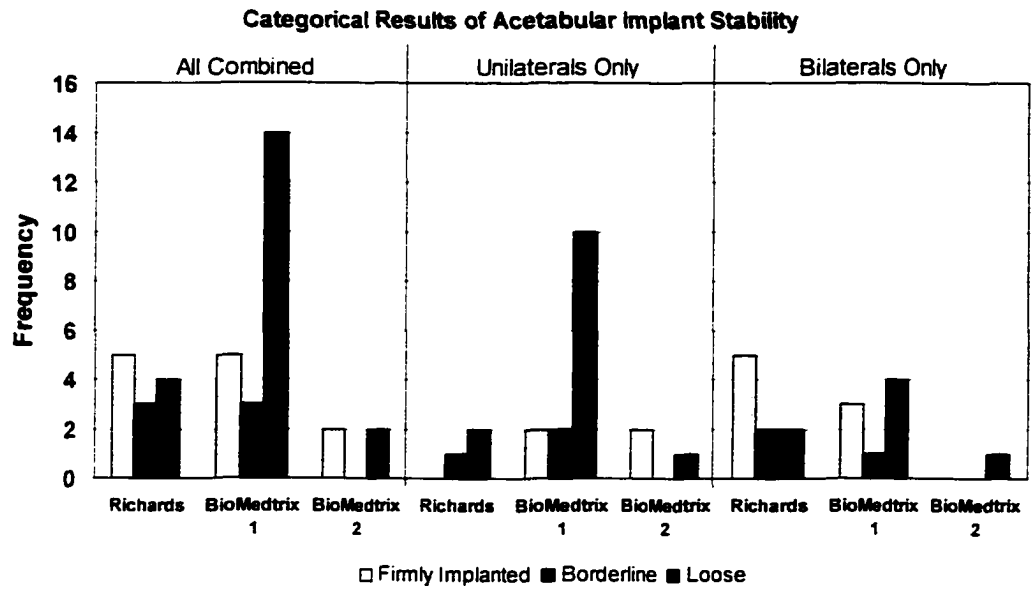

Figure 4.11 - Categorical results of non-destructive mechanical testing of acetabular components for implant stability.

Chapter 5

Putting It All Together

5.1. Introduction

5.1.1. Human Total Hip Arthroplasty

5.1.1.1. Analysis of Femoral and Acetabular Component Data

To the best of the author's knowledge, there have been no published reports of autopsy retrieval studies of human total hip arthroplasty (THA) that attempted to correlate the performance of the acetabular component and the femoral component together in order to ascertain whether or how the failure of one component affects the performance of the other. This may be due, in part, to lack of statistical power because of the small number of specimens in some of these studies (e.g. 16 femoral components [1] and 14 acetabular components [2]).

Jasty *et al.* [3] studied the volumetric wear of 22 acetabular components retrieved at autopsy and 106 revision retrievals. Multivariate regression analysis was used to correlate volumetric wear of the acetabular components, made of ultra high molecular weight polyethylene (UHMWPE), against demographic data from the chart (e.g., age, weight, femoral head size, implant design). A significant positive correlation was found between femoral head size and volumetric wear rate (VWR). However, no data was

presented on the performance of the femoral components against which the acetabular components had articulated.

The only reports that have discussed failure of matched acetabular and femoral components in human THA are outcomes studies that provide information on cases of aseptic loosening (*See introductory sections of Chapters 3 & 4*) [4-6]. From these studies, it is apparent that there is a disconnect between aseptic loosening of the acetabular component and aseptic loosening of the femoral component. The evidence from the literature is that the initiating event for aseptic loosening of the human femoral component is mechanical in nature [1, 7-8]. The rate of aseptic loosening of the femoral component is higher in the first five years after surgery, but then the rate of loosening lowers and remains constant with time [9]. By contrast, the initiating event for aseptic loosening of the acetabular component appears to be biological in nature [2-3, 8]. A complex biological reaction is initiated when submicron-sized wear debris from the acetabular component made of the UHMWPE comes in contact with the intraarticular edge of the bone/cement interface. The ultimate result of this biological reaction is the loss of bone in the areas containing UHMWPE wear debris followed by interposition of soft tissue between the bone and the polymethyl methacrylate (PMMA) bone cement. The loss of bone and the growth of the soft tissue leads to an aseptic loosening rate for human acetabular components that increases with time and can become close to exponential in nature [2, 8].

5.1.2. Wear Debris

Because of the relationship between UHMWPE wear and osteolysis that results in aseptic loosening of the acetabular component, the reduction of UHMWPE wear in

human THA is currently a major focus in orthopaedic research [10-13]. One method that human orthopaedic surgeons and researchers have developed for reducing UHMWPE wear is to highly crosslink the material. *In vitro* wear testing performed on highly crosslinked UHMWPE resulted in lower wear rates than for conventional UHMWPE. It is hoped that this decreased wear will reduce osteolysis and subsequent aseptic loosening in the future.

An experimental study, performed in dogs to study the results of large loads of artificially introduced debris [14], found no radiographic evidence of osteolytic lesions or radiolucencies; however, bone resorption was apparent upon microscopic examination.

5.1.3. Canine Total Hip Arthroplasty

In Chapter 3, the femoral component was tested, and the resulting data was analyzed for the femoral component alone. The acetabular component received similar treatment in Chapter 4. However, neither of these components operates alone, and the interaction between the two components and their failure mechanisms needs to be addressed.

The level of osteolysis detected in human THA can be extensive, but there have been no similar reports related to clinical canine THA, to the best of the author's knowledge. In addition, to the author's best knowledge, prior to this study there had been no research to determine whether dogs generated comparable amounts of wear debris to that generated by humans.

5.2. Hypotheses

The first hypothesis was that retrievals with higher wear rates of the UHMWPE would have higher rate of loosening for the femoral component. In one study of human

THAs retrieved at autopsy [7]. femoral components with debonding at the proximal PMMA/metal interface allowed UHMWPE wear debris to infiltrate the debonded area which triggered an osteolytic response in the proximal femur. If the same response was found in canine THA. increased loosening of the femoral component at the PMMA/metal interface would be expected to correlate positively with increased UHMWPE wear.

The second hypothesis was that acetabular components that displayed a larger volume of UHMWPE wear would also have higher amounts of wear debris contained in the soft tissues surrounding the implant.

The third hypothesis was that acetabular components that were loose would have higher levels of wear debris in the surrounding soft tissues. Several of the acetabular components had large chunks of PMMA debris loose in the joint. Some components were no longer supported by PMMA around the rim. If the cement mantle was cracking and breaking and releasing debris into the surrounding tissue. it stood to reason that the acetabular component would become loosened in view of lack of support by the PMMA..

The fourth hypothesis was that there would be increased implant-on-implant damage to the acetabular component when the femoral component was loosened. If the femoral component were loose within the femur. it would not maintain proper alignment of the femoral head with respect to the acetabular component. thus leading to increased damage to the acetabular component.

5.3. Methods

5.3.1. Femoral and Acetabular Component Data

The methods used to analyze the canine femoral and acetabular components and the

data collected using those methods are described in Chapters 3 and 4. Using that data, the questions to be answered in this chapter include:

1. Whether data from analysis of the acetabular component correlate with measures of failure of the femoral component and the generation of wear debris.
2. Whether data from analysis of the femoral component correlate with measures of failure of the acetabular component and the generation of wear debris.

Briefly, the data include demographic data taken from the chart (*See Chapter 3*), results of mechanical testing of the femoral component (*See Chapter 3*), measurements taken from contact radiographs of the intact femora (*See Chapter 3*), measurements taken from contact radiographs of transverse slices of the femora (*See Chapter 3*), volumetric wear measurements of the acetabular components (*See Chapter 4*), wear damage scores of the acetabular components (*See Chapter 4*), results of mechanical testing of the acetabular components (*See Chapter 4*), and amounts of wear debris isolated from surrounding soft tissues (described below).

5.3.2. Isolation of Wear Debris From Joint Capsule Tissue

At the time that the soft tissues were removed from the hemipelves and femora, tissue from the pseudocapsule was saved and frozen for future analysis. Shanbhag's method for isolation of wear debris was used [15] (*See Appendix J – Wear Debris Isolation Method*). Three grams of tissue were minced and placed in Papain solution and incubated in a water bath at 37°C for 48 hours. This tissue digest was then mixed with 9 ml of 95% ethanol and centrifuged. The supernatant was discarded, and the pellet was

resuspended in potassium hydroxide (KOH). After 5 minutes of sonication, the digest was incubated in the water bath for 16 hours. After centrifugation and discarding of the supernatant, the pellet was resuspended in equal parts ethanol and hexane in order to separate UHMWPE from other metal, PMMA, and bone debris. After centrifugation, the UHMWPE debris was carefully removed from the ethanol/hexane interface. Keeping the two debris samples separate, the debris was resuspended in KOH and incubated in the water bath overnight. The specimens were centrifuged, and the supernatant was discarded. The particles were washed three times in distilled water, which involved washing in distilled water, sonication, and allowing the specimen to sit in the water bath overnight. After the final distilled water wash, the specimen was centrifuged, the supernatant discarded, and the debris was suspended in ethanol and stored for future analysis.

The debris fractions were dried and weighed using an analytical scale to determine amounts of the debris fractions relative to the weight of the digested tissue sample. The amount of debris was normalized for the size of the specimen (i.e., units of mg debris per gram of tissue sample).

5.3.3. Statistical Analysis

Statistical analysis was performed using SAS software (SAS Institute, Cary, NC). Statistical analysis was performed with the assistance of the Center for Applied Statistical Expertise (CASE) in the Statistics Department at CSU. The low number of specimens and the large number of variables in this study presented challenges for statistician and researcher.

The SAS factor procedure [16] was used to perform principal component analysis in

order to identify highly correlated variables. These results were analyzed in combination with expert opinion of engineers and veterinary surgeons in order to select variables that could be combined into index variables and thus reduce dimensionality (i.e., number of variables). Square root transformations were used for those indices that did not have a normal distribution in order to allow the use of parametric statistics.

Simple and multiple linear regression analyses were performed with bone/PMMA index, bone/metal index, PMMA/metal subsidence, and PMMA/metal ML translation (from femoral component), TVW, VWR, and PE micromotion (from acetabular component) as the dependent variables. For multiple linear regression, two model selection methods were used in attempting to determine the best model for predicting the selected dependent variables [16-17]. The best selection method calculates the coefficient of determination (R^2) for all possible models for each number of variables being considered (e.g., one to four variables models). The models with the greatest R^2 are selected for each number of variables (*See Appendix F for sample output*). The backward selection method starts by fitting the multiple regression model containing all the possible independent variables. At each step, the variable that makes the smallest contribution to the model (i.e., smallest F statistic) is deleted. This process continues until an F statistic for a particular model meets the significance criteria that is preset by the investigator.

In addition, simple linear regression for all variables vs. implant duration were also performed to look for time-dependent trends.

5.4. Results

Just as was seen in human THA [4-6], there does not appear to be a connection in canine THA between aseptic loosening of the femoral component and aseptic loosening of the acetabular component (*See Figure 5.1*). Of 14 cases with a firmly implanted femoral component, six articulated against loose acetabular components. Of 24 cases with a loose femoral component, eight were matched with a firmly implanted acetabular component. Only 4 (10.5%) of 38 specimens had both femoral and acetabular components firmly implanted; whereas, 14 (36.8%) cases had both components loose. In addition, bilateral implants appeared to be more stable for both components than unilateral implants. These results were not significant by Chi-Square analysis.

When frequency distributions were calculated by manufacturer (*See Figure 5.2*), there was a trend that the Richards implants tended to be more stable than the BioMedtrix implants. These results were not significant by Chi-Square analysis.

5.4.1. Statistical Analysis

The statistically significant correlations from the simple linear regression analysis are presented (*See Table 5.1*). There were no significant correlations for the dependent variables, TVW and PE micromotion.

Multiple linear regression analysis was performed using backward and best model selection methods in an attempt to find a model that could be used to predict the dependent variables based on the combination of femoral component data, acetabular component data, and wear debris data. It was hoped that this analysis would demonstrate that femoral component data would appear as predictors of acetabular component wear and loosening and that acetabular component data would appear as predictors of femoral

component loosening. There were no clear-cut superior models for any of the dependent variables. Representative samples of possible models for each of the dependent variables are presented (*See Table 5.2*). Variables that appeared most often in these models are presented (*See Table 5.3*).

5.5. Discussion

This is the first report that provides benchmark data on the postmortem retrieval analysis of clinical canine THAs. This is also the first study of postmortem retrievals of THA that incorporated extensive and sophisticated statistical analysis method.

One limitation of the Shanbhag method of wear debris isolation [15] was that the 70% ethanol solution used to store the final product softened the PMMA component of the wear debris and caused it to consolidate into one lump during centrifugation. The ethanol took on the color of the PMMA that led to the conclusion that some of the wear debris was dissolved in the ethanol. This had not been mentioned as a problem in work done by either Shanbhag *et al.* [15] or Campbell *et al.* [18]. Several specimens had copious amounts of white debris in the miscellaneous debris fraction. Since the soft tissue of these specimens had hard lumps within the tissue, the white debris may be a digestion of ectopic calcification.

There was a significant positive correlation between VWR and the bone/PMMA index (*See Figure 5.3*), the bone/metal index (*See Figure 5.4*), and minimum PMMA (*See Figure 5.5*). The significant positive correlation between VWR and the measures of loosening of the femoral component (i.e., bone/PMMA index and bone/metal index) appear to agree with human THA literature. In human studies, acetabular components

retrieved at revision displayed markedly higher volumetric wear than those retrieved at autopsy (*See Table 4.1*) [3, 19], and increased VWR of canine acetabular components when the femoral component had loosened was expected. The correlation was not as strong at for the bone/metal index, probably because there were more implants loose at this interface, and the level of loosening and damage was thus more advanced. Perhaps the advanced damage at this interface and the introduction of secondary failure mechanisms confounded the relationship between VWR and bone/metal index. The greatest average micromotion occurred in subsidence at the bone/metal interface. The correlation between VWR and the bone/PMMA interface was stronger, perhaps because this would be an interface that failed secondary to failure of the bone/metal interface for these implants, and that secondary failure was not as advanced at the bone/PMMA interface.

Minimum PMMA was also positively correlated with VWR. Since thin cement mantles have been implicated in increased rates of aseptic loosening of the femoral component in both canine and human THA (*See Chapter 3*) [8, 20] and since the radiographic findings of Chapter 3 reinforced these findings (*See Table 3.6 – GZ indices*), it was expected that minimum PMMA would negatively correlate with VWR. This correlation is perhaps a statistical anomaly due to the low numbers of specimens in this study and bears further investigation. Only 6 cases had a minimum PMMA of greater than 1 mm, and this skewing of the data may explain this anomaly. Minimum PMMA did not correlate with loosening of the femoral components in Chapter 3 (*See Table 3.5*), but it was negatively correlated with implant duration. This negative correlation may be due to an increasing awareness by veterinary orthopaedic surgeons in recent years of the

need to properly centralize the distal tip of the femoral component in an attempt to decrease the incidence of aseptic loosening of the femoral component.

There was significant negative correlation (*See Table 5.1*) between the bone/PMMA index and the rim and creep indices and a significant positive correlation between the bone/PMMA index and the miscellaneous wear debris fraction; however, none of these were strong correlations (i.e., $R^2 < 0.20$). The negative correlation between bone/PMMA and the creep index mirrors the negative correlation between VWR and the creep index found in Chapter 4 (*See Table 4.5*). Perhaps with increased loosening of the femoral component, the implant-on-implant damage, which causes creep, decreased since the femoral component was more likely to move within the femur before the femoral neck could apply high enough forces to the UHMWPE to cause creep. This explanation may also explain the negative correlation between damage to the rim of the acetabular component and the bone/PMMA index.

The positive correlation between the bone/PMMA index and the miscellaneous wear debris fraction as well as the positive correlation between the bone/metal index and PE debris fraction was expected since more wear debris would be generated with increased loosening of the femoral component.

There was significant positive correlation between the bone/metal index (*See Table 5.1*) and the embedded metal index. Only seven acetabular components had a non-zero score for embedded metal, and three of them were matched against femoral components that were loose upon manual manipulation and not mechanically tested. Only four acetabular components with a non-zero embedded metal index were matched against femoral components that were mechanically tested, and all four of these femoral

components tested loose at the PMMA/metal interface. Since a loose femoral component moving against the PMMA would generate metal debris, the positive correlation between bone/metal index and embedded metal index would also be expected.

A possible relationship between the thickness of the cement mantle and centralization of the distal tip of the femoral component with VWR of the acetabular component appeared as well. There was a positive correlation between VWR and the GZ 9-10 index (middle and distal zones on cranial side – ML view). This agrees with the negative correlation between GZ 12-13 index (middle and distal zones on caudal side – ML view) and the bone/PMMA index in Chapter 3 (*See Table 3.6*) since there was a positive correlation between VWR and both femoral component dependent variables. This meant that as the cement mantle on the cranial side of the femoral component increased (and the cement mantle on the caudal side of the femoral component decreased), volumetric wear and loosening at the bone/PMMA interface increased.

There was a negative correlation between VWR and the GZ 2-3 index (middle and distal zones on lateral side – CC view) as well as a negative correlation between both femoral component dependent variables and GZ 2-3 index (middle and distal zones on lateral side – CC view). This means that as the cement mantle on the lateral side of the femoral component decreased, VWR increased and motion of the femoral component increased at both interfaces. This relationship was further supported by the positive correlation between VWR and both femoral component dependent variables.

Shape index 2 (*See Figure 3.14 and Glossary C - Variables*) also appeared in several of the possible models for both femoral dependent variables and for VWR. The relationships between these three dependent variables and the GZ 9-10 index (middle and

distal zones on cranial side – ML view) and GZ 12-13 index (middle and distal zones on caudal side – ML view) are probably interrelated with the shape index 2. In Chapter 3, it was found that as the femoral medullary canal became thinner in the cranial-caudal direction, loosening of the femoral component increased. The shape index 2 also correlated positively with VWR in the backward selection model. This relationship is further supported by the positive correlation between VWR and both femoral component variables (*See Figures 5.3 & 5.4*).

The positive correlation between TVW and UHMWPE inner diameter may be a reflection of the older Richards acetabular components with a larger UHMWPE inner diameter versus the newer BioMedtrix acetabular components with newer cementing techniques and a smaller UHMWPE inner diameter. Some of the TVW correlations (i.e., with UHMWPE inner diameter) may be a reflection of the implant design rather than a true correlation with an independent variable.

There were no clear-cut models developed using multiple linear regression methods that could be used to predict failure of the femoral and acetabular components. This may be due, in part, to the low number of specimens in the Richards and BioMedtrix #2 groups and the variability of the data. However, the variables that will be of most importance in future studies were those that appeared in more than one possible model (i.e., listed in the results section above). Despite the fact that no superior models were identified, there was still value for having performed this sophisticated statistical analysis. The factor analysis used to create index variables (*See Chapters 3 & 4*) resulted in the surprising finding of a relationship between the shape of the canine femoral canal and aseptic loosening of the femoral component (*See Chapter 3*).

There were multiple possible models identified for the femoral dependent variables that contained the miscellaneous wear debris fraction as well as a number of variables from the acetabular data, including creep index, rim index, embedded metal index, and 3BW index. In addition, there were multiple possible models identified for the acetabular dependent variables that contained the both wear debris fraction as well as a number of variables from the femoral data, including minimum PMMA, shape index 2, area index, femoral head angle, GZ 2-3 index (middle and distal zones on lateral side – CC view), GZ 9-10 index (middle and distal zones on cranial side – ML view), distance index, and radiolucency index 1.

Interesting findings from the multiple linear regression analysis (*See Table 5.2*) included the following:

1. For bone/PMMA index:
    1. The negative correlation with the UHMWPE damage indices for acetabular rim, creep, and third body wear.
    2. The positive correlation with the UHMWPE damage index for embedded metal.
    3. The positive correlation with the miscellaneous debris fraction.
2. For bone/metal index:
    1. The negative correlation with the UHMWPE damage indices for acetabular rim and the fire hydrant cut-out.
    2. The positive correlation with the UHMWPE damage index for embedded metal.
    3. The negative correlation with the number of implants.

3. For TVW:
    1. The positive correlation with the femoral shape index 2, minimum PMMA, and distance 3.
    2. The negative correlation with the BM1 index.
4. For VWR:
    1. The positive correlation with minimum PMMA, radiolucency index 1, and GZ 9-10 index (middle and distal zones on cranial side – ML view).
    2. The negative correlation with the GZ 2-3 index (middle and distal zones on lateral side – CC view).
    3. The positive correlation with the miscellaneous debris fraction.

There are a number of possible relationships between femoral dependent variables and wear debris or acetabular data and between acetabular dependent variables and wear debris or femoral data that need more research. With larger sample sizes for each implant design, the results of the multiple linear regression analysis may be able in the future to define a superior model for identifying variables that can predict failure of the femoral and acetabular components.

The findings that unilateral THA in dogs did not perform as well as bilateral THA (*See Chapters 3 and 4*) was supported further when comparing femoral and acetabular component together (*See Figure 5.1*). The unilateral group contained only one specimen with both components firmly implanted; whereas, the bilateral group contained three specimens with both components firmly implanted. The unilateral group contained 11 of the 14 retrievals that had both femoral and acetabular components loose.

The Richards implant design, despite being the implants with the longest durations

and the older surgical techniques, tended to perform better than the BioMedtrix implant designs (*See Figure 5.2*). Nine of the 12 Richards retrievals were bilateral as opposed to 8 of 22 BioMedtrix #1 and 1 of 4 BioMedtrix #2. The performance of the Richards implants may have performed better for that reason. Twelve of the 14 specimens that had both components loose were BioMedtrix implants; however, 7 BioMedtrix #1 femoral components were firmly implanted, 5 of which were bilaterals. This results strongly suggests that the issue is not so much the implant design but rather whether the implant was bilateral or unilateral.

From the results of the owner survey (*See Chapter 2*) [21], it is apparent that owners are unaware that their dogs may be in pain. Humans with aseptic loosening of the femoral component and periprosthetic remodeling of the femur commonly experience bone pain, thus causing the patient to undergo revision surgery [22]. The level of periprosthetic remodeling seen in the canine femora in this study suggest that these dogs suffered a painful condition. In contrast, humans with aseptic loosening of the acetabular component often remain asymptomatic and therefore clinically successful. This may also be the case with canine THA. As long as the loose acetabular components remain asymptomatic, no intervention may be necessary other than thorough clinical follow-up.

5.6. Conclusions

The results of this dissertation study determined that:

1. The first hypothesis, that retrievals with higher UHMWPE wear rates would have higher rates of loosening of the femoral component, was supported by the significant positive relationship found between VWR and bone/PMMA

index (*See Figure 5.3*) and between VWR and bone/metal index (*See Figure 5.4*).

2. The second hypothesis, that implants with increased wear would have increased wear debris in the surrounding soft tissues, was supported by the significant positive correlation between VWR and the miscellaneous debris fraction that appeared in several of the multiple regression models (*See Table 5.2*).
3. The third hypothesis, that loose femoral component would positively correlate with increased wear debris in the surrounding soft tissues, was supported by results of both the simple and multiple linear regression analysis (*See Tables 5.1 & 5.2*). The miscellaneous debris fraction was positively correlated with the bone/PMMA index, and the PE debris fraction was positively correlated with the bone/metal index. Human revision retrievals, known to have failed, have higher wear rates than postmortem retrievals [3, 19]; therefore, it would be reasonable to expect increase wear with component failure in the dog as well.
4. Rather than seeing increased implant-on-implant damage with increased loosening of the femoral component in support of the fourth hypothesis, the creep index was negatively correlated with the bone/PMMA index.

There were two findings in this research project that were quite surprising. The first was with regard to whether dogs with bilateral DJD should have unilateral or bilateral THA. The existing surgical paradigm in place before the beginning of the present study held that unilateral surgery was adequate for treating bilateral DJD. That paradigm was

not supported by the findings of this study. The negative correlation between the number of implants and the femoral dependent variables does not support the use of unilateral THA in dogs with bilateral DJD. Bilateral implants maintained stability of the femoral and acetabular components to a much greater degree than unilateral implants. Dogs with bilateral DJD should undergo bilateral THA for the best results. Unfortunately, the cost of the surgery will continue to be a major consideration for the owners of dogs with DJD.

The second and most surprising finding was that the shape of the medullary canal was related to aseptic loosening of the femoral component and the VWR of the acetabular component. Basically, what was found in the course of statistical analysis of the data was that the measure of the width of the femoral medullary canal in Gruen zone 4 (in CC view) (*See Figure 3.6*) was positively correlated with aseptic loosening at the bone/PMMA interface. This meant that as the width of the femur in the medial-lateral direction increased, loosening of the femoral component increased (*See Figure 3.14*). Conversely, the measure of the width of the femoral medullary canal in Gruen zone 11 (in ML view) was negatively correlated with aseptic loosening at the bone/PMMA interface. This meant that as the width of the femur in the CC direction decreased, loosening of the femoral component increased. As in human studies [3, 19], increased UHMWPE wear is seen with increased failure of the implants.

Perhaps one way to deal with the shape issue in the canine femur is to redesign the femoral component to ensure that the width of the femoral component is decreased in the cranial-caudal direction in order to maximize the cement mantle in that direction. The shape of the femoral components seems to support this statement. The distal tip of the BioMedtrix femoral components is round with two small grooves. The Richards femoral

component was more rectangular in shape and was thinner in the cranial-caudal direction. The rectangular shape increases the thickness of the cement mantle in the cranial-caudal direction. This may be one possible explanation for why Richards femoral components performed better despite the much longer implant durations and earlier generation cementing techniques. This finding is surprising because of the sharp corners on this design that have been shown to cause stress concentrations in the PMMA. Human postmortem retrieval studies showed radial cracks initiated from sharp corners. In this study, the bilateral vs. unilateral effect may predominant and explain the better performance of the Richards components.

Owners who are willing and able to pay for THA for their dogs appear enthusiastic at the chance to become involved in research that has the potential to help dogs with DJD in the future.

5.7. Acknowledgements

Pat Campbell, Ph.D. – for technical assistance on wear debris isolation and tissue digestion: Jim zum Brunnen of the Statistics Department at CSU for statistical analysis:

5.8. References

1) Maloney WJ, Jasty M, Burke DW, O'Connor DO, Zalenski EB, Bragdon C, Harris WH. Biomechanical and Histologic Investigation of Cemented Total Hip Arthroplasties: A Study of Autopsy-Retrieved Femurs After *In Vivo* Cycling. *Clinical Orthopaedics and Related Research*, 1989; 249: 129-140.

2) Schmalzried TP, Kwong LM, Jasty M, Sedlacek RC, Haire TC, O'Connor DO, Bragdon CR, Kabo JM, Malcolm AJ, Harris WH. The Mechanism of Loosening of Cemented Acetabular Components in Total Hip Arthroplasty: Analysis of Specimens Retrieved at Autopsy. *Clinical Orthopaedics and Related Research*, 1992; 274: 60-78.

3) Jasty M. Goetz DD. Bragdon CR. Lee KR. Hanson AE. Elder JR. Harris WH. Wear of Polyethylene Acetabular Components in Total Hip Arthroplasty: An Analysis of One Hundred and Twenty-Eight Components Retrieved at Autopsy or Revision Operations. *The Journal of Bone and Joint Surgery*. 1997; 79-A: 349-358.

4) Mulroy WF. Estok DM. Harris WH. Total Hip Arthroplasty with Use of So-Called Second-Generation Cementing Techniques: A Fifteen-Year-Average Follow-Up Study. *The Journal of Bone and Joint Surgery*. 1995; 77-A: 1845-1852.

5) Klapach AS. Callaghan JJ. Goetz DD. Olejniczak JP. Johnston RC. Charnley Total Hip Arthroplasty With Use of Improved Cementing Techniques: A Minimum Twenty-Year Follow-Up. *The Journal of Bone and Joint Surgery*. 2001; 83-A: 1840-1848.

6) Iorio R. Eftekhar NS. Kobayashi S. Grelsamer RP. Cemented Revision of Failed Total Hip Arthroplasty: Survivorship Analysis. *Clinical Orthopaedics and Related Research*. 1995; 316: 121-130.

7) Jasty M. Maloney WJ. Bragdon CR. O'Connor DO. Haire T. Harris WH. The Initiation of Failure in Cemented Femoral Components of Hip Arthroplasties. *The Journal of Bone and Joint Surgery*. 1991; 73-B: 551-558.

8) Schmalzried TP. Maloney WJ. Jasty M. Kwong LM. Harris WH. Autopsy Studies of the Bone-Cement Interface in Well-Fixed Cemented Total Hip Arthroplasties. *The Journal of Arthroplasty*. 1993; 8: 179-188.

9) Harris WH. Sledge CB. Total Hip and Total Knee Replacement (First of Two Parts). *New England Journal of Medicine*. 1990; 323: 725-731.

10) Muratoglu OK. Bragdon CR. O'Connor DO. Jasty M. Harris WH. A Novel Method of Cross-Linking Ultra-High-Molecular-Weight Polyethylene to Improve Wear, Reduce Oxidation, and Retain Mechanical Properties. *The Journal of Arthroplasty*, 2001; 16: 149-160.

11) Endo MM. Barbour PSM. Barton DC. Fisher J. Tipper JL. Ingham E. Stone MH. Comparative Wear and Wear Debris Under Three Different Counterface Conditions of Crosslinked and Non-Crosslinked Ultra High Molecular Weight Polyethylene. *Bio-Medical Materials and Engineering*, 2001; 11: 23-35.

12) Kurtz SM. Pruitt LA. Jewett CW. Foulds JR. Edidin AA. Radiation and Chemical Crosslinking Promote Strain Hardening Behavior and Molecular Alignment in Ultra High Molecular Weight Polyethylene During Multi-Axial Loading Conditions. *Biomaterials*. 1999; 20: 1449-1462.

13) McKellop H. Shen FW. Lu B. Campbell P. Salovey R. Development of an Extremely Wear-Resistant Ultra High Molecular Weight Polyethylene for Total Hip

Replacements. *Journal of Orthopaedic Research*. 1999; 17: 157-167.

14) Kraemer WJ. Maistrelli GL. Fornasier V. Binnington A. Shao JF. Migration of Polyethylene Wear Debris in Hip Arthroplasties: A Canine Model. *Journal of Applied Biomaterials*. 1995; 6: 225-230.

15) Shanbhag AS. Jacobs JJ. Glant TT. Gilbert JL. Black J. Galante JO. Composition and Morphology of Wear Debris in Failed Uncemented Total Hip Replacement. *The Journal of Bone and Joint Surgery*. 1994; 76-B: 60-67.

16) SAS Institute. Inc. *SAS/STAT User's Guide, Version 6, 4th ed.*. SAS Institute. Inc.. Cary. NC. 1990.

17) Campbell P. Ma S. Yeom B. McKellop H. Schmalzried TP. Amstutz HC. Isolation of Predominantly Submicron-Sized UHMWPE Wear Particles From Periprosthetic Tissues. *Journal of Biomedical Materials Research*. 1995; 29: 127-131.

18) Ott RL. More on Multiple Regression. *An Introduction to Statistical Methods and Data Analysis, 4th ed.* Duxbury Press. Belmont. California. Chapter 12; 1993: 647-766.

19) Sychterz CJ. Moon KH. Hashimoto Y. Terefenko KM. Engh Jr CA. Bauer TW. Wear of Polyethylene Cups in Total Hip Arthroplasty: A Study of Specimens Retrieved Post Mortem. *The Journal of Bone and Joint Surgery*. 1996; 78-A: 1193-1200.

20) Edwards MR. Egger EL. Schwarz PD. Aseptic Loosening of the Femoral Implant after Cemented Total Hip Arthroplasty in Dogs: 11 Cases in 10 Dogs (1991-1995). *Journal of the American Veterinary Medical Association*.1997; 211: 580-586.

21) Skurla CT. Egger EL. Schwarz PD. James SP. Owner Assessment of the Outcome of Total Hip Arthroplasty in Dogs. *Journal of the American Veterinary Medical Association*. 2000; 217: 1010-1012.

22) Georgiou AP. Cunningham JL. Accurate Diagnosis of Hip Prosthesis Loosening Using a Vibrational Technique. *Clinical Biomechanics*. 2001; 16: 315-323.

5.9. Tables

Table 5.1					
Dependent Variable	**Independent Variable**	**Pearson's rho**	**R^2**	**p**	**Power**
VWR	Bone/PMMA index	0.636	0.404	<0.001	0.988
	Min. PMMA	0.480	0.230	0.005	0.839
	Bone/Metal index	0.405	0.164	0.033	0.584
Bone/PMMA index	Rim index	-0.427	0.182	0.013	0.721
	Misc. debris	0.376	0.141	0.037	0.560
	Creep index	-0.350	0.122	0.046	0.522
Bone/metal index	Embedded metal index	0.475	0.226	0.009	0.771
	PE debris	0.431	0.186	0.025	0.632
PMMA/metal subsidence	Bone area	0.378	0.143	0.047	0.518
	UHMWPE debris	0.596	0.356	0.001	0.937
PMMA/metal ML translation	Void index	-0.394	0.156	0.042	0.541
	BM2 index	0.429	0.184	0.023	0.645
	UHMWPE outer diameter	0.400	0.160	0.035	0.574
	UHMWPE thickness	0.432	0.187	0.022	0.653
	Embedded metal index	0.404	0.163	0.033	0.582

Table 5.1 – Results of simple linear regression analysis by dependent variable in order of descending R^2. The sign of the Pearson's rho indicates whether the correlation between the dependent and independent variables is negative or positive.

Table 5.2					
Selection Method	**Dependent Variable**	**Model R^2 / p**	**Independent Variable**	**Parameter Estimate**	**Par. p**
Backward	Bone/PMMA index	0.850 <0.001	GZ 12-13 index	-6.791	<0.001
			Additional problem	-3.651	0.007
			Shape index 2	7.020	<0.001
			Rim index	-0.579	0.002
			Creep index	-1.457	<0.001
			Embedded metal index	9.551	<0.001
			3BW index	-0.713	0.003
Best – 2 variable	Bone/PMMA index	0.501 <0.001	Implant duration	-0.841	<0.001
			Shape index 2	7.373	<0.001
Best – 2 variable	Bone/PMMA index	0.408 0.001	GZ 12-13 index	-5.949	0.005
			Radioluc. index 1	7.178	<0.001
Best – 3 variable	Bone/PMMA index	0.624 <0.001	Implant duration	-0.978	<0.001
			GZ 12-13 index	-3.989	0.010
			Shape index 2	7.618	<0.001
Best – 4 variable	Bone/PMMA index	0.691 <0.001	GZ 12-13 index	-5.895	<0.001
			Radioluc. index 1	6.365	<0.001
			Rim index	-0.790	<0.001
			Misc. debris	0.039	0.028
Backward	Bone/metal index	0.416 0.003	GZ 5-6 index	7.549	0.006
			Crack index	11.479	0.002
Best – 2 variable	Bone/metal index	0.502 <0.001	Shape index 2	4.045	0.001
			Embedded metal index	9.174	<0.001
Best – 2 variable	Bone/metal index	0.490 0.001	Crack index	7.111	0.010
			Embedded metal index	9.190	0.001
Best – 3 variable	Bone/metal index	0.690 <0.001	Number of implants	-8.119	<0.001
			Area index	-0.147	<0.001
			Rim index	-1.011	<0.001
Best – 4 variables	Bone/metal index	0.774 <0.001	GZ 12-13 index	-4.777	0.008
			Crack index	6.369	0.006
			Rim index	-0.887	0.002
			Embedded metal index	10.634	<0.001
Backward	PMMA/metal subsidence	0.671 <0.001	Crack index	189.3	0.001
			UHMWPE debris	36.96	<0.001
Best – 2 variables	PMMA/metal subsidence	0.613 <0.001	Crack index	182.5	0.002
			UHMWPE debris	35.71	<0.001
		0.458	Creep index	20.21	NS

Best – 2 variables	PMMA/metal subsidence	0.001	Creep index	20.21	NS
Best – 3 variables	PMMA/metal subsidence	0.600 <0.001	UHMWPE debris	19.19	<0.001
			Rim index	-9.29	NS
			UHMWPE debris	38.20	<0.001
Best – 4 variables	PMMA/metal subsidence	0.761 <0.001	Void index	-38.10	0.012
			Crack index	211.6	<0.001
			Rim index	-11.58	0.015
			UHMWPE debris	34.93	<0.001
Backward	PMMA/metal ML translation	None			
Best – 2 variables	PMMA/metal ML translation	0.431 0.001	Femoral head angle	-2.477	0.002
			Embedded metal index	120.75	0.001
Best – 2 variables	PMMA/metal ML translation	0.376 0.004	Number of implants	-59.20	0.008
			Void index	-32.41	0.008
Best – 3 variables	PMMA/metal ML translation	0.559 <0.001	Femoral head angle	-2.58	0.001
			UHMWPE thickness	7.92	0.017
			Embedded metal index	105.28	0.001
Best – 4 variables	PMMA/metal ML translation	0.650 <0.001	Femoral head angle	-3.12	<0.001
			Distance 3	43.55	0.025
			UHMWPE thickness	7.59	0.013
			Embedded metal index	79.22	0.009
Backward	TVW	0.801 <0.001	PE ID	0.011	<0.001
Best – 2 variable	TVW	0.562 <0.001	Implant duration	0.004	<0.001
			PE ID	0.013	<0.001
Best – 2 variable	TVW	0.496 0.001	BM1	-0.022	0.001
			PE ID	0.011	0.002
Best – 3 variable	TVW	0.656 <0.001	Implant duration	0.005	<0.001
			Minimum PMMA	0.014	<0.001
			PE ID	0.012	0.008
Best – 4 variables	TVW	0.734 <0.001	Implant duration	0.004	<0.001
			Minimum PMMA	0.015	<0.001
			Area index	-0.0003	0.010
			PE ID	0.015	<0.001
			Femoral head angle	0.0001	0.001
			GZ 9-10 index	0.006	<0.001
			Distance index	-0.004	0.004

			Radioluc. index 1	0.004	<0.001
			Shape index 2	0.005	<0.001
			PE thickness	-0.0008	<0.001
			Rim index	-0.0008	<0.001
Best – 2 variable	VWR	0.518 0.001	Minimum PMMA	0.004	0.002
			Misc. debris	3.4 E-5	0.034
Best – 2 variable	VWR	0.449 0.002	Minimum PMMA	0.004	<0.001
			GZ 2-3 index	-0.003	0.043
Best – 3 variable	VWR	0.628 <0.001	Minimum PMMA	0.003	0.003
			Rim index	-0.0006	0.006
			Misc. debris	4.3 E-5	0.001
Best – 4 variable	VWR	0.671 <0.001	Miniumum PMMA	0.003	0.001
			PE ID	0.002	0.014
			Rim index	-0.0006	0.003
			Misc. debris	4.6 E-5	0.001
Backward	PE micromotion	None			
Best – 2 variable	PE micromotion	0.272 0.023	Torque	-0.786	0.009
			PE debris	-0.022	NS
Best – 2 variable	PE micromotion	0.229 0.035	Radioluc. index 1	0.122	NS
			Torque	-0.782	0.012
Best – 3 variable	PE micromotion	0.384 0.019	Shape index 2	0.080	NS
			Torque	-0.876	0.004
			PE debris	-0.034	0.026
Best – 4 variables	PE micromotion	0.451 0.028	Void index	-0.039	NS
			Shape index 2	0.091	NS
			Torque	-0.906	0.003
			PE debris	-0.036	0.021

Table 5.2 - Representative example of results of multiple linear regression analysis using backward and best model selection methods. The parameter estimate indicates whether the correlation is negative or positive (NS = not significant).

Table 5.3			
Dependent Variable	**Correlation Direction**	**Independent Variable**	**Data Source**
Bone/PMMA index	Positive	Shape index 2	Femoral component
		Radiolucency index 1	
		Embedded metal index	Acetabular component
		Misc. debris	Wear debris
	Negative	Implant duration	Chart
		GZ 12-13 index	

		Additional problem	Femoral component
		Rim index	Acetabular component
		Creep index	
		3BW index	
Bone/metal index	Positive	GZ 5-6 index	Femoral component
		Crack index	
		Shape index 2	
		Embedded metal index	Acetabular component
	Negative	Number of implants	Chart
		GZ 2-3 index	Femoral component
		GZ 12-13 index	
		Area index	
		Rim index	Acetabular component
		Cutout index	
PMMA/metal subsidence	Positive	Crack index	Femoral component
		Creep index	Acetabular component
		UHMWPE debris fraction	Wear debris
	Negative	Rim index	Acetabular component
PMMA/metal ML translation	Positive	UHMWPE thickness	Chart
		Distance 3	Femoral component
		Embedded metal index	Acetabular component
	Negative	Number of implants	Chart
		Femoral head angle	Femoral component
		Void index	
TVW	Positive	Implant duration	Chart
		UHMWPE inner diameter	
		Shape index 2	Femoral component
		Distance 3	
		Minimum PMMA	

		Creep index	Acetabular component
	Negative	BMI index	Chart
		Area index	Femoral component
		Quadrant index	Acetabular component
VWR	Positive	UHMWPE inner diameter	Chart
		Femoral head angle	Femoral component
		GZ 9-10 index	
		Radiolucency index 1	
		Shape index 2	
		Minimum PMMA	
		Misc. debris	Wear debris
	Negative	UHMWPE thickness	Chart
		GZ 2-3 index	Femoral component
		Distance index	
		Rim index	Acetabular component
PE micromotion	Negative	Torque	Acetabular component
		UHMWPE debris	Wear debris

Table 5.3 – Trends found during multiple linear regression analysis.

5.10. Figures

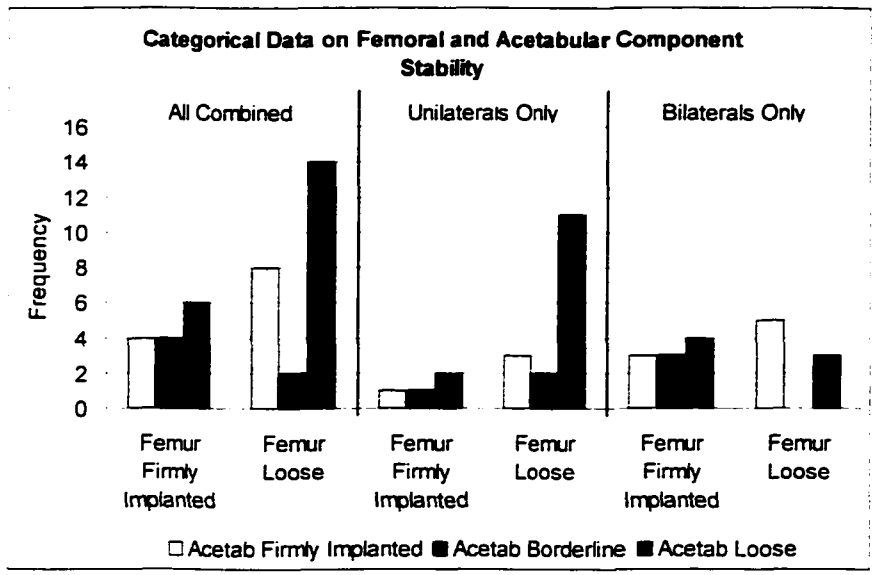

Figure 5.1 – Categorical data on mechanical stability of femoral and acetabular components by bilaterals vs. unilaterals.

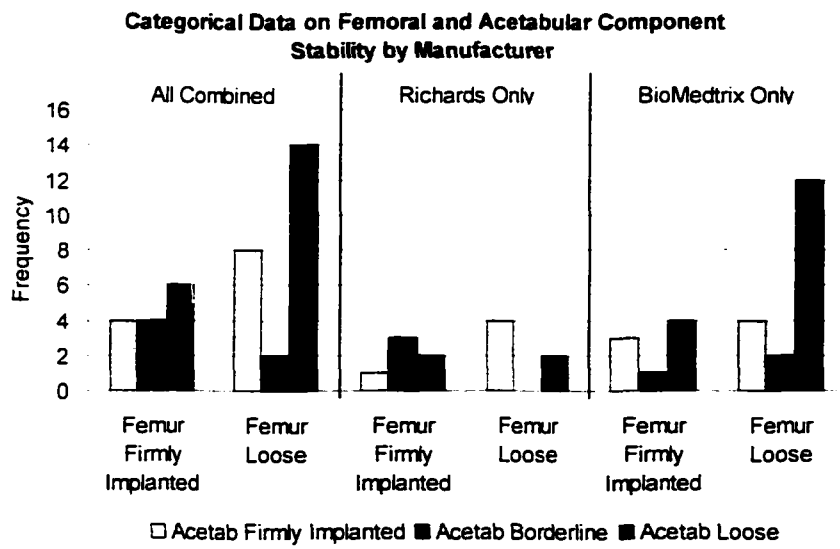

Figure 5.2 – Categorical data on mechanical stabiliyt of femoral and acetabular components by manufacturer.

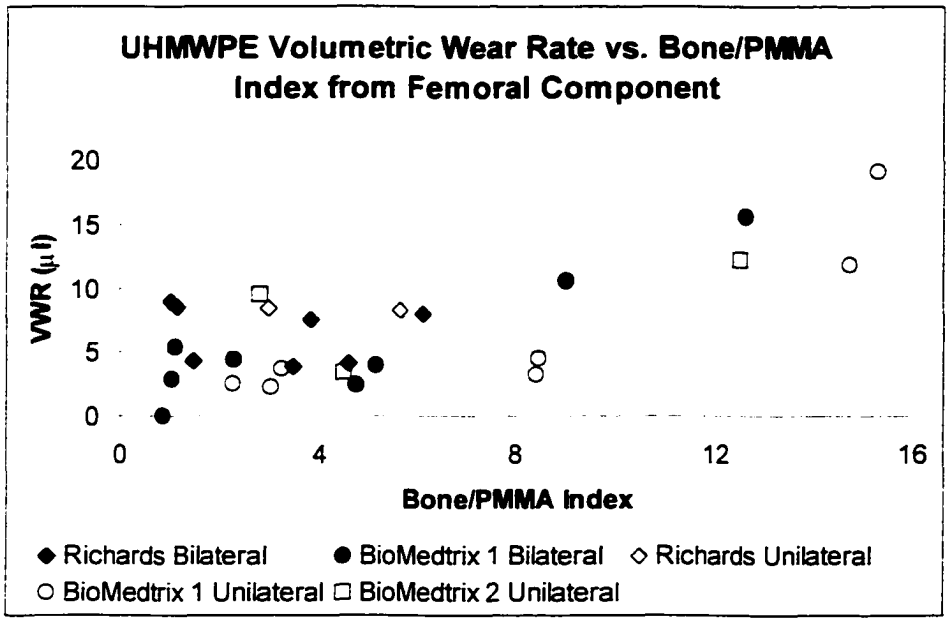

Figure 5.3 – Significant positive correlation between UHMWPE volumetric wear rate and bone/PMMA index from mechanical testing of femoral component (R^2 = 0.40, $p < 0.001$).

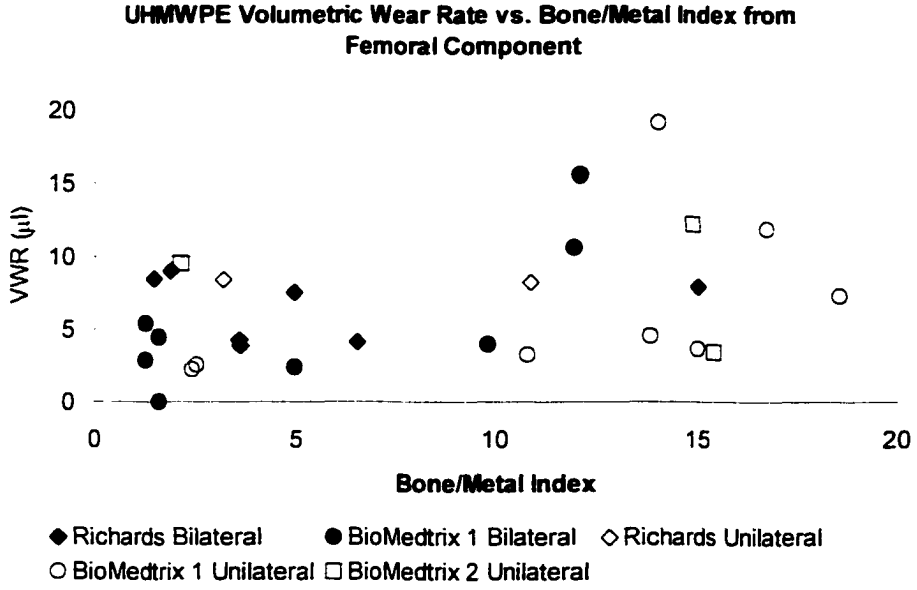

Figure 5.4 – Significant positive correlation between UHMWPE volumetric wear rate and bone/metal index from mechanical testing of femoral component (R^2 = 0.16, $p = 0.033$).

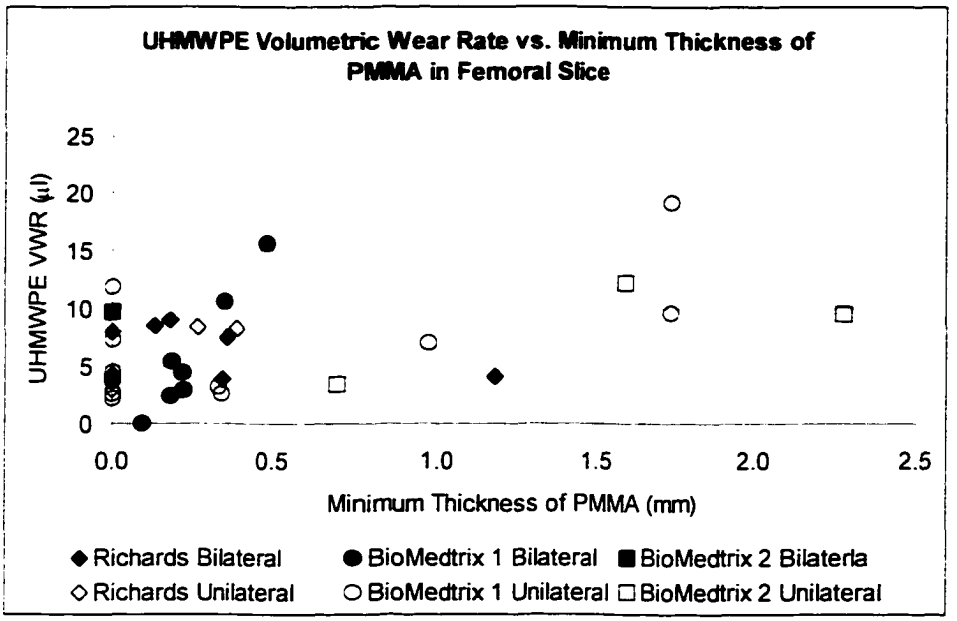

Figure 5.5 – Significant positive correlation between UHMWPE volumetric wear rate and minimum thickness of PMMA in femoral slice ($R^2 = 0.23$, $p = 0.005$).

Chapter 6

Discussion and Conclusions for Veterinary Clinicians

6.1. Introduction

The surgical paradigm in existence at the beginning of the present study held that dogs with bilateral degenerative joint disease (DJD) could be adequately treated with unilateral total hip arthroplasty (THA). Owners and veterinary surgeons alike spoke of how dogs with unilateral THA and bilateral DJD would make adjustments to their gait and put more weight on the implanted side than the intact, diseased side.

One of the major goals of the present study was to provide the veterinary orthopaedic surgeon with information regarding the long-term performance of clinical THA in dogs with the intention of improving future clinical success of canine THAs. The perceived clinical success rate of approximately 95% (*See Tables 3.1 & 4.3*), based on retrospective studies [1-7], is hard to improve upon.

Despite the fact that postmortem retrieval studies cannot be controlled, much has been learned about the performance and failure mechanisms of THAs in humans through postmortem retrieval studies [8-12], and that knowledge could not be gained in any other way. Knowledge about the initiating failure events for the femoral and acetabular components has led to improved surgical technique, implant design, and surgical

outcome in human THA, and it is hoped that similar findings in postmortem retrievals of canine THAs in the present study will be utilized to improve surgical technique and implant design for future canine THA as well.

Other than retrospective outcome studies [1-7], based on follow-up office visits and subjective owner surveys, that presented data with respect to the incidence of aseptic loosening requiring revision surgery, there was very little information in the literature with regard to the long-term performance of clinical canine THA. Indications from these studies were that the incidence of aseptic loosening requiring revision surgery was low in canine THA (*See Tables 3.1 & 4.3*) [1-7]. However, Edwards *et al.* [7] reported a problem with aseptic loosening requiring revision of the BioMedtrix #1 femoral component in 11 (7.2%) of 152 cases with follow-up periods ranging from 26 to 74 months. The study by Edwards *et al.* [7] was the only study providing data on the current implant manufacturer, BioMedtrix.

Prior to the present study, there were no postmortem retrieval studies of clinical canine THA that provided information with regard to the mechanical stability and wear of the implants. The manner and degree of wear and damage to the acetabular component made of ultra high molecular weight polyethylene (UHMWPE) were unknown. The mechanical stability of the femoral and acetabular components after long-term cycling *in situ* was unknown. In order to improve the future performance of canine THA, it is important to gain information about the performance of implanted canine THAs. It was unknown how the three different implant designs would perform relative to each other; although, there were indications that the BioMedtrix #1 implant was associated with increased incidence of aseptic loosening [7] and may not have performed

as well as the Richards and BioMedtrix #2 implants. The shapes of the femoral components were quite different among the three designs (*See Figures 1.3, 1.4 & 1.5*), and the optimum shape for the canine femoral component had not been studied.

The effect of the quality of the cement mantle on the mechanical stability of the THA implants was also unknown. The Richards components, the earliest implants used, had been implanted using older generation cementing techniques than the BioMedtrix implants, and it was unknown what effect the quality of the cement mantle had on the performance of the clinical canine THAs. It was hoped that all of these questions would be answered by the present study, and that recommendations could be made to veterinary surgeons that would lead to improved outcomes in the same manner that human postmortem retrieval studies led to improved surgical techniques and outcomes of human THA.

6.2. Research Findings

6.2.1. Femoral Component

More than half of the femoral components (63.2%) in the present study were loose (*See Figure 3.11*). This contrasts sharply with the 84% positive response to the subjective owner survey discussed in Chapter 2 [13]. The older, Richards femoral components performed better than either the BioMedtrix #1 or BioMedtrix #2 designs, despite older generation cementing techniques. Most surprising of all in the present study, bilateral femoral components performed better than unilateral femoral components. This may explain why the older Richards implants fared better since 9 of 12 were bilateral.

Improper positioning of the distal tip of the femoral component, resulting in thin cement mantles or contact of the distal tip with bone, has been implicated as a predictor of aseptic loosening of the femoral component in both human and canine THA [7-10], and the findings of the present study seem to support these previous findings. Measures of cement mantle thickness on contact radiographs of intact femora in Gruen zones 2 and 3 (middle and distal zones of lateral side - cranial-caudal (CC) view) were negatively correlated with loosening at both interfaces in several of the possible models identified in the multiple linear regression analysis. The most common sites for implant/bone contact or the thinnest PMMA were caudal (11), caudal-lateral (7), or lateral (5). There needs to be a minimal PMMA thickness in order to reduce the stress concentrations in the PMMA.

Another surprising finding in this study that resulted from the sophisticated statistical analysis methods was related to the shape of the medullary canal of the femur. In the analysis of contact radiographs made of the intact femora, measurements of the width of the femoral canal were made in Gruen zones (GZ) 4 (below distal tip of implant, ML width of femoral canal - in CC view) and 11 (below distal tip of implant, CC width of femoral canal - in medial-lateral (ML) view) (*See Figure 3.6*). The measurement made of GZ 4 reflected the width of the femoral canal in the ML direction (*See Figure 3.14*). The measurement made of GZ 11 reflected the width of the femoral canal in the CC direction. A shape effect was detected during multiple linear regression analysis. The measures of loosening of the femoral component were positively correlated with the ML width of the femoral canal (from GZ 4 in CC view) and were negatively correlated with the CC width of the femoral canal (from GZ 11 in ML view). This meant that femora that were wider in the ML direction and narrower in the CC direction tended to have loose femoral

components: whereas, femora that were wider in the CC direction and narrower in the ML direction tended to have firmly implanted femoral components.

This shape finding is reinforced by observations made with regard to the cross-sectional geometry of the distal stem of the Richards versus the BioMedtrix femoral components. The Richards femoral component was more rectangular in shape, and the thinner aspect was in the CC direction. The BioMedtrix designs are both round at the distal end of the femoral stem with two small grooves (one on the cranial side and the other on the caudal side) that run the distal length of the femoral stem. Perhaps the Richards components were thin enough in the cranial-caudal direction that, even in femora that were thin in the cranial-caudal direction, an adequate polymethyl methacrylate (PMMA) cement mantle could be achieved to maintain femoral implant stability for long periods of time. Thin cement mantles have been found, in both human and canine THA, to be predictors of future aseptic loosening of the femora components [7-10], and a finite element analysis study [14] found increased shear stress and micromotion at the PMMA/metal interface when the PMMA thickness was 2 mm or less. Thus, future designs for canine femoral components need to return to a more rectangular or oval shape on the distal end of the femoral stem with the thinner aspect being in the cranial-caudal direction in order to ensure that the cement mantle will be sufficiently thick in all directions around the distal tip of the femoral component. According the the review by Huiskes and Verdonschot [15], sharp corners on the femoral implant and thin PMMA mantles increases stress in the PMMA. Care needs to be taken in the use of sharp corners in femoral component design; however, the Richards femoral components performed better than the BioMedtrix #1 and #2 despite the sharp corners.

Two postmortem retrievals from the present study had femoral components that were so loose they could easily be removed from the femora. Both of the femoral components had damage on the lateral side of the femoral stem. One implant was scratched in a manner that indicated that the implant had been rotating within the stem. The other femoral component was polished to a mirror finish on the lateral side of the femoral stem. These observations in combination with statements from orthopaedic veterinary surgeons performing revision THA led to an early belief that rotational stability was the key issue for the redesign of a canine femoral component. However, the mechanical testing data for the femoral components did not support these early observations. Of the 29 femoral components (*See Table 3.3*) that were mechanically tested (9 were so loose that they were not tested), 14 tested as firmly implanted (i.e., firm in both subsidence and ML translation at both the bone/PMMA and PMMA/metal interfaces). Six femoral components tested as loose in all four tests, and five tested loose in both directions at the PMMA/metal interface but firm in both directions at the bone/PMMA interface. No implants tested loose at the bone/PMMA interface and firm at the PMMA/metal interface. The remaining four femoral components were unique. Two implants tested loose only at the PMMA/metal interface in subsidence. One implant tested loose in both directions at the PMMA/metal interface and in ML translation at the bone/PMMA interface. One implant tested loose in both directions at the PMMA/metal interface and in subsidence at the bone/PMMA interface.

Considering that there were only four implants that had a mismatch between subsidence and ML translation testing at the same interface, it is difficult to draw definitive conclusions. However, three of these four implants tested as loose in

subsidence and firm in ML translation at the same interface, in direct contradiction to the belief that rotational stability is the key. These results provide preliminary data to support published reports from human postmortem retrieval studies that indicate that femoral components fail mechanically at the PMMA/metal interface first with debonding of the PMMA/metal interface as the initiating event [8-10]. This failure in canine THA, as in human THA, appears to be in subsidence first.

In addition, if the metal implant's distal tip is in contact with the endosteal surface, failure may occur at the bone/PMMA interface. One implant (*See Table 3.3*) was grossly loose with the PMMA still attached to the metal, and movement at the bone/PMMA interface had polished the outer surface of the PMMA smooth. There were four grossly loose femoral components with soft tissues at the bone/PMMA interface. In those cases, the failure was too advanced to determine at which interface the failure began.

These results indicate that the rotational damage seen on the femoral components is not related to initiating failure events. However, further research and an increase in the number of tested specimens is required to verify these findings. The data suggests that perhaps the initial failure occurs in subsidence. Eventually, as the debonding of the PMMA/metal interface progresses, the PMMA cracks and the femoral component begins to rotate within the cement mantle, thus causing the rotational markings on the femoral stems. This rotational scoring and burnishing would result from secondary or tertiary failure mechanisms.

6.2.2. Acetabular Component

More than half of the acetabular components (52.6%) in the present study were loose (*See Figure 4.9*). This contrasts sharply with the 84% positive response to the subjective

owner survey discussed in Chapter 2 [13]. The older, Richards femoral components tended to perform better than either the BioMedtrix #1 or BioMedtrix #2 designs, despite older generation cementing techniques. Similar to findings in the femoral component analysis, bilateral acetabular components performed better than unilateral femoral components.

Visual inspection of the acetabular components revealed a high level of implant-on-implant and third body wear damage to the UHMWPE implant. Wear patterns were different from those seen in human THA retrievals. The entire articulating surface was worn and damaged. In many cases, the rim of the acetabular component was no longer supported by PMMA. In some cases, particles of PMMA (up to 1 cm long) were found loose in the joint capsule. Perhaps impingement of the femoral neck on the acetabular component caused high forces on the PMMA (a relatively brittle, amorphous polymer that is below its glass transition temperature at body temperature), causing it to crack and break, thus leading to high levels of third body wear damage caused by PMMA debris getting between the femoral head and the UHMWPE articulating surface.

Great care needs to be taken during canine total hip replacement surgery to ensure that the cement mantle fully supports the acetabular component while reducing the amount of excess PMMA left in the surgical field. Reducing damage to the PMMA mantle and subsequent third body wear damage should be one of the veterinary surgeon's goals.

Loosening of the acetabular component was positively correlated with the total UHMWPE damage score. There were no observations of large-scale osteolysis, as reported in human THA. These two factors led to the conclusion that the initiating event

for failure of the canine acetabular component is mechanical in nature.

Based on observations of high levels of implant-on-implant damage, particularly on the corners and on the fire hydrant cut-out rim, there is a need to redesign the acetabular component to reduce the probability of impingement damage while at the same time preventing the possibility of post-surgical luxations.

6.2.3. Interaction Between Femoral, Acetabular, and Wear Debris Data

This is the first postmortem retrieval study that attempted to connect measures of failure of the femoral component with measures of failure of the acetabular component. This is also the first study of postmortem retrievals that incorporated extensive and sophisticated statistical analysis methods.

There was a significant positive correlation between volumetric wear rate (VWR) of the acetabular component with loosening (i.e., failure) of the femoral component. In human studies, acetabular components retrieved at revision (i.e., considered to have failed) had displayed markedly higher volumetric wear than components retrieved at autopsy (i.e., considered to be clinically successful). The correlation between VWR and failure of the femoral component confirms that the same relationship exists in the dog.

6.3. Discussion

The average VWR of 6.7 mm^3 per year in the canine acetabular components was an order of magnitude lower than published wear rates for human THA (*See Table 4.1*) [12]. This may mean that the dog experiences a lower UHMWPE wear debris load, which may explain why dogs do not display the level of osteolysis seen in human THA.

The incidence of loosening of the femoral and acetabular components in this canine

postmortem retrieval study is alarmingly high. It became quickly apparent that the results of the mechanical testing for implant stability of the femoral and acetabular components did not support the existing surgical paradigm. Despite the fact that many of the bilateral THAs were of very long duration, many remained firmly implanted. More than half of both the femoral and acetabular implants were loose, overall. Perhaps the dogs with bilateral DJD and unilateral THA are overloading their artificial joints in order to favor the more painful contralateral joint.

The BioMedtrix #1 implant design was already associated with aseptic loosening problems [7], and the present study confirmed this. The distal half of the femoral stem in both BioMedtrix designs is round with two small grooves on the cranial and caudal aspects. These grooves were intended to provide rotational stability.

There appears to be a disconnect between owner perceptions and actual performance of canine THA, and more thorough follow-up with objective methods of evaluation need to be incorporated to ensure the best quality of live for the canine THA patient. From the results of the owner survey (*See Chapter 2*) [13], it is apparent that owners are unaware that their dogs may be in pain. Humans with aseptic loosening of the femoral component and periprosthetic remodeling of the femur commonly experience bone pain, thus causing the patient to undergo revision surgery [16]. The level of periprosthetic remodeling seen in the canine femora in this study suggests that these dogs suffered a painful condition. In contrast, humans with aseptic loosening of the acetabular component often remain asymptomatic and therefore clinically successful. This may also be the case with canine THA. As long as the loose acetabular components remain asymptomatic, no intervention may be necessary other than thorough clinical follow-up.

6.4. Conclusions

This was the first postmortem retrieval study in canine THA of this scale with regard to the number of implants and the degree of analysis performed. The results of this dissertation study point out the need to:

1. Improve the design of the femoral stem for better stability by improving the shape of the cross-section of the femoral stem;
2. Improve the design of the acetabular cup and femoral head/neck to reduce implant-on-implant impingement;
3. Improve surgical technique to prevent cracking and breaking of PMMA mantle around the acetabular components, which increases third-body wear of the acetabular component;
4. Improve surgical technique to ensure proper centralization of the femoral component to ensure that the PMMA mantle is at least 2 mm thick in all directions.

With regard to point #3 above, there were very few cracks found in the femoral cement mantle; so most of the cement debris may be generated by PMMA breaking away from the acetabular rim and the proximal end of the femur. Therefore, great care needs to be exercised by the veterinary orthopaedic surgeon to reduce or prevent the generation of large pieces of PMMA debris which have been shown to cause large amounts of third body damage to the implants in this study. Great care also needs to be exercised to ensure that the medullary canal of the femur and the acetabular area of the pelvis are well prepared before cementing the implants in place. Greater consideration needs to be given to performing bilateral THA in dogs with bilateral DJD. Veterinary orthopaedic surgeons

at the Colorado State University Veterinary Teaching Hospital have already changed their surgical paradigm by taking the steps described above.

6.5. References

1) Maloney WJ, Jasty M, Burke DW, O'Connor DO, Zalenski EB, Bragdon C, Harris WH. Biomechanical and Histologic Investigation of Cemented Total Hip Arthroplasties: A Study of Autopsy-Retrieved Femurs After *In Vivo* Cycling. *Clinical Orthopaedics and Related Research*, 1989; 249: 129-140.

2) Jasty M, Maloney WJ, Bragdon CR, O'Connor DO, Haire T, Harris WH. The Initiation of Failure in Cemented Femoral Components of Hip Arthroplasties. *The Journal of Bone and Joint Surgery*, 1991; 73-B: 551-558.

3) Schmalzried TP, Maloney WJ, Jasty M, Kwong LM, Harris WH. Autopsy Studies of the Bone-Cement Interface in Well-Fixed Cemented Total Hip Arthroplasties. *The Journal of Arthroplasty*, 1993; 8: 179-188.

4) Schmalzried TP, Kwong LM, Jasty M, Sedlacek RC, Haire TC, O'Connor DO, Bragdon CR, Kabo JM, Malcolm AJ, Harris WH. The Mechanism of Loosening of Cemented Acetabular Components in Total Hip Arthroplasty: Analysis of Specimens Retrieved at Autopsy. *Clinical Orthopaedics and Related Research*, 1992; 274: 60-78.

5) Jasty M, Goetz DD, Bragdon CR, Lee KR, Hanson AE, Elder JR, Harris WH. Wear of Polyethylene Acetabular Components in Total Hip Arthroplasty: An Analysis of One Hundred and Twenty-Eight Components Retrieved at Autopsy or Revision Operations. *The Journal of Bone and Joint Surgery*, 1997; 79-A: 349-358.

6) Lewis RH, Jones Jr JP: A Clinical Study of Canine Total Hip Arthroplasty. *Veterinary Surgery*, 1980; 9: 20-23.

7) Gofton N, Sumner-Smith G: Total Hip Prosthesis for Revision of Unsuccessful Excision Arthroplasty. *Vet Surg*, 11: 134-139, 1982.

8) Olmstead ML, Hohn RB, Turner TM: A five-year study of 221 total hip replacements in the dog. *J Am Vet Med Assoc*, 183: 191-194, 1983.

9) Parker RB, Bloomberg MS, Bitetto W, Rodkey WG: Canine Total Hip Arthroplasty: A Clinical Review of 20 Cases. *J Am Vet Med Assoc*, 20: 97-104, 1984.

10) Olmstead ML: Total Hip Replacement in the Dog. *Semin Vet Med Surg (Small Animal)*, 2: 131-140, 1987.

11) Paul HA. Bargar WL. A Modified Technique for Canine Total Hip Replacement. *J Am Anim Hosp Assoc.* 23: 13-18. 1987.

12) Edwards MR. Egger EL. Schwarz PD: Aseptic Loosening of the Femoral Implant after Cemented Total Hip Arthroplasty in Dogs: 11 Cases in 10 Dogs (1991-1995). *Journal of the American Veterinary Medical Association.* 1997: 211: 580-586.

13) Skurla CT. Egger EL. Schwarz PD. James SP. Owner Assessment of the Outcome of Total Hip Arthroplasty in Dogs. *Journal of the American Veterinary Medical Association.* 2000: 217: 1010-1012.

14) Ramaniraka NA. Rakotomanana LR. Leyvraz PF. The Fixation of the Cemented Femoral Component: Effects of Stem Stiffness. Cement Thickness and Roughness of the Cement-Bone Surface. *The Journal of Bone and Joint Surgery*: 2000: 82-B: 297-303.

15) Huiskes R. Verdonschot N. BioMechanics of Artificial Joints: The Hip. *Basic Orthopaedic Biomechanics. 2nd ed.*. edited by Van C. Mow and Wilson C. Hayes. Lippincott-Raven Publishers. Philadelphia. Chapter 11: 1997: 395-460.

16) Georgiou AP. Cunningham JL. Accurate Diagnosis of Hip Prosthesis Loosening Using a Vibrational Technique. *Clinical Biomechanics.* 2001: 16: 315-323.

Chapter 7

Performance of Total Hip Arthroplasty in Dogs vs. Humans – Discussion and Conclusions for Researchers

7.1. Introduction

Dogs are the animal model of choice for total hip arthroplasty (THA) [1]; however, recent experimental studies are of relatively short duration (< 2 years in most cases), are performed in dogs without degenerative joint disease (DJD), and utilize cementless implants that are not commercially available to the clinical veterinary orthopaedic surgeon [2-10]. The long-term performance of clinical canine THA was unknown prior to the present study. The only data with regard to aseptic loosening (*See Tables 3.1 & 4.3*) was contained in follow-up studies that used subjective owner observations or clinical office visits [11-17].

The value of postmortem retrieval studies has been demonstrated in human THA [18-22]. While these studies are difficult to control, they remain valuable because the knowledge gained from studying clinically successful THAs postmortem cannot be gained by any other method. The initiating events for the failure of human THA were found through these studies. The initiating event in the failure of human femoral components is mechanical in nature, beginning with debonding of the polymethyl

methacrylate (PMMA)/metal interface distally and proximally [18-20]. By contrast, the initiating event in the failure of the human acetabular component, made of ultra high molecular weight polyethylene (UHMWPE), is biological in nature, beginning with the generation of submicron-sized UHMWPE wear debris, the dispersion of this debris into the intraarticular margin of the bone/PMMA interface, and a complex biological reaction to the debris resulting in osteolysis [21-22]. Unfortunately, there was little statistical data analysis performed in the human postmortem retrieval studies, and there was no information in the literature with regard to the effect of failure of the femoral component on performance of the acetabular component and vice versa.

7.2. Research Findings

7.2.1. Femoral Component

More than half of the femoral components (63.2%) in the present study were loose (*See Figure 3.11*). This contrasts sharply with the 84% positive response to the subjective owner survey discussed in Chapter 2 [23]. The older, Richards femoral components performed better than either the BioMedtrix #1 or BioMedtrix #2 designs, despite older generation cementing and surgical techniques. Most surprising of all in the present study, bilateral femoral components performed better than unilateral femoral components.

Improper positioning of the distal tip of the femoral component, resulting in thin cement mantles or contact of the distal tip with bone, has been implicated as a predictor of aseptic loosening of the femoral component in both human and canine THA [17-20], and the findings of this study support these previous findings. Measures of cement

mantle thickness on contact radiographs of intact femora in Gruen zones 2 and 3 (middle and distal zones on lateral side - cranial-caudal (CC) view) were negatively correlated with loosening at both interfaces in several of the possible models identified in the multiple linear regression analysis.

Another surprising finding in this study that resulted from the sophisticated statistical analysis methods was related to the shape of the medullary canal of the femur. In the analysis of contact radiographs made of the intact femora, measurements of the width of the femoral canal were made in Gruen zones (GZ) 4 (distal to distal tip of implant, ML width of femoral canal – in CC view) and 11 (distal to distal tip of implant, CC width of femoral canal - (ML) view) (*See Figure 3.6*). The measurement made of GZ 4 reflected the width of the femoral canal in the ML direction (*See Figure 3.14*). The measurement made of GZ 11 reflected the width of the femoral canal in the CC direction. A shape effect was detected during multiple linear regression analysis. The measures of loosening of the femoral component were positively correlated with the ML width of the femoral canal (from GZ 4 in CC view) and were negatively correlated with the CC width of the femoral canal (from GZ 11 in ML view). This meant that femora that were wider in the ML direction and narrower in the CC direction tended to have loose femoral components; whereas, femora that were wider in the CC direction and narrower in the ML direction tended to have firmly implanted femoral components (*See Figure 3.14*). This effect has not been studied in the human.

This shape finding is reinforced by observations made with regard to the cross-sectional geometry of the distal stem of the Richards versus the BioMedtrix femoral components. The Richards femoral component was more rectangular in shape, and the

thinner aspect was in the CC direction. The BioMedtrix designs are both round at the distal end of the femoral stem with two small grooves (one on the cranial side and the other on the caudal side) that run the distal length of the femoral stem. Perhaps the Richards components were thin enough in the CC direction that, even in femora that were thin in the CC direction, an adequate PMMA cement mantle could be achieved to maintain femoral implant stability for long periods of time. Thin cement mantles have been found, in both human and canine THA, to be predictors of future aseptic loosening of the femora components [17-20], and a finite element analysis study [24] found increased shear stress and micromotion at the PMMA/metal interface when the PMMA thickness was 2 mm or less. Thus, future designs for canine femoral components need to return to a more rectangular or oval shape on the distal end of the femoral stem with the thinner aspect being in the CC direction in order to ensure that the cement mantle will be sufficiently thick in all directions around the distal tip of the femoral component.

Two postmortem retrievals from the present study had femoral components that were so loose they could easily be removed from the femora. Both of the femoral components had damage on the lateral side of the femoral stem. One implant was scratched in a manner that indicated that the implant had been rotating within the stem. The other femoral component was polished to a mirror finish on the lateral side of the femoral stem. These observations in combination with statements from orthopaedic veterinary surgeons performing revision THA led to an early belief that rotational stability was the key issue for the redesign of a canine femoral component. However, the mechanical testing data did not support these early observations. Of the 29 femoral components (*See Table 3.3*) that were mechanically tested (9 were so loose that they were not tested), 14 tested as

firmly implanted (i.e., firm in both subsidence and ML translation at both the bone/PMMA and PMMA/metal interfaces). Six femoral components tested as loose in all four tests, and five tested loose in both directions at the PMMA/metal interface but firm in both directions at the bone/PMMA interface. No implants tested loose at the bone/PMMA interface and firm at the PMMA/metal interface. The remaining four femoral components were unique. Two implants tested loose only at the PMMA/metal interface in subsidence. One implant tested loose in both directions at the PMMA/metal interface and in ML translation at the bone/PMMA interface. One implant tested loose in both directions at the PMMA/metal interface and in subsidence at the bone/PMMA interface.

Considering that there were only four implants that had a mismatch between subsidence and ML translation testing at the same interface, it is difficult to draw definitive conclusions. However, three of these four implants tested as loose in subsidence and firm in ML translation at the same interface, in direct contradiction to the belief that ML translational stability is the key. These results provide preliminary data to support published reports from human postmortem retrieval studies that indicate that femoral components fail mechanically at the PMMA/metal interface first with debonding of the PMMA/metal interface as the initiating event [18-20]. This failure, as in human THA, appears to be in subsidence first.

These results indicate that the ML translational damage seen on the femoral components is not related to initiating failure events. However, further research and an increase in the number of tested specimens is required to verify these findings. The data seems to suggest that perhaps the initial failure occurs in subsidence. Eventually, as the

debonding of the PMMA/metal interface progresses, the PMMA cracks and the femoral component begins to rotate within the cement mantle, thus causing the ML translational markings on the femoral stems. This rotational scoring and burnishing would result from secondary or tertiary failure mechanisms.

7.2.2. Acetabular Component

More than half of the acetabular components (52.6%) in the present study were loose (*See Figure 4.9*). This contrasts sharply with the 84% positive response to the subjective owner survey discussed in Chapter 2 [23]. The older, Richards femoral components tended to perform better than either the BioMedtrix #1 or BioMedtrix #2 designs, despite older generation cementing techniques. Similar to findings in the femoral component analysis, bilateral acetabular components performed better than unilateral femoral components.

Visual inspection of the acetabular components revealed a high level of implant-on-implant and third body wear damage to the UHMWPE implant. Wear patterns were different from those seen in human THA retrievals. The entire articulating surface was worn and damaged, in contrast to human acetabular components that have characteristic high wear and low wear regions that may be separated by a wear ridge [25]. The levels of damage seen in the canine acetabular components are not commonly seen in human retrievals, either at autopsy or revision surgery.

In many of the canine postmortem retrievals, the rim of the acetabular component was no longer supported by PMMA. In some cases, particles of PMMA (up to 1 cm long) were found loose in the joint capsule. Perhaps impingement of the femoral neck on the acetabular component caused high forces on the PMMA (a relatively brittle,

amorphous polymer that is below its glass transition temperature at body temperature), causing it to crack and break, thus leading to high levels of third body wear damage caused by PMMA debris getting between the femoral head and the UHMWPE articulating surface.

Loosening of the acetabular component was positively correlated with the total UHMWPE damage score. There were no observations of large-scale osteolysis, as reported in human THA. These two factors lead to the conclusion that the initiating event for failure of the canine acetabular component is mechanical in nature. High levels of osteolysis, common findings in human THA, were not observed in the canine retrievals.

7.2.3. Interaction Between Femoral, Acetabular, and Wear Debris Data

This is the first postmortem retrieval study that attempted to connect measures of failure of the femoral component with measures of failure of the acetabular component. This is also the first study of postmortem retrievals that incorporated extensive and sophisticated statistical analysis methods.

There was a significant positive correlation between volumetric wear rate (VWR) of the acetabular component with loosening of the femoral component. In human studies [22], acetabular components retrieved at revision (i.e., considered to have failed) had displayed markedly higher VWRs than components retrieved at autopsy (i.e., considered to be clinically successful). The correlation between VWR and loosening of the femoral component confirms that the same relationship exists in the dog.

The possible relationships that were identified between femoral dependent variables and the wear debris and acetabular data and between the acetabular dependent variables and the wear debris and femoral data will require further analysis with a larger number of

specimens to identify definite relationships between failure mechanisms of the acetabular and femoral components; however, some interesting trends were identified and invite further study. Loosening of the femoral component was negatively correlated with the creep index, 3BW index, and rim index for the acetabular components. Not surprisingly, there was a positive correlation between loosening of the femoral component and the embedded metal index for the acetabular component. VWR was negatively correlated with the thickness of the PMMA in the distal, lateral aspect of the femur.

Unfortunately, the number of specimens was too small to allow for the selection of a clearly superior model to predict failure of the femoral and acetabular components through the use of multiple linear regression, but some interesting trends were identified for future study.

7.3. Discussion

The average VWR of 6.7 mm^3 per year in the canine acetabular components was an order of magnitude lower than published wear rates for human THA (*See Table 4.1*) [22]. This may mean that the dog experiences a lower UHMWPE wear debris load, which may explain why dogs do not display the level of osteolysis seen in human THA.

Despite the differences in hip loading and femoral morphology, the dog remains a valuable animal model for THA studies; however, there are some limitations to conclusions that can be drawn from experimental studies performed in dogs. Dogs do not display age-related changes in their femora as are seen in humans [26-27], and levels of osteolysis reported in human THA studies were not seen in the present postmortem retrieval study. The canine femur is straighter proximally than the human femur, and this

shape difference needs to be accounted for in the selection of experimental implants for use in canine studies [26-27]. In addition, the medullary canal is larger relative to the length of the femur in the dog than in the human [28], and the femur flares more proximally in the dog than in the human. Since the cortical area remains constant, the proximal femoral cortex is thinner than in the remainder of the femoral shaft.

In addition, dogs can make subtle adjustments in their gait, and previous gait studies have found that dogs do not consistently load their hip joint between gait cycles. Dogs display wide variation in their walking gait cycles, and they quite often walk with their hind limbs offset from their front limbs (i.e., crab-walking) [29]. There were differences in gait between breeds. Dogs also load their hip joints with a lower percentage of their body weight [30-32]. Measurements taken to determine the magnitude and direction of principle strain in canine and human femora indicate found that the direction is similar in both species (i.e., 15-20 degrees off the long axis of the femur), but the magnitude of the strain in the canine femur is much less than in the human femur [33-34].

The incidence of loosening of the femoral and acetabular components in this canine postmortem retrieval study is alarmingly high. It became quickly apparent from the results of the mechanical testing for implant stability of the femoral and acetabular that bilateral THAs tended to perform better than unilateral THAs. Despite the fact that many of the bilateral THAs were of very long duration and had been implanted using previous generation cementing and surgical techniques, many remained firmly implanted. But unilateral THAs tended to have a higher proportion of loose components (*See Figures 3.11, 4.9, & 5.1*). More than half of both the femoral and acetabular implants were loose.

The BioMedtrix #1 implant design was already associated with aseptic loosening

problems [17]. and our findings confirmed this. The distal half of the femoral stem in both BioMedtrix designs is round with two small grooves on the cranial and caudal aspects. These grooves were intended to provide rotational stability. Despite the known aseptic loosening problems. seven BioMedtrix #1 (5 were bilaterals) femoral components were firmly implanted. This results suggests that the bilateral vs. unilateral issue has greater impact than implant design.

7.4. Conclusions

This was the first postmortem retrieval study in canine THA of this scale with regard to the number of implants and the degree of analysis performed. Findings from this research study include:

1. Dogs wear their implants at a much lower VWR than humans (order of magnitude lower). UHMWPE wear debris is therefore not as prevalent within the joint in dogs as compared to humans.
2. Dogs are flawed as an animal model for THA in humans. Dogs do not exhibit age-related changes in their bones that humans experience. Osteolytic changes seen in human THA related to UHMWPE wear debris were not noted in this canine postmortem retrieval study.
3. Dogs displayed a higher level of damage to the acetabular components. including implant-on-implant and third body wear damage. Despite that damage. the VWR was an order of magnitude lower than that seen in human acetabular components. Perhaps the osteolytic reaction to UHMWPE wear debris observed in humans was not present in dogs due to the much lower

load of wear debris in the dog as a result of the lower VWR.

4. More than half of the acetabular components were loose. The initiating event for loosening of the acetabular component in the dog appears to be mechanical in nature, not biological as in the human.
5. More than half of the femoral components were loose. The initiating event for loosening of the femoral component appears to be mechanical in nature, similar to that seen in human THA.
6. Loosening of the femoral component was positively correlated with VWR. This correlation and other correlations that were identified during multiple linear regression analysis indicate that loosening of the femoral component correlates with failure measures on the acetabular component and VWR on the acetabular component correlates with failure measures on the femoral component.

The possible relationships that were identified between femoral dependent variables and the wear debris and acetabular data and between the acetabular dependent variables and the wear debris and femoral data will require further analysis with a larger number of specimens to identify definite relationships between failure mechanisms of the acetabular and femoral components: however, some interesting trends were identified and invite further study.

7.5. References

1) An YH, Friedman RJ. *Animal Models in Orthopaedic Research*. CRC Press, Boca Raton, Chapter 3: 1998.

2) Anderson GI, Podworny N, Jain R, Kwok AWL, Waddell JP. Hydroxyapatite

Application Effect on Micromotion Around Acetabular and Femoral Components in the Dog. *Transactions of Fifth World Biomaterials Congress*. 1996: 176.

3) Bobyn JD. Jacobs JJ. Tanzer M. Urban RM. Aribindi R. Sumner DR. Turner TM. Brooks CE. The Susceptibility of Smooth Implant Surfaces to Periimplant Fibrosis and Migration of Polyethylene Wear Debris. *Clinical Orthopaedics and Related Research*. 1995; 311: 21-39.

4) Bobyn JD. Pilliar RM. Binnington AG. Szivek JA. The Effect of Proximally and Fully Porous-Coated Canine Hip Stem Design on Bone Modeling. *Journal of Orthopaedic Research*. 1987; 5: 393-408.

5) Dowd JE. Schwendeman LJ. Macaulay W. Doyle JS. Shanbhag AS. Wilson S. Herndon JH. Rubash HE. Aseptic Loosening in Uncemented Total Hip Arthroplasty in a Canine Model. *Clinical Orthopaedics and Related Research*. 1995; 319: 106-121.

6) Finkelstein JA. Anderson GI. Waddell JP. Richards RR. Hearn TC. Schemitsh E. A Study of Micromotion and Appositional Bone Growth to a Canine Madreporic-Surfaced Femoral Component. *The Journal of Arthroplasty*. 1994; 9: 317-324.

7) Harvey EJ. Bobyn JD. Stackpool GJ. Tanzer M. Comparative Peri-Implant Femoral Bone Remodeling with Isoelastic and Hypoelastic Noncemented Canine Hip Prostheses. *Transactions of the 43rd Meeting of the Orthopaedic Research Society*. 1997: 307.

8) Maistrelli GL. Mahomed N. Fornasier V. Antonelli L. Li Y. Binnington A. Functional Osseointegration of Hydroxyapatite-Coated Implants in a Weight-Bearing Canine Model. *The Journal of Arthroplasty*. 1993: 8: 549-554.

9) Vanderby Jr R. Manley PA. Kohles SS. McBeath AA. Fixation Stability of Femoral Components in a Canine Hip Replacement Model. *Journal of Orthopaedic Research*. 1992: 10: 300-309.

10) Walenciak MT. Zimmerman MC. Harten RD. Ricci JL. Stamer DT. Biomechanical and Histological Analysis of an HA Coated. Arc Deposited CPTi Canine Hip Prosthesis. *Journal of Biomedical Materials Research*. 1996; 31: 465-474

11) Lewis RH. Jones Jr JP: A Clinical Study of Canine Total Hip Arthroplasty. *Veterinary Surgery*. 1980; 9: 20-23.

12) Gofton N. Sumner-Smith G. Total Hip Prosthesis for Revision of Unsuccessful Excision Arthroplasty. *Veterinary Surgery*. 1982; 11: 134–139.

13) Olmstead ML. Hohn RB. Turner TM. A Five-Year Study of 221 Total Hip Replacements in the Dog. *Journal of the American Veterinary Medical Association*.

1983: 183: 191–194.

14) Parker RB. Bloomberg MS. Bitetto W. *et al.*. Canine Total Hip Arthroplasty: A Clinical Review of 20 Cases. *Journal of the American Veterinary Medical Association*. 1984: 20: 97–104.

15) Olmstead ML. The canine cemented modular total hip prosthesis. *Journal of the American Animal Hospital Association*. 1995: 31: 109-124.

16) Paul HA. Bargar WL. A Modified Technique for Canine Total Hip Replacement. *Journal of the American Animal Hospital Association*. 1987: 23: 13–18.

17) Edwards MR. Egger EL. Schwarz PD: Aseptic Loosening of the Femoral Implant after Cemented Total Hip Arthroplasty in Dogs: 11 Cases in 10 Dogs (1991-1995). *Journal of the American Veterinary Medical Association*. 1997: 211: 580-586.

18) Maloney WJ. Jasty M. Burke DW. O'Connor DO. Zalenski EB. Bragdon C. Harris WH. Biomechanical and Histologic Investigation of Cemented Total Hip Arthroplasties: A Study of Autopsy-Retrieved Femurs After *In Vivo* Cycling. *Clinical Orthopaedics and Related Research*. 1989: 249: 129-140.

19) Jasty M. Maloney WJ. Bragdon CR. O'Connor DO. Haire T. Harris WH. The Initiation of Failure in Cemented Femoral Components of Hip Arthroplasties. *The Journal of Bone and Joint Surgery*. 1991: 73-B: 551-558.

20) Schmalzried TP. Maloney WJ. Jasty M. Kwong LM. Harris WH. Autopsy Studies of the Bone-Cement Interface in Well-Fixed Cemented Total Hip Arthroplasties. *The Journal of Arthroplasty*. 1993: 8: 179-188.

21) Schmalzried TP. Kwong LM. Jasty M. Sedlacek RC. Haire TC. O'Connor DO. Bragdon CR. Kabo JM. Malcolm AJ. Harris WH. The Mechanism of Loosening of Cemented Acetabular Components in Total Hip Arthroplasty: Analysis of Specimens Retrieved at Autopsy. *Clinical Orthopaedics and Related Research*. 1992: 274: 60-78.

22) Jasty M. Goetz DD. Bragdon CR. Lee KR. Hanson AE. Elder JR. Harris WH. Wear of Polyethylene Acetabular Components in Total Hip Arthroplasty: An Analysis of One Hundred and Twenty-Eight Components Retrieved at Autopsy or Revision Operations. *The Journal of Bone and Joint Surgery*. 1997: 79-A: 349-358.

23) Skurla CT. Egger EL. Schwarz PD. James SP. Owner Assessment of the Outcome of Total Hip Arthroplasty in Dogs. *Journal of the American Veterinary Medical Association*. 2000: 217: 1010-1012.

24) Ramaniraka NA. Rakotomanana LR. Leyvraz PF. The Fixation of the Cemented Femoral Component: Effects of Stem Stiffness. Cement Thickness and Roughness of

the Cement-Bone Surface. *The Journal of Bone and Joint Surgery*; 2000: 82-B: 297-303.

25) James SP. Lee KR. Beauregard GP. Rentfrow ED. McLaughlin JR: Clinical Wear of 63 Ultrahigh Molecular Weight Polyethylene Acetabular Components: Effect of Starting Resin and Forming Method. *Journal of Biomedical Materials Research (Applied Biomaterials)*. 1999; 48: 374-384.

26) Kuo TY. Skedros JG. Bloebaum RD. Comparison of Human. Primate. and Canine Femora: Implications for Biomaterials Testing in Total Hip Replacement. *Journal of Biomedical Materials Research*. 1998; 40: 475-489.

27) Bloebaum RD. Ota DT. Skedros JG. Mantas JP. Comparison of Human and Canine External Femoral Morphologies in the Context of Total Hip Replacement. *Journal of Biomedical Materials Research*. 1993; 27: 1149-1159.

28) Sumner Jr DR. Devlin TC. Winkelman D. Turner TM. The Geometry of the Adult Canine Proximal Femur. *Journal of Orthopaedic Research*. 1990; 8: 671-677.

29) Adrian MJ. Roy WE. Karpovich PV. Normal Gait of the Dog: An Electrogoniometric Study. *American Journal of Veterinary Research*. 1966; 27: 90-95.

30) Page AE. Allan C. Jasty M. Harrigan TP. Bragdon CR. Harris WH. Determination of Loading Parameters in the Canine Hip *in Vivo*. *Journal of Biomechanics*. 1993; 26: 571-579.

31) Davy DT. Kotzar GM. Brown RH. Heiple KG. Goldberg VM. Heiple Jr KG. Berilla J. Burstein AH. Telemetric Force Measurements across the Hip after Total Hip Arthroplasty. *The Journal of Bone and Joint Surgery*. 1988; 70-A: 45-50.

32) Arnoczky SP. Torzilli PA. Biomechanical Analysis of Forces Acting About the Canine Hip. *American Journal of Veterinary Research*. 1981; 42: 1581-1585.

33) Finlay JB. Chess DG. Harkie WR. Rorabeck CH. Bourne RB. An Evaluation of Three Loading Configurations for the In Vitro Testing of Femoral Strains in Total Hip Arthroplasty. *Journal of Orthopaedic Research*. 1991; 9: 749-759.

34) Jasty M. Page A. Henshaw R. Bragdon C. Cargill E. Harris WH. Long Duration Measurement of In Vivo Strain Distribution in the Canine Femur. *Transactions of the 34th Annual Meeting of the Orthopaedic Research Society*. 1988: 236.

Chapter 8

Future Work

8.1. Work Currently in Progress on Current Specimens

There is a wealth of additional information contained in the 38 implants analyzed in this dissertation. There are at least 12 additional postmortem retrievals awaiting analysis, most shipped from veterinary orthopaedic surgeons at the University of California at Davis. Studies already in progress include:

1. The complete analysis of contact radiographs of the femora in conjunction with complete analysis of serial clinical radiographs is already in progress as the master's thesis project for Dan Frankel, DVM, a resident at the CSU VTH. One issue with this study is that clinical radiographs are not available on every case, and the radiographs were not made at fixed time periods after surgery (a consideration for enhancing future follow-up).

8.2. Future Projects from Current Specimens

Future potential studies include:

1. The histological analysis of the slices taken from the femora.
2. The complete digital analysis of the contact radiographs of the 2 mm femoral

slices.

3. Scanning electron microscopy (SEM), FTIR, or XPS analysis of the wear debris isolated from the joint capsule along with SEM analysis of the articulating surface of the acetabular components.
4. Scanning electron microscope analysis of 2 mm femoral slices and Morse taper of femoral stem.
5. Analysis of the acetabular component, including assessment of alignment or misalignment of the acetabular component in the hemipelvis, slicing of the acetabular component/hemipelvis construct, histological analysis of slices designated for histology, SEM analysis of slices designated for further assessment of wear mechanisms.

8.3. Redesign of the Canine THA Implant for Improved Stability

In an unpublished study performed in 1996 at CSU Orthopaedic Biomechanics Laboratory, a test method was developed with the intention of testing the rotational stability of a femoral component cemented with varying cement mantle thicknesses in an artificial femur (i.e., blocks of maple wood). The experimental design involved mounting the artificial femur vertically in the mechanical testing machine (MTS, Eden Prairie, MN) and applying a torque to the femoral neck of the implant until destructive failure occurred. The test results were inconclusive, and one of the conclusions reached was that the destructive test did not recreate physiological loading conditions experienced by these implants *in situ*.

A better experimental design would involve implanting a femoral component in a

femur retrieved from a cadaver, mounting it in the MTS in a saline water bath held at body temperature, and cycling the implant/femur construct through a set number of loading cycles designed to imitate peak loading of the joint in the walking gait. While this test in non-living bone would not result in active bone remodeling, as would be seen in a living specimen, the effects of fatigue on the cement mantle could be studied.

The shape effect found in the present study and presented in Chapter 3 must be taken into effect in this experimental design. For example, matched artificial femora with controlled femoral canal geometries could be used for matched comparisons of the performance of two different femoral component designs.

8.4. Improvements to Current Methods

8.4.1. Survey Improvements

The survey instrument developed (*See Chapter 2*) and used in this dissertation study needs to be revised, based on owner and surgeon feedback. Better information could be attained by using this survey prior to and at various set times after (e.g., 6 months and 1, 2, and 5 years) surgery in order to get a time-dependent response from owners. This would provide valuable information with regard to when the THA starts to degrade or fail in comparison to when additional health problems related to aging appear and complicate THA follow-up.

8.4.2. Reduction in Dimensionality

Some reduction in the dimensionality of the data can already be determined. For example, during the measurement of the contact radiographs of intact femora, veterinary surgeons did not see anything of clinical relevance for the most proximal Gruen zones.

These zones were dropped from the data analysis and could be dropped from future studies. Care must be taken in deleting variables from future data collection; however, the maximum thickness of PMMA in the femoral slice appeared to have limited value during the data analysis. Further analysis of the multiple linear regression analysis logs should allow for the selection of additional variables that do not need to be collected in the future.

8.4.3. Improvements to Mechanical Testing of Acetabular Components

During mechanical testing, the loading jig was rotated through 2 degrees of rotation, but during data analysis it was found that one degree of rotation was adequate for determining whether an acetabular component was firmly implanted or loose.

Improvements need to be made to the mounting jig to allow the mounted hemipelvis to be mounted more rigidly on the MTS machine. Improvements also need to be made to the jig that applied the torque to the rim of the acetabular component. The four pins in the loading jig used in the present study placed an asymmetric load on the rim of the acetabular component. The loading jig needs to be redesigned so that a load would also be applied to the fire hydrant cut-out in order to achieve a more symmetric application of the load to the acetabular component.

8.5. Future Large Scale Projects

This dissertation research project has served to determine owner willingness to become involved in research aimed at the eventual improvement of total hip arthroplasty (THA) implant design and surgical technique for humans as well as dogs. Dog owners, who are willing and able to pay to have a surgery of this magnitude performed on their

dogs, enthusiastically embraced the opportunity to help with research projects designed to help dogs with similar conditions in the future.

8.5.1. Multi-Center Study

The early results of this pilot study have led to the start of a collaborative, multi-center research project with researchers at the veterinary colleges at North Carolina State University, Iowa State University, and the University of California at Davis for more thorough analysis of postmortem retrievals.

8.5.2. Experimental Materials/Designs in Client-Owned Dogs

Another possible future project involves offering reduced surgical and follow-up expenses to owners of dogs with degenerative joint disease (DJD) by offering them the opportunity to sign up for a long-term clinical follow-up study. This would be a controlled study to compare conventional THA implant materials (i.e., the results of the present work) and designs with new or experimental materials and designs.

Human orthopaedic surgeons are currently implanting acetabular components made of highly crosslinked ultra high molecular weight polyethylene (UHMWPE) in clinical patients without the benefit of animal testing. This material would be an excellent candidate for a study of this type.

The follow-up visits, at fixed times post-surgery, would include force plate gait analysis to determine the degree of weight-bearing on the implanted hip compared to the contralateral hip. Ciprofloxacin scans, in which the antibiotic, ciprofloxacin, is tagged to technetium, are useful in determining whether THA loosening is related to infection [1]. The technetium- ciprofloxacin cocktail is injected and becomes incorporated into dividing bacteria. In the presence of infection, high levels of technetium will be detected

on scans in the area of the implant. Testing of metal ions in blood and urine, performed at Iowa State University, would provide information related to wear and/or corrosion of the metallic femoral component. Radiographs would be taken at every visit to provide clinical radiographs at set times post-THA. The owners would also agree to donate their dogs' hemipelves and femora for detailed engineering, radiographic, and histological analysis upon the deaths of their dogs, whether from natural causes or owner-selected euthanasia.

While the duration of the implant *in situ* would remain uncontrolled, there would be ample opportunity for the collection of controlled, time-dependent data from more thorough clinical follow-up examinations.

8.6. References

1) Yapar Z, Kibar M, Yapar AF, Togrul E, Kayeselcuk U, Sarpel Y. The Efficacy of Technetium-99m Ciprofloxacin (Infecton) Imaging in Suspected Orthopaedic Infection: A Comparison With Sequential Bone/Gallium Imaging. *European Journal of Nuclear Medicine*, 2001; 28: 822-830.

Glossary

GLOSSARY A - MEDICAL TERMINOLOGY

Acetabulum – (*n.*) the large cup-shaped cavity on the lateral surface of the os coxae in which the head of the femur articulates [**acetabular** – *adj.*]

Anterior – (*adj.*) situated in front of or in the forward part of an organ. toward the head end of the body: a term used in reference to the ventral or belly surface of the body

Anteversion – (*n.*) the forward tipping or tilting of an organ

Arthroplasty – (*n.*) plastic surgery of a joint or of joints: the formation of movable joints [**Charnley's hip a.**, a hip reconstruction operation involving insertion of Charnley's prosthesis to form a low-friction joint]

Aseptic – (*adj.*) free from infection or septic material: sterile

Autopsy – (*n.*) the postmortem examination of a body. Called also necropsy

Bilateral – (*adj.*) having two sides. or pertaining to both sides

Cancellous – (*adj.*) of a reticular. spongy. or lattice-like structure: said mainly of bony tissue

Caudal – (*adj.*) in embryology and nonhuman anatomy. denoting a position more toward the caudal. or tail: in human anatomy. a synonym of inferior

Cortical – (*adj.*) pertaining to or of the nature of a cortex or bark

Cranial – (*adj.*) pertaining to the cranium. or to the anterior (in animals) or superior (in humans) end of the body

Distal – (*adj.*) remote: farther from any point of reference; opposed to proximal

Dorsal – (*adj.*) denoting a position more toward the back surface than some other object of reference: same as posterior in human anatomy and superior in the anatomy of quadrupeds

Ectopic – (*adj.*) arising in an abnormal site or tissue

Endosteal – (*adj.*) pertaining to the endosteum; occurring or located within a bone

Femur – (*n.*) the bone that extends from the pelvis to the knee, being the longest and largest bone in the body; its head articulates with the acetabulum of the hip bone, and distally the femur, along with the patella and tibia, forms the knee joint [**femora** – *plural*; **femoral** – *adj.*]

Flexion – (*n.*) the act of bending or condition of being bent

In Situ – (*adj.*) in the natural or normal place; confinced to the site of origin without invasion of neighboring tissues

In Vitro – (*adj.*) within a glass; observable in a test tube; in an artificial environment

In Vivo – (*adj.*) within the living body

Inferior – (*adj.*) situated below, or directed downward; a term used in reference to the lower surface of an organ or other structure, or to the lower of two (or more) similar structures

Lateral – (*adj.*) denoting a position farther from the median plane or midline of the body or of a structure

Medial – (*adj.*) pertaining to the middle; closer to the median plane or the midline of a body or structure

Medullary – (*adj.*) pertaining to the marrow or to any medulla; resembling narrow

Necropsy – (*n.*) examination of a body after death; see autopsy (usually used in reference to animals)

Osteolysis – (*n.*) dissolution of bone; applied especially to the removal or loss of the calcium of bone

Osteoporosis – (*n.*) reduction in the amount of bone mass, leading to fractures after minimal trauma

Periosteum – (*n.*) a specialized connective tissue covering all bones [**periosteal** – *adj.*]

Posterior – (*adj.*) situated in back of, or in the back part of, or affecting the back part of a structure; a term used in reference to the back or dorsal surface of the body; in lower animals, it refers to the caudal end of the body

Postmortem – (*adj.*) occurring or performed after death

Proximal – (*adj.*) nearest; closer to any point of reference; opposed to distal

Retroversion – (*n.*) the tipping of an entire organ in a posterior direction

Superior – (*adj.*) situated above, or directed upward: a term used in reference to a structure occupying a position near the vertex

Synovia – (*n.*) a transparent alkaline viscid fluid, resempling the white of an egg, secreted by the synovial membrane, and contained in joint cavities, bursai, and tendon sheaths [**synovial** – *adj.*]

Unilateral – (*adj.*) affecting but one side

Valgus – (*adj.*) bent outward, twisted: denoting a deformity in which the angulation of the part is away from the midline of the body

Varus – (*adj.*) bent inward: denoting a deformity in which the angulation of the part is toward the midline of the body

Ventral – (*adj.*) denoting a position more toward the belly surface than some other object of reference: same as anterior in human anatomy

***** NOTE *** All definitions, unless otherwise noted are from:**

Dorland's Illustrated Medical Dictionary, 28th edition, W.B. Saunders Company, Philadelphia, 1994.

GLOSSARY B - ACRONYMS

ANOVA – Analysis of variance.

CASE – Center for Applied Statistical Expertise in the Statistics Department at CSU.

CC – Cranial-caudal radiographic view.

Co-Cr – Cobalt-chromium alloy commonly used to make femoral components.

CSU – Colorado State University.

DJD – Degenerative joint disease.

FEA – Finite element analysis.

JRF – Joint reaction force.

KOH – Potassium hydroxide.

ML – Medial-lateral radiographic view.

OIRP – Orthopaedic Implant Retrieval Program.

BW – Body weight.

PMMA – Polymethyl methacrylate bone cement.

RMD – Relative motion device. Used in mechanical testing for stability of the femoral component.

SAS – Statistical Analysis System. SAS Institute. Cary. NC.

THA – Total hip arthroplasty.

Ti-6Al-4V – Titanium alloy commonly used to make femoral components.

TJA – Total joint arthroplasty.

TVW – Total volumetric wear of the UHMWPE acetabular component (μl).

UHMWPE – Ultra high molecular weight polyethylene.

VTH – Veterinary Teaching Hospital.

VWR – Volumetric wear rate of the UHMWPE acetabular component (μl / year).

Calculated value = TVW / ID.

3BW – Third body wear.

GLOSSARY C - VARIABLES

Demographic Data (from Chart):

Age – Age at surgery (years).

BM1 – 1 = BioMedtrix #1 implant design. 0 = Richards or BioMedtrix #2 implant design. Numeric version of implant design. used in multiple linear regression.

BM2 – 1 = BioMedtrix #2 implant design. 0 = Richards or BioMedtrix #1 implant design. Numeric version of implant design. used in multiple linear regression.

Implant Duration - Implant duration (years).

Implant Design – Richards. BioMedtrix #1. or BioMedtrix #2.

Number of Implants - 1 = the dog had unilateral THA. 2 = the dog had bilateral THA.

Weight – Weight of dog at surgery (kg).

Femoral Component Index Variables (Chapter 3):

Additional Problem – 1 = the dog had unilateral THA in the presence of other disease conditions (e.g.. bilateral DJD. trauma). 0 = the dog had unilateral THA with no other disease conditions or the dog had bilateral THA.

Area Index – Mean of the areas of metal and PMMA calculated during digital image analysis of the femoral slice (mm^2).

Bone/Metal Index – Square root transformation of the mean of subsidence and ML translation micromotion measurements taken between the bone and the femoral component during mechanical testing (square root of μm).

Bone/PMMA Index – Square root transformation of the mean of subsidence and ML translation micromotion measurements taken at the bone/PMMA interface of the femoral component during mechanical testing (square root of μm).

Crack Index – Mean of the length of cracks in the PMMA in CC and ML contact radiographs of intact femora. If the mean was greater than one. the value was set to one (0 = no cracks. 1 = cracks detected).

Distance Index – Square root transformation of the mean of the distance between the PMMA and metal centroids and the distance between the bone and metal centroids calculated during digital image analysis of the femoral slice (square root of mm).

GZ 11 Index – Square root transformation of the minimum and maximum thicknesses of PMMA in Gruen zone 11 on the ML contact radiographs of intact femora (square root of mm).

GZ 12-13 Index – Square root transformation of the minimum and maximum thicknesses of PMMA in Gruen zones 12 and 13 on the ML contact radiographs of intact femora (square root of mm).

GZ 2-3 Index – Square root transformation of the minimum and maximum thicknesses of PMMA in Gruen zones 2 and 3 on the CC contact radiographs of intact femora (square root of mm).

GZ 4 Index – Square root transformation of the minimum and maximum thicknesses of PMMA in Gruen zone 4 on the CC contact radiographs of intact femora (square root of mm).

GZ 5-6 Index – Square root transformation of the minimum and maximum thicknesses of PMMA in Gruen zones 5 and 6 on the CC contact radiographs of intact femora (square root of mm).

GZ 9-10 Index – Square root transformation of the minimum and maximum thicknesses of PMMA in Gruen zones 9 and 10 on the ML contact radiographs of intact femora (square root of mm).

Radiolucency Index 1 – Mean of the width and length of radiolucencies at the bone/PMMA interface in the CC and ML contact radiographs of intact femora. If the mean was greater than one. the value was set to one. (0 = no radiolucencies. 1 = radiolucencies detected).

Radiolucency Index 2 – Mean of the width and length of radiolucencies at the PMMA/metal interface in the CC and ML contact radiographs of intact femora. If the mean was greater than one. the value was set to one (0 = no radiolucencies. 1 = radiolucencies detected).

Shape Index 1 - Mean of GZ 4 index and GZ 11 index.

Shape Index 2 – GZ 4 index minus GZ 11 index.

Void Index – Square root transformation of the mean of the number of voids in the PMMA in the CC and ML contact radiographs of intact femora.

Femoral Component Variables (Chapter 3):

Bone Area – Area of cortical bone taken during digital image analysis of femoral slice

(mm^2).

Bone/Metal ML translation – Micromotion measurement made in ML translation at PMMA/metal interface during mechanical testing of femoral component (μm).

Bone/Metal Subsidence – Micromotion measurement made in subsidence at PMMA/metal interface during mechanical testing of femoral component (μm).

Bone/PMMA ML translation – Micromotion measurement made in ML translation at bone/PMMA interface during mechanical testing of femoral component (μm).

Bone/PMMA Subsidence – Micromotion measurement made in subsidence at bone/PMMA interface during mechanical testing of femoral component (μm).

Distance 3 – Distance between centroid of bone and centroid of PMMA taken during digital image analysis of femoral slice (mm^2).

Femoral Head Angle – Angle of the head of the femoral component as measured in the ML radiographic view (Anteversion is positive; retroversion is negative).

Femur Category – Results of mechanical testing of femoral component (Firm, Loose, Grossly loose).

Minimum PMMA – Minimum thickness of cement mantle taken during digital image analysis of femoral slice (mm).

PMMA/Metal ML translation – Difference between bone/PMMA ML translation and bone/metal ML translation (μm).

PMMA/Metal Subsidence – Difference between bone/PMMA subsidence and bone/metal subsidence (μm).

Acetabular Component Index Variables (Chapter 4):

3BW Index – Mean of the total UHMWPE damage scores across all zones of the acetabular component for embedded PMMA debris, scratching, removal of machine marks, abrasion, macroscopic removal of UHMWPE, and yellowing.

Creep Index – Mean of the total UHMWPE damage scores across all zones of the acetabular component for creep and pitting.

Cut-Out Index – Mean of the total UHMWPE damage scores for the cranial corner, the caudal corner, and the rim of the 45° fire hydrant cut-out on the acetabular component.

Embedded Metal Index – Presence or absence of embedded metal (black debris) in any zone on the acetabular component (0 = no black debris. 1 = black debris detected).

Quadrant Index – Mean of the total UHMWPE damage scores for each of the four quadrants of the articulating surface on the acetabular component.

Rim Index – Mean of the total UHMWPE damage scores for the cranial half and the caudal half of the rim on the acetabular component.

Acetabular Component Variables (Chapter 4):

Acetabulum Category – Results of mechanical testing of acetabular component (Firm. Borderline. Loose).

PE ID – Inner diameter of UHMWPE acetabular component (mm).

PE Micromotion – Micromotion measurement made during mechanical testing for implant stability of the acetabular component.

PE OD – Outer diameter of UHMWPE acetabular component (mm).

PE Thickness – Thickness of UHMWPE in acetabular component (mm).

Torque – Maximum torque applied during mechanical testing of acetabular component (N mm).

Total PE Score – Grand total of damage score for acetabular component.

TVW – Total volumetric wear of acetabular component (μl).

VWR – Volumetric wear rate of acetabular component (μl / year).

Appendix

APPENDIX A - OWNER ASSESSMENT SURVEY

Canine Hip Replacement Research Survey

Instructions:

Please circle the response that is most appropriate to describe the results of your dog's hip replacement surgery. Upon completing the survey, please fold this survey form and place it in the postage-paid envelope. Thank you for your contribution to improving hip replacement implants for both canines and humans!

1. Was your dog receiving pain medication prior to the hip replacement?
   1 Yes, daily.
   2 Yes, several times per week.
   3 Yes, infrequently.
   4 No

2. Did the hip replacement appear to decrease your dog's pain?
   1 Yes, completely.
   2 Yes, somewhat.
   3 No.
   4 My dog did not appear to be in pain before surgery.

3. Did the hip replacement increase your dog's function?
   1 Yes, a lot.
   2 Yes, somewhat.
   3 No, my dog's function is the same.
   4 No, my dog's function is worse.

4. How would you rate the results of your dog's hip replacement surgery?
   1 Excellent.
   2 Good.
   3 Fair.
   4 Poor.

5. Hip replacement surgery is expensive. In considering the results of your dog's hip replacement surgery, do you feel that the surgery was worth the expense?

1 Yes, definitely.
2 Yes, probably.
3 No, probably not.
4 No, definitely not.

6. Now that you have learned a lot about hip replacement surgery in dogs, if you could go back in time and make the same decision again, would you choose to have this surgery for your dog again?
1 Yes, definitely.
2 Yes, probably.
3 No, probably not.
4 No, definitely not.

7. How much did your dog's hip replacement surgery improve your dog's quality of life?
1 More improvement than I ever thought possible.
2 A great improvement.
3 A moderate improvement.
4 A slight improvement.
5 No improvement.
6 It lessened the quality of my dog's life.

8. Compared with the period prior to your dog's hip replacement, would you say your dog's health is now better, about the same, or worse?
1 Better.
2 Same.
3 Worse.

9. How well does your dog perform running since the hip replacement surgery?
1 My dog runs at will with no restriction.
2 Half day running activity causes apparent discomfort.
3 One hour running activity causes apparent discomfort.
4 Less than a half hour running activity causes apparent discomfort.
5 My dog cannot run without discomfort.

10. How well does your dog perform walking since the hip replacement surgery?
1 My dog walks at will with no restriction.
2 Half day walking activity causes apparent discomfort.
3 One hour walking activity causes apparent discomfort.
4 Less than a half hour walking activity causes apparent discomfort.
5 My dog cannot walk without discomfort.

11. Do you still have to give pain medication to your dog since hip replacement surgery?
1 Yes, daily.
2 Yes, several times per week.

3 Yes. infrequently.
4 No.

If your dog had both hips replaced. please skip to question 13.

12. If your appears to be in discomfort since the hip replacement surgery. where does the source of the discomfort appear to be?
    1 The hip that was replaced appears to be the primary cause of discomfort.
    2 The other hip appears to be the primary cause of discomfort.
    3 My dog does not appear to be in discomfort.

13. If your have any further comments concerning the outcome of your dog's hip replacement surgery. or if you feel that we have left anything out of this survey. please provide us with your comments in the space provided.

_____

_____

_____

_____

_____

_____

14. Please provide us with our correct address:
    1 The address to which you sent this survey is correct.
    2 My correct address is:

_____

_____

_____

_____

15. Is your dog still alive?
    1 Yes.
    2 No.

16. If your dog is no longer alive. could you please tell us how and approximately

when your dog died?

_____

_____

_____

_____

If your dog is no longer alive, thank you for your cooperation in filling out this survey. You need proceed to further. If your dog is still alive, please proceed on to the next question.

17. We are looking for owners who would consider donating their dog's hips at the time of their dog's death. One benefit of this gift is that CSU will provide free euthanasia services and cremation for your dog. Could you consider the possibility of donating your dog's hips at the time of his or her death?
    1 Yes, please send me more information.
    2 No.

If you have any questions about this survey or would prefer to respond to this survey over the phone, please call Sean Brevard at the CSU Veterinary Teaching Hospital at (970) 221-4535.

APPENDIX B - CALIBRATION OF RELATIVE MOTION DEVICE

Calibration Jig (See Figure Below):

1. Piece of Teflon™, 1 5/8 inch by 1 5/8 inch by 0.50 inch.
   a. Used as "implant" against which the point of the RMD pin rested.
2. Four pieces of Teflon™, 3/8 inch by 3/8 inch by 0.50 inch with pieces of duct tape on tops and bottoms (3/8 inch by 3/8 inch sides).
   a. Used as supports for the aluminum plate.
   b. Used as guide for Teflon™ "implant".
3. Aluminum plate, 2.5 inch by 2.5 inch by 0.25 inch.
   a. Used as "bone" to which RMD "t" was glued.
   b. Contained 0.25 inch hole drilled in center of 2.5 inch by 2.5 inch side of plate.
   c. Contained semi-circular groove of 0.275 inch radius drilled as shown in figure below to allow piston of the 2 inch micrometer to move along the groove.
4. Additional piece of scrap aluminum plate, 0.25 inch thick.
5. Two springs.
6. MTS extensometer.
7. Assorted C-clamps.

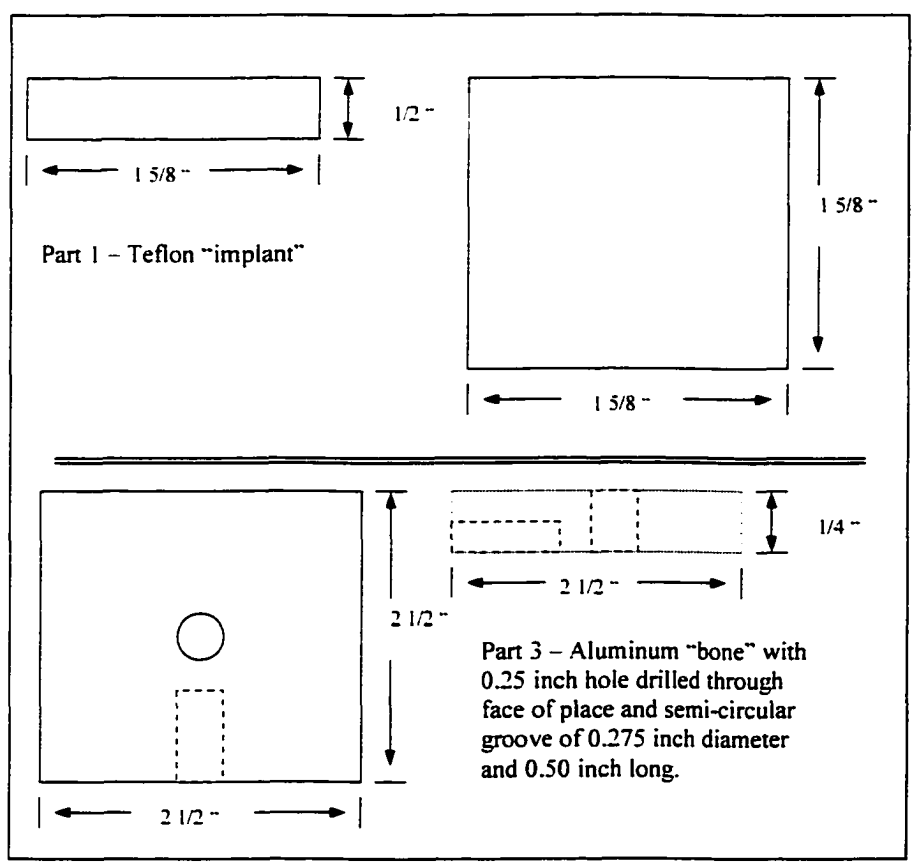

Calibration Method:

1. Using metal 5 minute epoxy, glue RMD "t" to aluminum bone (Part 3 above). Allow epoxy 4 hours to set.
2. Using shelf mounted on MTS upright linear bearing as the base, place aluminum "bone" (Part 3) with four small Teflon™ pieces (Part 2 above) as corner supports so that the Teflon™ "implant" (Part 1 above) will have room to slide under the aluminum "bone" and between the Teflon™ corner supports.
3. Clamp aluminum "bone" to mounting plate using C-clamps. Tighten the clamp enough to hold the constuct in place while still allowing the Teflon™ "implant" to slide between the base and the aluminum "bone."
4. Thread RMD Part 2 onto RMD "t" and place RMD pin into hole through RMD "t." Place RMD Part 2 so that one of the 5 slots is perpendicular to the groove in the aluminum "bone." Tighten set screw.
5. Put 2 inch micrometer into position so that it is anchored against the flat end of the aluminum "bone" and the piston fits into the groove and sets against the Teflon™ "implant."
6. Place two springs between Teflon™ "implant" and piece of scrap aluminum (Part 4 above). Clamp aluminum scrap to base so that springs press the Teflon™ "implant" against the piston of the micrometer.
7. Attach extensometer to RMD using rubber bands or springs.
8. Remove pin from extensometer and zero extensometer output on MTS pod.
9. Take zero readings of both extensometer reading on MTS pod and micrometer.
10. Move micrometer ~0.0005 inch and take extensometer reading.
11. Repeat step 10 until the extensometer measures 300 microns.
12. Repeat steps 7 through 11 several times until sufficient data has been collected to calculate a calibration curve with 95% prediction confidence levels.
13. Parameter estimate for the micrometer (dependent) variable is the conversion factor to convert extensometer reading to motion detected at the tip of the RMD pin.

Correction Factors for Three RMD "t"s:

1. RMD "t" #1 = 1.139
2. RMD "t" #2 = 1.095
3. RMD "t" #3 = 1.190
4. To calculate motion at the tip of the pin, divide extensometer reading by correction factor.

Sample Calibration Curve Calculations (SAS Output):

1. **Sample SAS Output – Regression Procedure Used to Calculate 95% Prediction Confidence Limits for RMD Calibration Curve**

```
RMD 3 Calibration - All Trials Combined - SI Units                    33
                                          17:52 Tuesday, May 14, 2002

The REG Procedure
```

Model: MODEL1
Dependent Variable: ExtensSI

Analysis of Variance

Source	DF	Sum of Squares	Mean Square	F Value	Pr > F
Model	1	98500	98500	6042.30	<.0001
Error	34	554.26001	16.30176		
Corrected Total	35	99054			

Root MSE	4.03754	R-Square	0.9944
Dependent Mean	109.18833	Adj R-Sq	0.9942
Coeff Var	3.69778		

a. Parameter estimate for variable, MicroSI, is the correction factor to convert extensometer data to movement at the head of the pin.

Parameter Estimates

Variable	DF	Parameter Estimate	Standard Error	t Value	Pr > |t|
Intercept	1	-4.01495	1.60428	-2.50	0.0173
MicroSI	1	1.19025	0.01531	77.73	<.0001

RMD 3 Calibration - All Trials Combined - SI Units 34
17:52 Tuesday, May 14, 2002

The REG Procedure
Model: MODEL1
Dependent Variable: ExtensSI

Output Statistics

b. Predicted error for calibration curve is the range of the 95% CL Predict, shown below.

Obs	Dep Var ExtensSI	Predicted Value	Std Error Mean Predict	95% CL Mean		95% CL Predict	
1	23.3800	26.2174	1.2618	23.6531	28.7817	17.6207	34.8140
2	38.6800	38.3103	1.1332	36.0073	40.6133	29.7880	46.8327
3	59.0800	56.4497	0.9556	54.5077	58.3917	48.0178	64.8817
4	74.1000	71.5659	0.8289	69.8813	73.2504	63.1895	79.9423
5	86.2300	86.6820	0.7326	85.1933	88.1708	78.3428	95.0213
6	98.5000	98.7750	0.6861	97.3806	100.1694	90.4521	107.0979
7	116.1500	116.9144	0.6802	115.5320	118.2968	108.5935	125.2353
8	131.8600	132.0305	0.7343	130.5383	133.5228	123.6907	140.3704
9	145.9200	147.1467	0.8314	145.4570	148.8364	138.7693	155.5241
10	160.8100	162.2629	0.9587	160.3146	164.2111	153.8295	170.6963
11	173.4900	177.3790	1.1056	175.1321	179.6259	168.8717	185.8864
12	189.2000	192.4952	1.2655	189.9235	195.0669	183.8963	201.0941
13	21.7300	26.2174	1.2618	23.6531	28.7817	17.6207	34.8140
14	37.3000	41.3335	1.1022	39.0936	43.5735	32.8280	49.8391
15	53.1500	56.4497	0.9556	54.5077	58.3917	48.0178	64.8817
16	69.1400	71.5659	0.8289	69.8813	73.2504	63.1895	79.9423

17	83.3400	86.6820	0.7326	85.1933	88.1708	78.3428	95.0213
18	97.8100	101.7982	0.6796	100.4171	103.1793	93.4775	110.1189
19	112.8400	116.9144	0.6802	115.5320	118.2968	108.5935	125.2353
20	127.5900	132.0305	0.7343	130.5383	133.5228	123.6907	140.3704
21	143.1600	147.1467	0.8314	145.4570	148.8364	138.7693	155.5241
22	157.0800	162.2629	0.9587	160.3146	164.2111	153.8295	170.6963
23	172.9300	177.3790	1.1056	175.1321	179.6259	168.8717	185.8864
24	188.1000	192.4952	1.2655	189.9235	195.0669	183.8963	201.0941
25	27.3800	26.2174	1.2618	23.6531	28.7817	17.6207	34.8140
26	44.1900	41.3335	1.1022	39.0936	43.5735	32.8280	49.8391
27	61.2900	56.4497	0.9556	54.5077	58.3917	48.0178	64.8817
28	75.3500	71.5659	0.8289	69.8813	73.2504	63.1895	79.9423
29	89.9600	86.6820	0.7326	85.1933	88.1708	78.3428	95.0213
30	106.2200	101.7982	0.6796	100.4171	103.1793	93.4775	110.1189
31	122.2100	116.9144	0.6802	115.5320	118.2968	108.5935	125.2353
32	138.7500	132.0305	0.7343	130.5383	133.5228	123.6907	140.3704
33	152.6700	147.1467	0.8314	145.4570	148.8364	138.7693	155.5241
34	168.5200	162.2629	0.9587	160.3146	164.2111	153.8295	170.6963
35	184.6500	177.3790	1.1056	175.1321	179.6259	168.8717	185.8864
36	198.0200	192.4952	1.2655	189.9235	195.0669	183.8963	201.0941

The REG Procedure
Model: MODEL1
Dependent Variable: ExtensSI

Output Statistics

Obs	Residual	Std Error Residual	Student Residual	-2-1 0 1 2	Cook's D
1	-2.8374	3.835	-0.740	| *| |	0.030
2	0.3697	3.875	0.0954	| | |	0.000
3	2.6303	3.923	0.671	| |* |	0.013
4	2.5341	3.952	0.641	| |* |	0.009
5	-0.4520	3.971	-0.114	| | |	0.000
6	-0.2750	3.979	-0.0691	| | |	0.000
7	-0.7644	3.980	-0.192	| | |	0.001
8	-0.1705	3.970	-0.0430	| | |	0.000
9	-1.2267	3.951	-0.310	| | |	0.002
10	-1.4529	3.922	-0.370	| | |	0.004
11	-3.8890	3.883	-1.001	| **| |	0.041
12	-3.2952	3.834	-0.859	| *| |	0.040
13	-4.4874	3.835	-1.170	| **| |	0.074
14	-4.0335	3.884	-1.038	| **| |	0.043
15	-3.2997	3.923	-0.841	| *| |	0.021
16	-2.4259	3.952	-0.614	| *| |	0.008
17	-3.3420	3.971	-0.842	| *| |	0.012
18	-3.9882	3.980	-1.002	| **| |	0.015
19	-4.0744	3.980	-1.024	| **| |	0.015
20	-4.4405	3.970	-1.118	| **| |	0.021
21	-3.9867	3.951	-1.009	| **| |	0.023
22	-5.1829	3.922	-1.321	| **| |	0.052
23	-4.4490	3.883	-1.146	| **| |	0.053

24	-4.3952	3.834	-1.146	|	**|	0.072
25	1.1626	3.835	0.303	|	|	0.005
26	2.8565	3.884	0.735	|	*	0.022
27	4.8403	3.923	1.234	|	**	0.045
28	3.7841	3.952	0.958	|	*	0.020
29	3.2780	3.971	0.826	|	*	0.012
30	4.4218	3.980	1.111	|	**	0.018
31	5.2956	3.980	1.331	|	**	0.026
32	6.7195	3.970	1.692	|	***	0.049
33	5.5233	3.951	1.398	|	**	0.043
34	6.2571	3.922	1.595	|	***	0.076
35	7.2710	3.883	1.872	|	***	0.142
36	5.5248	3.834	1.441	|	**	0.113

RMD 3 Calibration - All Trials Combined - SI Units 36
17:52 Tuesday, May 14, 2002

The REG Procedure
Model: MODEL1
Dependent Variable: ExtensSI

Sum of Residuals	0
Sum of Squared Residuals	554.26001
Predicted Residual SS (PRESS)	624.85659

Plot of Calibration Curve:

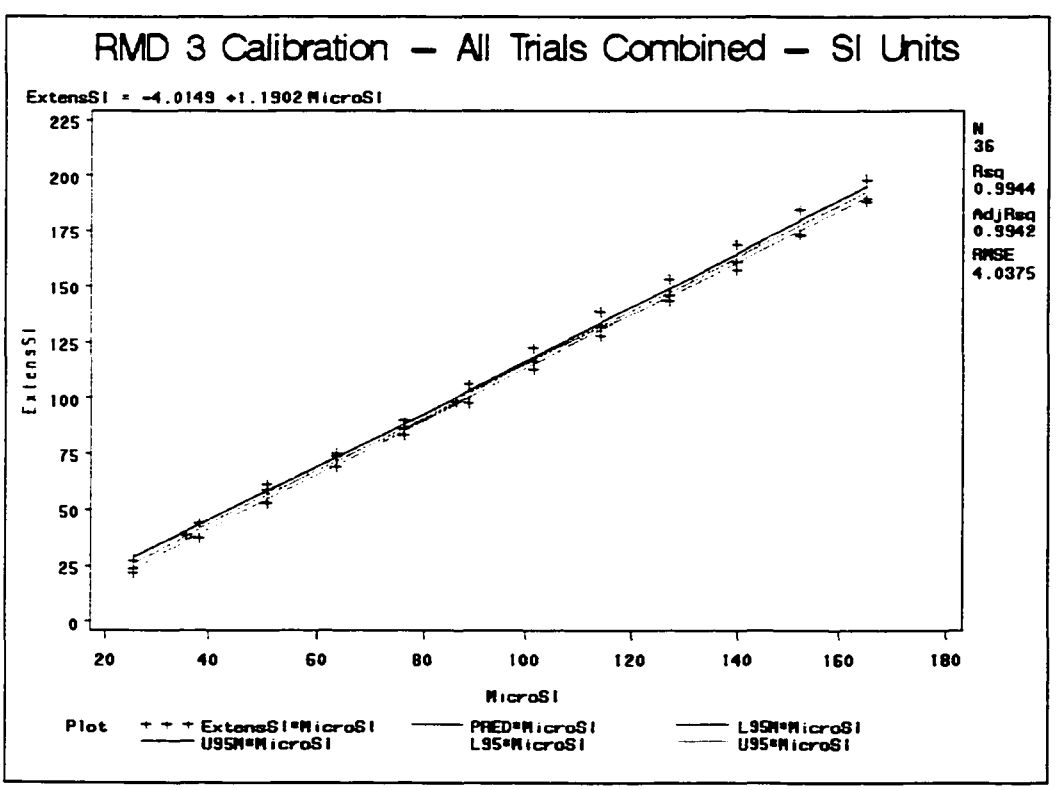

Plot of Mechanical Testing Results:

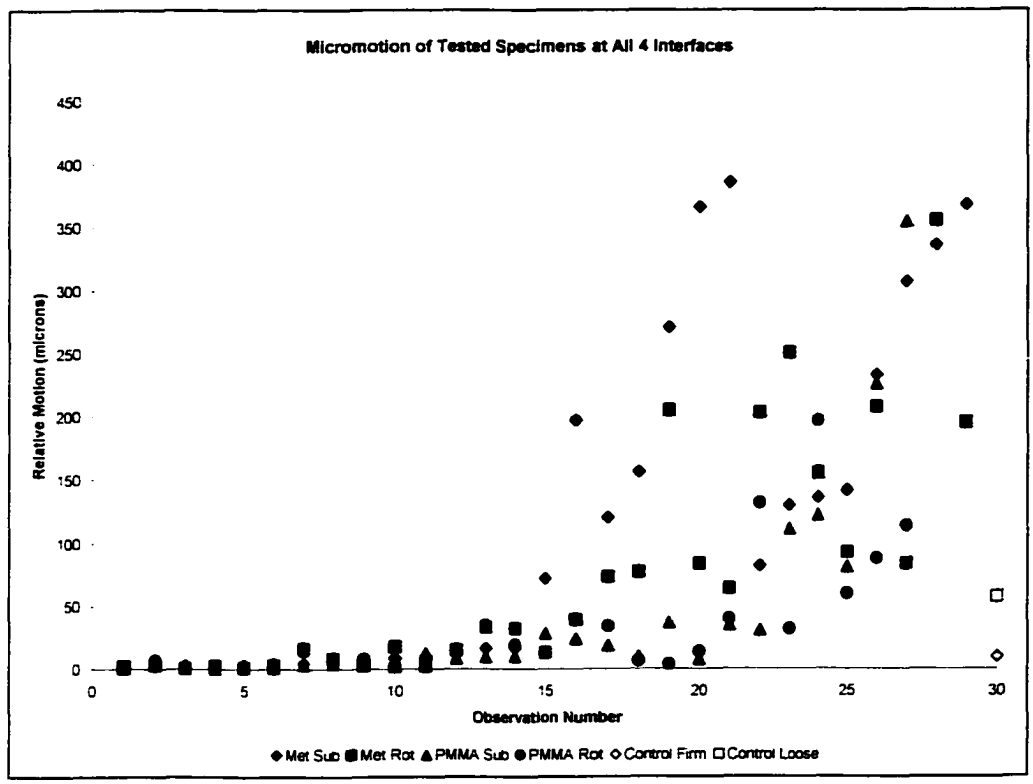

APPENDIX C - NON-DESTRUCTIVE MECHANICAL TESTING OF FEMORAL COMPONENTS

Sample Preparation Procedure for Mechanical Testing of Femoral Component:

1. Use CSU OIRP Femur Mechanical Testing Checklist to ensure that each required step is performed. This checklist is in the Excel file named "femlist.xls" and is in the worksheet labeled "Master." (See *Femoral Component Mechanical Testing Checklist* below)
2. This entire test must be completely run in one day due to the challenges of getting metal to stay glued to bone. Even though the femur is defatted, the fat continues to percolate up through the bone. This will cause the epoxy's bond to the bone to eventually fail. I discovered that you cannot even store the bone in the refrigerator overnight. The epoxy will usually fail by the next morning.
3. Prepare femur for mounting on MTS. Cut off condyles if necessary. Clamp femur in position using stand and 3-finger clamp such that the MTS will apply the load to the point on the femoral head that corresponds to the location of the peak load during walking (See Figure). Pot femur at proper angles using Dynacast. Allow Dynacast to set for 20-30 minutes.
4. From contact radiographs, estimate bone and PMMA thickness as well as placement of implant within the femur. Determine placement of hole to be drilled through bone.
   a. Usually, hole was placed ½" down from the lower edge of the implant collar in the thickest part of the implant and femur.
   b. Use cranial caudal radiograph to determine placement of hole.
   c. Use medial lateral radiograph to measure thickness of bone and PMMA.
5. Clean off tissue surrounding area where hole is to be drilled. Mark position of hole with a medium point Sharpie.
6. Wrap shaft of femur in saline-soaked paper towels. Place femur between 2 small pieces of wood shim. Clamp femur in vice which is clamped to platform on drill press.
7. Place ¼" end mill in drill press. Align drill press for proper placement of hole in femur. From radiograph measurements, set stop on drill press if necessary. Otherwise, note position of drill press when end mill is touching the bone and note expected position of drill press when PMMA should be reached.
8. Using drill press on slowest speed (220 RPM), carefully drill hole through bone to PMMA. Sometimes the drill press will try to run away when the bone/PMMA interface is reached. Watch carefully for different colors of bone vs. PMMA. This takes a soft touch and a little bit of practice.
9. Use coarse grit sandpaper to roughen up surface of bone around hole in preparation for gluing relative motion device (RMD) "t" in place.
10. Place femur in vent hood.
11. Defat bone by swabbing with alcohol then ether.
    a. Scrub and wipe down bone with denatured alcohol using cotton swabs.

b. Wipe bone down with 4x4 non-sterile gauze sponges.
c. The wiping pattern, especially when using ether, is critical. Use each gauze sponge for only one wipe. Do not rewipe with a used sponge. Start at hole and wipe outward. (See Figure). Wipe in 4 directions, starting at hole each time. The bone must be wet with alcohol before wiping, or it won't do any good.
d. Pour approximately 15 ml of ether into small beaker.
e. Pour a small amount of ether onto the bone and scrub with a cotton swab. Repeat this until the entire area around the bone has been scrubbed.
f. Pour a small amount of ether onto the bone one side of the hole (i.e., enough ether so that it does not evaporate before you can wipe it off with the gauze sponge). Wipe immediately with a clean 4x4 gauze sponge from the hole outward. Repeat this 3 more times around the hole (See Figure).
g. Repeat so that each direction has been wiped down twice.
h. Allow the femur to sit in the hood until the ether has evaporated from the bone.

12. Mix metal epoxy. Apply epoxy to bottom of RMD "t". Be careful not to get any epoxy on the threads of the "t". Set "t" in place with the bottom part seated into the ¼" hole in the femur. Allow the epoxy to set for at least 5 minutes before moving the femur.
13. Note which RMD "t" is being used on checklist.
14. Wrap femur in saline-soaked paper towels and plastic wrap. Do not wrap towels over the RMD "t". Do not let towels or plastic wrap touch the curing epoxy. Leave a small hole in the plastic wrap over the RMD "t" and the epoxy.
15. Place the wrapped femur so that the RMD "t" and the curing epoxy are under a lamp with a 40W light bulb. Allow the epoxy to cure for 1 hour under the light bulb.
16. Allow the epoxy to cure for an additional 3 hours at room temperature without the light bulb. This will give the epoxy 4 hours of total cure time before testing.

Femoral Component Mechanical Testing Procedure:

1. Warm up MTS. Mount jigs to MTS.
2. Double check to make sure that you are using the proper configuration file, tuning, data collection ranges, low pressure, load cell, and cable placement.
3. Calculate maximum and incremental loads from dog's weight.
   a. Peak load on the head of the femur is approximately 1.5 x body weight. Since the purpose of this test is to be relatively nondestructive, 75% of that peak load will be the maximum load applied to the head of the femur.
   b. Divide maximum test load by 5 to get increments for incremental loading.
4. Modify test program to apply proper loading sequence.
   a. The loading sequence used is to first use displacement control at a very slow loading rate until a preload of 2 lbf is reached. At this point, the program changes to force control. The 2 lbf preload is held for 10 seconds. Then the machine ramps up to the first load (1/5 of maximum load) over 5 seconds. Load 1 is held for 10 seconds. Then the machine ramps to the second load (2/5 of maximum load), etc. until the maximum load is reached. The machine then switches back to displacement control, and the femur is backed off until the femoral head is 0.1 inch above the test jig.

5. Manually test the RMD "t" to verify that it is firmly glued in place.
6. Spin RMD Part #2 onto "t" into first test position (i.e., either subsidence or ML translation testing) at the bone/PMMA interface.
   a. Each interface is tested in subsidence (i.e., slots of RMD perpendicular to long axis of femur) and ML translation (i.e., slots of RMD parallel to long axis of femur). The order of testing at each interface was randomized using an Excel spreadsheet and the random number generating function.
   b. The RMD is in the proper position when the slotted surface of Part #2 is level with the top of the RMD pin.
   c. Remove the pin from the RMD before mounting the femur in the MTS jig so that it does not fall out and get lost.
7. Mount femur upside down in MTS jig.
8. Place RMD pin into hole in RMD "t". Ensure that the 2 slots are at the same height. Tighten set screw on Part #2.
9. Mechanically test bone/PMMA relative motion. Use appropriate Testing Checklist (i.e., either "Subsidence" or "ML translation" worksheets from Excel file "femlist.xls."). Fill out Testing Checklist and circle which interface is being tested. The procedure is:
   a. Zero force.
   b. Make sure the pin is in place on the extensometer.
   c. Mount the extensometer to RMD.
   d. Lower actuator piston into test position. Place the implant into about 11.5 lbf compression.
   e. Remove the pin from the extensometer.
   f. Make sure the extensometer is still in place.
   g. Zero actuator displacement and extensometer.
   h. Note dataset name of output file for this test.
   i. Run test program.
   j. After test is completed, place pin back into extensometer.
   k. Raise the actuator position.
   l. Remove the extensometer from the RMD.
   m. For at least the first test run, quickly graph the data file to ensure that the data looks good (i.e., make sure the pin did not slip out of position during the test).
   n. Ideally, repeat the above steps until 4 good tests have been run. Sometimes, especially during the bone/metal relative motion tests, the pin sometimes slips or pops out of position during the test. This makes it difficult to get 4 good tests run. In this case, try for at least 2 good tests.
10. Loosen RMD set screw. Spin RMD Part #2 into second test position. Tighten the RMD set screw.
11. Mechanically test bone/PMMA relative motion using Testing Checklist as described above.
12. Remove pin from RMD. Remove femur from MTS jig.
13. Mount femur in vise on bench.
14. Using handheld drill with 3/16" end mill or other drill bits as necessary, carefully drill through PMMA to prosthesis.
15. This is a tricky part, and sometimes the RMD would pop off during this procedure.

16. If the femoral implant is not parallel to the surface of the bone. the end mill will not be enough. You will have to use other drill bits to get all the PMMA drilled out.
17. Use canned air to occasionally remove PMMA bits during drilling. Check progress using 70° endoscope and fiber optic light source.
18. Mount femur in MTS jig.
19. Loosen RMD set screw. Place RMD Pin into hole of RMD "t". Spin RMD Part #2 onto "t" into first test position (i.e., either subsidence or ML translation testing) for the bone/prosthesis relative motion testing.
20. Mechanically test bone/prosthesis relative motion using Testing Checklist as described above.
21. Loosen RMD set screw. Spin RMD Part #2 into second test position. Tighten the RMD set screw.
22. Mechanically test bone/prosthesis relative motion using Testing Checklist as described above.
23. Remove pin from RMD. Remove femur from MTS jig.
24. Remove RMD "t" from bone. This can usually be done manually at this point.
25. Rewrap femur and return it to the freezer.
26. Backup data to Zip disk.
27. Soak RMD "t" overnight in acetone in order to soften the epoxy. Clean the epoxy off the next morning. This may require the use of a chisel and hammer. I would mount a nut in the vise and screw the RMD "t" into the nut when I needed to use the chisel and hammer.
28. Rinse the RMD "t" with fresh acetone before using it again.

Femoral Component Mechanical Testing Checklist (Part 1):

CSU OIRP Femur Mechanical Testing Checklist

Case ID _____ Last Name _____

Side _____ RMD "t" _____

Implant Type & Size _____ Date _____

Sample Preparation

___ 1 Photograph and radiograph femurs
___ 2 From radiograph, estimate bone and PMMA thickness. Determine placement of RMD. Mark spot on femur
AP View [ ] ML View [ ]
___ 3 Mount femur in vise
___ 4 Align drill press. Set stop for drilling through bone to PMMA (from x-ray measurements)
___ 5 Using 1/4" end mill, CAREFULLY drill hole through bone to PMMA
___ 6 Place femur in vent hood.
___ 7 Prepare bone by swabbing with alcohol then ether
___ 8 Mix epoxy. Apply to RMD "t" and bone. Set "t" in place.
___ 9 Note which "t" is used (top of page)
___ 10 Allow epoxy to set for 20 minutes. Keep femur wrapped in saline soaked towels.
___ 11 Prepare femur for mounting in MTS. Cut off condyles (if necessary) and mount at proper angles using Dynacast.
___ 12 Warm up MTS. Mount jigs to MTS.
___ 13 Double check config, tuning, data collection ranges, low pressure, load cell being used, cable placement.
___ 14 Calculate maximum and incremental loads from body weight. Modify test program loads.
Weight [ ] *1.5*0.75 = [ ] <= Max Ld Ld / 5 = [ ] <= Increments
___ 15 Manually test RMD "t" to verify that it is firmly glued in place
___ 16 Mount femur in MTS jig. Wrap femur in saline-soaked towels

___ 17 Spin RMD Part #2 onto "t" into proper position for _____ testing.
NOTE For subsidence, slot perpendicular to long axis of femur. For ML Translation, slot parallel to long axis of femur
___ 18 Place Pin into RMD. Ensure that 2 slots are at same height. Tighten set screw on Part #2
___ 19 Mechanically test bone/PMMA interface (Go to Test Checklist)

___ 20 Loosen RMD set screw. Spin RMD Part #2 into position for _____ testing.
___ 21 Mechanically test bone/PMMA interface (Go to Test Checklist).
___ 22 Remove femur from MTS jig. Remove RMD Pin.
___ 23 Mount femur in vise
___ 24 Using 3/16" end mill, CAREFULLY align drill press so that end mill will not touch sides of RMD
___ 25 Set stop for drilling through PMMA to prosthesis. Extend hole to prosthesis
___ 26 Mount femur in MTS jig. Wrap femur in saline-soaked towels

___ 27 Loosen RMD set screw. Spin RMD Part #2 into position for _____ testing.
___ 28 Place Pin into RMD. Ensure that 2 slots are at same height. Tighten set screw on Part #2
___ 29 Mechanically test bone/PMMA interface (Go to Test Checklist).

___ 30 Loosen RMD set screw. Spin RMD Part #2 into position for _____ testing.
___ 31 Mechanically test bone/PMMA interface (Go to Test Checklist)
___ 32 Remove femur from MTS jig. Remove RMD Pin and Part #2.
___ 33 Mount femur in vise. Remove "t" from bone
___ 34 Rewrap femur and return to freezer
___ 35 Backup data to Zip disk.

Femoral Component Mechanical Testing Checklist (Part 2):

CSU OIRP Femur Mechanical Testing Checklist
Subsidence Tested First

Case ID _____ Last Name _____

Side _____ RMD "t" _____

Implant Type & Size _____ Date _____

Relative Motion Being Tested Bone/PMMA Bone/Prosthesis

Test Checklist	Subsidence Test #1	Subsidence Test #2	Subsidence Test #3	Subsidence Test #4	ML Transl Test #1	ML Transl Test #2	ML Transl Test #3	ML Transl Test #4
1 Zero force								
2 Make sure pin is in place on extensometer								
3 Mount extensometer to RMD								
4 Lower actuator piston into test position								
5 Remove extensometer pin								
6 Make sure extensometer is still in place								
7 Zero displacement and extensometer								
8 Note dataset name for test								
9 Run test program								
10 Place pin back into extensometer								
11 Raise actuator piston								
11 Remove extensometer from RMD								
12 For first test run, graph data file								

Femoral Component Mechanical Testing Checklist (Part 3):

CSU OIRP Femur Mechanical Testing Checklist
ML Translation Tested First

Case ID _____ Last Name _____

Side _____ RMD "t" _____

Implant Type & Size _____ Date _____

Relative Motion Being Tested Bone/PMMA Bone/Prosthesis

Test Checklist	ML Transl Test #1	ML Transl Test #2	ML Transl Test #3	ML Transl Test #4	Subsidence Test #1	Subsidence Test #2	Subsidence Test #3	Subsidence Test #4
1 Zero force								
2 Make sure pin is in place on extensometer								
3 Mount extensometer to RMD								
4 Lower actuator piston into test position								
5 Remove extensometer pin								
6 Make sure extensometer is still in place								
7 Zero displacement and extensometer								
8 Note dataset name for test								
9 Run test program								
10 Place pin back into extensometer								
11 Raise actuator piston								
11 Remove extensometer from RMD								
12 Graph data file								

Sample Output from Mechanical Testing:

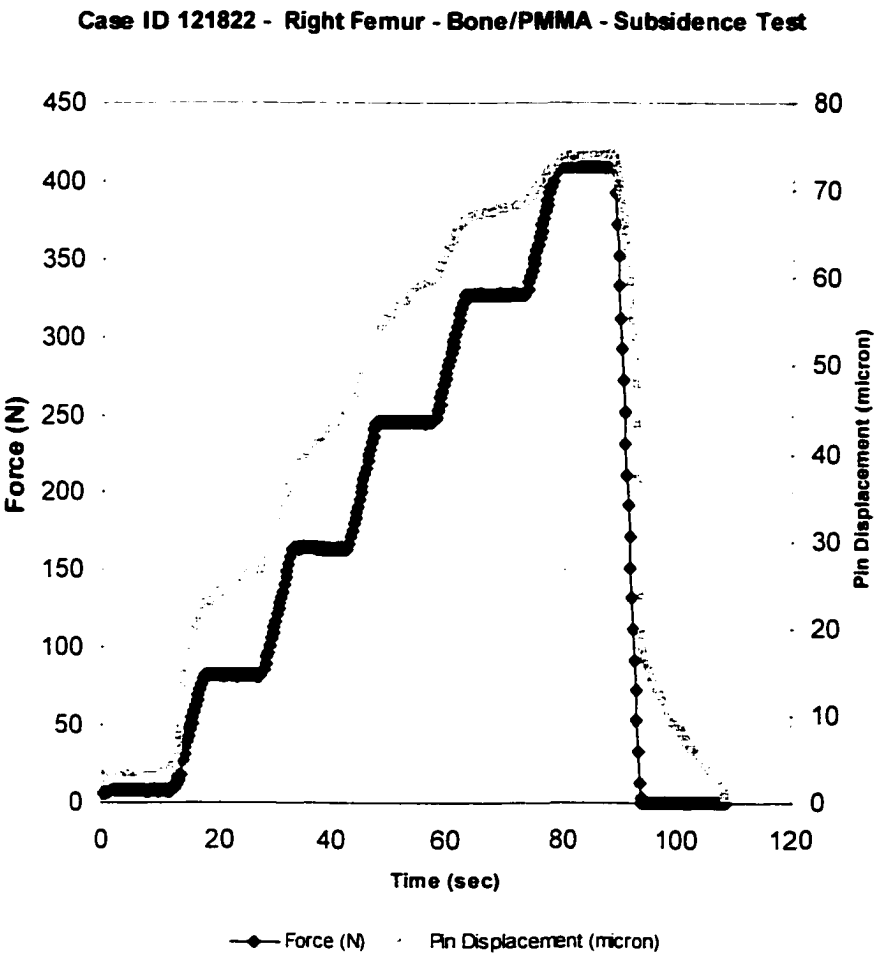

APPENDIX D - GRADING OF FEMORAL RADIOGRAPHS

Femoral Radiograph Evaluation Form

Case ID: _____ Birth Date: _____

Surgery Date: _____ Death Date: _____

Age at Surgery (mos): _____ Implant Duration (mos): _____

Implant Mfr: _____

Implant Size: _____ Implant Side: Right / Left

Bilateral / Unilateral If bilateral, side implanted first: Right / Left
If bilateral, time between surgeries (mos): _____

Radiograph Evaluation:

Contact Radiograph / Clinical Radiograph Date & Views: _____

Cerclage Wires (i.e., Number & Location) _____

_____

Additional Hardware: _____

_____

Other Disease Conditions (e.g., Stifle OA): _____

_____

Add'l Observations on
Femoral Radiographs: _____

_____

_____

_____

Subsidence (related to fixed landmarks on femur)
_____ No
_____ Yes (_____ mm) Within cement / With cement
Resorption of calcar: No / Yes
Resorption or hypertrophy of shaft: No / Yes

Resorption (zones: _____) Hypertrophy (zones: _____)
[CC View] Position of distal tip of stem (qualitative): Neutral / Valgus / Varus
[ML View] Position of distal tip of stem (qualitative): Neutral / Cranial / Caudal
In contact? Yes / No

[ML View] Position of femoral head: Anteverted (____°) / Normoverted / Retroverted (____°)
Greater trochanter: Not osteomized / Osteomized

[ML View] Position of femoral head: Anteverted (____°) / Normoverted / Retroverted (____°)
Greater trochanter: Not osteomized / Osteomized
Ectopic ossification: No / Yes

Cranial-Caudal (Anterior-Posterior in Human) View						
	Cement thickness		Number of voids (pores) and Void Size (mm)	Crack Number/Length of each (mm)	Radiolucency at Bone-PMMA Interface (mm)	Radiolucency at PMMA-Metal Interface (mm)
	Max Width (mm)	Min Width (mm)				
Zone 1					L: W:	L: W:
Zone 2					L: W:	L: W:
Zone 3					L: W:	L: W:
Zone 4					L: W:	L: W:
Zone 5					L: W:	L: W:
Zone 6					L: W:	L: W:
Zone 7					L: W:	L: W:

Medial-Lateral View						
	Cement thickness		Number of voids (pores) and Void Size (mm)	Crack Number/Length of each (mm)	Radiolucency at Bone-PMMA Interface (mm)	Radiolucency at PMMA-Metal Interface (mm)
	Max Width (mm)	Min Width (mm)				
Zone 1					L: W:	L: W:
Zone 2					L: W:	L: W:
Zone 3					L: W:	L: W:
Zone 4					L: W:	L: W:
Zone 5					L: W:	L: W:
Zone 6					L: W:	L: W:
Zone 7					L: W:	L: W:

APPENDIX E - SLICING OF FEMORA

Plan Cuts:

1. Use contact radiographs made using the Faxitron. These radiographs need to have the modified Gruen zones already marked on them.
2. Measure length from top of Gruen zone 1/7 to bottom of zone 3/5 (mm).
3. Measure length from top of Gruen zone 1/7 to distal tip of implant.
4. Calculate length of each Gruen zone.
5. Measure distance from top of Gruen zone to bottom of implant collar. Plan placement of first cut based on this landmark.
   a. If collar is 3 mm into zone, cut at collar's edge.
   b. If collar is 4 mm or less into zone, cut at collar's edge.
   c. If collar's edge is less than 3 mm into zone, line up first cut at collar's edge and then move the implant to the 3 mm mark.
   d. If collar's edge is more than 4 mm into zone, line up first cut at collar's edge and then back implant back to 3 mm.
6. Plan remainder of cuts.
   a. 2 mm thick SEM cuts will be made at the proximal end and distal end of each of the 3 zones. These cuts will be placed 3 mm into the zone.
   b. There will be a 6 mm cut at the 1/7 & 2/6 boundary and at the 2/6 & 3/5 boundary.
   c. The thickness of the slices in the center of each zone will vary depending on the length of the implant.
   d. The 13^{th} cut, at the 3/5 & 4 boundary is made thick enough to include the distal tip of the implant in that cut.
   e. The 14^{th} cut makes the 7^{th} SEM slice. This slice is made past the distal tip of the implant and has only PMMA in the bone.

Exakt Cutting Methodology:

1. Exakt recommends using their 0.3 mm interrupted blade for cutting through the metal implant. This blade costs approximately $1200 each.
2. Set up the Exakt saw with the appropriate blade. You must be trained on how to mount the blade and make sure that it is making cuts perfectly parallel with a slide mounted on the vacuum mount of the rocker arm.
   a. Make sure that the thinner of the 2 feed weights is in place. Since we are cutting metal, we don't want to put too much weight and stress on the blade.
3. Using the rocker arm cuts the cutting time for each slice by 2/3. However, don't use the rocker arm if the bone must be mounted at an odd angle. As long as the femur can rotate inline with the rocker arm's piston, it works fine. If you have to offset the femur, though, the blade may jump around as the rocker arm rotates. This would be bad.

4. Cut off the distal condyles of the femur so that the grips can be used on the cylindrical length of the femur. Plan this cut so that it is at least 3-4 cm past the 14th cut. This will give you enough femur to mount in the jig without obstructing all 14 cuts. This cut is made with the femur held in your hands. Be careful. The blade can grab onto the specimen if you are applying too much pressure to the blade.
5. Wrap the distal end of the femur in gauze and mount in the jig.
   a. If the femur is not perfectly cylindrical, you may need to fold the gauze in places to get the grips to hold the femur firmly.
   b. If possible, line up the longitudinal axis of the femur with the part of the jig that mounts to the rocker arm.
6. Mount the jig to the rocker arm.
   a. Make sure that the longitudinal axis of the femur is inline with or at least parallel with the longitudinal axis of the rocker arm.
   b. Use a level to make sure the proximal length of the femur (before the femur starts to curve caudally) is parallel to the floor.
7. If the rocker arm's set screw is not all the way to the right side of the little window, spin the rocker arm (not the dial – it takes too long and will kill your hands) until the set screw is to the far right side of the window.
8. Move the carriage of the rocker arm until the collar's edge is inline with the blade. Tighten the clamps to hold the carriage in place.
   a. If necessary, dial in any necessary adjustments to properly place the first cut relative to the collar's edge.
9. Tighten the rocker arm set screw and the metal knob on top of the rocker arm assembly. Put the plastic cover in the window to prevent water from spraying into the window.
10. Turn on the Exakt saw.
    a. I was cutting at speed 8.
    b. Slowly turn the speed up. I would start at 3 and give it 5 seconds. Then I would give an additional 5 seconds for each incremental increase in blade speed.
    c. Make sure the water pump is on (green switch).
11. Cut the first slice.
    a. Don't turn on the rocker arm until the blade has cut a bit into the bone.
    b. For the thick slices, I used the 3 dot setting on the rocker arm.
    c. For the 2 mm slices, I used the 2 dot setting on the rocker arm.
12. Each specimen is placed into a specimen cup with 70% ethanol.
    a. I used 8 oz specimen cups for the 5 thickest slices and pieces, and 4 oz specimen cups for the remaining thinner slices (2 mm and 6 mm slices). This was done to save storage space.
    b. Each specimen cup should have a piece of index card with the slice's identification written in pencil. Pencil won't fade in the ethanol.
13. Dial in each subsequent slice.
    a. Loosen the metal knob and set screw on the rocker arm.
    b. Turn the dial 10 times for each mm thickness of the slice. (I kept tick marks in a notebook for each 1 turns.)
    c. Tighten the metal knob and set screw.
    d. Continue slicing.

14. When the set screw gets too close to the left side of the window, you will need to move the carriage forward.
    a. Wind the rocker arm until the set screw is once again at the right side of the window.
    b. Loosen the clamps that hold the carriage in place.
    c. Place the bone in line with the blade.
    d. Move the carriage until the bone is very close to, but not touching, the blade. I made sure I could slip a sticky note between the blade and the specimen.
    e. Pull the bone back from the blade.
    f. Tighten the clamps to hold the carriage in its new position.
    g. Dial in the thickness of the next slice.
    h. NOTE – Never move the carriage before a 2 mm thick slice. If possible, move the carriage just before making the thickest slices

APPENDIX F - SAMPLE SAS OUTPUT: MULTIPLE LINEAR REGRESSION ANALYSIS

1. Sample SAS Output – Multiple Linear Regression – Backward Selection Method

The REG Procedure
Model: MODEL1
Dependent Variable: s_pmma s_pmma

Backward Elimination: Step 19

Analysis of Variance

Source	DF	Sum of Squares	Mean Square	F Value	Pr > F
Model	6	379.70951	63.28492	11.58	<.0001
Error	18	98.37778	5.46543		
Corrected Total	24	478.08729			

Variable	Parameter Estimate	Standard Error	Type II SS	F Value	Pr > F
Intercept	2.17150	2.17784	5.43366	0.99	0.3319
minpmma	4.63227	0.99020	119.60985	21.88	0.0002
area_met_pmma	-0.11739	0.02336	138.04390	25.26	<.0001
s_dist	-1.88827	1.48130	8.88113	1.62	0.2186
mean_s_cc4ml11	2.25893	0.51940	103.37827	18.91	0.0004
diff_s_cc4ml11	6.16871	1.37855	109.43848	20.02	0.0003
bm1	5.95411	1.10258	159.38089	29.16	<.0001

Bounds on condition number: 1.7171, 52.538

Backward Elimination: Step 20

a. **R^2 Value for Backward Selection Model:**

Variable s_dist Removed: R-Square = 0.7756 and C(p) = 1.6148

Analysis of Variance

Source	DF	Sum of Squares	Mean Square	F Value	Pr > F
Model	5	370.82838	74.16568	13.14	<.0001
Error	19	107.25891	5.64521		
Corrected Total	24	478.08729			

The REG Procedure
Model: MODEL1
Dependent Variable: s_pmma s_pmma

Backward Elimination: Step 20

b. **Backward Selection Model:**

Variable	Parameter Estimate	Standard Error	Type II SS	F Value	Pr > F
Intercept	0.39120	1.69834	0.29953	0.05	0.8203
minpmma	5.09915	0.93498	167.90655	29.74	<.0001
area_met_pmma	-0.12242	0.02340	154.56517	27.38	<.0001
mean_s_cc4ml11	2.01592	0.49103	95.15014	16.86	0.0006
diff_s_cc4ml11	5.97157	1.39219	103.86265	18.40	0.0004
bm1	5.62088	1.08862	150.49994	26.66	<.0001

Bounds on condition number: 1.6014, 33.429

All variables left in the model are significant at the 0.0110 level.

Summary of Backward Elimination

Step	Variable Entered	Variable Removed	Label	Number Vars In	Partial R-Square	Model R-Square	C(p)
1		s_cc23	s_cc23	22	0.0002	0.9845	22.0098
2		femdur	femdur	21	0.0007	0.9838	20.0541
3		s_void_nbr	s_void_nbr	20	0.0003	0.9835	18.0757
4		s_ml1213	s_ml1213	19	0.0014	0.9821	16.1672
5		age	age	18	0.0007	0.9814	14.2125
6		wt_kg	wt_kg	17	0.0006	0.9808	12.2491

Summary of Backward Elimination

Step	F Value	Pr > F
1	0.01	0.9371
2	0.09	0.7950
3	0.06	0.8202
4	0.34	0.5910
5	0.19	0.6782
6	0.18	0.6851

The REG Procedure
Model: MODEL1
Dependent Variable: s_pmma s_pmma

Summary of Backward Elimination

Step	Variable Entered	Variable Removed	Label	Number Vars In	Partial R-Square	Model R-Square	C(p)
7		cccrk_nbr	cccrk_nbr	16	0.0006	0.9802	10.2883
8	crk_len		crk_len	17	0.0006	0.9808	12.2491
9		crk_len	crk_len	16	0.0006	0.9802	10.2883
10		ccvoid_area	ccvoid_area	15	0.0004	0.9798	8.3134
11		bm2	bm2	14	0.0007	0.9792	6.3581
12		luc1	luc1	13	0.0028	0.9763	4.5423
13		s_cc56	s_cc56	12	0.0119	0.9645	3.3156
14		luc2	luc2	11	0.0234	0.9410	2.8421
15		mlvoid_area	mlvoid_area	10	0.0198	0.9212	2.1324
16		nbr_imp	nbr_imp	9	0.0355	0.8857	2.4441
17		area_bone	area_bone	8	0.0250	0.8608	2.0696
18		fem_head	fem_head	7	0.0207	0.8401	1.4163
19		s_ml910	s_ml910	6	0.0459	0.7942	2.4047
20		s_dist	s_dist	5	0.0186	0.7756	1.6148

Summary of Backward Elimination

Step	F Value	Pr > F
7	0.22	0.6536
8	0.22	0.6536
9	0.22	0.6536
10	0.16	0.7030
11	0.31	0.5934
12	1.36	0.2712
13	5.52	0.0386
14	7.91	0.0157
15	4.37	0.0569
16	6.31	0.0249
17	3.28	0.0904
18	2.38	0.1428
19	4.88	0.0412
20	1.62	0.2186

2. Sample SAS Output – Multiple Linear Regression – Best Selection Method

The REG Procedure
Model: MODEL1
Dependent Variable: s_pmma

R-Square Selection Method

Number in Model	R-Square	Variables in Model
1	0.2810	luc1
1	0.2327	femdur
1	0.1629	diff_s_cc4ml11
1	0.1363	nbr_imp
1	0.1172	minpmma
2	0.5304	femdur diff_s_cc4ml11
2	0.4615	s_ml1213 luc1
2	0.3957	s_cc56 luc1
2	0.3812	s_cc23 luc1
2	0.3537	femdur luc1
3	0.6531	femdur s_cc23 diff_s_cc4ml11
3	0.6208	femdur area_met_pmma diff_s_cc4ml11
3	0.6145	s_cc56 s_ml1213 luc1
3	0.6049	femdur s_ml1213 diff_s_cc4ml11
3	0.5832	femdur s_cc56 diff_s_cc4ml11
4	0.6912	femdur area_met_pmma s_cc56 diff_s_cc4ml11
4	0.6787	femdur area_met_pmma s_ml910 diff_s_cc4ml11
4	0.6770	femdur s_cc23 luc2 diff_s_cc4ml11
4	0.6767	minpmma s_cc56 s_ml1213 luc1
4	0.6736	femdur s_cc23 s_cc56 diff_s_cc4ml11
5	0.7756	minpmma area_met_pmma mean_s_cc4ml11 diff_s_cc4ml11 bm1
5	0.7395	femdur s_cc56 s_ml1213 luc1 diff_s_cc4ml11
5	0.7280	femdur cccrk_nbr area_met_pmma s_cc56 diff_s_cc4ml11
5	0.7280	femdur area_met_pmma s_cc56 crk_len diff_s_cc4ml11
5	0.7265	minpmma s_cc56 s_ml1213 luc1 diff_s_cc4ml11
6	0.8148	minpmma area_met_pmma s_ml1213 mean_s_cc4ml11 diff_s_cc4ml11 bm1
6	0.8122	wt_kg minpmma area_met_pmma mean_s_cc4ml11 diff_s_cc4ml11 bm1
6	0.7994	age minpmma area_met_pmma mean_s_cc4ml11 diff_s_cc4ml11 bm1
6	0.7968	minpmma fem_head area_met_pmma mean_s_cc4ml11 diff_s_cc4ml11 bm1
6	0.7942	minpmma area_met_pmma s_dist mean_s_cc4ml11 diff_s_cc4ml11 bm1
7	0.8659	wt_kg minpmma area_met_pmma s_ml1213 mean_s_cc4ml11 diff_s_cc4ml11 bm1
7	0.8534	minpmma area_met_pmma s_cc56 s_dist mean_s_cc4ml11 diff_s_cc4ml11 bm1

← Note that this R^2 value is larger than the other four 2-variable models, but only 1 of these variables were in the backward model

← Note – no superior model

← Note – no superior model

APPENDIX G - WEAR GRADING FORM FOR ACETABULAR COMPONENT

UHMWPE Wear Grading Form

Case ID _____ Name _____

Implant Side _____ Implant Size _____ Implant Mfr _____

Grading Criteria:	Quadrant I (Cranial – Dorsal)	Quadrant II (Caudal – Dorsal)	Quadrant III (Caudal – Ventral)	Quadrant IV (Cranial – Ventral)	Cranial Corner	Caudal Corner	Rim of Cut-Out	Cranial Rim of Cup	Caudal Rim of Cup	Score Subtotal
1. Creep (Deformation).										
2. Pitting.										
3. Embedded PMMA debris.										
4. Embedded metal debris.										
5. Scratching.										
6. Absence of machine marks.										
7. Abrasion (Tufting).										
8. Non-scratch macroscopic removal of PE.										
9. Yellowing.										
SCORE SUB-TOTALS:										

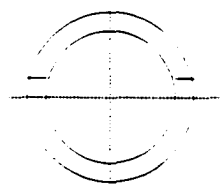

APPENDIX H - CALIBRATION OF LASER TEST METHOD

Calibration Jig:

1. A board was mounted to the MTS actuator so that the flat surface of the board was perpendicular to the MTS actuator (i.e., parallel with the floor).
2. Concentric circles were drawn on the board with the radii of the different sized acetabular components. The location of the cut-out corners was marked on the board (i.e., -22° from the negative x-axis).
3. A bone pin and laser mirror were mounted to the bottom of the board at the location of the cut-out corner on the acetabular component.
   a. Laser mirror was mounted
4. The laser mirror was mounted so that the laser spot on the wall could be marked through ±2° rotation of the MTS actuator (i.e., laser beam did not strike the MTS upright bearings during the test).

Calibration Method:

1. A laminated dry-erase calendar poster was taped to the wall of the laboratory to provide a smooth surface for recording the laser spots on the wall.
2. Tractor-feed continuous form computer printer paper was taped to the laminated poster so that the laser spot at the zero position was in the center of the paper.
   a. The paper was taped to the wall with the tape on the perforated tractor feed strips on the sides of the paper. This made for easy removal of the paper from the wall at the end of the test. The paper was torn from the tractor-feed strips in one piece. The tractor-feed strips were then removed from the poster and discarded.
   b. The paper was marked with the position relative to a fixed position on the wall.
   c. Using a carpenter's level, a line was drawn under the laser spot in order to indicate level on the paper for future reference during measurement.
   d. The test date, test being performed, and the output dataset from the MTS system were written on the paper.
3. The calibration program started at zero degrees and rotated the actuator clockwise to 2° in 0.2° increments. The program held at each increment for 15 seconds to allow the operator enough time to mark the laser spot on the paper. The program then returned the actuator to zero, and held for 15 seconds. Then the actuator was rotated to –2 ° in 0.2° increments. The program held at each increment for 15 seconds to allow the operator to mark the laser spot on the paper. The program then returned the actuator to zero to end the test.
   a. The spot was outlined in pencil on the paper. There were two ovals drawn for each spot. There was an intense inner spot and a more diffuse outer spot.
4. The test was repeated multiple times in order to calculate a calibration curve.
5. The test was also repeated at different angles in the z-direction (i.e., vertical on the

laboratory wall) to determine the effect on rotation in the y-direction (i.e., horizontal on the laboratory wall).

   a. The origin was placed at the center of rotation of the MTS actuator with the x-axis perpendicular to the laboratory wall and the y-axis parallel to the laboratory wall.

6. The calibration curve in the y-direction was very linear through more than 5 degrees of rotation (*See Plot of Calibration Curve, below*).
   a. This allowed for an area of the laboratory wall to be considered to be within the calibration zone. The laser mirrors for the test specimens were mounted so that the laser spot fell within the calibrated zone on the laboratory wall.
   b. One degree of rotation in the y-direction resulted in the laser spot moving approximately 138 mm on the wall.
7. The calibration curves were made in both clockwise and counter-clockwise rotation in order to facilitate testing right and left acetabular components.
   a. The loading direction for the actual testing was chosen based on the rotation that would more likely result from the direction of the peak joint reaction force in stance during walking gait.
   b. Left acetabular components were rotated counter-clockwise.
   c. Right acetabular components were rotated clockwise.
8. Using SAS calculate a calibration curve with 95% prediction confidence levels.
9. Generate a similar calibration curve for motion in the z-direction.

Sample Calibration Curve Calculations (SAS Output):

1. **Sample SAS Output - Regression Procedure Used to Calculate 95% Prediction Confidence Limits for Y-Direction Calibration Curve for PE Laser:**

```
                    Laser hip test calibration                          14
                                        14:52 Monday, January 14, 2002

---------------------------------- type=pe -----------------------------------

                          The REG Procedure
                            Model: MODEL1
                        Dependent Variable: y

                          Analysis of Variance

                                   Sum of           Mean
Source                     DF      Squares         Square    F Value    Pr > F

Model                       1      1247174        1247174     272231    <.0001
Error                      52    238.22805        4.58131
Corrected Total            53      1247412


          Root MSE            2.14040    R-Square     0.9998
          Dependent Mean     24.61574    Adj R-Sq     0.9998
          Coeff Var           8.69525
```

Parameter Estimates

Variable	DF	Parameter Estimate	Standard Error	t Value	Pr > |t|
Intercept	1	-0.98309	0.29537	-3.33	0.0016
deg	1	137.94650	0.26439	521.76	<.0001

Parameter Estimates

Variable	DF	95% Confidence Limits	
Intercept	1	-1.57580	-0.39038
deg	1	137.41597	138.47703

---------- type=pe ----------

The REG Procedure
Model: MODEL1
Dependent Variable: y

Output Statistics

Obs	Dep Var y	Predicted Value	Std Error Mean Predict	95% CL Mean		95% CL Predict	
1	0	-0.8891	0.2953	-1.4818	-0.2965	-5.2248	3.4466
2	-53.0000	-53.5743	0.3276	-54.2316	-52.9170	-57.9193	-49.2293
3	-109.0000	-108.4778	0.3872	-109.2548	-107.7009	-112.8426	-104.1131
4	-165.0000	-163.8567	0.4640	-164.7878	-162.9256	-168.2515	-159.4619
5	-221.2500	-218.7602	0.5499	-219.8637	-217.6567	-223.1947	-214.3257
6	2.5000	0.8539	0.2948	0.2623	1.4454	-3.4817	5.1894
7	58.5000	56.2327	0.2975	55.6357	56.8297	51.8964	60.5690
8	111.7500	111.3739	0.3354	110.7009	112.0469	107.0265	115.7214
9	166.0000	166.5151	0.3985	165.7155	167.3148	162.1463	170.8839
10	221.0000	221.6563	0.4769	220.6993	222.6133	217.2560	226.0567
11	277.0000	276.7975	0.5643	275.6651	277.9299	272.3557	281.2393
12	0	-0.7307	0.2953	-1.3232	-0.1381	-5.0664	3.6050
13	-52.5000	-53.3366	0.3274	-53.9935	-52.6797	-57.6816	-48.9917
14	-107.7500	-108.7155	0.3875	-109.4930	-107.9380	-113.0803	-104.3507
15	-164.5000	-163.8567	0.4640	-164.7878	-162.9256	-168.2515	-159.4619
16	-221.2500	-218.9979	0.5503	-220.1022	-217.8936	-223.4326	-214.5632
17	2.5000	1.0915	0.2947	0.5001	1.6830	-3.2440	5.4271
18	59.5000	55.7574	0.2973	55.1607	56.3540	51.4211	60.0936
19	114.0000	111.1362	0.3352	110.4637	111.8088	106.7889	115.4836
20	168.0000	166.5151	0.3985	165.7155	167.3148	162.1463	170.8839
21	221.5000	221.6563	0.4769	220.6993	222.6133	217.2560	226.0567
22	274.5000	276.5598	0.5639	275.4282	277.6914	272.1182	281.0014
23	0	-0.7307	0.2953	-1.3232	-0.1381	-5.0664	3.6050
24	-52.0000	-53.0989	0.3271	-53.7554	-52.4425	-57.4439	-48.7540
25	-107.2500	-108.4778	0.3872	-109.2548	-107.7009	-112.8426	-104.1131
26	-163.7500	-163.6190	0.4637	-164.5495	-162.6886	-168.0137	-159.2244
27	-220.7500	-218.7602	0.5499	-219.8637	-217.6567	-223.1947	-214.3257
28	3.0000	1.8046	0.2945	1.2135	2.3956	-2.5309	6.1401

29	60.2500	56.2327	0.2975	55.6357	56.8297	51.8964	60.5690
30	168.7500	166.7528	0.3988	165.9525	167.5531	162.3838	171.1217
31	222.2500	221.8940	0.4773	220.9362	222.8517	217.4935	226.2945
32	274.7500	277.2728	0.5651	276.1389	278.4068	272.8307	281.7150
33	0	-1.4437	0.2955	-2.0367	-0.8507	-5.7795	2.8921
34	-52.2500	-53.5743	0.3276	-54.2316	-52.9170	-57.9193	-49.2293
35	-106.2500	-108.9532	0.3878	-109.7313	-108.1750	-113.3181	-104.5882
36	-162.5000	-164.0944	0.4644	-165.0262	-163.1625	-168.4893	-159.6994
37	-219.0000	-219.2356	0.5507	-220.3406	-218.1305	-223.6705	-214.8007
38	3.0000	1.0915	0.2947	0.5001	1.6830	-3.2440	5.4271
39	60.0000	56.2327	0.2975	55.6357	56.8297	51.8964	60.5690
40	114.0000	111.3739	0.3354	110.7009	112.0469	107.0265	115.7214
41	168.0000	166.2774	0.3982	165.4784	167.0765	161.9087	170.6461
42	222.0000	221.8940	0.4773	220.9362	222.8517	217.4935	226.2945
43	274.5000	276.5598	0.5639	275.4282	277.6914	272.1182	281.0014
44	0	1.0915	0.2947	0.5001	1.6830	-3.2440	5.4271
45	-55.0000	-53.8120	0.3278	-54.4697	-53.1543	-58.1571	-49.4669
46	-111.0000	-108.7155	0.3875	-109.4930	-107.9380	-113.0803	-104.3507

---------- type=pe ----------

The REG Procedure
Model: MODEL1
Dependent Variable: y

Output Statistics

Obs	Residual
1	0.8891
2	0.5743
3	-0.5222
4	-1.1433
5	-2.4898
6	1.6461
7	2.2673
8	0.3761
9	-0.5151
10	-0.6563
11	0.2025
12	0.7307
13	0.8366
14	0.9655
15	-0.6433
16	-2.2521
17	1.4085
18	3.7426
19	2.8638
20	1.4849
21	-0.1563
22	-2.0598
23	0.7307
24	1.0989

25	1.2278
26	-0.1310
27	-1.9898
28	1.1954
29	4.0173
30	1.9972
31	0.3560
32	-2.5228
33	1.4437
34	1.3243
35	2.7032
36	1.5944
37	0.2356
38	1.9085
39	3.7673
40	2.6261
41	1.7226
42	0.1060
43	-2.0598
44	-1.0915
45	-1.1880
46	-2.2845

---------- type=pe ----------

The REG Procedure
Model: MODEL1
Dependent Variable: y

Output Statistics

Obs	Dep Var y	Predicted Value	Std Error Mean Predict	95% CL Mean		95% CL Predict	
47	-167.5000	-163.8567	0.4640	-164.7878	-162.9256	-168.2515	-159.4619
48	-223.5000	-218.7602	0.5499	-219.8637	-217.6567	-223.1947	-214.3257
49	0	0.8539	0.2948	0.2623	1.4454	-3.4817	5.1894
50	55.0000	56.2327	0.2975	55.6357	56.8297	51.8964	60.5690
51	109.5000	111.3739	0.3354	110.7009	112.0469	107.0265	115.7214
52	163.5000	166.2774	0.3982	165.4784	167.0765	161.9087	170.6461
53	218.0000	221.6563	0.4769	220.6993	222.6133	217.2560	226.0567
54	271.0000	276.5598	0.5639	275.4282	277.6914	272.1182	281.0014

Output Statistics

Obs	Residual
47	-3.6433
48	-4.7398
49	-0.8539
50	-1.2327
51	-1.8739
52	-2.7774

53	-3.6563
54	-5.5598

Sum of Residuals	0
Sum of Squared Residuals	238.22805
Predicted Residual SS (PRESS)	260.27769

Plot of Calibration Curve:

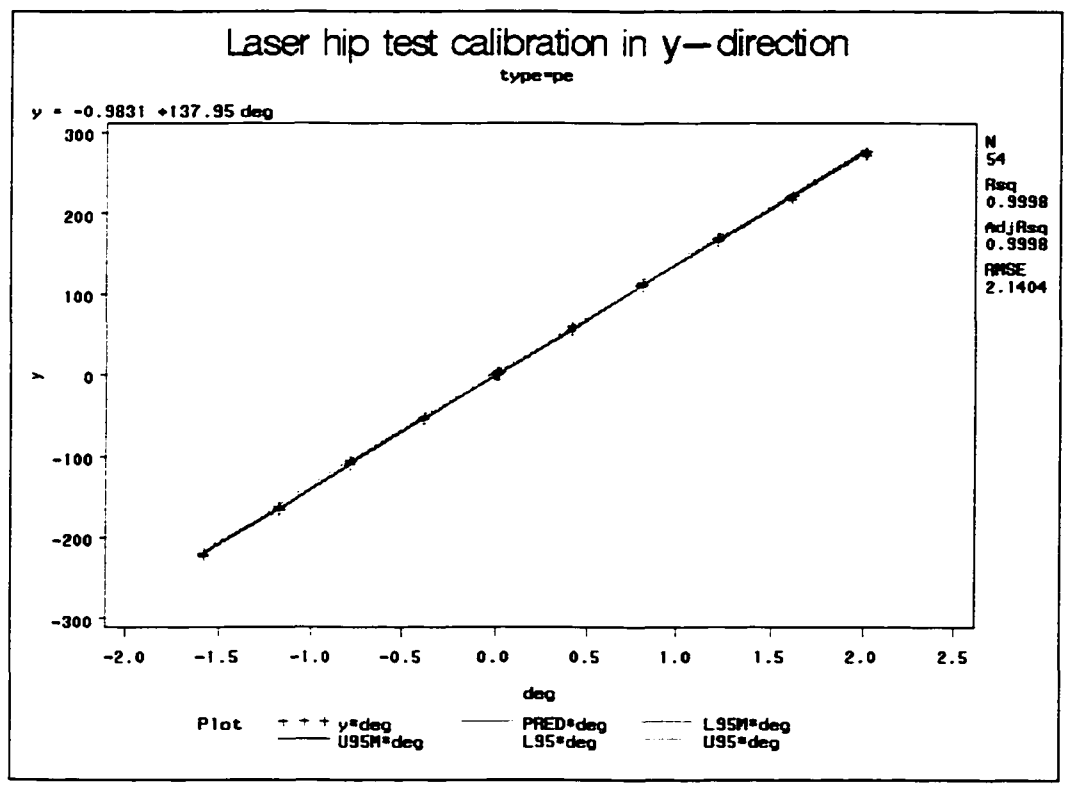

Sample Output From Calibration Curve:

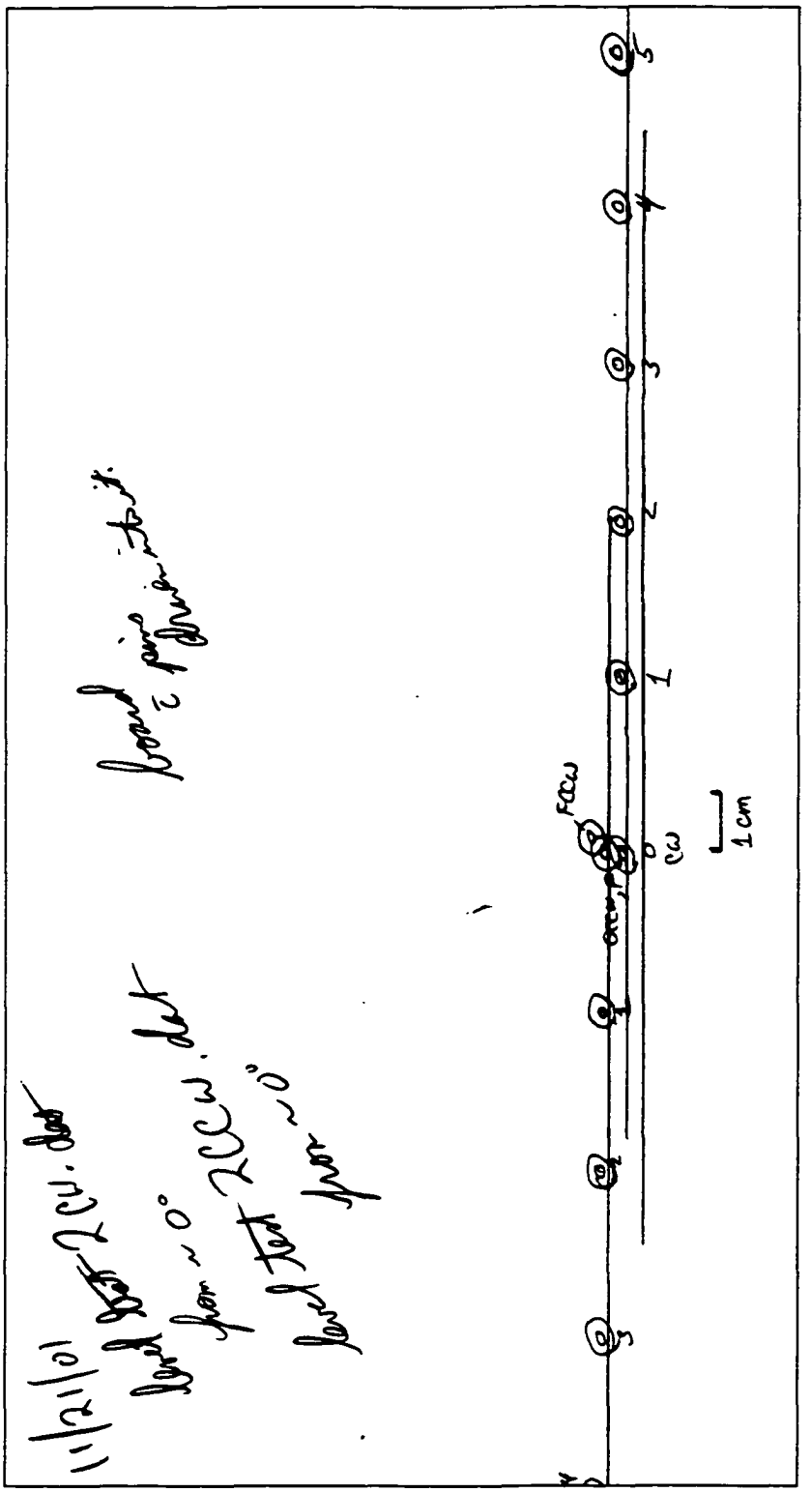

APPENDIX I - MECHANICAL TESTING OF ACETABULAR COMPONENTS

Sample Pre-Preparation:

1. Store specimen in freezer at -20°C. Thaw in refrigerator overnight.
2. If entire pelvis is intact, cut in ½ with big red bone chopper.

Sample Preparation Procedure for Mechanical Testing:

1. Place potting jig on bottom plate of mounting jig on MTS machine. Center using rubber bands.
2. Place bone on potting jig and center UHMWPE acetabular cup.
3. Mount laser in drill chuck.
4. Place guide on rim of cup and align laser with acetabular cup until proper placement of the bone is achieved.
5. Mark placement of screws in bone. These screws will be embedded in Dynacast and hold the bone in place.
6. Remove bone from potting jig. Place screws in bone.
7. Keep bones covered with saline-soaked paper towels during process to keep bones from drying out. Leave acetabular cup exposed.
8. Cover paper towels with plastic wrap. Keep in place with packaging tape.
9. Make sure that screws are sticking through paper towels and plastic wrap.
10. Line potting jig with plastic wrap.
11. Place bone in potting jig and align acetabular cup again.
12. Cut shims to fit around bone and form last 2 sides of potting jig. Hold shims in place using whatever you can think of (other shims, rubber bands, tape, etc.)
13. Mix Dynacast in fume hood.
14. Pour Dynacast into potting jig. Allow to set for a minimum of 20 minutes.
15. Remove potting jig from MTS machine.
16. Disassemble potting jig to remove test specimen from potting jig.
17. Using drill guide, drill 0.035 surgical pin into PE cup. Remove pin and glue it into PE cup using Super Glue™.
18. Drill 0.035 surgical pin into bone.

Measurements of Fixed Points in the Room:

1. MTS machine measurements.
    a. Between inside of 2 uprights = 21 inches (tape measure).
    b. From inside of upright to center of rotation = 10.5 inches (tape measure).
    c. Diameter of uprights = 5 inches (tape measure).
    d. From outside of upright to inside of gray upright = 2 5/8 inches (tape measure).
    e. Diameter of gray upright = 1 ¾ inches (tape measure).
    f. Distance from center of gray upright to outer edge of mounting bracket = 1 ½

inches (tape measure).

2. Room measurements.
   a. Distance from center of gray upright on MTS to wall = 122 5/8 inches (tape measure).
   b. Length of vertical line drawn from (a) to horizontal drawn from upper left corner of outlet plate = 24 7/8 inches (tape measure).
   c. Length of horizontal line drawn from upper left corner of outlet plate to vertical line (b) = 6 5/8 inches (tape measure).
3. Misc. measurements.
   a. Thickness of reference bar = 0.1868 inches (caliper).
   b. Thickness of surgical pins = 0.0338 inches (caliper).
   c. Thickness of laser mirrors = 0.075 inches (caliper).
   d. Width and height of laser mirrors = 0.493 inches (caliper).
   e. Distance between points 1 & 2 on laser A (PE laser) = 25.5 mm (compass & metal ruler).
   f. Distance between points 1 & 2 on laser B (Bone laser) = 23.5 mm (compass & metal ruler).

Acetabular Cup Mechanical Testing Procedure:

4. Determine which direction to rotate jig (left hip rotate ____ / right hip rotate ____).
5. Mount testing jig to its bottom plate.
6. Mount test specimen in testing jig. Align cup using laser and drilling guide.
7. Double check to make sure that you are using the proper configuration file, tuning, data collection ranges, load cell, and cable placement.
8. Replace laser with upper test jig in hydraulic wedge grip.
9. Make sure that surgical pin in PE cup is short enough to fit under upper test jig.
10. Using Super Glue™, glue laser mirrors to pins. Align mirrors so that they are vertical and align with length of the room.
11. Lower crosshead so that jig can be lowered into rim of PE cup.
12. Turn hydraulic pressure to low pressure.
13. Zero force and torque.
14. Lower upper test jig into place until pins are digging into rim of acetabular cup. Force applied should be 20 lbf or less.
15. Zero angle.
16. Place laser warning signs on doors.
17. Using compass and metal ruler, make distance measurements (mm) before testing:
    a. Reference bar to NW corner of bottom plate of testing jig (ref_l1)___ ___ ___
    b. Reference bar to SW corner of bottom plate of testing jig (ref_l2).___ ___ ___
    c. Reference bar to pin 4 on upper jig (jig_l4). ___ ___ ___
    d. Reference bar to pin 3 on upper jig (jig_l3). ___ ___ ___
    e. Reference bar to bone pin (bone_pin_lr). ___ ___ ___
    f. Bone pin to pin 4 on upper jig (bone_pin_l4). ___ ___ ___
    g. Bone pin to pin 3 on upper jig (bone_pin_l3). ___ ___ ___
    h. Reference bar to PE pin (pe_pin_lr). ___ ___ ___
    i. PE pin to pin 1 on upper jig (pe_pin_l1). ___ ___ ___

j. PE pin to pin 2 on upper jig (pe_pin_l2). ___ ___ ___

18. Mount lasers in their jigs (laser B = bone laser) and align laser beams in centers of mirrors.
19. Using compass and metal ruler, make distance measurements (mm) before testing:
    a. PE laser point 1 to reference bar (laser_a_r1). ___ ___ ___
    b. PE laser point 1 to bone pin (laser_a_b1). ___ ___ ___
    c. PE laser point 2 to reference bar (laser_a_r2). ___ ___ ___
    d. PE laser point 2 to bone pin (laser_a_b2). ___ ___ ___
    e. Bone laser point 1 to reference bar (laser_b_r1). ___ ___ ___
    f. Bone laser point 1 to bone pin (laser_b_b1). ___ ___ ___
    g. Bone laser point 2 to reference bar (laser_b_r2). ___ ___ ___
    h. Bone laser point 2 to bone pin (laser_b_b2). ___ ___ ___
20. Mount paper onto dry-erase poster on wall.
21. Using level, draw horizontal line from each laser dot.
22. Using tape measure, mark horizontal and vertical distance from upper left corner of reference outlet plate to any point on the paper.
23. On paper, note date, specimen tested, and data set name containing test data.
24. Run test program (CTS_hip_testing).
    a. Mark zero location of bone and cup laser lights. Mark with "0" and either "Bone" or "PE".
    b. Mark location of laser point after each incremental increase in load. Mark points 1-5.
    c. Mark final location of laser point at conclusion of test.

Calculation of Non-Dimensionalized PE Micromotion:

$$chord(small\_angles) = r\theta(radians) = \frac{d}{2} * \theta(\deg) * \frac{\pi}{180}$$

$$circumference = 2 * \pi * r = d * \pi$$

$$PE\_micromotion = \frac{\frac{d}{2} * \theta * \frac{\pi}{180}}{d * \pi} = \frac{\theta}{360}$$

Sample Output From Mechanical Testing of a Firmly Implanted Acetabular Component:

Larger figure = UHMWPE laser. Inset figure = Bone laser. Level line is parallel to 1 cm mark.

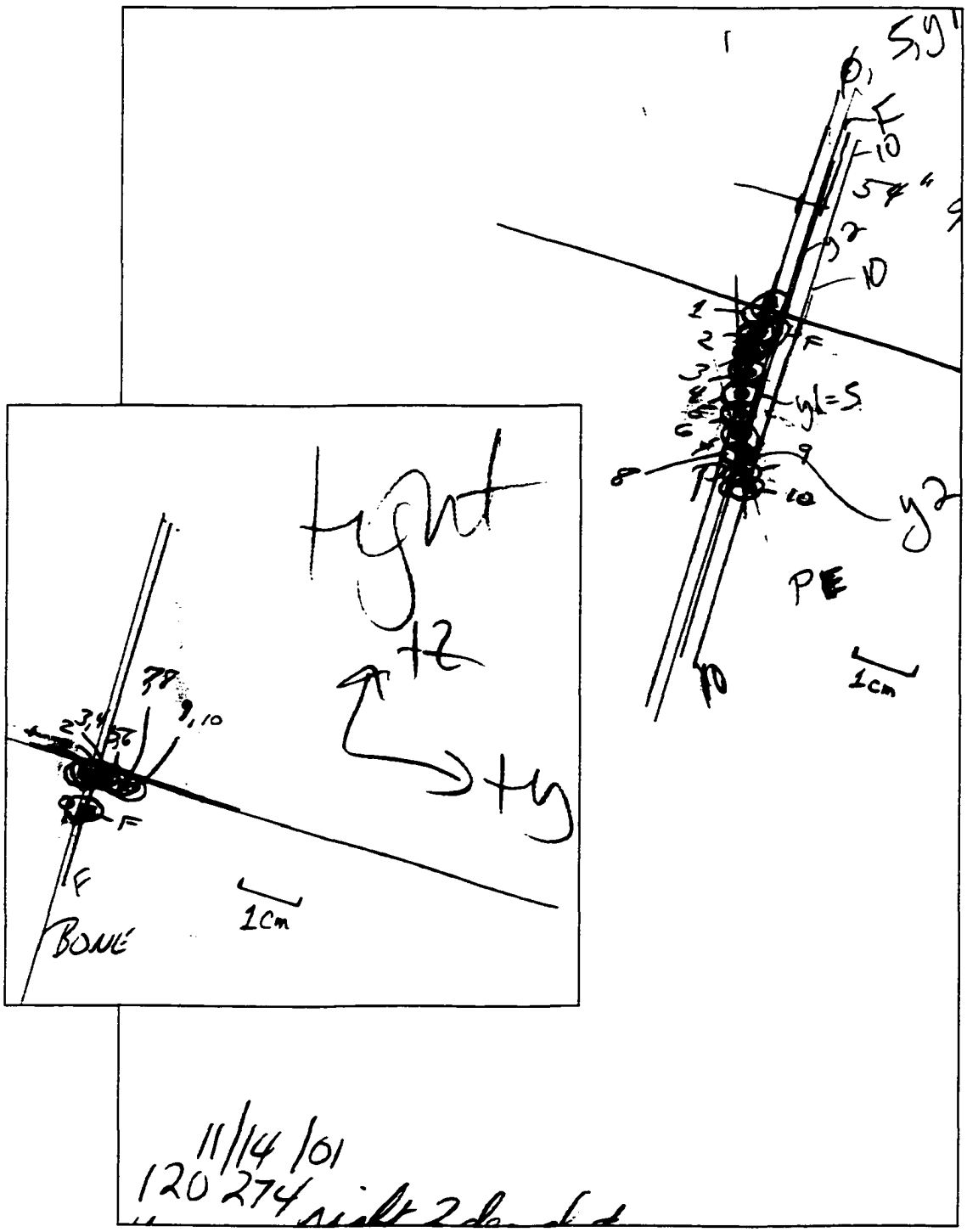

Sample Output From Mechanical Testing of a Loose Acetabular Component:

Larger figure = UHMWPE laser. Inset figure = Bone laser. Level line is parallel to 1 cm mark.

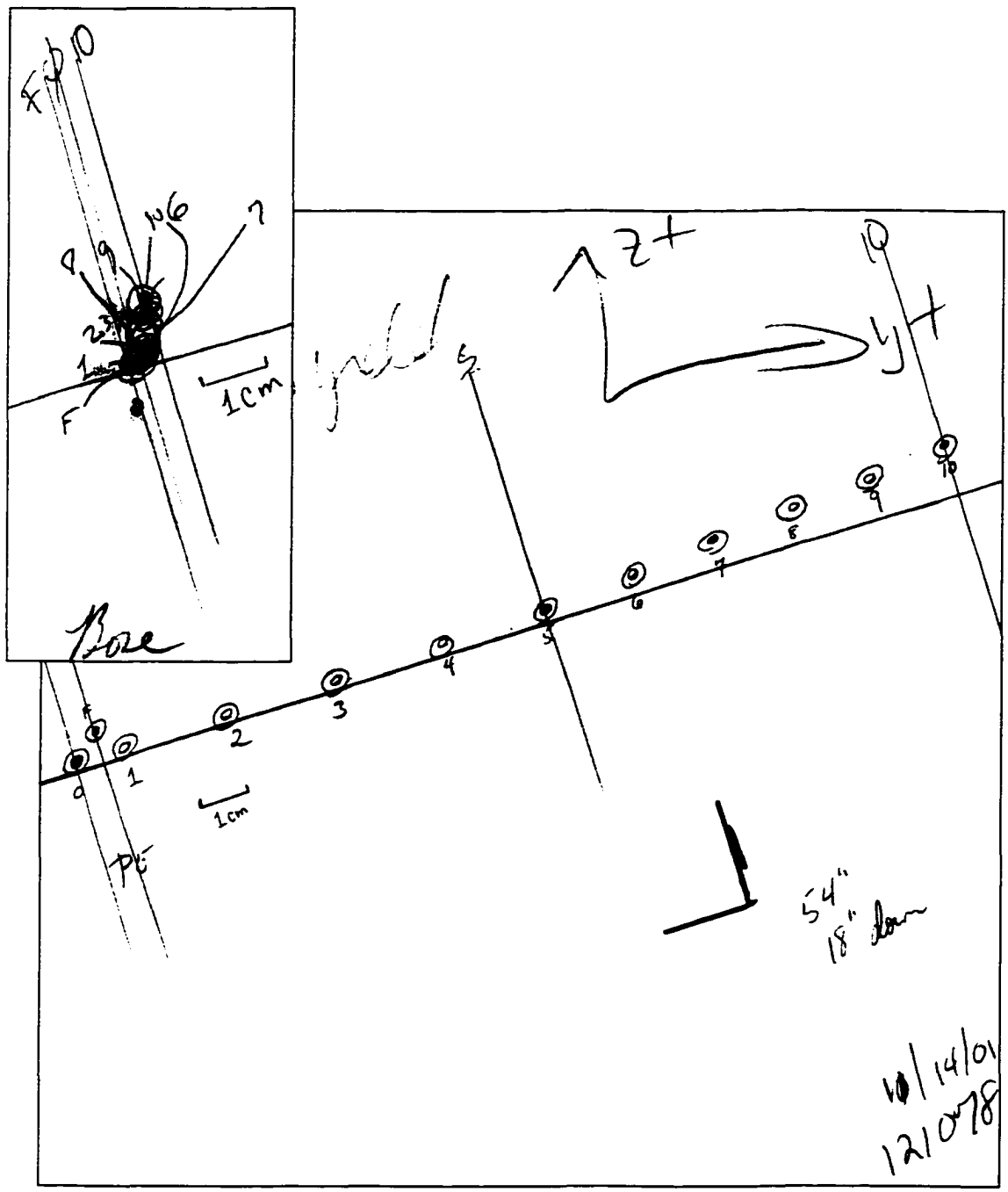

APPENDIX J - WEAR DEBRIS ISOLATION METHOD

Reagents:

1. Reagent #1 – Papain.
   a. 0.3 mg/ml papain buffered in PBS supplemented with 0.02 M EDTA and 0.02 M N-acetyl-L-cysteine.
2. Reagent #2 – 4M KOH.
3. Saline.
4. 95% ethyl alcohol.
5. Hexane.
6. Distilled water.

Equipment:

1. Centrifuge capable of spinning specimens at 1500 x gravity.
2. Centrifuge tubes.
3. Test tube rack for water bath.
4. Capped test tubes for digestion.
5. Volumetric flasks.
6. Magnetic stir bars.
7. Magnetic stir plate.
8. Heated water bath (37°C).
9. Transfer pipettes for removing supernatant.
10. Pipetteman or Eppendorf pipette that delivers 5µl.
11. Smooth polycarbonate filter with pore size of 1.0 and 0.1 µm (???).
12. Carbon paint (EM Center provides).
13. Vortexing mixer.
14. Sonicating water bath.
15. SEM stubs.
16. Dessicator.
17. Sputter coater.
18. SEM & EDX.
19. FTIR (for UHMWPE id).
20. Image analysis software (for particle size analysis).

Particle Retrieval Procedure:

1. Store specimen in freezer at -20°C. Thaw in refrigerator overnight.
2. Cut 3g samples of tissue for each digestion.
3. Place tissue specimen and 3 ml of Papain solution in test tube.

4. Incubate in a water bath at 37°C for 48 h.
5. Mix tissue digest with 9 ml of 95% ETOH.
6. Transfer tissue digest to centrifuge tubes.
7. Centrifuge for 60 min at 1500 x g.
8. Discard supernatant.
9. Suspend pellet in 6 ml 4M KOH (2 ml/g tissue).
10. Ultrasonicate for 5 min.
11. Hydrolyze for 16 h.
12. Separate UHMWPE particles from other metal and bone mineral debris.
    a. Mix equal volumes of hexane and ETOH.
    b. Spin tube vigorously using vortex mixer(?).
    c. Using transfer pipette, remove debris collected at hexane-ETOH interface.
13. Keeping UHMWPE debris and other sediment separate, clean debris of any remaining denatured protein by re-digestion in 4M KOH.
    a. Incubate overnight at 56°C.
14. Wash particles 3x in distilled water.
    a. Wash in distilled water.
    b. Sonicate for 4 minutes.
    c. Let sit at unknown temperature for 16 h.
    d. Centrifuge at 1500 x gravity for 30 min.
    e. Repeat at least 2 more times.
15. Suspend particles in 3 ml ETOH.